Preclinical Evaluation of Cell-based Tissue Engineering Constructs in Animal Models of Pelvic Organ Prolapse

Stuart Emmerson

Bsc (Hons) (Biochemistry and Molecular Biology)

The Ritchie Centre, Hudson Institute of Medical Research
Department of Obstetrics and Gynaecology
Faculty of Medicine, Nursing and Health Sciences
Monash University, Melbourne, Australia

A thesis submitted for the degree of *Doctor of Philosophy* at

Monash University in 2019

Supervisors

Prof. Caroline Gargett

The Ritchie Centre, Hudson Institute of Medical Research and Monash University, Department of Obstetrics and Gynaecology,

Melbourne, VIC, Australia

Prof. Jerome Werkmeister

CSIRO Manufacturing

The Ritchie Centre, Hudson Institute of Medical Research

Melbourne, VIC, Australia

Notice 1

Under the Copyright Act 1968, this thesis must be used only under the normal conditions of scholarly fair dealing. In particular, no results or conclusions should be extracted from it, nor should it be copied or closely paraphrased in whole or in part without the written consent of the author. Proper written acknowledgement should be made for any assistance obtained from this thesis.

Notice 2

I certify that I have made all reasonable efforts to secure copyright permissions for third-party content included in this thesis and have not knowingly added copyright content to my work without the owner's permission.

Declaration

This thesis is an original work of my research and contains no material which has been accepted for the award of any other degree or diploma at any university or equivalent institution and that, to the best of my knowledge and belief, this thesis contains no material previously published or written by another person, except where due reference is made in the text of the thesis.

Signature:

Name: Stuart James Emmerson

Date: 10/06/2019

Table of Contents

Declaration 4
Acknowledgements 8
List of Abbreviations 10
Summary 12
Publications and Abstracts 13
Thesis including published works declaration 15
Chapter 1: General Introduction 19
1.1. Pelvic Organ Prolapse 20
1.1.1. Surgical Reconstruction for Treatment of POP 20
1.1.2. Transvaginal augmented mesh implant for treatment of POP 21
1.1.3. Transvaginal Mesh characteristics 21
1.1.4. Mesh-Tissue Interaction 22
1.1.5. Alternative Mesh Designs to PP for Hernia Repair 23
1.1.6. Gelatin-coated Polyamide Mesh 24
1.1.7. Biodegradable Decellularized Materials 25
1.2. Vaginal Wall Structure 26
1.2.1. Effect of Parity 27
1.2.2. Damage to the Pelvic Support Structure Contributes to Reduced Pelvic Organ Support 28
1.3. Tissue Engineering 28
1.3.1. Stem Cells 28
1.3.2. Candidate Cells for Tissue Engineering Applications for POP 29
1.3.2.1. Skeletal Muscle Derived Stem Cells 29
1.3.2.2. Fibroblasts and Myoblasts 30
1.3.2.3. Mesenchymal Stem Cells 31
1.3.2.4. Adipose-derived Mesenchymal Stem Cells 32
1.3.2.5. Placenta-derived Mesenchymal Stem Cells 33
1.4. Endometrium as a Novel Source of MSC 34
1.4.1. Endometrial Mesenchymal Stem Cells 35
1.4.2. Prospective Isolation of eMSC from Biopsies and Hysterectomy 38
1.4.3. eMSC Phenotype and Gene Profile 39
1.4.4. Inhibition of eMSC Spontaneous Differentiation 40
1.5. Immune Response to Implanted Mesh 41
1.5.1. Role of Macrophages in Wound Repair 41

1.5.2. M1 Pro-inflammatory Macrophages 42
1.5.3. M2 Pro-wound Healing Macrophages 43
1.5.4. eMSC Modulation of the Macrophage Response 44
1.6. Preclinical Animal Trial Models for Assessment of POP Mesh **45**
1.6.1. Small Animal Rodent Models 45
1.6.2. Primate Models in Preclinical Trials 47
1.6.3. Large Animal Models in Preclinical Trials 47
1.6.3.1. Sheep as an Animal Model of POP and POP Surgery 48
1.6.3.2. ECM and Smooth Muscle Composition of the Vaginal Wall 48
1.6.3.3. Biomechanical Properties of the Vaginal Wall 49
1.6.3.4. Sheep-adjusted POP-Q Measurement for Detecting Vaginal Weakness 50
1.6.4. Pressure Sensor Measurement of Vaginal Wall Weakness 51
1.7. Rationale for Study **52**
1.8. Aims and Hypothesis **54**
Chapter 2: Ovine Multiparity: Implication for Pelvic Organ Prolapse **56**
Introductory Statement 57
2.1 Abstract 58
2.2 Introduction 58
2.3 Results 59
2.4 Discussion 62
2.5. Methods 67
2.6. References 68
Chapter 3: Optimising Ovine Surgery Models for Preclinical Trials **71**
Introductory Statement 73
3.1. Abstract 74
3.2. Introduction 75
3.3. Methods 77
3.4. Results 84
3.5. Discussion 93
3.6. Conclusion 96
Chapter 4: Composite Mesh Design for Delivery of Autologous Mesenchymal Stem Cells **98**
Introductory Statement 99
4.1. Abstract 101
4.2. Introduction 102

4.3. Methods 104
4.4. Results 110
4.5. Discussion 115
5. Conclusion 121
4.7. Acknowledgements 121
4.8. Tables 121
4.9. Figures 123
Chapter 5: General Discussion **133**
References **140**
Appendices **157**
Chapter 4 Appendices Images 157
Published Review – World Journal of Stem Cells 158

Acknowledgements

The number one person whom deserves my acknowledgement is my supervisor, Professor Caroline Gargett. She has shown me enormous patience and mentoring, and I hold that my ability to make it to the end of a doctorate is a reflection on her quality as a supervisor. I owe the arc of my improvement over 4 years to her guidance. Likewise, I wish to thank my co-supervisor Professor Jerome Werkmeister for his insight and contributions, without which I would not have gotten as far as I had with my PhD project.

I also want to acknowledge the laboratory colleagues both in the Gargett Laboratory and The Ritchie Centre as a whole, who have offered their experience and expertise. Particularly, I'd like to thank Ker Sin Tan, who had the unenviable role of teaching a new PhD student the required techniques and who remained a source of know-how for whom I am forever grateful. I would also like to thank Dr James Deane who shared his knowledge of fluorescent microscopy, Dr Fiona Cousins who helped with qPCR analysis, Dr Shayanti Mukherjee who assisted with sheep post-mortems and Dr Ilias Nitsos who performed the sheep euthanasia.

I would also like to extend a sincere thanks to our collaborators at CSIRO, especially Jacinta White and Aditya Vashi who were fantastic sources of advice and assistance on staining and imaging analysis during the early years of the POP project. I also want to thank Dr Sharon Edwards who provided wonderful expertise on and preparation of our experimental mesh and biomechanical testing.

I want to give another sincere thanks to our collaborators at the Monash Animal House and Monash Health. Dr Anne Gibbon provided invaluable expertise for sheep anaesthesia and monitoring as well as Dr Joan Melendez and Dr Paivi

Karjalainen who both kindly contributed their gynaecological surgery skills to make our animal model testing possible. Dr Anna Rosamilia also deserves special thanks for her gynaecological insight to both our scientific and surgical work. I also wish to acknowledge that this research was supported by an Australian Government Research Training Program (RTP) Scholarship.

Finally, I want to thank those closest to me in my family, partner and friends, all of whom have supported and remained with me during the ups and downs of a doctorate. If I could sum up my doctoral experience with a single proverb, it would be that one falls down seven times, but gets up eight. Without my family, partner and all of those mentioned above, there would have been no eighth time for me. Thank you all.

List of Abbreviations

Adipose derived mesenchymal stem cells	adMSC
Adult stem cells	ASC
Bone marrow mesenchymal stem cells	bmMSC
Buccal mucosal fibroblasts	BMF
Embryonic stem cells	eSC
Endometrial Mesenchymal Stem Cells	eMSC
Endometrial stromal fibroblasts	eSF
Expanded Polytetrafluoroethylene	ePTFE
Extra Cellular Matrix	ECM
Fetal placental mesenchymal stem cells	fpMSC
Fibulin 3	FBLN3
Fibulin 5	FBLN5
Glycosaminoglycan	GAG
Hematopoietic stem and progenitor cells	HSPC
Homeobox Protein Hox-A13	HOXA13
Human embryonic stem cells	hESC
Inducible nitric Oxide Synthase	iNOS
Induced pluripotent stem cells	iPSC
Insulin-like Growth Factor 1	IGF1
International Federation of Adipose Therapeutics and Science	IFATS
International Society for Cellular Therapy	ISCT
Lysyl oxidase like-1	LOXL1
Maternal placental mesenchymal stem cells	mpMSC
Mesenchymal stem cells	MSC
Metalloproteinases	MMPs
Muscle derived stem cells	MDSC
Pelvic floor disorders	PFD
Pelvic Organ Prolapse	POP
Pelvic Organ Prolapse Quantification	POP-Q
Polyamide	PA
Polyamide + gelatin	PA/G
Polyetheretherketone	PEEK

Polyvinylidene fluoride	PVDF
Reactive Oxygen Species	ROS
Side population cells	SP cells
Stromal Vascular Fraction	VSF
Superparamagnetic iron oxide nanoparticle	SPION
Sushi Domain-containing 2	SUSD2
Tissue Engineering	TE
Tissue non-specific alkaline phosphatase	TNAP
Transforming Growth Factor Beta	TGF-β
Transforming-growth factor beta receptor	TGFβR
Vascular endothelial growth factor	VEGF

Summary

The aim of this doctorate thesis "Pre-clinical Evaluation of Cell-based Tissue Engineering constructs in Animal Models of Pelvic Organ Prolapse" is to investigate the use of endometrial mesenchymal stem cells (eMSC) to rehabilitate damaged vaginal tissue and modulate the immune system when seeded onto polyamide mesh constructs and inserted into the vaginal walls of multiparous sheep animal models. The vaginal tissue of nulliparous, primiparous and multiparous sheep were first characterised using histological and biomechanical methods, and tested for POP susceptibility using an ovine-modified Pelvic Organ Prolapse Quantification (POP-Q) system and a novel pressure sensor device. These methods observed that multiparity thins the muscularis of the vaginal wall and increases the content of elastic fibre, which was correlated with POP-Q measurements that were indicative of POP susceptibility and tissue which was very flexible and poor at resisting applied forces. Next, autologous eMSC were isolated from the uteral lining of multiparous ewes, labelled with Iodex, and either seeded onto polyamide mesh coated in gelatin (eMSC/PA/G) and implanted into the vaginal walls of sheep, or was mixed with gelatin as the first step and then applied to polyamide mesh that was already implanted in the vaginal walls of sheep as part of a two-step protocol (PA + eMSC/G). After 30 days the tissues were harvested, and histological, fluorescent microscopy and qPCr techniques were used to observe the superior integration of PA + eMSC/G into the vaginal walls of sheep compared with eMSC/PA/G as no instance of exposure was observed in PA + eMSC/G explants, which corresponded with less disruption to the muscularis of the vaginal wall, reduced myofibroblast response, retention of elastic fibre content and a downplayed pro-inflammatory M1 macrophage response.

The result of this thesis demonstrated several important findings. The first was that sheep are a good animal model for POP research and treatment. Second, that implanted, autologous eMSC can reduce the trauma and damage incurred by vaginal tissue during the implantation of mesh in the treatment of POP. And third, that the delivery mechanism for stem cells into vaginal tissue has a significant impact on the future rehabilitation of damaged tissue and efficacy of implanted cells.

Publications and Abstracts

Peer-reviewed journal articles

Emmerson S, Young N, Rosamilia A, Parkinson L, Edwards SL, Vashi AV, Davies-Tuck M, White J, Elgass K, Lo C, Arkwright J, Werkmeister JA, Gargett CE, *Ovine multiparity is associated with diminished vaginal musuclaris, increased elastic fibres and vaginal wall weakness: implication for pelvic organ prolapse*. *Scientific Reports*, 2017: 7:45709 (vol 7 article 45709).

Published Review Articles

Emmerson S, Gargett C, Endometrial mesenchymal stem cells as a cell based therapy for pelvic organ prolapse, *World Journal of Stem Cells*, 2016 May 26; 8(5): 202-15

Submitted Journal Articles

Emmerson S, Mukherjee S, Melendez J, Cousins F, Edwards SL, Karjalainen P, Ng M, Tan, KS, Darzi S, Bhakoo K, Rosamilia A, Werkmeister JA, Gargett CE, Composite mesh design for delivery of autologous mesenchymal stem cells influences mesh integration, exposure and biocompatibility in an ovine model of pelvic organ prolapse, *Biomaterials*, submitted 2019, March.

Presentations

Emmerson S, Karjalainen P, Mukherjee S, Melendez J, Edwards SL, Rosamilia A, Werkmeister JA, Gargett CE, "Composite autologous stem cell and polyamide graft in the ovine prolapse model: comparing 2 delivery systems, integration and biocompatibility", International Continence Society, Gothenburg, Sweden Sept 3-6, 2019, accepted for Poster Presentation.

Emmerson S, Mukherjee S, Melendez J, Karjalainen P, Rosamilia A, Cousins F, Edwards, Tan KS, Werkmeister JA, Gargett CE, "Biocompatibility of Polyamide/Gelatin Mesh with or Without Endometrial MSC in Ovine Model of Pelvic Organ Prolapse", Tissue Engineering and Regenerative Medicine International Society, Kyoto, Sept 4-7, 2018, accepted for Poster Presentation.

Emmerson S, Mukherjee S, Melendez J, Karjalainen P, Rosamilia A, Cousins F, Edwards, Tan KS, Werkmeister JA, Gargett CE, "Biocompatibility of Polyamide/Gelatin Mesh with or without Endometrial MSC in Ovine Model of Pelvic Organ Prolapse", International Society of Stem Cell Research 2018 Melbourne Conference, Melbourne, Jun 20-30, 2018, Poster Presentation.

Emmerson S, Mukherjee S, Melendez J, Karjalainen P, Rosamilia A, Cousins F, Edwards, Tan KS, Werkmeister JA, Gargett CE, "Effect of Multiparity on Ovine Vaginal Tissue", UroGynaecological Society of Australia Annual Meeting, Melbourne, March 31-April 1, 2017, poster Presentation "Effect of Multiparity on Ovine Vaginal Tissue."

Emmerson S, Mukherjee S, Melendez J, Karjalainen P, Rosamilia A, Cousins F, Edwards, Tan KS, Werkmeister JA, Gargett CE, "Effect of Parity on Ovine Vaginal Wall Tissue Properties.", Australian Gynaecological Endoscopy & Surgery XVII Pelvic Floor Symposium & Workshop, Melbourne, July 15-16, 2016, Free Communication Presentation.

Emmerson S, Mukherjee S, Melendez J, Karjalainen P, Rosamilia A, Cousins F, Edwards, Tan KS, Werkmeister JA, Gargett CE, "Effect of Parity on Ovine Vaginal Wall Tissue Properties", 8th National Symposium on Advances in Gastrointestinal & Urogenital Research, Melbourne, November 25th, 2016, Presentation.

Awards

- Hudson Institute, Next Big Idea Ward, 1st Place Student Entry, 2018.
- The Ritchie Centre 3MT People's Choice Award, 2018.
- Hudson Institute, Next Big Idea Award, 2nd Place, 2017.
- The Ritchie Centre 3MT People's Choice Award, 2017.
- The Ritchie Centre 3MT People's Choice Award, 2016.
- The Ritchie Centre 3MT 1st Place Junior Category, 2016.
- AGES XVII Pelvic Floor Symposium, Best Free Communication Presentation, 2016.

Thesis including published works declaration

I hereby declare that this thesis contains no material which has been accepted for the award of any other degree or diploma at any university or equivalent institution and that, to the best of my knowledge and belief, this thesis contains no material previously published or written by another person, except where due reference is made in the text of the thesis.

This thesis includes 1 original papers published in peer reviewed journals and 1 submitted publications. The core theme of the thesis is tissue engineering and stem cell biology. The ideas, development and writing up of all the papers in the thesis were the principal responsibility of myself, the student, working within The Ritchie Centre under the supervision of Prof. Caroline Gargett.

(The inclusion of co-authors reflects the fact that the work came from active collaboration between researchers and acknowledges input into team-based research.)

In the case of Chapter *2 & 4* my contribution to the work involved the following:

Thesis Chapter	Publication Title	Status *(published, in press, accepted or returned for revision, submitted)*	Nature and % of student contribution	Co-author name(s) Nature and % of Co-author's contribution*	Co-author(s), Monash student Y/N*
2	Ovine multiparity is associated with diminished vaginal muscularis, increased elastic fibres and vaginal wall weakness: implication for pelvic organ prolapse	Published	75% collecting data, experimental work and writing.	1) **Natharnia Young,** sheep surgery 5% 2) **Anna Rosamilia** 3) **Luke Parkinson** Concept and experimental work 5% 4) **Sharon L. Edwards** Experimental work and draft editing 2% 5) **Aditya V. Vashi5** Experimental work 1% **6) Miranda Davies-Tuck** Statistical assistance 1%	No for all.

				7) **Jacinta White** Image analysis assist 1% 8) **Kirstin Elgass** Image analysis macros 9) **Camden Lo** Image analysis macros **10) John Arkwright** Fibre optic expertise **11) Jerome A. Werkmeister** concept and draft editing, 5% **12) Caroline E. Gargett** concept and draft editing, 5%	
4	Composite mesh design for delivery of autologous mesenchymal stem cells influences mesh integration, exposure and biocompatibility in an ovine model of pelvic organ prolapse	Under Review	75% collecting data, experimental work and writing.	1) **Shayanti Mukherjee** Post-mortem Assistance 2% 2) **Joan Melendez** Sheep Surgery 3% 3) **Fiona Cousins** qPCR Analysis assistance 1% 4) **Sharon L Edwards** Biomechanical analysis 1% 5) **Päivi Karjalainen** Sheep Surgery 4% **6) Michael Ng** IODEX supply 6) **Ker Sin Tan** Experimental assistance 3% 7) **Saeedeh Darzi** Experimental assistance 1%	No for all. Saeedeh Darzi (7) was recent doctorate graduate at Monash University.

				8) **Kishore Bhakoo** Iodex Supply 9) **Anna Rosamilia** Surgical expertise 10) **Jerome Werkmeister** concept and draft editing, 5% 11) **Caroline Gargett** concept and draft editing, 5%	

**If no co-authors, leave fields blank*

I have not renumbered sections of submitted or published papers in order to generate a consistent presentation within the thesis.

Student name: Stuart James Emmerson

Student signature: **Date:** 10/06/2019

I hereby certify that the above declaration correctly reflects the nature and extent of the student's and co-authors' contributions to this work. In instances where I am not the responsible author I have consulted with the responsible author to agree on the respective contributions of the authors.

Main Supervisor name: Caroline Gargett

Main Supervisor signature: **Date:** 10/06/2019

Chapter 1

General Introduction

1.1. Pelvic Organ Prolapse

POP is the herniation of pelvic organs into the vaginal cavity (**Figure 1)**. Symptoms are bladder, bowel and sexual dysfunction, including incontinence, which severely affects the quality of life of affected women [1]. POP affects 25% of all women in the USA and Western countries and is particularly prevalent in post-menopausal women. The main risk factors are vaginal birth delivery and aging, while obesity also contributes to POP recurrence [2]. A genetic predisposition for developing POP involves genes regulating collagen and elastic fibre synthesis, whose deficiency contributes to POP susceptibility [3]. As much of the world faces increasing obesity rates and an aging population, the prevalence and severity of POP will only increase over the coming years. The economic and healthcare costs are considerable, approximating US$1 billion each year [4].

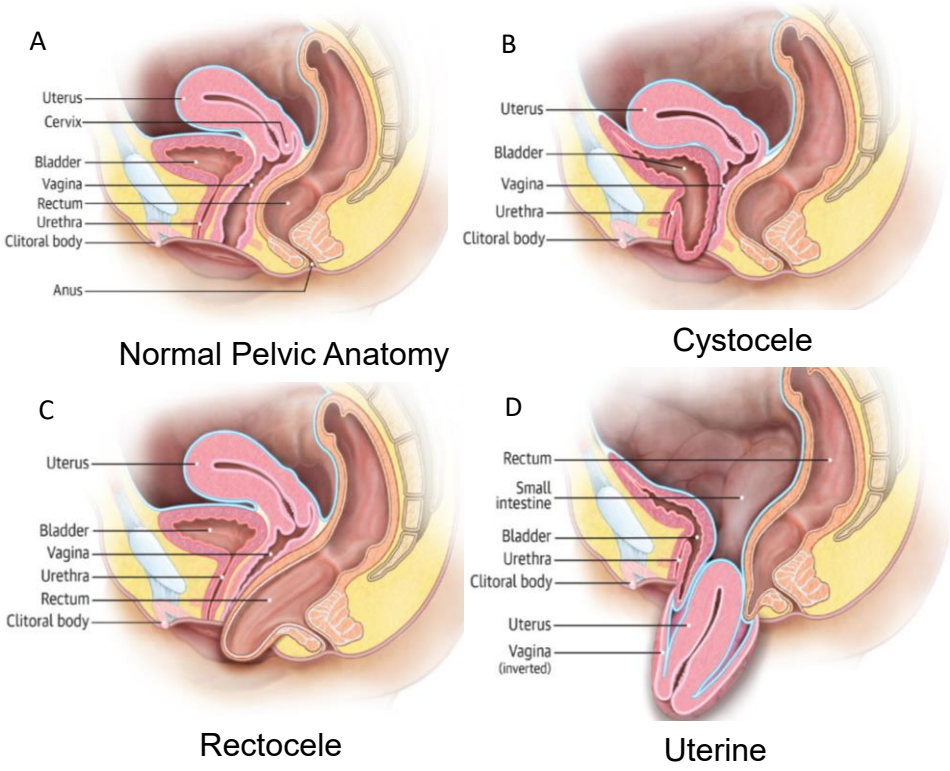

Figure 1: Pelvic organ prolapse. A) normal pelvic anatomy that undergoes **B)** bladder (cystocele), **C)** rectum (rectocycle) or **D)** uterine prolapse. (Reproduced with permission from [5])

1.1.1. Surgical Reconstruction for Treatment of POP

Currently the standard treatment for POP is native tissue repair conducted transvaginally (colporrhaphy) or abdominally (sacral colpopexy). This surgical treatment has a high failure rate with 30% of patients requiring one or more further surgeries due to recurrence of POP [6]. Additionally, reconstructive procedures in older women have complication rates from 15.5% to 33%, with the majority related to urinary tract infections, febrile morbidity and blood loss

requiring transfusion [7]. Indeed, the mortality from urogynecological surgery increases with each decade of life, with the most common complications occurring in women 80 years or older [8].

1.1.2. Transvaginal augmented mesh implant for treatment of POP

Augmented treatments for POP involving the implantation of polypropylene (PP) mesh into the vaginal wall to alleviate POP and support the pelvic organs has been available since 2005 after FDA approval in 2001 [9]. In addition to alleviating the herniation, synthetic mesh was intended to provoke a fibrotic response to thicken and strengthen the vaginal wall to protect against future instances of POP [10]. Though successful for many women, up to 10% require subsequent surgery while also enduring other complications such as pain, excessive fibrosis, mesh exposure into the vagina and erosion into the bladder or bowel, chronic inflammation and mesh shrinkage [7, 11, 12]. This led to the FDA releasing a Public Health Notification and Additional Patient Information in regards to these side effects, as well as worldwide recalls of several leading brands of mesh [12]. Similar bans have been issued in Australia, New Zealand and the United Kingdom. This has left many women with fewer options for treatment.

1.1.3. Transvaginal Mesh characteristics

The structural characteristics of hernia mesh, such as pore size (porosity), weight, production method (woven or knitted) have had enormous influence over the biocompatibility and efficacy of implanted mesh. Commercially available meshes are either woven or knitted, with woven mesh initially popular some decades ago **(Figure 2)** [13, 14]. These initial meshes were strong, providing support for herniated pelvic organs and protection against further prolapse [15-17]. However, they were quite stiff and heavy, and knitted polypropylene (PP) mesh was soon introduced as a replacement. Knitted PP had the advantage of strength, were chemically inert and borders did not fray after being cut to size. Furthermore, it retained relatively larger pore size while being more flexible and lighter than other meshes available at the time [14]. Though the optimal porosity is still under debate, it is a central consideration in new mesh development [17-19]. Recent meshes are usually monofilament (a single filament) but historically were initially multifilament (multiple filaments braided to make one thread). Monofilament mesh are less flexible but usually provide greater mechanical strength, while multifilament are more pliable and soft [20]. However, implanted monofilament mesh is less susceptible to infection, due to the lower surface area reducing bacterial adhesive ability and has less inaccessible

spaces for bacteria to hide from larger macrophages [14, 21]. This has prompted preference for monofilament mesh. In regards to weight, heavier and stiffer mesh have been associated with fibrotic scarring and chronic inflammation [22], as well as "stress shielding". This occurs when the heavier, stiffer mesh implant "shields" the resident tissues against the "stress" of herniation forces, which causes those tissues to adapt to the reduced stress by remodelling and undergoing atrophy [10]. This is avoided by using a more porous, pliable mesh that more closely matches the biomechanical properties of the vaginal wall, which assists the mesh to maintain its geometry by retaining pore shape [23, 24]. Though it might be tempting to sacrifice strength for lightweight flexibility, the geometry of implanted mesh comes under significant load force that can distort the pores and cause permanent deformation and loss of porosity [10].

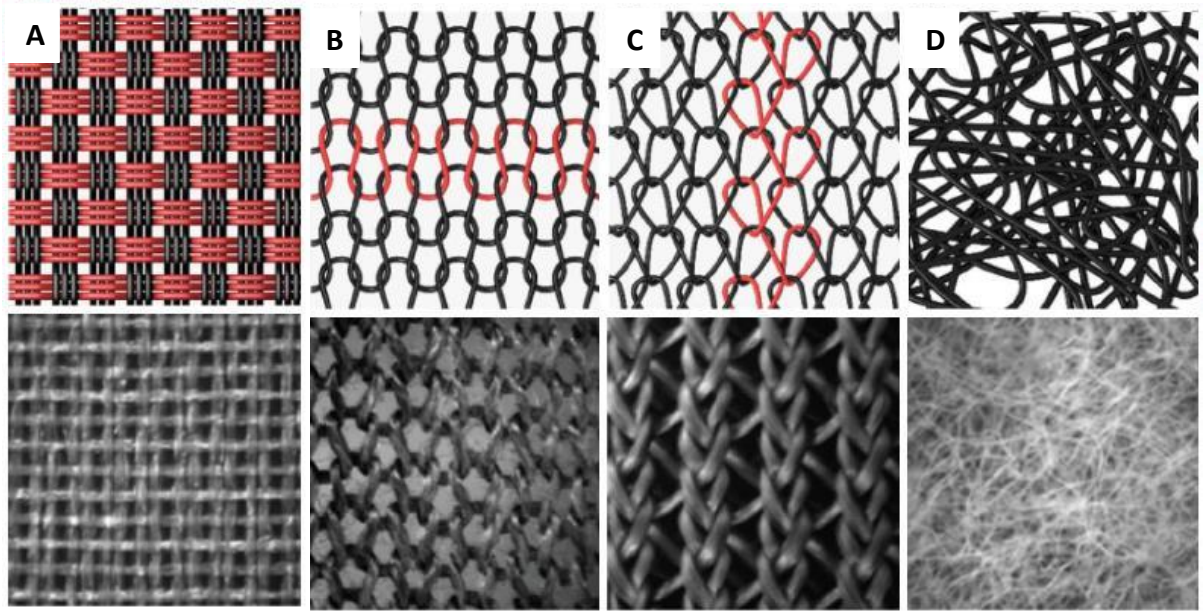

Figure 2: Different mesh types: A) woven mesh structure, **B)** knitted structure, **C)** warp-knitted structure and **D)** non-woven structure. (Reproduced with permission from [25])

1.1.4. Mesh-Tissue Interaction

The structural characteristics are an important consideration for not just the efficacy of the mesh itself, but its overall biocompatibility and integration into host recipient tissues. The porosity of the mesh has been investigated and is one of the most important aspects of mesh used for POP treatment [17]. Smaller pores have been associated with a greater risk of chronic inflammation and infection, as <10µm pore diameters inhibit the host macrophage response from accessing any bacterial colonies for phagocytosis [15]. Larger pore sizes permit the infiltration of leukocytes, both M1 and M2 macrophages, as well as fibrovascular ingrowth of

new tissues to facilitate superior mesh integration than those of smaller pore sizes [17]. The host immune response to implanted mesh has been a primary focus of mesh development research, particularly as chronic inflammation and fibrosis are two of the main complications of mesh implantation for POP treatment. Mesh materials, particularly the most commercially common PP mesh, typically evoke an inflammatory response that becomes chronic. Specialised collagen coatings of mesh have been investigated to reduce the immune response, with varied success. PP mesh coated with collagen demonstrated an improvement in prolapse-related symptoms and quality of life for human recipients compared to uncoated PP mesh, possibly due to improved biocompatibility of collagen coating for tissue adhesion [26]. Ovine animal models have been used to demonstrate the biocompatibility of PP mesh where individual filaments were coated with solubilized atelocollagen that exhibited superior vascularisation and collagen deposition compared to uncoated controls [27]. Other PP meshes are enveloped inside a solid collagen-coating. These have been associated with mesh exposure rates as high as 50% in larger animal models such as sheep and show reduced contractile force of ovine vaginal tissue after 180 days [28, 29]. Recently, fibrin glue-coated (consisting mostly of fibrinogen) PP meshes, used to deliver both mesenchymal stem cells (MSC) and MSC-derived exosomes reduced the inflammatory response [30]. Our group has been developing a gelatin coated mesh as delivery scaffolds for MSC as a potential treatment of POP, which has accelerated the wound healing process and reduced chronic inflammation [31-34]. However, as collagen- or gelatin-coating has produced inconsistent results with PP mesh, the question must be asked as to the future direction of transvaginal mesh itself. With FDA recalls and a recent ban of transvaginal mesh for POP surgery in Australia, transvaginal mesh requires significant improvement to both remain medically relevant and re-earn public trust.

1.1.5. Alternative Mesh Designs to PP for Hernia Repair

PP mesh is the most commonly used synthetic mesh for hernia repair, yet it is clear from its adverse effects that new materials are necessary. Polyester has demonstrated good biocompatibility due to being more hydrophilic while being very strong, with studies of abdominal implantations into patients having infection rates within acceptable parameters [35]. Likewise, the expanded polytetrafluoroethylene (ePTFE) material is highly hydrophobic limiting its biocompatibility, while polyvinylidene fluoride (PDVF) has had initially promising results but may find translation to clinical application difficult in the current climate of synthetic mesh bans [12]. Three new synthetic mesh designs for potential use in POP surgery were warp-knitted from different polymers; polyetheretherketone (PEEK), polyamide (PA) and

a gelatin-coated polyamide composite (PA/G). Of these, PA exhibited reduced stiffness and PA/G showed lower macrophage accumulation around individual filaments 90 days after implantation into a rat abdominal hernia model [31, 33]. These results suggested a flexible mesh with biomechanical properties closer to that of vaginal tissues is more promising than the stronger mesh. The gelatin coating of PA/G constructs could also serve as a scaffold for delivering stem cells to repair damaged vaginal tissue, a concept that could be trialled in larger animal models, such as sheep [33, 34].

1.1.6. Gelatin-coated Polyamide Mesh

A potential new application for FDA approved polyamide (PA) is for POP mesh, which is a monofilament, lightweight warp knitted mesh with diamond tulle pore construction [31]. Comparison with commercially available PP brands Polyform, Gynemesh PS and IntePro demonstrated that PA mesh was the most flexible of all mesh designs as measured by uniaxial biomechanical testing. It also exhibited similar strength to commercial PP meshes and closely matched the stiffness of human vaginal tissue [31] **(Figure 3B)**. An alteration to our basic PA was also compared. This alteration featured a glutaraldehyde-cross linked 12% porcine gelatin coating to create a PA/G construct, to offer a scaffold for cell seeding. With the gelatin coat, the PA/G mesh had increased bending rigidity compared to PA alone **(Figure 3A)** indicating reduced drapability, though it still exhibited similar burst strength **(Figure 3B)** [31]. The gelatin coat reduced flexibility but offered an invaluable method of cell delivery. Alternative methods of cross-linking could reduce the rigidity of the gelatin coat, such as ruthenium-based photo-crosslinking that produces more elastic gelatin scaffold for cells that could complement the PA meshes flexibility [36]. However, this use of ruthenium-based cross-linking has not yet been investigated *in vivo*. Both flexible and matching the tensile strength of vaginal tissue, it was decided that the new experimental PA mesh was worthy of further development for treating POP.

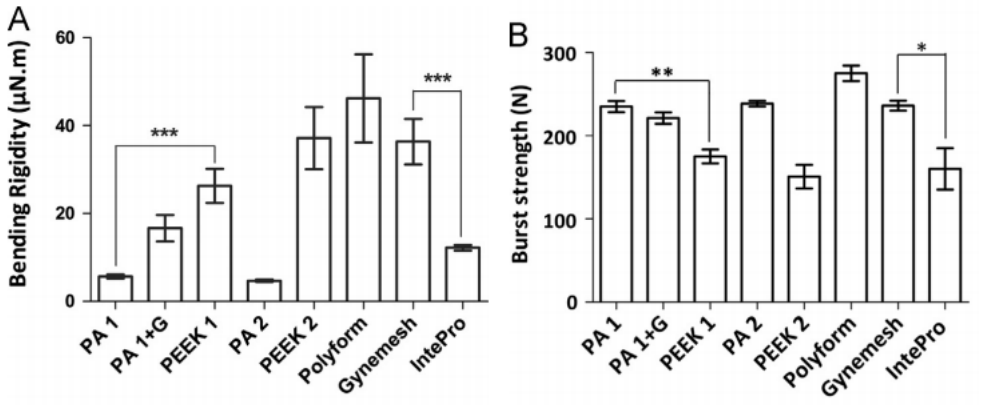

Figure 3: Mechanical properties of new meshes and commercial PP meshes: A) bending rigidity and **B)** burst strength. Data are expressed as mean ± SD (n=35). Statistical comparisons between meshes with least structural variables shown (PA1 vs. PA2, PA1 vs. PA1+G, PA1 vs. PEEK1, PEEK1 vs. PEEK2, Gynemesh vs. IntePro), with significantly different results noted $p \leq 0.05$ (*), $p < 0.01$ (**) and $p \leq 0.001$ (***). (Reproduced with permission from [31])

1.1.7. Biodegradable Decellularized Materials

A variety of materials have been devised to treat both abdominal herniations and pelvic organ prolapse, ranging from the use of human tissue, to non-absorbable synthetic mesh. One method involves scaffolds composed of mammalian extracellular matrices (ECM), which are acquired by decellarising tissue harvested from humans [37]. These are already used in surgical repair for musculotendinous tissue reconstruction and reconstructive breast surgery [37, 38]. Bioprosthetics, (grafts of a patient's own tissue) were originally proposed to alleviate the herniation and support the vagina and pelvic organs. Though autologous tissue usually avoids the foreign body reaction of synthetic materials, it lacks the mechanical strength to protect the tissue against further herniations [39, 40]. Further development of these grafts is required until they can be used as a feasible alternative to the most commonly used material, synthetic mesh [41, 42]. An interesting recent development has been to combine established mesh with polycaprolactone (PCL) degradable nanofiber scaffolds. When PCL was combined with PP and implanted into minipigs, the collagen accelerated in maturation with the implant itself becoming encased in flexible and elastic tissue with reduced mesh shrinkage [43]. However, the combination of PP and PCL degradable nanofibers produced a construct that was less resistant to forces [43]. Electrospun polylactic-co-glycolic acid (PLGA) with PCL nanofiber coating have been cultured with vaginal fibroblasts derived from patients suffering from POP and placed under mechanical straining *in vitro*. Genes associated with extracellular matrix synthesis (Collagen I, III, V and Elastin) and remodelling (αSMA, TGF-β1) were upregulated

in comparison to controls [44]. This suggests a future for degradable nanofibers for POP treatment in the wake of synthetic mesh bans.

1.2. Vaginal Wall Structure

The vaginal wall is composed of four layers **(Figure 4)**. The vaginal cavity is lined by stratified squamous epithelium. Beneath the epithelium is the lamina propria which is composed mostly of connective tissue and blood vessels. The third layer of the vaginal wall is the muscularis, comprised of bundles of smooth muscle cells, with the inner layer featuring circular smooth muscle and the outer layer longitudinal arrangements. The final layer is the adventitia, a layer of loose connective tissue composed mostly of blood vessels. Since the muscularis has a role in providing mechanical strength to the vaginal wall, it has been studied in women with POP investigating the hypothesis that deficiency in the muscularis would contribute to POP susceptibility. Indeed, histological analysis of POP tissue obtained from the anterior wall of women undergoing vaginal plastic surgery observed increased Collagen III fibrils which displaced the smooth muscle cells and appeared disorganised [45]. Another study showed reduced smooth muscle actin and increased collagen expression in the muscularis of women with POP [46]. If these alterations occurred before first vaginal birth, it could suggest a genetic predisposition caused remodelling of the vaginal wall increasing susceptibility to POP. This could be explored using nulliparous ovine animal models. Alternatively, the changes of ECM synthesis and gene expression could be a response to the tissue trauma incurred by POP, resulting in a remodelling of the vaginal wall layers. In either case, the vaginal wall composition and its relation to POP requires further exploration to refine methods of POP treatment.

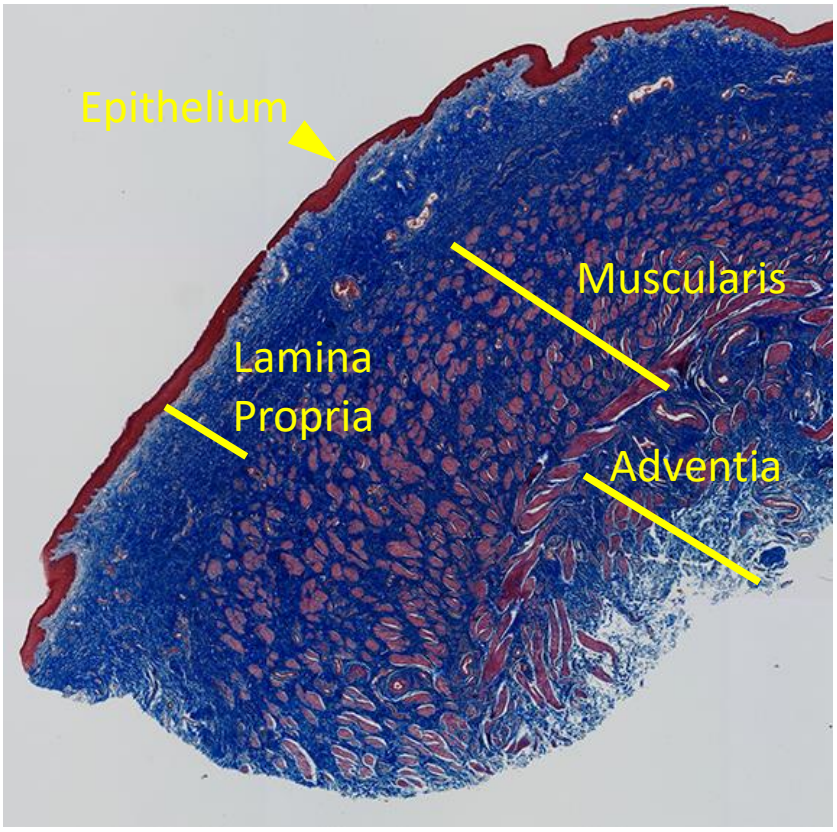

Figure 4: Four layers of the vaginal wall: Masson's trichrome stained ovine vaginal wall is composed of four distinct layers. The first is the epithelium (yellow arrow), beneath which is the lamina propria which is mostly composed of connective tissue (collagen). The third layer is the muscularis which is made-up inner circular smooth muscle cells and outer longitudinal smooth muscle cells. The final layer is the adventitia, a layer of connective tissue rich with blood vessels.

1.2.1. Effect of Parity

To date, the most common risk factor for POP susceptibility is child-birth due to the traumatic effect of the first child delivery on the vaginal wall, which causes the initial and most damage of all births [47]. However, the precise mechanisms underpinning the development of this vulnerability are not entirely understood. Recent investigations into the effect of parity on the vaginal wall using animal models have observed significant alteration of ECM composition, remodelling of the vaginal wall layers and reduction of tissue strength [48]. These alterations are likely due to overstretching of vaginal tissue as the baby transits the birth canal leading to tissue damage. Increased elastic fibres appear to be retained post-partum to compensate for birth-induced damage [49]. A decline in the epithelial thickness of the vaginal wall as a result of parity has also been observed, though the effect on the strength of the vaginal wall remains unknown [50, 51]. That this is due to the damage incurred by vaginal tissues during delivery is further supported by the reduced risk of POP among women who have undergone caesarean section instead of vaginal delivery [52].

1.2.2. Damage to the Pelvic Support Structure Contributes to Reduced Pelvic Organ Support

The majority of damage done to the vaginal wall and supporting architecture is incurred during the first delivery. Separation of connective tissue within the pelvic side wall has been associated with stress urinary incontinence and descent of the anterior wall [53]. This highlights the importance of the integrity of the 3 pelvic organ support structures for resisting POP; the pelvic floor muscles, vaginal wall endopelvic fascia and uterine suspensory ligaments. The pelvic floor skeletal muscles at risk of separation and damage due to childbirth can be influenced during pregnancy to prepare the vagina for childbirth (eg. increased elastin deposition) [54]. It is clear, then, that the effect of parity on the vaginal wall play central roles in resistance and vulnerability to POP, with more research required to both understand and overcome the effect of damage to the pelvic organ support structures that lead to loss of vaginal integrity and POP, and how to prevent it.

1.3. Tissue Engineering

Tissue engineering is a multidisciplinary field focused on combining living cells with synthetic scaffolds to produce tissue constructs that can be implanted as substitutes for damaged tissues or organs. Waiting times for organ donations are long and even when donations are made the incompatibility of donors and recipients is a persistent problem leading to rejection. This has created a massive world-wide demand for organs that tissue engineering could meet. One of the most promising recent innovations in this direction is 3D bio-printing, which has shown potential to create desired organs and tissues using a host's own cells (i.e autologous). However, the type of cell(s) employed is of central importance as this can significantly affect the construct effectiveness and compatibility. It is for this reason that stem cells, in the broader use of the term, have shown the most promise, as their pluripotency and/or multipotency, ability to differentiate into various desired lineages, has made them popular for various TE endeavours.

1.3.1. Stem Cells

The label "stem cells" is a broad and simplified term for cells that can self-renew and differentiate into a variety of cellular lineages and can be divided into three broad groups: embryonic stem cells (eSC), induced pluripotent stem cells (iPSC) and adult stem cells (ASC), and each has advantages and disadvantages to consider in the context of tissue engineering.

eSCs are derived from the inner cell mass of the blastocyst and differentiate into all three germ layers, giving them remarkable versatility and potential for targeted linear differentiation [55, 56]. However, the process of their extraction destroys the developing embryo, which has raised ethical concerns that have remained the centrepiece of any discussion surrounding the employment of these cells. Furthermore, the logistics of employing eSC is challenging due to the initial low cellular yield and the time and resource-intensive process of culturing and maintaining eSC cultures. The second group of stem cells, iPSC, have been heralded as a promising replacement for eSC, as they are acquired by reprogramming somatic cells with four transcription factors *Oct4* (Pou5f1), *Sox2*, *cMyc* and *Klf4* [57-59]. This gives rise to a small number of pluripotent stem cell colonies which can be directed to differentiate into desired cell types using the correct culture conditions. However, iPSC, much like eSC, require considerable time and resources for successful culturing and cell differentiation, which is itself a sensitive process. Additionally, iPSC derivation involves "reprogramming" by retrovirus-delivered transcription factors, which can unwittingly introduce genome mutations and errors, and is an explanation offered for why even autologous iPSC-derived cells have sometimes been rejected by a hosts immune system [60]. This is a significant barrier for replicable use in a standardised therapeutic employment, although there are clinical trials underway using these derivatives [61]. The final broad group of stem cells are known as Adult Stem Cells (ASC). These are undifferentiated cells found within existing tissues that can be directed into specific cell lineages of the tissue in which they reside with the appropriate induction conditions [62-64]. Unlike iPSC, ASCs do not require retrovirus delivered transcription factors as they already exist in an undifferentiated, although not pluripotent, state. This benefit means that ASC do not have to undergo "reprogramming" and, when used autologously, are safe from risk of host immune rejection. However, they are not immortal cells like iPSC. These properties make ASC promising candidates for cell-based therapies, particularly TE. Fortunately, knowledge of ASC and their applications is growing rapidly, as their many benefits have intensified research efforts.

1.3.2. Candidate Cells for Tissue Engineering Applications for POP

1.3.2.1. Skeletal Muscle Derived Stem Cells

Skeletal muscle has been identified previously as a potential source of progenitor stem cells capable of differentiating into myogenic cell lineages in rat models [65-68]. The use of skeletal

muscle stem cells to deliver gene therapy is being explored for treating muscular dystrophy and stress urinary incontinence, another pelvic floor disorder involving the urethra [66]. In addition, they are being used to regenerate both skeletal and cardiac muscle. As a potential source of cells for treating POP, muscle-derived stem cells (MDSC) are particularly attractive as they can now be isolated from human skeletal muscles and differentiated into skeletal myotubes, *in vitro* and *in vivo* [69]. The ability of MDSC to promote vaginal epithelial regeneration and vaginal wall repair in a rat model makes them candidates for treating POP [70]. However, to avoid the risk of immune rejection from allogeneic sources, MDSC are better derived from the patient's own muscle tissue. Such an autologous procedure is expensive and invasive, causing significant pain and morbidity for the patient. An alternative source of cells for POP treatment could prove more beneficial and practical for the patient.

1.3.2.2. Fibroblasts and Myoblasts

As major producers of collagen and an essential cell for the formation of connective tissue, fibroblasts have been suggested as an alternative cell source for TE [71]. Vaginal myofibroblasts from nulliparous women have higher contractile strength compared to those from parous women, suggesting that vaginal delivery and overstretching of the vaginal wall affects myofibroblast function [72]. However, the use of autologous vaginal fibroblasts from patients for treating their pelvic floor disorders raises concerns about the quality of cells utilised. Other studies have observed that vaginal fibroblasts derived from prolapsed tissues have impaired function, such as delayed fibroblast mediated collagen contraction and lower production of collagen synthesising enzymes [73]. This could be avoided if women have a vaginal biopsy to collect and cryopreserve fibroblasts before childbirth to obtain better quality cells, however such long-term planning and storage facilities are not available to most women. The invasive method of acquiring human vaginal fibroblasts and subsequent morbidity is another obstacle in their use as the main source of cells for a tissue engineering-based approach to treating POP. Buccal mucosal fibroblasts (BMF), however, offer a readily available and plentiful source of cells and could prove an alternative to human vaginal fibroblasts [74]. BMF are harvested from the inside of the cheek lining and express the typical MSC/fibroblast surface markers but do not function as MSC [75]. They produce important components of the extracellular matrix such as Collagen I, which is required for strengthening the vaginal walls to alleviate and prevent herniation [71, 76]. The interaction of BMF with various biodegradable scaffolds has been examined *in vitro* for potential treatment of pelvic floor disorders (PFD)

including POP [76]. Although BMF offer a potential candidate for the treatment of POP, they currently remain untested for this purpose in animal models and their ultimate suitability remains unknown.

1.3.2.3. Mesenchymal Stem Cells

MSC have been extensively used in cell-based therapies, predominantly for their anti-inflammatory and immunomodulatory non-stem cell properties [77, 78]. Though these cells fall under the umbrella of ASC, they are a distinct group that are of stromal origin. However, they also have potential for TE purposes for regenerating new tissues or promoting the activity of endogenous stem cells [79-81]. MSC populations have the capacity for self-renewal, are highly proliferative and differentiate into mesodermal and other lineages [82]. Recent advances in cellular identification using more specific markers have shown that MSC can be extracted from most tissues including bone marrow, umbilical cord, placenta, adipose and endometrium, although not all sources have demonstrated clonogenicity for their MSC populations [83-86]. Typically, MSC actively respond to stress or injury in a similar manner to cells of the innate immune system responding to pathogen exposure. When supplied systemically, exogenous MSC home to sites of injury in response to inflammation [87]. Here MSC operate in a paracrine manner by secreting large amounts of diverse proteins, growth factors, cytokines and chemokines that promote a variety of effects including neo-angiogenesis, tissue regeneration and remodelling, immune cell activation, suppression of inflammation and cellular recruitment [79, 80, 88-90]. The potential of MSC as a cell-based therapy has also been explored in numerous clinical applications. The ability to direct bone marrow MSC differentiation into other cell types and lineages has shown that these cells maintain a phenotype lacking tissue-specific characteristics until exposed to signals in damaged tissues [91]. MSC obtained from dental pulp have been used to repair related tissues such as periodontal ligament, dental papilla and dental follicle [92]. Likewise, urine derived stem cells (UDSC), have demonstrated restoration of sphincter function after vaginal distention injury in rats [93]. The ability of adipose tissue and bone marrow MSC to act as precursor cells has also been exploited by directing their differentiation toward the chondrogenic lineage to produce cartilage-synthesising chondrocytes [94]. Although MSC show promise as cell-based therapies, more understanding of their mechanism of action is needed. Indeed, early clinical use of MSC has not always met expectations, often producing inconsistent results [95]. This may be due to lesser refined methods of isolating and cultivating MSC resulting in the administration of

fibroblasts and myofibroblasts rather than undifferentiated MSC [96]. Until recently, production of significant numbers of MSCs posed a challenge, as the regenerative potential of MSC declined during culture expansion [34, 97], which is required due to the small numbers of perivascular MSC present within tissues [98]. For tissue engineering applications and tissue repair following ischemia (e.g., cardiac muscle), local rather than systemic delivery is desirable and will likely result in greater local concentration of MSC at the desired tissue site, even when the mechanism of action is paracrine [99]. A further consideration is allogeneic vs autologous, as autologous cells avoid immune rejection. Seeding MSC onto scaffolds, such as polyamide/gelatin (PA/G) for POP appears to produce better outcomes in preclinical studies [34]. MSCs are a versatile and promising stem/stromal cell which can be used for a variety of regenerative medicine applications. Additionally, MSC have greater capacity to regenerate tissues from which they are derived [78]. Therefore, MSC obtained from the lining of the uterus could be useful in the development of treatments for other regions of the female reproductive tract, e.g., vaginal wall tissue in cases of POP. This could occur from two places: the placenta and the endometrium itself.

1.3.2.4. Adipose-derived Mesenchymal Stem Cells

Adipose derived mesenchymal stem cells (adMSC) are isolated from fat and have emerged as a popular source of multipotent and self-renewing MSC for cell-based therapies. Multipotent cells were first acquired by centrifuging mechanically and enzymatically digested adipose tissue and then culturing the ensuing pellet, the Stromal Vascular Fraction (SVF) [86]. These cells exhibit common MSC markers CD90, CD71, CD105/SH2 and SH3, and their observed adipogenic, osteogenic, chondrogenic and myogenic differentiation pathways *in vitro* marked them as multipotent stem cells worthy of further investigation for MSC-based therapy applications [86]. In addition to their multipotent potential, stromal vascular fraction (SVFs) have demonstrated anti-inflammatory properties when co-cultured with monocytes through increased expression of interleukin-6 and interleukin-10 [100]. Due to the heterogenous nature of the SVF, further efforts were made to refine the isolation process to separate the genuine adMSC from the surrounding cells. This culminated in a joint statement by the International Federation for Adipose Therapeutics and Science (IFATS) and the International Society for Cellular Therapy (ISCT), which identified adipose stem cells as positive for CD13, CD29, CD44, CD73, CD90 andCD105 and varying levels of CD34, while negative for CD31, CD24, CD235a [101]. The varying CD34 expression has been controversial for the identification and isolation of adMSC. adMSC in early culture highly express CD34, however this sharply

declines with increasing time spent in culture [102, 103]. CD34 is a glycosylated transmembrane protein and has served as a marker for hematopoietic stem and progenitor cells (HSPC). Its precise function is unknown, due to many tissue specific post-translational and post-transcriptional modifications. However, current evidence suggests CD34 enhances proliferation, blocks stem cell differentiation and promotes cell morphogenesis [104, 105]. CD34 doubtless plays an important role within adMSC, and its loss of expression on culturing suggests they undergo similar spontaneous differentiation as do other sources of MSC [106]. Nevertheless, both CD34+ and CD34- adMSC have been used in tissue engineering to regenerate bone tissue in Labradors [107], in stimulating human osteogenic markers *in vitro* [107], treatment of induced myocardial infraction in rats [108] and neovascularisation during peritoneal grafting in mice [109]. However, despite their promise and employment in tissue engineering, their use in cell-based tissue engineering for treating POP has several hurdles. Most research conducted with adMSC has used adipose tissue derived from cosmetic surgery off-cuttings. As POP is a condition mostly affecting post-menopausal age women, acquiring adipose tissue would be an invasive procedure for autologous adMSC acquisition, and one that risks further surgical complications for older surgical patients. Therefore, until the methods of their initial acquisition can be refined to less-invasive means, adMSC are not an ideal candidate for cell-based tissue engineering treatment of POP.

1.3.2.5. Placenta-derived Mesenchymal Stem Cells

The placenta is a large tissue connecting the mother and her infant during pregnancy, discarded as waste after the child is born. The main purpose of the placenta is to provide oxygen, nutrients and protective immune molecules from the mother to the infant. As a fetomaternal organ that develops from the endometrium, the placenta is composed of two main components: the maternal placenta (decidua basalis) and the fetal placenta (chorion frondosum). The placenta is rich with blood vessels and MSC which can be isolated from either the fetal (fpMSC) or maternal (mpMSC) placenta. fpMSC exhibit strong immunosuppressive and angiogenic properties, and differentiation potential into various lineages, such as chondrocytes, adipocytes and osteoblasts [110-112]. mpMSC have exhibited surface markers common to other MSC [113], with mpMSC isolated from the decidua basalis during the second trimester showing significantly higher proliferative ability than adult bmMSCs [114]. mpMSC also exhibit similar mesodermal differentiating ability except for the adipogenic lineage, in which bmMSC were superior [115]. fpMSC isolated from the chorion and amnion, during the first and second trimester show mesodermal lineage differentiation and neuronal cells with appropriate cell

markers for each lineage [113], showing their multipotency. The angiogenic and immunomodulatory properties of pMSC have been demonstrated through use of their exosome derivatives in mouse models to alleviate the ischemia after transplantation into diabetic nude rats [116, 117]. However, pMSC (including fpMSC and mpMSC) are currently not well-suited for tissue engineering applications, such as POP. This is because POP usually occurs in women of menopausal age long after the opportunity to harvest pMSC for treatment has passed. Though it is possible that forward thinking women could have their pMSC stored in biobanks for such a purpose, this is an expensive solution. A more practical solution would be to utilise an MSC based tissue engineering treatment on cells that can be acquired from a patient when they are needed.

1.4. Endometrium as a Novel Source of MSC

The endometrial lining of the uterus serves as the site of embryo implantation, placentation and the development of the embryo and foetus during pregnancy [118]. The upper functional layer of the human endometrium undergoes extensive growth, differentiation and shedding each menstrual cycle under the influence of sex steroid hormone fluctuations [119]. Following menstruation, the remaining basal layer regenerates the new functional layer, which undergoes rapid cellular proliferation followed by differentiation **(Figure 5)**. If an embryo does not implant, the terminally differentiated epithelium and stroma is shed during menstruation [120]. Much like the continuously renewing small intestinal mucosa, the endometrial mucosa undergoes many cycles of regeneration during a woman's lifetime, indicative of its highly dynamic and regenerative capacity.

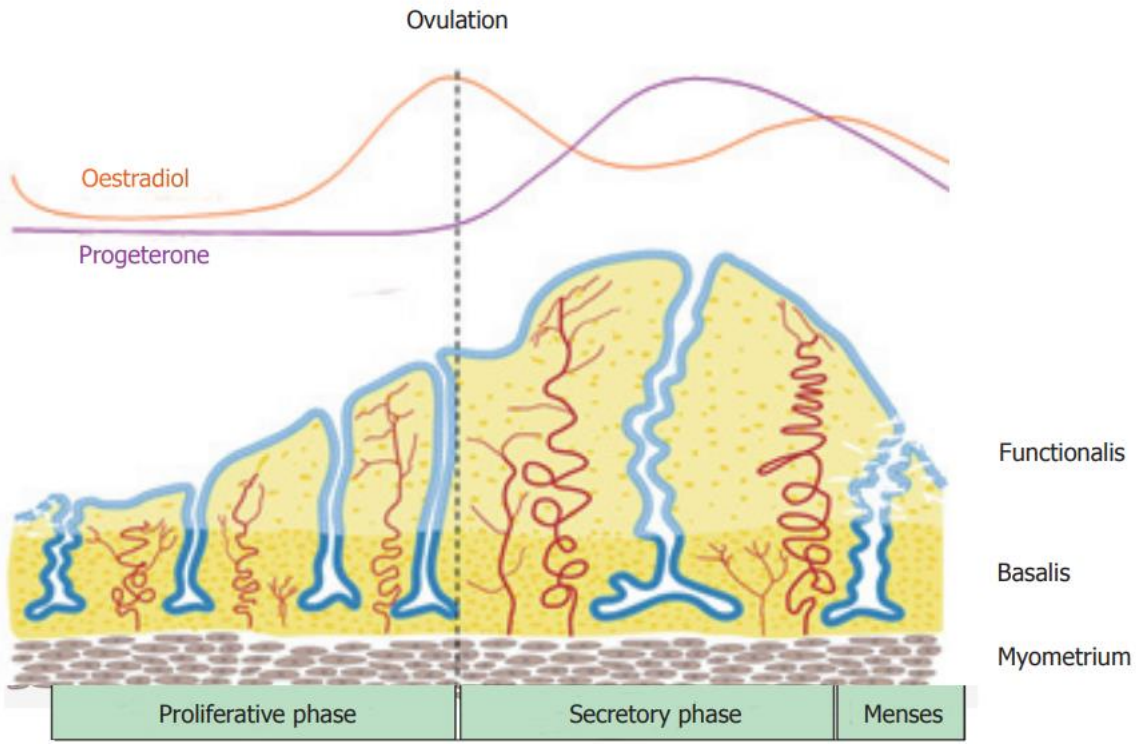

Figure 5: Schematic showing changes in the human endometrium during the menstrual cycle, illustrating the growth, differentiation and shedding of the functionalis layer. The functionalis layer regenerates 4-10 mm during the proliferative phase (10d) as cells proliferate in response to rising circulating estrogen levels. During the secretory phase, progesterone induces differentiation of the epithelium and stroma to generate an endometrium receptive to implantation of an embryo. This entire process occurs over 400 times during a woman's reproductive life indicating the regenerative potential of human endometrium. (Reproduced with permission from [119])

1.4.1. Endometrial Mesenchymal Stem Cells

The existence of stem/progenitor cells within the endometrium and their role as progenitor cells for regenerating endometrial tissue has only recently been reported 15 years ago. Endometrial MSC (eMSC) are clonogenic and multipotent, differentiating into four mesodermal lineages: osteoblasts, chondrocytes, smooth muscle cells and adipocytes *in vitro* **(Figure 6)** and expressing the typical pattern of MSC surface markers [84, 121, 122]. Endometrial side population (SP cells) also demonstrate MSC properties [123, 124]. Serial clonal culture shows that clonogenic eMSC undergo self-renewal *in vitro* and have high proliferative potential [84]. The population of clonogenic eMSC within human endometrium is small, approximating 1.3%, necessitating the identification of specific surface markers to allow their prospective isolation and enrichment from endometrial biopsies [125, 126].

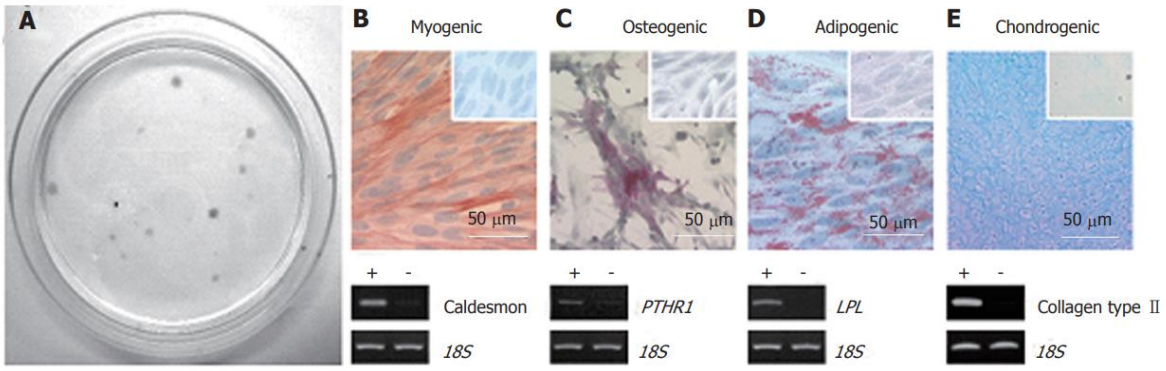

Figure 6: Endometrial mesenchymal stem cells. A) Colony Forming Units – Fibroblast (CFU-F) differentiate into 4 mesodermal lineages from a single clonogenic cell. **B-E)**; **B)** myoctes**, C)** osteocytes**, D)** adipocytes, **E)** chondrocytes. PTHR1, parathyroid hormone 1 receptor; LPL, lipoprotein lipase, key markers of osteogenic and adipogenic cells respectively. (Reproduced with permission from [84].)

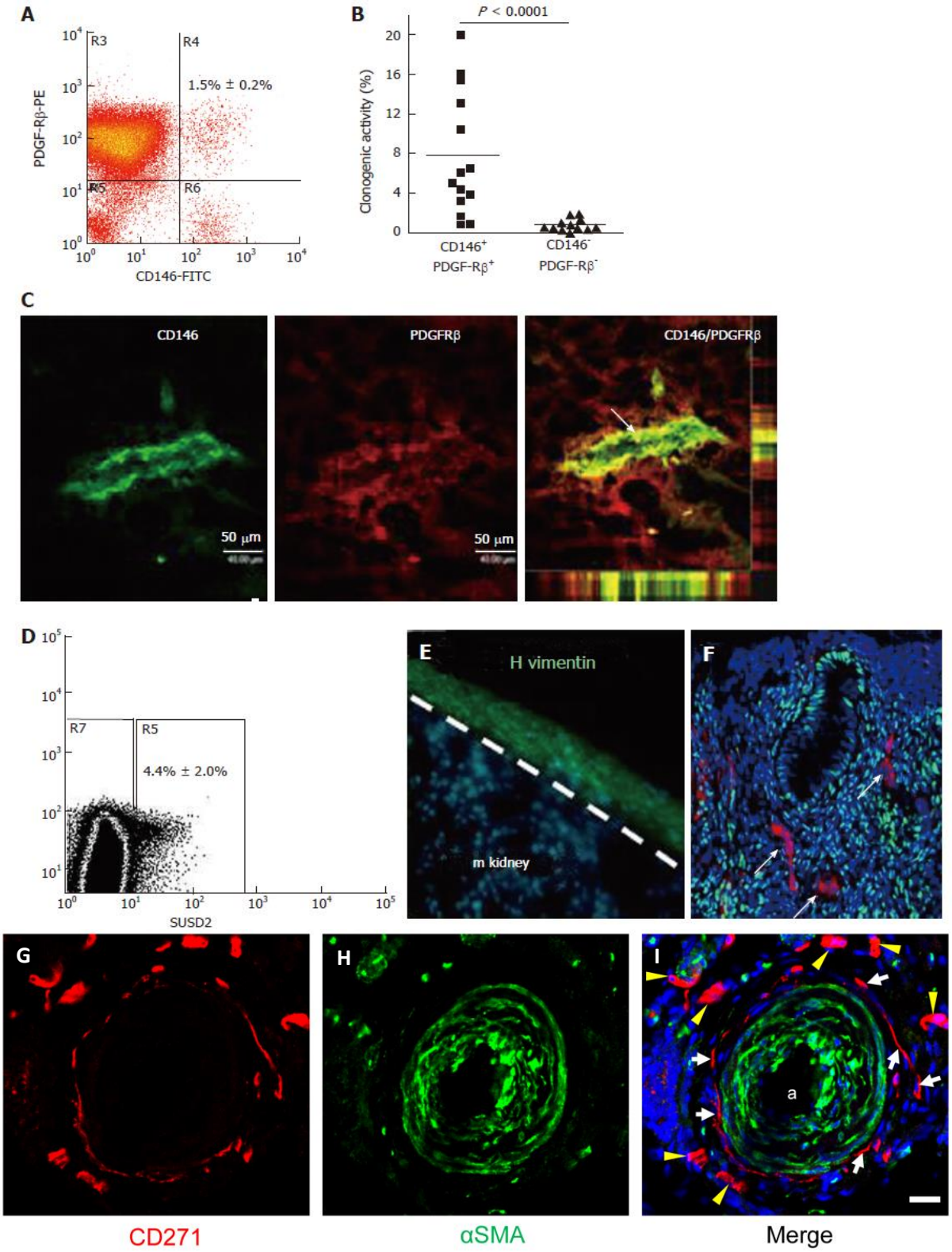

Figure 7: Specific enrichment for endometrial mesenchymal stem cells using surface markers. Flow cytometry plot of CD146+ /CD140b (PDGRRβ)+ fraction **A)** which contains most of the clonogenic endometrial stromal cells **B)** and reveals their pericyte identity *in vivo* **C)**; SUSD2+ cells in endometrial cell suspensions **D)** which **E)** reconstitute human vimentin+ stromal tissue when transplanted under the kidney capsule of NSG mice, and **F)** have a perivascular location in human endometrium. SUSD2+ cells (red) do not express estrogen receptor-α (green), but endometrial stromal cells do (DNA blue). **G)** Ovine CD271+ eMSC (red, yellow arrows) were close to **H)** αSMA vascular regions (green), suggesting an **I)** adventitia location within the endometrium. The white arrow indicates perivascular SUSD2+ cells. (Reproduced from [123, 126-129] with permission).

1.4.2. Prospective Isolation of eMSC from Biopsies and Hysterectomy

To exploit the regenerative ability of human eMSC, they must first be isolated from the heterogeneous population of cells obtained from dissociated endometrial tissue. Ideally this requires the identification of unique surface markers on eMSC to reveal their *in vivo* niche and separate them from undesired stromal fibroblasts and other cells. Indeed, several sets of specific surface markers have been identified on eMSC [125, 127]. Almost all clonogenic human endometrial stromal cells with MSC properties are found in the $CD140b^{+}CD146^{+}$ population, comprising 1.5% of the stromal fraction [125]. These markers revealed a perivascular niche for eMSC adjacent to endothelial cells suggesting they are pericytes **(Figure 7)**. The transcriptome of the expressing $CD140b^{+}CD146^{+}$ cells indicates they are distinct from $CD140b^{-}CD146^{+}$ endothelial cells, but more similar to endometrial $CD140b^{+}CD146^{-}$ stromal fibroblasts [130]. To obtain these co-expressing cells, a flow cytometry sorter must be used, which limits the utility of this marker set, given the damaging effects of automated cell sorting on cell viability [125]. To overcome this problem a single perivascular marker was sought for isolating eMSC. The W5C5 antibody identified a population of perivascular endometrial stromal cells with typical MSC properties that also reconstituted stromal tissue *in vivo* when transplanted beneath the kidney capsule [127]. The $W5C5^{+}$ cells comprised 4.4% of endometrial stromal cells. The epitope recognised by the W5C5 antibody is the Sushi Domain-containing 2 (SUSD2) adhesion molecule [131]. A single marker enables magnetic bead sorting, a gentler protocol than using a cell sorter as evidenced by increased clonogenicity of SUSD2+ cells compared to $CD140b^{+}CD146^{+}$ cells [127]. TNAP (tissue non-specific alkaline phosphatase) is another single marker that identifies eMSC but has less utility as the epitope is also expressed by endometrial epithelial cells [132]. Another perivascular marker (AOC3), identified by RNA sequencing $SUSD2^{+}$ and $SUSD2^{-}$ cells, may have utility for isolating eMSC [133], but the common bone marrow MSC marker Stro-1 does not enrich for endometrial stromal cells with MSC properties [126]. These markers revealed that the perivascular eMSC were found in both the functionalis and basalis layers of human endometrium, indicating that eMSC will be found in menstrual blood and can be isolated from biopsies and curettage as well as hysterectomies [96, 134]. eMSC can also be obtained from post-menopausal women following short term (8 week) estrogen replacement which regenerates their atrophic endometrial tissue [128]. Collection of menstrual blood or an endometrial biopsy are convenient sources not requiring anaesthesia, with the latter available as a simple office-based procedure. Such tissue sources are ideal for cell-based therapies. Despite their great promise, eMSC and menstrual blood MSC have yet to be significantly explored as therapeutic agents for cell therapies. There are certain

endometrial disorders where caution may be required e.g endometriosis. However, this disorder affects young infertile women who will not have the opportunity to develop POP. Indeed, it will be important to ensure no underlying uterine or other pathology (e.g. malignant tumour) in identifying suitable patients for cell harvesting to treat their POP. For example, should a woman have uterine cancer, it would not be possible to use her eMSC for cell-based therapies. Similarly, it would also be contraindicated to use another source of autologous MSC in case tumour cells have spread to organs such as bone. Additionally, research has demonstrated that the thin endometrium of post-menopausal women contains a population of W5C5+ eMSC [128]. This endometrium could be regenerated by use of exogenous estrogen [128]. In ewes, eMSCs isolated from nulliparous ewes are more proliferative than those harvested from older, multiparous ewes, suggesting a donors age affects the overall quality of cells [135]. Whether this impacts the eMSCs ability to induce wound healing effects when implanted into recipient tissues remains to be investigated, however this is an important consideration due to the majority of women receiving potential eMSC-based POP treatment being of an older demographic. These important issues should be considered in developing the potential of eMSC as cell-based therapies. Large animal models are usually required to provide data for regulatory bodies prior to translating potential cell-based therapies into the clinic. If autologous applications are being evaluated, it becomes necessary to derive MSC from species such as ovine, porcine, canine, equine and non-human primates [129, 136]. Often antibodies used as biomarkers to derive MSC from human or mouse do not cross react with these species. For example, neither CD140b, CD146 nor SUSD2 cross react with ovine endometrial tissue [129]. However, the bone marrow MSC surface marker CD271 [137] cross reacts with ovine endometrial stromal cells enriching for eMSC demonstrating clonogenicity, *in vitro* self-renewal and the ability to differentiate into adipogenic, myogenic, osteogenic and chondrogenic lineages [129]. The $CD271^+$ ovine eMSC were identified in a perivascular niche around arterioles and venules *in vivo*, but unlike human eMSC which have a pericyte location, ovine $CD271^+$ stromal cells occupied the adventitia in the periphery of these vessels **(Figure 7G-I)**. In human bone marrow and adipose tissue, vascular adventitial cells show similar MSC properties as those located in the pericyte position [138].

1.4.3. eMSC Phenotype and Gene Profile

Cell fate decisions made by somatic stem cells to self-renew or undergo differentiation depends upon the cellular microenvironment or niche from signals emanating from cells and extracellular matrix that comprise this niche [139]. In this context, understanding both the extrinsic and intrinsic gene regulation pathways operating in undifferentiated eMSC and their more differentiated progeny could shed light on their function in endometrial regeneration. Gene expression profiling comparing purified endometrial cell populations of $CD140b^{+}CD146^{+}$ eMSC, $CD140b^{+}CD146^{-}$ stromal fibroblasts (eSF) and $CD140b^{-}CD146^{+}$ endothelial cells showed that eMSC differentially expressed 762 and 1518 genes, respectively [130]. The eMSC gene expression profile was typical of adult stem cells, showing upregulation of *TGF*β, *FGF2*, *WNT*, *IGF* and Hedgehog signalling pathways in comparison with the endometrial stromal fibroblasts and endothelial cells. The expression of SUSD2 was also elevated in the double positive eMSC population. G-protein coupled receptor and cAMP-mediated signalling were also upregulated in the $CD140b^{+}CD146^{+}$ population, similar to genes involved in maintaining the undifferentiated state of bone marrow MSC. The $CD140b^{+}CD146^{+}$ population also showed upregulation of immunomodulatory and immunosuppressive genes [130]. eMSC displayed increased expression of Cyclin D1 (*CCND1*) which ensures their progression through the G1 phase of the cell cycle [130]. Gene profiling confirmed human eMSC as pericytes, while RNA sequencing of cultured endometrial $SUSD2^{+}$ and $SUSD2^{-}$ cells revealed 134 differentially expressed genes, with many of those in the $SUSD2^{+}$ population characteristic of perivascular cells [133]. The *in vivo* differentiation pathway for eMSC is to decidualised perivascular cells and decidual cells of the endometrial stroma, a process mediated by the post-ovulation sex steroid hormone, progesterone, *via* production of cAMP. The perivascular location of eMSC in the spiral arterioles renders them well situated to participate in the regeneration of the uterine lining and formation of the placenta during embryo implantation and subsequent pregnancy [133].

1.4.4. Inhibition of eMSC Spontaneous Differentiation

The current understanding of eMSC signalling reinforces their ability to self-new, differentiate into various lineages and their immunomodulator properties. Gene profiling comparisons between FACS-isolated eMSC ($CD146^{+}/CD140b^{+}$) and eSF ($CD146^{-}$/CD140b+ revealed 550 differently up-regulated genes between eMSC and eSF and 1370 genes down-regulated using principal component analysis and hierarchal clustering [140]. The eMSC transcriptome was characterised by increased expression of pericyte-markers, hypoxia-related genes, genes

involved in adult stem cells and growth factor signalling pathways, which all support a common set of genes shared by the eMSC lineage [140]. Interestingly, when cultured *in vitro*, eMSC display down-regulated expression of 211 eMSC lineage genes (81% of total), and up-regulation of eSF lineage genes (55% of total) indicating spontaneous differentiation during culture expansion [141, 142]. However, non-cultured eMSC exhibited increased expression of *NOTCH2NI* and *NOTCH2* Notch signalling pathway (associated with proliferative signals during neurogenesis), SLIT ligands (secreted proteins involved with neural development) and growth factors such as transforming growth factor beta (TGF-β), Hedgehog and insulin-like growth factor 1 (*IGF1)* stem cell signalling pathways compared to eSF suggesting their capacity for self-renewal and lineage differentiation [140]. Similarly, increased growth factor expression was also observed in menstrual blood-derived MSC/stromal fibroblasts *in vitro*, such as pro-angiogenesis vascular endothelial growth factor (*VEGF*) when cultured in hypoxic conditions [143]. The TGF-β receptor signalling pathway was recently identified as having a major role in the spontaneous differentiation of eMSC to eSF [142]. Indeed, inhibiting transforming-growth factor beta receptor (TGFβR) signalling using the selective inhibitor A83-01, a molecule that acts via SMAD2/3 phosphorylation, prevented spontaneous eMSC differentiation [142]. When administered to cultures of human SUSD2+ eMSC, SUSD2-expressing cells are retained in serum free cultures, while spontaneous differentiation is halted [142]. This suggests the TGFβR-SMAD2/3 signalling pathway is important in the maintenance of stemness of cultured the eMSC population. It also suggests that A83-01 could be a valuable inhibitor of eMSC spontaneous differentiation *in vitro* to generate an eMSC product for clinical use [142]. A83-01 has been used to generate highly purified undifferentiated SUSD2+ human eMSC after culture expansion, which makes it a valuable tool for maintaining quality cultures for MSC-based clinical purposes [144].

1.5. Immune Response to Implanted Mesh

1.5.1. Role of Macrophages in Wound Repair

Macrophages have a significant role in wound repair, both in pro-inflammatory and pro-wound healing capacities. Immediately following tissue injury, neutrophils and monocytes of the innate immune system secrete pro-inflammatory cytokines, such as interleukin-1 beta and tumor necrosis factor alpha [145-147]. These cytokines assist with recruiting pro-inflammatory neutrophils and monocytes from the blood stream, with the latter differentiating into M1 "pro-

inflammatory" macrophages **(Figure 8)** that phagocytose bacteria, cellular debris and damaged tissue while walling off the site of damage [148-150]. This, combined with a simultaneous coagulation process, assists with decreasing blood loss and shielding the vulnerable wound site from further infiltration by bacteria or foreign antigens. As the inflammatory response continues M1 macrophages switch to a M2 macrophage phenotype which mediate the wound healing process by **(Figure 8)** releasing various signals that promote angiogenesis, fibroplasia and ECM remodelling [151]. This clearly shows that M1 and M2 macrophages play an eminent role in wound repair, and that modulating their function has significant potential for tissue engineering applications.

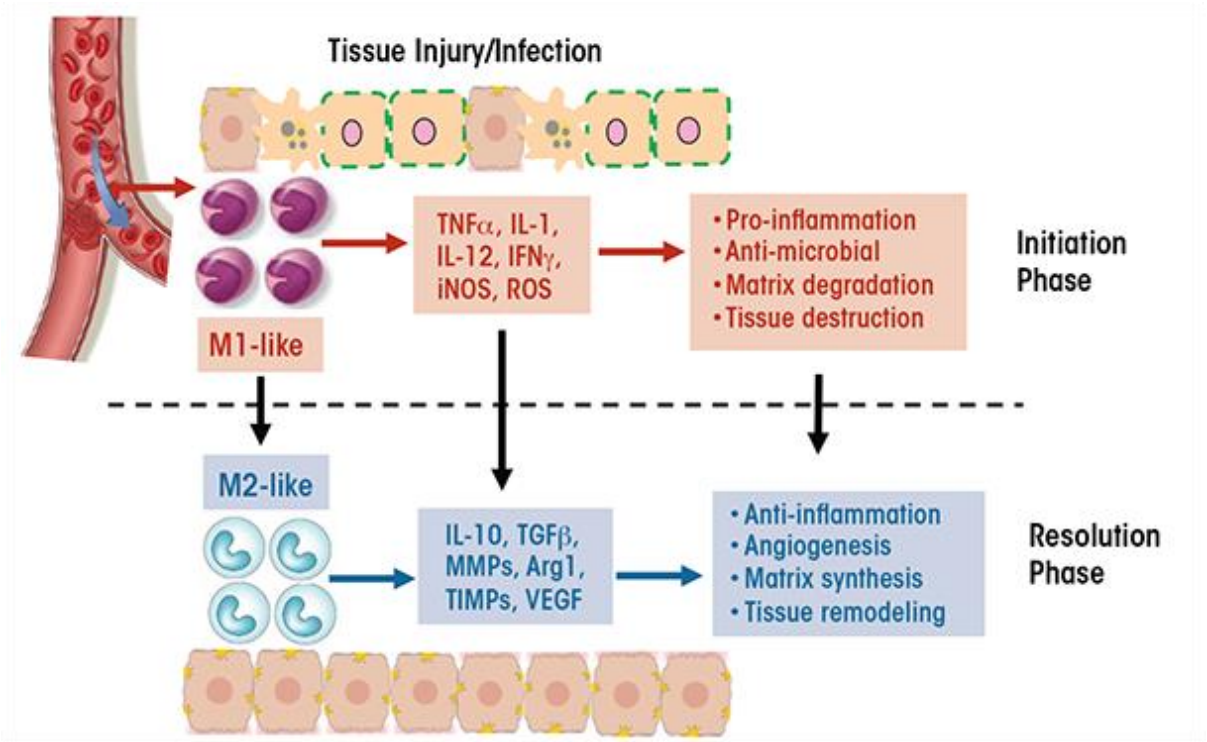

Figure 8: Macrophage plasticity during wound site repair. Neutrophils and chemo-signals attract monocytes to the wound site, which give rise to the M1 macrophage "pro-inflammatory" phenotype. M1 macrophages release pro-inflammatory cytokines and induced nitric oxide synthase (iNOS) and reactive oxygen species (ROS), as well as take up foreign bacteria, debris and dead cells to sterilise the wound site and clear dead tissue. M2 macrophages emerge in the healing phase where they produce growth factors, participate in tissue remodelling and assist with angiogenesis. (Diagram reproduced with permission from [152].)

1.5.2. M1 Pro-inflammatory Macrophages

Following the platelet response to a wound, the damaged tissue release chemokines that attract circulating white blood cells from the blood stream. The first to arrive are polymorphonuclear neutrophils which release Reactive Oxygen Species (ROS) to help clean the wound site, and

soon apoptose once this is done [145]. The second white blood cell type to arrive are monocytes, that differentiate into M1 pro-inflammatory macrophages which then proceed to further clean the wound by taking up foreign antigens and cellular debris **(Figure 8)** [153, 154]. M1 macrophages also produce various chemokines and pro-inflammatory cytokines that further stimulate the innate immune system to ensure removal of damaged tissue and debris. As the inflammatory response progresses, the pro-inflammatory M1 phenotype will transition into a pro-wound healing M2 phenotype [150, 151]. The exact stimulus for this polarisation is not yet fully known, but current literature suggests temporal-microenvironmental cues within the wound site instigate the transition. This suggests that several adverse effects observed following transvaginal mesh implantation, such as chronic inflammation, are due to the mesh material itself which is too large for effective cellular removal **(Figure 9)**.

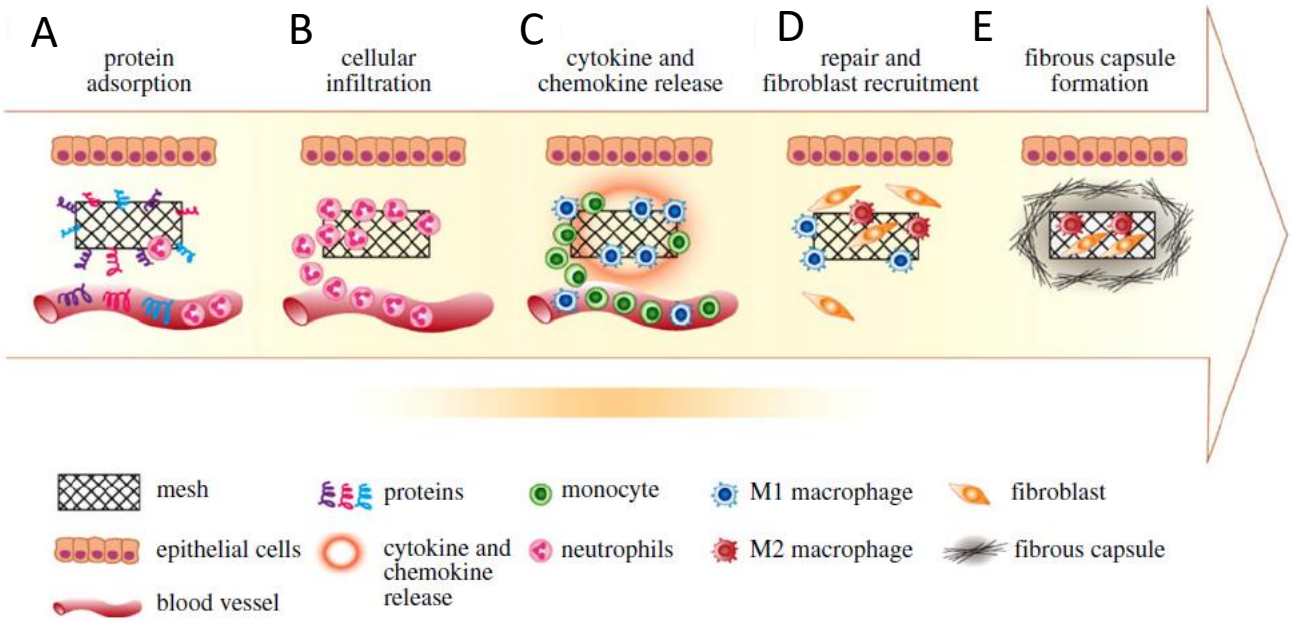

Figure 9: Diagram of the Foreign Body Response to Implanted Biomaterials. A) Protein adsorption, **B)** cellular infiltration and acute inflammation, **C)** chronic inflammation, cytokine release and further cell recruitment, **D)** fibroblast recruitment and collagen matrix deposition and **E)** formation of fibrous capsule. (Reproduced with permission from [144])

1.5.3. M2 Pro-wound Healing Macrophages

The M2 macrophage phenotype arises during the remodelling stage of wound healing and is central to ECM remodelling and angiogenesis. There is current debate whether the M2 population arises from M1 conversion to M2 phenotypes, or whether M2 macrophages are independently recruited to a wound site, with current evidence supporting the latter or even an overlap of both processes [155-157]. Current literature also suggests that the binding of

interleukin-4 and interleukin-13 to a common interleukin-4 receptor alpha chain induces the M2 phenotype, marked by increased expression of macrophage CD206, a mannose receptor [158]. As the M2 population increases at a wound site, it plays a key role in promoting the migration and proliferation of fibroblasts and endothelial cells, among others, by secreting anti-inflammatory cytokines and growth factors **(Figures 8 and 9)** [159]. M2 macrophages also synthesise and release metalloproteinases (MMPs) which remove the temporary tissue of the wound site by remodelling the ECM, further enhanced by the attracted fibroblasts and endothelial cells [160-162]. M2 macrophages also assist with neovascularisation, by aligning with blood vessels and assisting with fusing them together during angiogenesis [163]. If the M1 macrophages are the sterilising agents of the immune system then the M2 macrophages are the builders, thus their designation as pro-wound healing macrophages.

1.5.4. eMSC Modulation of the Macrophage Response

A promising property of eMSC is their modulation of the inflammatory and innate immune response at a wound site to accelerate the M1 to M2 polarisation, and thus induce swifter wound healing. The capacity to modulate the innate immune system from a pro-inflammatory to a pro-wound healing is a property shared by most MSC types [164]. eMSC, likewise, modulate the innate immune system as observed in preclinical studies involving eMSC-seeded TE constructs implanted into immunocompromised rodents [32, 34]. eMSC promoted the accumulation of macrophages that changed within a month to a M2 phenotype. By 90 days the overall leukocyte infiltration was greatly reduced in tissues that received an eMSC/PA/G implant compared to PA/G alone [34]. In immunocompetent mice, eMSC reduced the early M1 macrophage response at 3 days after mesh implantation while promoting an increase in the M2 population at both 3 and 7 days [165]. The removal of implanted human eMSC by the recipient innate immune system was greater in immunocompetent than immunocompromised mice as demonstrated by the longer persistence of eMSC in immunocompromised mice implanted with an eMSC/PA/G TE construct [32, 34]. Clearly the two-way relationship between implanted eMSC and the immune system, particularly M1 and M2 macrophages, is critical for their use in TE constructs to treat POP. Current literature suggests that preclinical trials would be best served using autologous eMSC to ensure their persistence beyond 30 days [129, 166].

1.6. Preclinical Animal Trial Models for Assessment of POP Mesh

As outlined earlier **(Section 1.1.2)** there are substantial problems with current mesh augmentation of POP surgery. The use of autografts increases morbidity at the donor tissue site, biological materials often fail due to their rapid and unpredictable degradation [167], and synthetic PP mesh is biomechanically too stiff and often erodes into adjacent organs [168]. A better solution may be to combine the advantages of both the synthetic and biological approaches. This could utilise a polyamide synthetic mesh coated with gelatin (PA/G) as a scaffold to support the prolapsed tissue and provide a vehicle upon which to deliver eMSC to sites of vaginal damage [33, 34]. As eMSC have exhibited immunomodulatory effects and are easily obtainable during an office-based biopsy, they could be an ideal candidate for implantation. The eMSC could serve by modulating the inflammatory and immune responses, assisting the regeneration of lost or damaged tissue or promoting endogenous stem/progenitor cell populations to initiate repair which mesh alone cannot do [168, 169].

1.6.1. Small Animal Rodent Models

Our team has developed a non-degradable, polyamide (PA) mesh with biomechanical properties more closely matching vaginal tissue when coated with gelatin [33] to provide a substrate for seeding with SUSD2+ eMSC **(Figure 10A)**. This tissue engineering construct was then implanted into a subcutaneous defect on the dorsum of immunocompromised rats and assessed at several time points over 90 days [34]. In the explanted eMSC/PA/G tissue complexes, greater neovascularisation was observed early on at 7 days compared with PA/G controls. Initially there was a greater influx of M1 inflammatory macrophages around the eMSC-seeded mesh. At 30 days these macrophages had changed to a M2 wound healing phenotype and by 90 days there were fewer CD68+ macrophages around the eMSC/PA/G filaments in comparison to PA/G alone, indicating a milder chronic inflammatory response in the long term. Importantly, in these studies the cellular response at the mesh tissue interface was assessed quantitatively in 50mm increments around individual filaments using image analysis rather than subjective scoring [33, 34]. Similar quantities of new rat collagen were generated around the P/AG mesh filaments, irrespective of the inclusion or not of eMSC, which was derived from recipient rat fibroblasts rather than derivatives of the implanted human eMSC. However, this new collagen around the eMSC/PA/G mesh filaments showed physiological crimping by scanning electron microscopy, while more scar-like collagen was deposited around the PA/G mesh without eMSC **(Figure 10B-C)** [170]. This deposition of

physiological collagen likely contributed to the improved biomechanical properties of the mesh/tissue complexes harvested at 90 days, where a longer toe region and lower stiffness was observed in the stress strain curves of the eMSC/PA/G mesh compared with PA/G alone **(Figure 10D)** [34]. The improved tissue organisation around the mesh filaments shown by histological staining suggests that eMSC promoted tissue regeneration and improved the biocompatibility of the synthetic PA/G mesh [34, 170]. In this xenogeneic model, the eMSC survived a maximum of 14 days, indicating that they exerted a paracrine effect in promoting vascularisation and reducing fibrosis similar to MSC effects on many other tissues [80]. However, the percentage of SUSD2+ cells in the single sample of passage 6 cells used for the entire study was only 10%. It will be of interest to determine whether more than a paracrine effect will be observed if > 90% of the cells are SUSD2+, which is now a possibility by culturing them in A83-01-containing medium [142]. A83-01 is a selective inhibitor of TGF-B that blocks phosphorylation of Smad2/3 and has been observed to block apoptosis and senescence in eMSC and retain stemness **(Section 1.4.4)**[142].

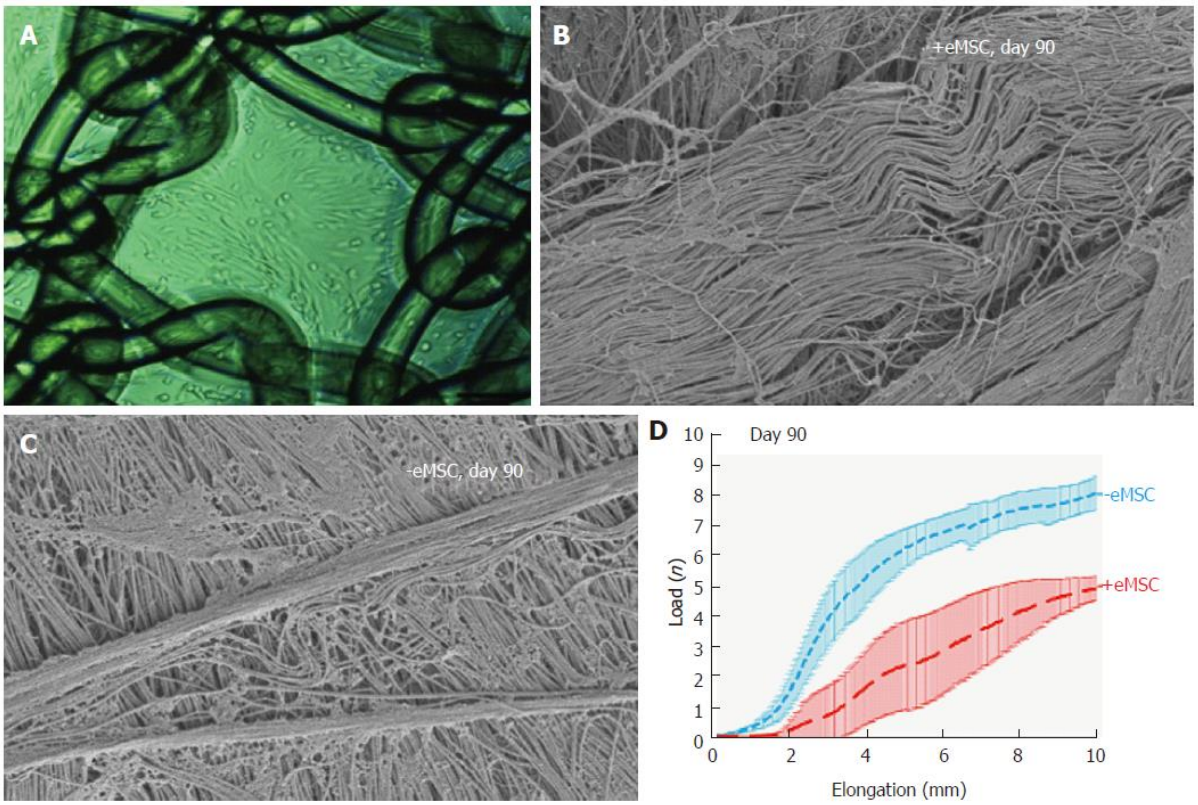

Figure 10: Human eMSC improves biocompatibility of PA/G constructs in a fascial wound defect in nude rats: **A)** PA/G mesh seeded with 100,000 eMSC**. B)** Physiological crimped collagen deposited around eMSC/PA/G constructs, **C)** scar-like collagen in PA/G mesh alone as observed by scanning electron microscopy (SEM) and **D)** load-elongation curves of explanted meshes with (red) and without (blue) eMSC showing less stiffness (slope) and longer toe region for mesh seeded with eMSC, indicating improved biomechanical properties (Reproduced with permission from [34, 170])

Despite the significant biological differences between human females and rodents, mouse models have proven invaluable for the investigation of the underlying biochemical mechanisms involved in the development of POP. The use of genetically modified mice has allowed exploration of the genetic underpinnings of POP, such as lysyl oxidase like-1 (LOXL1), an enzyme involved in elastin biosynthesis within vaginal tissue, and fibulins 3 and 5 (FBLN3, FBN5 respectively) which regulate expression of collagen and elastin. Depletion of either LOXL1 or FBLN5 has been associated with POP [171-174]. The LOXL1 deficient mouse creates a POP-like condition where the mice develop an obvious bulge in the perineal region. It would be of interest to determine if an injectable MSC-based cell therapy alleviates the prolapse symptoms of LOXL1 deficient mice. While extremely useful for investigating genetic contribution and mechanism of action, transgenic mice are limited in their utility as models for exploring TE based treatments for POP due to the small size of their vagina.

1.6.2. Primate Models in Preclinical Trials

Various primate animal models have been proposed and used for the study of both POP and potential treatments, each with their advantages and disadvantages [175, 176]. Nonhuman primates are considered to be the best model for POP, particularly the Rhesus macaque, due to a highly equivalent pelvic anatomy with women. Similarly, macaques deliver high head-to-body ratio babies. These equivalencies have prompted research into the effect of parity on vaginal tissue using Rhesus macaques, with studies observing diminished mechanical strength and disruption of collagen alignment in parous vaginal walls [50], undoubtedly contributed to spontaneous POP observed in multiparous Rhesus macaques, similar to women. Although Rhesus macaques are an equivalent and promising model for POP investigation, widespread use of these animals is hampered by considerable costs in acquisition, housing and maintenance. Additionally, animal ethic committees typically place particularly stringent conditions for researchers seeking to use primates, due to their humanlike characteristics [177].

1.6.3. Large Animal Models in Preclinical Trials

Larger animal models are growing in popularity for POP research due various advantages. Cows have been suggested as an animal model for the study of POP, due to observed spontaneous POP in the later stages of their pregnancies. The underlying vulnerabilities to POP are similar to women, with increased intra-abdominal pressure contributing to the prevalence of POP in cattle raised for beef. The effect of diet on the preponderance has also been observed

in swine, with POP induced in gilts as young as 4 months old via a specific diet of mouldy corn (through an unknown mechanism) [178]. However, neither of these animals are in widespread use as an experimental model, due to the enormous cost of acquisition and housing for cows and the relatively little knowledge of the pig genital tract and pelvis. Additionally, sows deliver litters compared to typically single child delivery among women, which distances their equivalence.

1.6.3.1. Sheep as an Animal Model of POP and POP Surgery

Of the large animal models available for assessing cell-based therapies for POP, the domestic sheep is the most promising candidate due to their ready availability and physiological similarity to the human female pelvis in size and structure [166, 168]. Ewes also have a similar oestrus cycle of 17 days, a long labour and deliver a foetus with a large head to body ratio that is closer to humans than rodents [176, 179]. Like humans, ewes undergo spontaneous POP with similar frequency and predisposing factors, such as parity, age and breeds with a large rump [29, 176]. Although the ovine species are quadrupeds with a horizontal rather than vertical pelvic floor subject to differing forces, the overall arrangement of the pelvic organs and the similar vaginal dimensions to women make them a useful model for assessing new mesh and tissue engineering constructs [96, 166, 168]. Additionally, the ovine vagina has a similar histological structure, biochemical and biomechanical properties to that of women [180] with the most common form of prolapse in sheep involving the bladder (cystocele) [181], similar for women. Finally, our group has taken the Pelvic Organ Prolapse-Quantification (POP-Q) method of measuring vaginal wall distensibility and adapted it for use in sheep to select for older, multiparous ewes that are equivalent to multiparous women with vaginal wall weakness [182, 183]. Sheep have already been vaginally implanted with various POP mesh materials for evaluation of their efficacy and adverse effects for their use in female pelvic reconstructive surgery [167, 169, 179, 184, 185], and are being proposed for training surgeons in vaginal surgery specifically for treating POP in women [186].

1.6.3.2. ECM and Smooth Muscle Composition of the Vaginal Wall

The biochemical and biomechanical properties of ovine vaginal tissue have already been examined by quantitative histological imaging, biochemical collagen/GAG/elastin assays and biomechanical analyses, providing a platform for the evaluation of next generation eMSC-seeded mesh in the ovine vaginal repair model [54, 180, 187]. Changes to the composition of these layers **(Section 1.2)** and their relative contribution to POP susceptibility is still being

explored [11, 54]. Neither is it known how such changes are reflected in POP-Q measurements[183] or vaginal wall weakness [182]. However, a relationship between ECM proteins and POP has been identified in women, with a high content of immature collagen III associated with POP [188]. While collagens type I and III increase with prolapse, others have suggested that the ratio of collagen type III to type I decreases [189]. Irrespective, it appears that the collagen remodels with the onset of prolapse in women, due to increased expression of matrix metalloproteinases (MMP)-2 and -12 [190]. This is further exacerbated during the progression of prolapse by an increase in other matrix metalloproteinases, active MMP-9 and a decrease in fibulin 5, essential for elastogenesis [191]. There is also a decrease in the transcriptional regulator, Homeobox protein Hox-A13 (HOXA13), which controls the expression of ECM associated genes involved in elastic fibre homeostasis [192] in vaginal tissue [190]. Elastic fibres play an important role in the mechanical properties of the vaginal wall, allowing the tissue to extend and return to its original shape without damage [193-195] particularly during pregnancy [174] and delivery. Disruption of elastic fibre synthesis by the absence of LOXL1 or knock out of Fibulin 5 [191] contributes to spontaneous POP in mice **(Section 1.6.1)** [73, 196]. Likewise, the reduction of non-vascular smooth muscle in the vaginal wall has been associated with POP. Anterior vaginal tissue acquired from women undergoing hysterectomies exhibits a decreased fraction of non-vascular smooth muscle compared with women who had not undergone POP [197], as well as a greatly increased apoptotic index [198].

1.6.3.3. Biomechanical Properties of the Vaginal Wall

Understanding the biomechanical properties of the vaginal wall is valuable for treating POP. The uniaxial and multiaxial biomechanical properties of synthetic mesh have often been measured as a means to gauge stiffness and strength [31]. Uniaxial testing on vaginal tissue from ovariectomised ewes generated a Youngs Modulus of different regions within the vaginal canal **(Figure 11)**. This observed stronger (higher maximum stress) vaginal tissue in the proximal region (close to the cervix) of the canal, and weaker vaginal tissue in the distal region [180]. This region is also the most commonly affected by POP [199]. The stiffness and flexibility of vaginal tissue is seen as a means of determining POP susceptibility. The POP-Q system has been developed to gauge vaginal wall weakness by measuring the distensibility of the vaginal tissue at specific points [200]. The vaginal tissues of prolapsed, pregnant, Fibulin-5 knockout mice exhibited decreased stress resistance and higher distensibility [196, 201]. These biomechanical properties are similar in the prolapsed vaginal tissue of women, which is

significantly more flexible and less pressure-resistant than non-prolapsed tissue [202, 203]. It is possible that these characteristics are the result of prolapse[203], and it is currently unknown if POP-Q correlates with the biomechanical properties of the vaginal wall. Collagen deposition could be an important contributor to the biomechanical properties of the vaginal wall implanted with a mesh, if not through quantity of collagen deposited, then perhaps through its organisation, with more organised collagen fibrils perhaps contributing to biomechanically equivalence in PA mesh [170, 180].

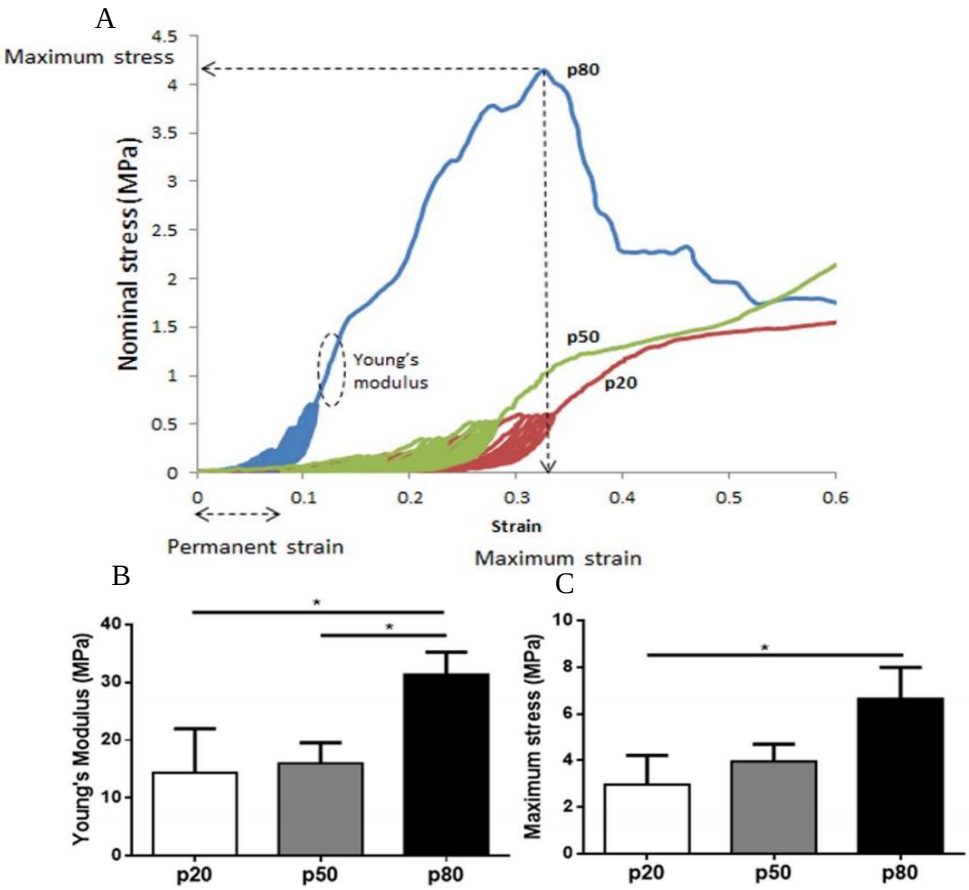

Figure 11: Biomechanical evaluation of ovine vaginal tract: A) A stress-strain curve of ovariectomised ovine vaginal tissue with Young's Modulus (dotted circle) indicating maximum stress (MPa) and strain with **B)** Youngs Modulus (MPa) and **C)** maximum stress (MPa). p20 (20% of total vaginal length), p50 (50% of total vaginal length) and p80 (80% of total vaginal length). (Reproduced with permission from [180])

1.6.3.4. Sheep-adjusted POP-Q Measurement for Detecting Vaginal Weakness

The contributors to POP vulnerability are currently being explored in large animal models [180, 183]. The Pelvic Organ Prolapse Quantification (POP-Q) is a points-based measurement system that has been developing to measure the distensibility of vaginal wall tissue in women. The basis for this system is measuring (in cm) the distensibility of the vaginal wall tissue at

specific points along the vaginal canal **(Figure 12)**. These measurements range from -3cm (the least distensible, indicating no vaginal wall weakness) to +3cm (the most distensible, signifying weakened vaginal wall), with POP defined as descent into the introitus or beyond (scores of 0≥) [183]. There are 6 measurements made in women, however only 5 were possible when adapting this system for measuring vaginal wall weakness in ewes **(Figure 12)**.

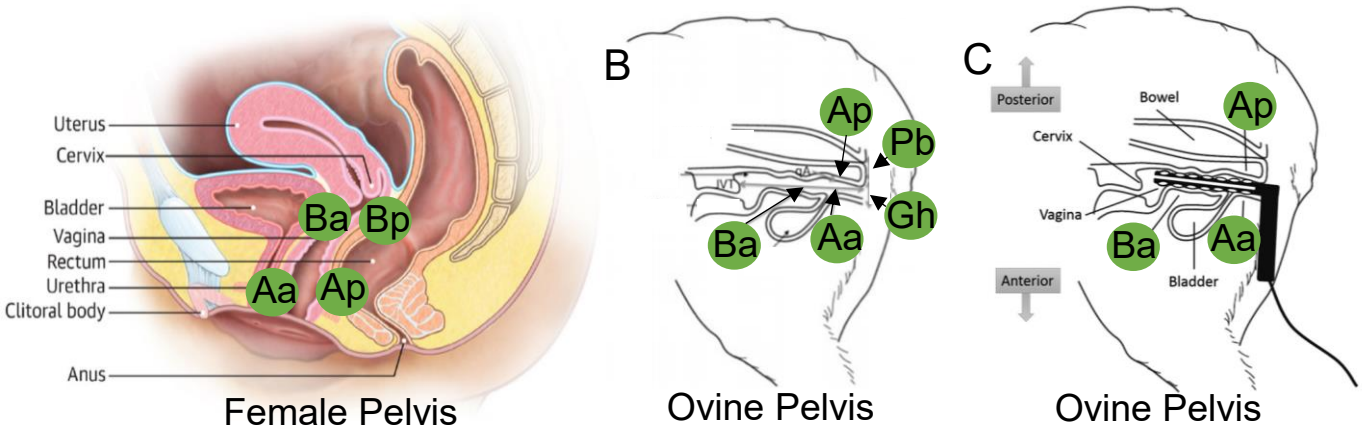

Figure 12: Pelvic organ prolapse quantification points of measurement and positioning of the fibre-optic speculum. A) The 4 main positions of distensibility measurement are Posterior Point A (Ap), Posterior Point B (Bp), Anterior Point A (Aa) and Anterior Point B (Ba) along the vaginal wall **B)** while ovine POP-Q measures these four points plus Perineal Body (Pb) and Genital Hiatus (Gh). **C**) When using the fiber-optic speculum (coloured in black), the upper speculum blade is positioned along the posterior wall incorporating Ap, with the lower blade positioned along the anterior wall to incorporate Ba and Aa regions. (Diagrams reproduced and adapted with permission from [5, 183, 204])

These points are Anterior Point A (Aa), Posterior Point A (Ap), Anterior Point B (Ba), Genital Hiatus (Gh) and Perineal Body (Pb). Increasing parity showed increasing vaginal wall weakness and distensibility, as measured by this modified POP-Q [183]. Nulliparous ewes exhibited an average of -3 for Aa, Ap and Ba, while multiparous ewes had a median of -1 and an interquartile range of -2 to 0, with a strong association with parity [183]. The effect of parity was further observed when nulliparous and parous vaginal tissue was assessed by biomechanical testing and nulliparous tissue exhibited greater resistance to deformity due to mechanical forces (permanent strain) [183, 205]. However, a clear association between histological composition of the vaginal wall and POP-Q measurements has yet to be demonstrated.

1.6.4. Pressure Sensor Measurement of Vaginal Wall Weakness

An additional quantification of vaginal wall weakness to the POP-Q is a novel pressure sensor device that measures distributed pressures along the anterior and posterior vaginal walls via sensors embedded in two blades of a standard human speculum [204]. This modified vaginal

speculum incorporating a series of pressure sensors placed 10mm apart, which is inserted into the vagina and records the pressure exerted by the vaginal wall along its length upon dilation of the speculum **(Figure 12)** [204]. The vaginal pressure sensor has shown great promise, despite being a new and developing technology. In initial trials using ovine models, it was able to detect pressure variations between anterior and posterior walls, as well as between pressure points along each wall [204]. Additionally, the use of a pressure sensor device, as opposed to manual measurement of vaginal tissue distensibility (POP-Q), allows for objective measurement of weakness along the vaginal wall. Though still under development, the pressure sensor device shows potential as a system to quickly acquire accurate data across both vaginal walls that could be used in conjunction with conventional POP-Q.

1.7. Rationale for Study

POP is a common, debilitating and costly condition with serious consequences for human health, happiness, quality of life and economic well-being. Abdominal operations to treat this condition are incredibly invasive, while transvaginal mesh has undergone severe restrictions due to numerous adverse effects, such as mesh erosion and chronic inflammation and is banned in many countries. The development of a next generation, cell-based tissue engineering solution is paramount for the treatment of a condition that afflicts one quarter of the female population. The incidence will only increase as women live longer and changes in family establishment practices such as delayed first childbirth increase the incidence of POP.

I will use an ovine model to explore the effects of parity on the vaginal wall using histological analysis of collagen organisation, elastin and smooth muscle content and biomechanical properties as well as clinical measures POP-Q and pressure sensor measured vaginal weakness. This will establish a detailed physiological understanding of the ovine vaginal wall that we can use as baseline for our pre-clinical evaluation of gelatin-coated PA scaffolds using an autologous multiparous ewe model with characterised weakened vaginal tissue and matched between experimental groups. In this model I will harvest ovine eMSC from individual ewe's endometrium for generating the TE constructs using autologous cells.

A detailed characterisation of the ovine vaginal wall will enable us to determine if autologous ovine eMSC, when combined with gelatin-coated PA mesh and implanted into the vaginal wall, will influence wound healing. We will measure this capacity by assessing the foreign body

response to the mesh and promotion of tissue integration via modulating the innate immune response, angiogenesis, collagen deposition and rehabilitation of damaged tissue. We intend that this could potentially lead to development of an autologous mesenchymal stem cell-based therapy for women suffering POP. This data will also assist with comparing two designs for mesh delivery of eMSC into the vaginal wall: an *in vitro* prepared eMSC/PA/G composite featuring glutaraldehyde-based gelatin coating and a two-step protocol featuring eMSC mixed with a ruthenium-based gelatin mixture before being applied to implanted PA mesh *in situ*.

We are developing a tissue engineering approach for treating women with POP. Our goal is to evaluate our new polyamide/gelatin TE constructs matched to the biomechanical properties of human vaginal tissue and seeded with autologous ovine eMSC using an ovine preclinical vaginal surgery model [168, 169] **(Figure 13)**. As ewes develop spontaneous POP [176, 206], we will identify the level of vaginal wall weakness for individual ewe to select multiparous ewes with "POP" for generating matched experimental groups based on POP-Q measurements. This will provide a model most closely matching women with POP in which we will evaluate two mesh designs for delivery of autologous therapeutic eMSC, to more accurately determine the effect of our TE constructs **(Figure 12)**.

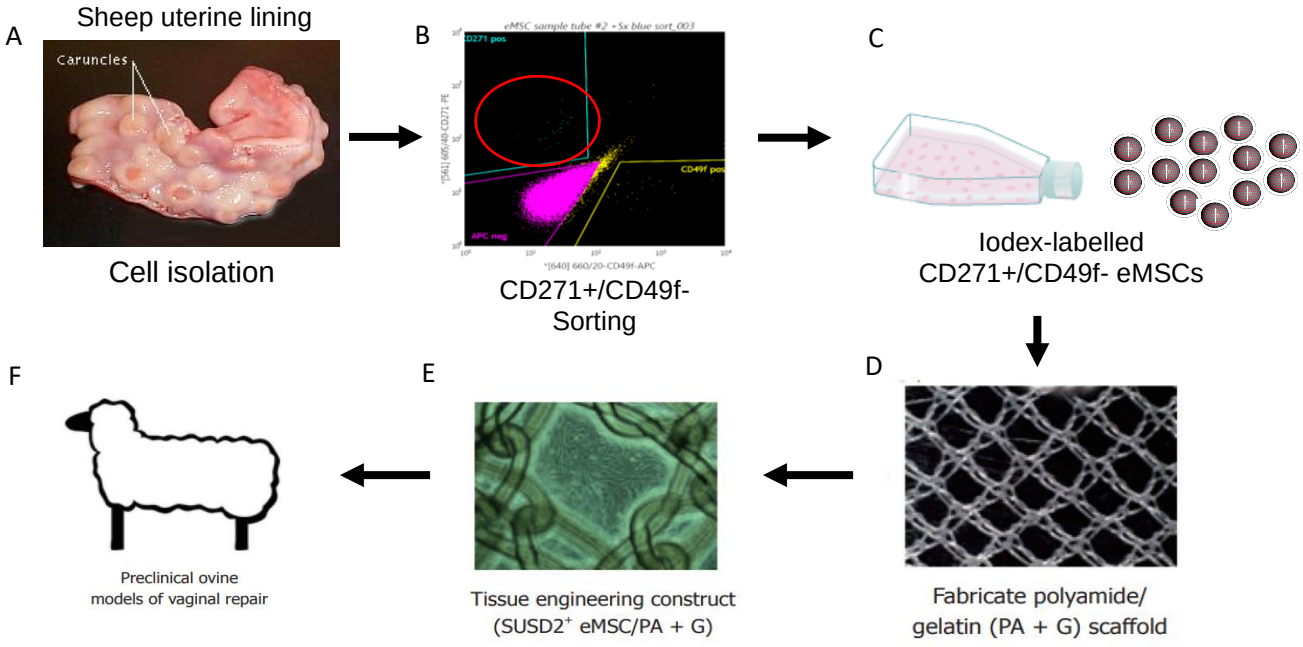

Figure 13: Isolation and application of eMSC and new PA/G mesh evaluation in pelvic organ prolapse vaginal repair. A) ovine uteri are acquired by hysterectomy and single cell isolation performed on the endometrial tissue, then **B)** eMSC are selected using $CD271^{+}/CD49f^{-}$ FACS, followed by **C)** culture expansion and 24-hour labelling with IODEX before **D)** seeding onto in house fabricated PA/G scaffolds which will create an **E)** eMSC/PA/G tissue engineering construct for implantation into **F)** an ovine large animal preclinical model selected for vaginal weakness by POP-Q to assess their efficacy in vaginal repair of parous ewes with evidence of POP (Adapted from [31, 34] with permission).

1.8. Aims and Hypothesis

This thesis aimed to evaluate a potential cell-based tissue engineering solution to pelvic organ prolapse using ovine autologous endometrial mesenchymal stem cells and comparing delivery on a glutaraldehyde cross-linked gelatin-coated polyamide mesh (PA/G) and a ruthenium cross-linked gelatin onto implanted PA mesh in an ovine preclinical vaginal surgery model.

Aim I

Define the relationship between POP-Q, pressure sensor, vaginal tissue histology, biochemical composition and biomechanical properties in nulliparous and parous ewes.

Hypothesis I

The vaginal wall of multiparous ewes will exhibit alteration of ECM components (mature and immature collagen and elastic fibres), smooth muscle content and display lower tensile strength than nulliparous ewes which will correlate with POP-Q and pressure sensor measurements.

Aim II

To establish the ovine vaginal surgery model for assessing autologous SPION-labelled ovine eMSC delivered on a PA/G synthetic mesh.

- To optimise SPION cellular labelling of eMSC.
- To confirm the presence of SPION-labelled eMSC in ovine vaginal tissue following transvaginal implantation on PA/G scaffolds.

Hypothesis II

FITC-labelled SPIONs are a non-toxic cell labelling tool that can be used to track eMSC *in vivo* after implantation into multiparous ewes selected by POP-Q for vaginal wall weakness.

Aim III

- To compare biocompatibility and cell delivery of two designs of transvaginal mesh seeded with or without autologous ovine eMSC: one featuring glutaraldehyde-based crosslinked gelatin-coated PA mesh (PA/G), and the second a PA mesh first implanted and then receiving a ruthenium-based gelatin/autologous eMSC mixture that is photosealed *in situ* (PA).
- To determine the retention of implanted autologous eMSC and to assess their effect on the extracellular matrix and inflammatory response to the implanted gelatin-coated and non-coated PA mesh.

Hypothesis III

In an autologous ovine model of POP using multiparous ewes with objectively measured vaginal wall weakness:

- Transvaginal insertion of PA mesh with ruthenium-based *in situ* crosslinked gelatin with or without autologous ovine eMSC will show less erosion and superior biocompatibility compared to PA coated with stiffer glutaraldehyde-based gelatin coated PA (PA/G) constructs with or without eMSC after implantation.
- Autologous ovine eMSC will survive for an extended period of time (≥30 days) *in vivo*.
- Autologous eMSC will modulate the innate immune response to PA/G and PA mesh improving tissue integration, reducing mesh tissue complex stiffness and improving biocompatibility.

Chapter 2

Ovine multiparity is associated with diminished vaginal muscularis, increased elastic fibres and vaginal wall weakness: implication for pelvic organ prolapse

Introductory Statement

Pelvic Organ Prolapse (POP) is a common condition worldwide, affecting close to 25% of the female population [207, 208]. This condition usually occurs in post-menopausal women who have undergone at least one vaginal child delivery [47]. Established literature suggests that it is the first vaginal delivery that inflicts the lasting damage on the vaginal wall, but the mechanisms of how this contributes to POP is not yet fully understood.

I hypothesised that parity weakens the vaginal wall by remodelling the composition of the layers that constitute the wall itself and does so in ways that reduce its ability to resist the forces applied by POP. To investigate this hypothesis, we used ovine-adapted Pelvic Organ Prolapse Quantification (POP-Q) and a novel new pressure sensor device to assess the distensibility of the vaginal tissue of nulliparous, primiparous and multiparous ewes. We then correlated these measurements with quantified data gathered from histological, biochemical and biomechanically analysis of the vaginal walls of these same ewes.

This project was a collaborative effort between the Gargett Laboratory of The Ritchie Centre (Clayton, Australia), the Commonwealth Scientific Industrial Research Organisation (CSIRO, Clayton, Australia), researchers at Flinders University (Adelaide, South Australia) and gynaecologists at Monash Health (Clayton, Australia). Animal surgery, POP-Q measurements and post-mortems were conducted by Dr Natharnia Young and Dr Anna Rosamilia with the assistance of Dr Anne Gibbon. The novel pressure sensor device was designed by Dr Luke Parkinson and Dr Jon Arkwright, and it was operated by Aditya Vashi and Prof. Jerome Werkmesiter to acquire measurements from our animal models. I gathered tissue samples and performed all histological experiments and analysis (using ImageJ macros supplied by Dr Camden Lo and Dr Kirstin Elgass). Dr Sharon Edwards performed biomechanical analysis on the vaginal tissue explants and Aditya Vashi performed the biochemical analysis. I also want to acknowledge Jacinta White of CSIRO for helping with Sirius-Red staining, which I used to determine total collagen content. Finally, I want to acknowledge Dr Miranda Davies-Tuck who assisted with statistical analysis.

www.nature.com/scientificreports

SCIENTIFIC REPORTS

OPEN

Ovine multiparity is associated with diminished vaginal muscularis, increased elastic fibres and vaginal wall weakness: implication for pelvic organ prolapse

Received: 23 August 2016
Accepted: 03 March 2017
Published: 04 April 2017

Stuart Emmerson[1,2], Natharnia Young[3], Anna Rosamilia[2,3], Luke Parkinson[4], Sharon L. Edwards[5], Aditya V. Vashi[5], Miranda Davies-Tuck[1,2], Jacinta White[5], Kirstin Elgass[6], Camden Lo[6], John Arkwright[4], Jerome A. Werkmeister[2,5,*] & Caroline E. Gargett[1,2,*]

Pelvic Organ Prolapse (POP) is a major clinical burden affecting 25% of women, with vaginal delivery a major contributing factor. We hypothesised that increasing parity weakens the vagina by altering the extracellular matrix proteins and smooth muscle thereby leading to POP vulnerability. We used a modified POP-quantification (POP-Q) system and a novel pressure sensor to measure vaginal wall weakness in nulliparous, primiparous and multiparous ewes. These measurements were correlated with histological, biochemical and biomechanical properties of the ovine vagina. Primiparous and multiparous ewes had greater displacement of vaginal tissue compared to nulliparous at points Aa, Ap and Ba and lower pressure sensor measurements at points equivalent to Ap and Ba. Vaginal wall muscularis of multiparous ewes was thinner than nulliparous and had greater elastic fibre content. Collagen content was lower in primiparous than nulliparous ewes, but collagen organisation did not differ. Biomechanically, multiparous vaginal tissue was weaker and less stiff than nulliparous. Parity had a significant impact on the structure and function of the ovine vaginal wall, as the multiparous vaginal wall was weaker and had a thinner muscularis than nulliparous ewes. This correlated with "POP-Q" and pressure sensor measurements showing greater tissue laxity in multiparous compared to nulliparous ewes.

POP is the herniation of pelvic organs into the vaginal cavity. Symptoms are bladder, bowel and sexual dysfunction, including incontinence which severely affects the quality of life of affected women[1–3]. POP affects 25% of all women in the USA and Western countries, and is particularly prevalent in post-menopausal women[4,5]. The main risk factors are vaginal delivery and ageing, in addition to obesity contributing to POP recurrence[6,7]. A genetic predisposition for developing POP appears to involve genes regulating collagen and elastic fibre synthesis[8–10]. Despite the prevalence of POP, little is understood about the underlying mechanisms affecting the integrity of the vaginal wall that leads to POP. For example, little is known about the effect of parity on vaginal wall structure and function and how these change in women who develop POP. Animal models reflecting human POP are important in developing new treatments for POP.

We are developing a tissue engineering approach for treating POP with the goal of using an ovine preclinical vaginal surgery model to evaluate a new polyamide/gelatin composite scaffold seeded with endometrial mesenchymal stem cells[11,12]. Similar to women, ewes develop spontaneous POP[13,14], but the pathophysiological mechanisms that underpin POP are not well understood. We have therefore developed a novel pressure sensor device

[1]The Ritchie Centre, Hudson Institute of Medical Research, Clayton, Victoria, 3168, Australia. [2]Monash University, Department of Obstetrics and Gynaecology, Clayton, Victoria, 3168, Australia. [3]Monash Health, Clayton, Victoria, 3168, Australia. [4]School of Computer Science, Engineering and Mathematics, Flinders University, Bedford Park, South Australia 5042, Australia. [5]CSIRO Manufacturing, Clayton, Victoria, 3168, Australia. [6]MicroImaging, Hudson Institute of Medical Research, Clayton, Victoria, 3168, Australia. *These authors contributed equally to this work. Correspondence and requests for materials should be addressed to C.E.G. (email: caroline.gargett@hudson.org.au)

to detect changes in vaginal wall pressures along the length of the anterior and posterior walls to better diagnose weakened regions that might be associated with POP[15]. In addition, we have adapted the pelvic organ prolapse quantification (POP-Q) system, a clinical score of POP for assessing the ewe vagina[16]. The POP-Q measures vaginal tissue displacement at four points within the vaginal wall which are associated with POP; points A and B on the anterior wall (Aa, Ba), which are associated with anterior vaginal wall POP (cystocele), and points A and B posterior (Ap, Bp)[17] which is the region vulnerable to posterior vaginal wall POP (rectocele and enterocele, respectively). In ewes, this system measures how far the tissue can be extended from its resting position for 3 of the POP-Q points using traction rather than during Valsalva manoeuver as is performed in women. Higher measurements indicate greater vaginal weakness and greater potential for developing POP.

The histological structure of human and ovine vaginal tissue is similar, comprising an epithelium, collagen-rich lamina propria and a muscularis containing smooth muscle[18]. Changes to the composition of these layers and their relative contribution to POP susceptibility is not well understood[19]. Neither is it known how such changes are reflected in POP-Q measurements or vaginal wall weakness. A relationship between extracellular matrix proteins (ECM) and POP has been identified, with a high content of immature collagen III associated with POP[20]. While collagen type I and III have been shown to increase with prolapse, others have suggested that the ratio of collagen type III to type I decreases[21]. Irrespective, it appears that the collagen remodels with the onset of prolapse, due to increased expression of matrix metalloproteinases (MMP)-2 and -12[22]. This is further exacerbated during the progression of prolapse by an increase in other matrix metalloproteinases, active MMP-9 and a decrease in fibulin 5, essential for elastogenesis[23]. There is also a decrease in the transcriptional regulator, Homeobox protein Hox-A13 (*HOXA13*), which controls the expression of ECM associated genes involved in elastic fibre homeostasis[24] in vaginal tissue[22]. Elastic fibres play an important role in the mechanical properties of the vaginal wall, allowing the tissue to extend and return to its original shape without damage[25] particularly during pregnancy[26]. Disruption of elastic fibre synthesis by the absence of lysyl oxidase like 1 (LOXL1) or knock out of Fibulin 5[23], an essential elastic fibre binding protein required for synthesis, contributes to spontaneous POP in mice[23,27].

Smooth muscle provides mechanical strength to tissue and viscoelasticity to the vagina, allowing for expansion during intercourse and vaginal delivery. There is a reduction in cross-sectional area of nonvascular vaginal smooth muscle in both the posterior and anterior wall in women with POP[28–30]. However the mechanism involved is not well understood[31]. A reduction in smooth muscle content of the vaginal muscularis may impact its biomechanical properties.

The purpose of this study was (1) to analyse "POP-Q" and pressure sensor measurement differences in ovine vagina and (2) to correlate these data with the collagen, elastic fibre and smooth muscle content and biomechanical properties of ovine vaginal tissue to determine if a relationship exists between ECM and smooth muscle content of the vagina, its biomechanical properties and susceptibility to POP by parity. We hypothesised that with increasing parity, ECM proteins and smooth muscle content decreases and is associated with altered biomechanical properties of ovine vaginal tissue. These altered properties will relate to vaginal tissue weakness, reflected in abnormal "POP-Q" measurements and changes in pressure distribution along the ovine vaginal wall.

Results

Vaginal weakness identified in multiparous ewes by "POP-Q" and pressure sensor measurements. Ovine vaginal wall displacement or tissue laxity was measured using a modified human POP-Q[32] to provide a clinical measure of vaginal wall weakness[18]. Our modified "POP-Q" measures the distance (cm) vaginal tissue can be displaced using traction, with −3 indicating no displacement and +3 maximal displacement with respect to the muco-cutaneous junction or urethra[16]. Ovine vaginal length was also measured for nulliparous (11.3 ± 0.4 cm), primiparous (13.0 ± 0.5 cm) and multiparous (14.3 ± 0.3 cm) ewes. Nulliparous ewes showed no vaginal displacement at the three "POP-Q" points assessed; Aa, Ap and Ba, generating baseline measurements of −3 for each point (Fig. 1A). Primiparous ewes showed no displacement at Aa and Ba, but more laxity at Ap compared to nulliparous ($p = 0.0026$). In contrast, multiparous ewes showed significantly more vaginal displacement at all 3 "POP-Q" points compared to nulliparous (Ap, $p < 0.001$; Aa, $p = 0.0011$; Ba, $p < 0.001$) and primiparous ewes (Aa, $p = 0.001$; Ba, $p < 0.001$) (Fig. 1A). The genital hiatus (Gh, Fig. 1A), a measure of the pelvic floor muscle support was significantly larger for primiparous compared with nulliparous ewes ($p = 0.0065$). The perineal body (PB) was reduced in multiparous ewes, compared to nulliparous ($p = 0.001$) (Fig. 1A). Ovine vaginal wall weakness was also measured with a novel pressure sensor device[15], which has eight fibre optic pressure sensors inserted 10 mm apart on each of the anterior and posterior blades of a modified speculum that enables the measurement of distributed pressure along both the posterior and anterior vaginal wall (Fig. 1B). Multiparous vaginal walls exerted significantly lower pressure than that of the nulliparous vagina in sensors 6–7 measurements, equivalent to point Ap ($p = 0.0053$) (Fig. 1B), while primiparous exhibited lower pressure in sensors 1–3 for the equivalent Ba region ($p = 0.003$) (Fig. 1B) measurements. No difference was found in vaginal pressure at sensors 6–7 of the lower blade (equivalent to "POP-Q" point Aa) for the three ewe groups (Fig. 1B). There was strong positive correlation between the "POP-Q" Ap measurement and Ap pressure ($r = 0.70$, $p = 0.003$), but not for points on the anterior wall, Aa or Ba (Table 1).

Ewe vaginal wall structure changes with parity. Masson's trichrome staining of the ovine vagina showed the typical layered structure, with a lamina propria beneath the epithelium and a deeper muscularis layer (Fig. 2A). The thickness of the lamina propria was similar between ewe groups; however the muscularis was significantly thinner in the multiparous, compared with the ovine vaginal wall ($p = 0.0018$) (Fig. 2B). The thickness of the muscularis was greater than the lamina propria in the nulliparous ($p = 0.0037$) and primiparous ($p = 0.0084$) ovine vagina, while these regions had similar thickness in the multiparous ewes (Fig. 2B). When the lamina propria and muscularis were combined to determine the total thickness of each wall, no significant

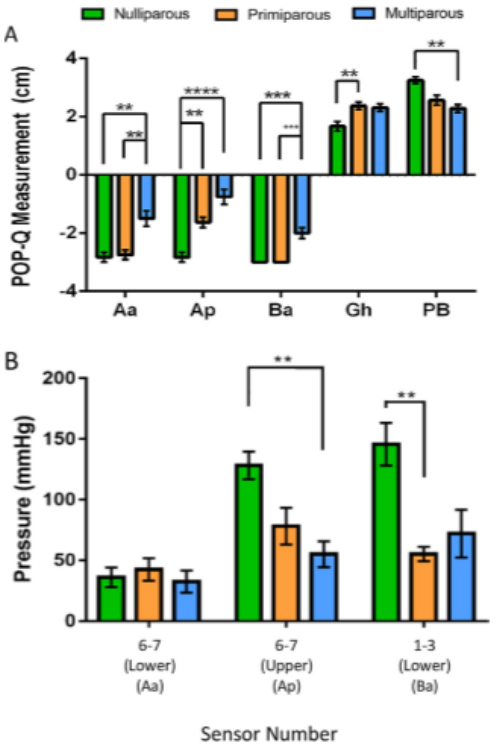

Figure 1. Modified POP-Q and pressure sensor measurements identify vaginal weakness in multiparous ewes. (**A**) "POP-Q" measurements in ovine nulliparous (green bars, n = 6), primiparous (orange bars, n = 8) and multiparous vaginal tissue (blue bars, n = 8). POP-Q points Aa and Ba are taken on the anterior wall 3 cm from the muco-cutaneous junction and 3 cm above the urethra (located in the vaginal wall), Ap 3 cm from the posterior muco-cutaneous junction. Gh; Genital hiatus; Pb, perineal body. (**B**) Pressure sensor measurements were taken from sensors detecting pressure in regions equivalent to Aa (anterior, distal sensors 6–7 on the lower blade), Ap (posterior, distal sensors 6–7 on the upper blade) and Ba (anterior, proximal sensors 1–3 on the lower blade). Data are mean +/− SEM, Pressure Sensor data from nulliparous n = 5, primiparous n = 6, multiparous n = 5 ewes/group. $^{**}p < 0.01$, $^{***}p < 0.001$, $^{****}p < 0.0001$.

differences were observed between all three ewe groups (Fig. 2C). However, when these regions are reported as percentage of total wall thickness, the lamina propria was ~50% thicker in the multiparous, compared with nulliparous and primiparous tissues ($p < 0.001$ and $p < 0.001$, respectively) (Fig. 2D). In contrast, the % muscularis of the multiparous ewes was significantly less than the nulliparous and primiparous ewes ($p < 0.001$, $p < 0.001$ respectively) (Fig. 2D). There was a strong negative correlation between "POP-Q" Aa and Ap and the muscularis thickness (Aa, $r = 0.61$, $p = 0.002$; Ap, $r = 0.75$, $p < 0.001$), indicating that the thin muscularis found in the multiparous ovine vagina is directly associated with vaginal wall weakness, particularly in the posterior compartment (Table 1).

Collagen content and organisation differs little with parity. Total collagen content of ovine vaginal tissue was measured biochemically using a hydroxyproline collagen assay, which showed significantly less collagen between nulliparous and primiparous tissues (Fig. 3A). Similarly, multiparous vaginal tissues had less collagen but this was not significant (Fig. 3A). Sirius Red birefringence was used to assess collagen organisation in the two layers of the ovine vagina (Fig. 3B,C). The percent area of both immature and mature collagen fibrils in the three ewe groups were similar in the lamina propria (Fig. 3D,E) and muscularis (Fig. 3F,G). There was a significant negative correlation between the muscularis immature collagen and the Ba pressure sensor measurement ($r = 0.70$, $p = 0.002$). However, there were no other significant correlations (Table 1).

Parity has no effect on smooth muscle content of the ovine vagina. Alpha Smooth Muscle Actin (αSMA) immunostaining showed the bilayer arrangement of smooth muscle bundles in the muscularis of the

Variable	Variable Correlation R-coefficients								
	Ap	Aa	Ba	Linear Stiffness	Max Load	Max Elongation	Ap Pressure	Aa Pressure	Ba Pressure
Ap Pressure	**0.7, 0.003**	0.6, 0.251	0.47, 0.063	0.280	0.74, 0.001	0.13, 0.634			
Aa Pressure	0.17, 0.518	0.04, 0.878	0.004, 0.989	0.32, 0.216	0.5, 0.041	0.08, 0.755			
Ba Pressure	0.51, 0.037	0.3, 0.244	0.27, 0.294	0.071, 0.790	0.37, 0.146	0.04, 0.859			
Lamina Propria	0.1, 0.66	0.15, 0.502	0.35, 0.106	0.33, 0.131	0.3, 0.171	0.29, 0.188	0.14, 0.602	0.11, 0.681	0.12, 0.634
Muscularis	0.75, <0.001	0.61, 0.002	0.54, 0.01	0.44, 0.038	0.7, <0.001	0.13, 0.564	0.58, 0.017	0.1, 0.699	0.42, 0.089
Collagen Lamina Immature	0.52, 0.014	0.45, 0.038	0.39, 0.75	0.3, 0.166	0.44, 0.042	0.36, 0.095	0.34, 0.195	0.21, 0.414	0.32, 0.215
Collagen Lamina Mature	0.24 0.281	0.43, 0.043	0.31, 0.165	0.11, 0.628	0.09, 0.685	0.38, 0.082	0.001, 0.996	0.19, 0.465	0.01, 0.967
Collagen Muscularis Immature	0.53, 0.011	0.47, 0.028	0.32, 0.146	0.23, 0.293	0.51, 0.015	0.13, 0.547	0.45, 0.080	0.1, 0.703	0.67, 0.002
Collagen Muscularis Mature	0.36, 0.103	0.51, 0.015	0.36, 0.104	0.055, 0.821	0.22, 0.331	0.11, 0.608	0.055, 0.842	0.19, 0.468	0.52, 0.032
Collagen% of Dry Weight	0.092, 0.169	0.045, 0.342	0.001, 0.887	0.001, 0.883	0.020, 0.533	0.015, 0.591	0.089, 0.263	0.066, 0.32	0.207, 0.067
αSMA Lamina	0.43, 0.047	0.18, 0.458	0.26, 0.246	0.25, 0.253	0.4, 0.068	0.28, 0.208	0.21, 0.428	0.055, 0.845	0.38, 0.132
αSMA Muscularis	0.09, 0.691	0.044, 0.835	0.055, 0.811	0.25, 0.26	0.15, 0.51	0.48, 0.023	0.055, 0.88	0.21, 0.421	0.22, 0.795
Elastic Fibres Lamina	**0.81, <0.001**	**0.67, 0.001**	0.51, 0.15	0.36, 0.98	0.52, 0.014	0.14, 0.538	0.43, 0.97	0.01, 0.976	0.46, 0.06
Elastic Fibres Muscularis	**0.65, 0.001**	**0.6, 0.003**	0.49, 0.021	0.35, 0.109	0.49, 0.019	0.17, 0.438	0.34, 0.194	0.09, 0.74	0.52, 0.032
Linear Stiffness	0.54, 0.01	0.27, 0.226	0.37, 0.091		**0.6, 0.002**	0.09, 0.681	0.28, 0.293	0.32, 0.216	0.07, 0.0790
Max Load	0.74, <0.001	0.57, 0.005	0.54, 0.009	**0.6, 0.002**		0.14, 0.545	0.74, 0.001	0.5, 0.041	0.37, 0.146
Max Elongation	0.06, 0.795	0.22, 0.321	0.3, 0.175	0.09, 0.681	0.14, 0.545		0.13, 0.634	0.08, 0.755	0.04, 0.859

Table 1. Correlation analyses of ovine vagina between POP-Q, pressure sensor, histological and biomechanical parameters. *Data are presented as r value, p value for each comparison. Benjamini-Hochberg procedure calculated a corrected significance value of $p < 0.0051$ to account for false discovery rate associated with multiple correlations. Values with underline are negative correlations, those in bold-underline were positively correlated.

ovine vagina (Fig. 4A). In the lamina propria, smooth muscle cells in the blood vessels were more prominent in multiparous tissue than nulliparous (Fig. 4A). The percentage area of smooth muscle as assessed by αSMA immunostaining was similar between the ewe groups in the lamina propria (Fig. 4B) and muscularis (Fig. 4C). Total α SMA percent area also showed no difference between ewe groups (Fig. 4D). Finally, there was no significant correlation between "POP-Q" measurements and % area of αSMA of the ovine vaginal wall compartments (Table 1).

Elastic fibre content increases with parity in the ovine vagina. Black-stained elastic fibres were predominant within both the lamina propria and muscularis of the multiparous (Fig. 5A,C) compared to the respective regions of the nulliparous vaginal wall. The elastic fibre content (%) with blood vessel contribution removed electronically (Fig. 5B,D) was increased in the lamina propria of primiparous and multiparous tissue compared to nulliparous ($p = 0.0126$, $p < 0.001$, respectively) (Fig. 5E). The vaginal muscularis of multiparous ewes also contained significantly greater elastic fibres than nulliparous ewes ($p = 0.003$) (Fig. 5E). Total elastic fibres in the entire vaginal wall was greater for primiparous and multiparous ewes compared with nulliparous ($p = 0.0296$, $p < 0.001$ respectively) (Fig. 5E). There was a positive correlation between the "POP-Q" measurement and the percent of elastic fibres within the lamina propria (Ap, $r = 0.81$, $p < 0.001$; Aa $r = 0.67$, $p = 0.001$) and the muscularis (Ap, $r = 0.65$, $p = 0.001$; Aa $r = 0.6$, $p = 0.003$). These correlations suggest that increased elastic fibres in the lamina propria and muscularis tissue may be associated with vaginal weakness.

Tensile strength and linear stiffness decreases with parity in the ovine vagina. Biomechanical properties of the ovine vaginal wall were assessed by biaxial tensiometry, using the ball burst method. Typical load (N) versus elongation (mm) curves suggested that multiparous tissue (orange) exhibited reduced maximum load-bearing ability compared to nulliparous (blue) and primiparous (red) tissue (Fig. 6A). Multiparous vaginal tissue exhibited significantly lower linear region stiffness (Fig. 6B) than nulliparous tissue ($p = 0.0093$) and was significantly weaker than both the nulliparous ($p = 0.0008$) and primiparous ($p = 0.0031$) ewes with a lower breaking load (Fig. 6C). Maximum elongation of vaginal tissue was also measured, but no differences were observed between the three groups (Fig. 6D). "POP-Q" measurement were negatively correlated with Ap and Aa measurements of maximum load (Ap, $r = 0.77$, $p < 0.001$; Aa, $r = 0.57$, $p = 0.005$), (Table 1). Maximum load also negatively correlated with the Ap pressure sensor measurement ($r = 0.74$, $p = 0.001$) (Table 1). Linear stiffness and maximum load results also correlated ($r = 0.6$, $p = 0.002$) and there was also a strong correlation of maximum load with thickness of the muscularis ($r = 0.7$, $p < 0.001$) (Table 1). Together these correlations indicate vaginal weakness detected by a clinical measurement and that changes in support measured by the pressure sensor are

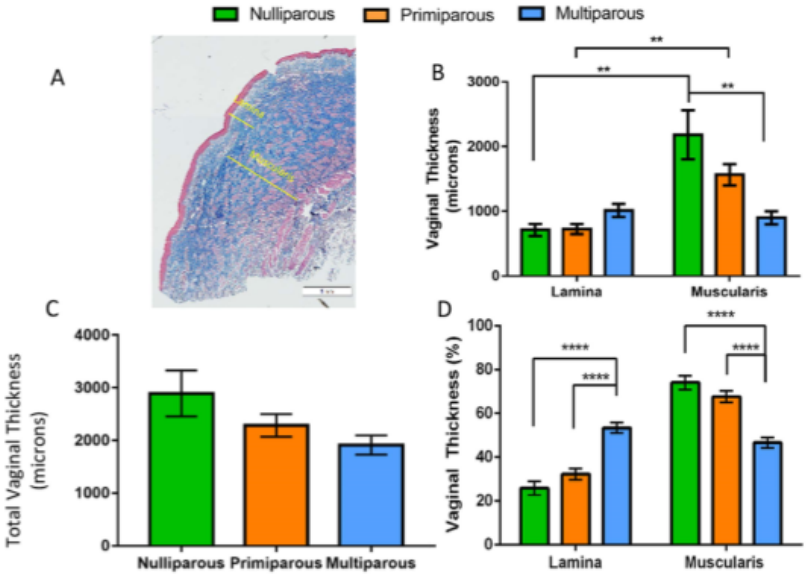

Figure 2. Dimensions of the ovine vaginal wall. (**A**) Mason's Trichrome Staining showing measurement of lamina propria and muscularis (yellow lines). Vaginal thickness of the (**B**) lamina propria and muscularis and (**C**) the total vaginal wall thickness. (**D**) lamina propria and muscularis as percent of vaginal wall depth. Scale Bar is 1 mm. Data are mean +/− SEM from nulliparous n = 6, primiparous and multiparous n = 8 ewes/group. $^{**}p < 0.01$, $^{***}p < 0.001$, $^{****}p < 0.0001$.

associated with a thin muscularis with increased elastic fibre content and decreased biomechanical strength of ovine vaginal tissue, particularly in the posterior vaginal wall.

Discussion

In our study we have shown that the ovine vaginal wall undergoes dynamic changes in physiological, structural, histological and physical properties as a result of increasing parity, with the greatest effect observed in multiparous ewes. We first observed significant differences in tissue displacement and pressure between parous groups using both modified "POP-Q" measurement and a new pressure sensor. Specifically, the multiparous vagina becomes thinner due to a loss of muscularis tissue, though density of the remaining smooth muscle is similar to both nulliparous and primiparous ewes. The elastic fibre content was greater within the primiparous and multiparous vagina muscularis and percent collagen is reduced in primiparous compared to nulliparous ewes. The vagina was also weaker and less stiff in multiparous ewes, compared to nulliparous and primiparous ewes, suggesting that the loss of muscle mass rather than elastic fibres is a significant contributor to higher "POP-Q" measurements and weaker biomechanical measurements. For the first time, our extensive correlation analysis shows a positive relationship between thickness of the vaginal muscularis and its mechanical strength, as well as a negative relationship between the ECM elastic fibre content and vaginal wall strength in the distal region of the anterior and posterior ovine vaginal wall.

Our correlative data suggests that the muscularis thins with increasing parity resulting in a disproportionately thicker, well vascularised lamina propria, which is associated with vaginal wall weakness, as measured by both clinical and biomechanical methods. Increased elastic fibre content in the weakened multiparous ovine vagina may be a compensatory mechanism for loss of muscularis. Our data also suggests that the decreased thickness of the muscularis may be a significant contributor to loss of vaginal wall strength and stiffness and that increasing parity has a considerable impact on this change in tissue compartment of the ovine vaginal wall. The similar percentage area of vaginal αSMA staining in the three groups of ewes suggests that the density of the muscle bundles is not altered in multiparous ewes. Rather, it appears that there is a loss of absolute levels of smooth muscle in the multiparous ewe vagina that may account for muscularis thinning. The total vaginal wall itself is not significantly thinner than that of nulliparous ewes, although there is a trend towards vaginal thinning from nulliparous to primiparous to multiparous ewes.

While significantly lower total collagen content was observed in the primiparous tissue than nulliparous using a biochemical assay, this was not replicated in our histological analysis using Sirius red birefringence, which may be less sensitive as it only measures collagen fibril organisation. Our data suggests that the nulliparous vaginal tissue contains more total collagen but has no relationship with ewe parity. As there was also no correlation

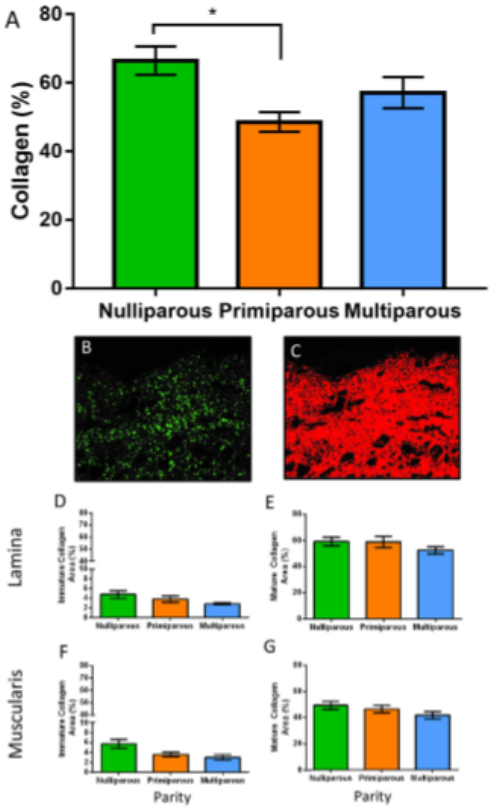

Figure 3. Collagen in the ovine vaginal wall. Biochemical analysis by hydroxyproline for (**A**) total collagen content as percent of dry weight. Birefringence images of Sirius Red stained tissues showing (**B**) green immature fibrils, and (**C**) red mature fibrils in the lamina propria. (**D**) immature and (**E**) mature collagen within the lamina propria of nulliparous (green bars), primiparous (orange bars) and multiparous (blue bars) ewes. (**F**) immature and (**G**) mature collagen within the muscularis. Data are mean+/− SEM from nulliparous n = 6, primiparous and multiparous n = 8 ewes/group.

observed between the collagen content and any other measurement, any effect this may have on the biomechanical properties and areas of weakness of the vaginal tissue remains unclear. Increased elastic fibre synthesis may have compensated for the loss of smooth muscle in the multiparous vagina. This increased elastic fibre content may account for the decreased tissue biomechanical strength and stiffness, along with the loss of muscularis, may account for the loss of tensile strength in multiparous vaginal tissue, compared to nulliparous and primiparous ewes. This was suggested by our "POP-Q" correlation results. Specifically, the muscularis elastic fibre content correlated positively with Ap and Aa measurements. Though a direct relationship requires further investigation, we are confident that a relationship exists due to our use of the Benjamini-Hochberg false discovery rate correction to calculate a stringent significance level of $P < 0.0051$, for which significance was met for only 15 out of a possible 141 correlations. Additionally, our previously reported POP-Q measurements in ewes had good-to-excellent intraclass correlation coefficients for Aa and Ap, but weaker for the Ba point[16]. In the present study, our correlations between POP-Q points Aa and Ap and histological and biomechanical data yielded very small P values in contrast to correlations with Ba providing further confidence in the accuracy of their measurement. Together these correlations may indicate POP susceptibility in the multiparous ewes. When considered as a whole, this suggests that the muscularis plays an important role in protecting the vaginal wall against herniation from pelvic organs, and its size reduction with accompanying smooth muscle and ECM alteration from repeated birth-induced injury may leave the vaginal wall vulnerable to prolapse. Our results support findings in the vaginal wall of multiparous menopausal women who are more susceptible to pelvic organ prolapse[31,33–36].

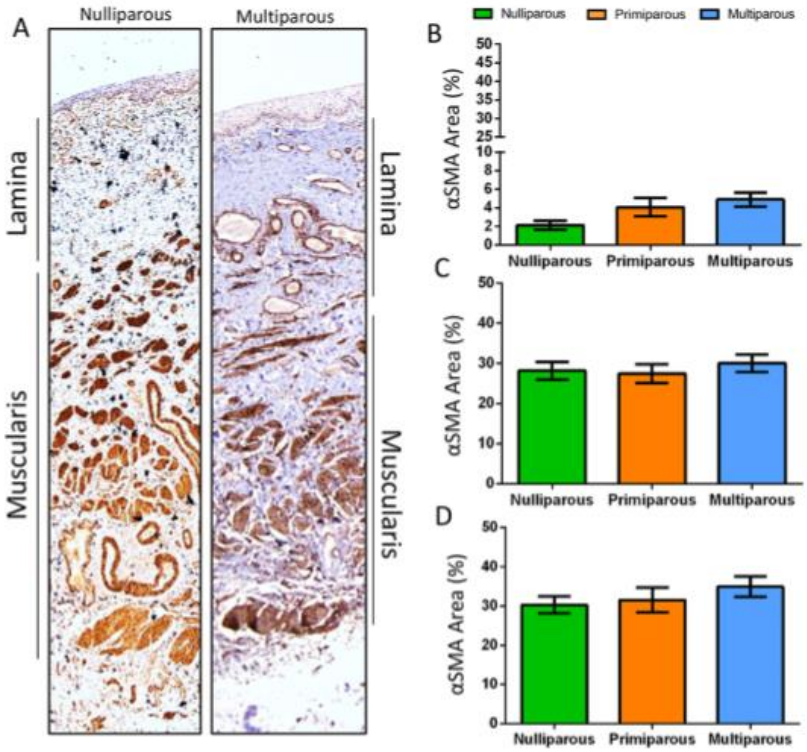

Figure 4. Smooth Muscle Content in the ovine vaginal wall by αSMA Immunohistochemistry. Images showing αSMA positive blood vessel vascularity of the ovine lamina propria of the vagina in **(A)** nulliparous and multiparous ewes. Quantification by image analysis of aSMA percent of the **(B)** lamina propria, **(C)** muscularis and the **(D)** total smooth muscle in vaginal tissue. Data are mean +/− SEM from nulliparous n = 6, primiparous and multiparous n = 8 ewes/group.

An earlier smaller study in ewes showed the multiparous muscularis was thicker than the nulliparous[18]. It also showed greater collagen content and lower elastic tissue associated proteins (ETAP) measured biochemically. However, these differences may be due to different methodologies and sample sizes used in these studies. The current study used greater sample sizes for each of the groups. It also employed histological and biochemical methods for assessing elastic fibre and total collagen content, quantifying immature and mature collagen by Sirius Red birefringence in contrast to SDS-PAGE to assess collagens type I and III[18]. Our histological measure of vaginal wall thickness was from multiple measurements per region in each sample rather than a single measurement reported in the earlier study. The limited correlation observed between conventional "POP-Q" measurement and the novel pressure sensor device indicate further refinement is needed for the device, with particular attention to the distinction between tissue displacement and vaginal wall pressure as predictors of POP vulnerability. However, this novel device holds value in that it is capable of measuring alterations in pressure along the lengths of the anterior and posterior vaginal wall, instead of a single measurement for both. This may be achieved by automating dilation of the speculum to minimise movement artefact and determining the maximum rate of pressure change versus dilation to accommodate variations in vaginal dimensions that may be associated with parity or vaginal weakness[15].

The results of our study align with the findings of others investigating the relationship between tissue composition and pelvic organ prolapse in other animal models. Our observations on collagen align with those performed in prolapsed tissue of rhesus macaques, where different collagen types and their ratio was not different to nulliparous controls, although there was less collagen alignment as observed under a polarising microscope[37]. Parous macaques also exhibited inferior biomechanical properties similar to our study. Smooth muscle is also significantly decreased due to increased apoptosis in human vaginal tissue obtained from women with POP[30,31]. Similar to the current study, the smooth muscle content was not diminished but rather the area the smooth muscle occupied had decreased[31]. Previous studies have reported that vaginal smooth muscle content of women with

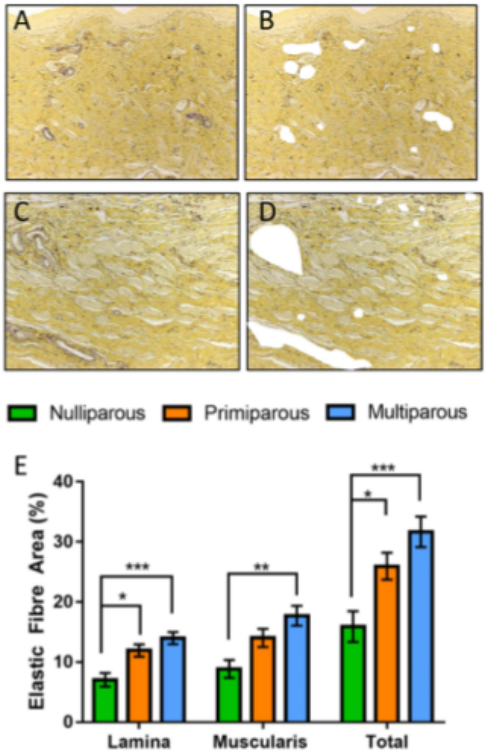

Figure 5. Elastic fibre content of ovine vaginal wall. Shown as black fibres in Hart's-stained tissue in representative images of multiparous (**A**) lamina propria with (**B**) blood vessels removed from analysis and in the (**C**) muscularis with (**D**) blood vessels removed from analysis. (**E**) Graph showing the image analysis quantification of elastic fibre area in tissue images with blood vessels electronically removed. n = 6, primiparous and multiparous n = 8 vaginal tissues/group. Data are mean +/− SEM, *p < 0.05, **p < 0.01, ***p < 0.001.

POP was diminished and disorganised[28,29]. However, in our study, we did not observe a disorganised muscularis in multiparous ewes, but rather a thinning of this entire layer, suggesting a unique adaptation in the ovine model not seen in parous women with POP. While our image analysis revealed a thinner muscularis in multiparous than in nulliparous ewes, we were unable to determine whether this was due to smaller smooth muscle cells or a reduction in smooth muscle cell number. Nevertheless, our study provides evidence that the net pathophysiological response of the altered vaginal muscularis is likely very similar in ewes and women.

The current understanding of elastic fibre synthesis within the vaginal wall, before and after child delivery, is limited and requires further investigation. As has been observed in Fibulin $5^{-/-}$ knockout mice, elastic fibre deficiency contributes to the structural weakness of the vaginal wall that leads to POP. In contrast, the weakened ovine vaginal wall of the primiparous and multiparous ewes at Ap, as evidenced by POP-Q and pressure sensor measurements, showed increased levels of elastic fibre content compared to nulliparous ewes. It is possible that elastic fibres are synthesised within the vaginal wall after lamb delivery as a compensatory mechanism for the loss of smooth muscle. Increased elastic fibre content of vaginal tissue from the prolapse site has also been observed women[10]. However, the precise relationship between increased elastic fibre content, vaginal wall weakness and POP requires further research.

Indeed, that our results aligned with those that used humans and macaques as models supports our selection of ewes as an investigational model. Our study also supports a recent report comparing the mechanical properties of ewe vagina in non-human primates and rodent models where parity had a negative impact on mechanical integrity[38]. Though further comparative studies between these species are warranted, the similarities already identified suggests that ewes can be used for further investigations. The ewe can serve as a model for measuring damage caused by the first vaginal delivery, known to be a major contributor to future POP[1]. Our observations in

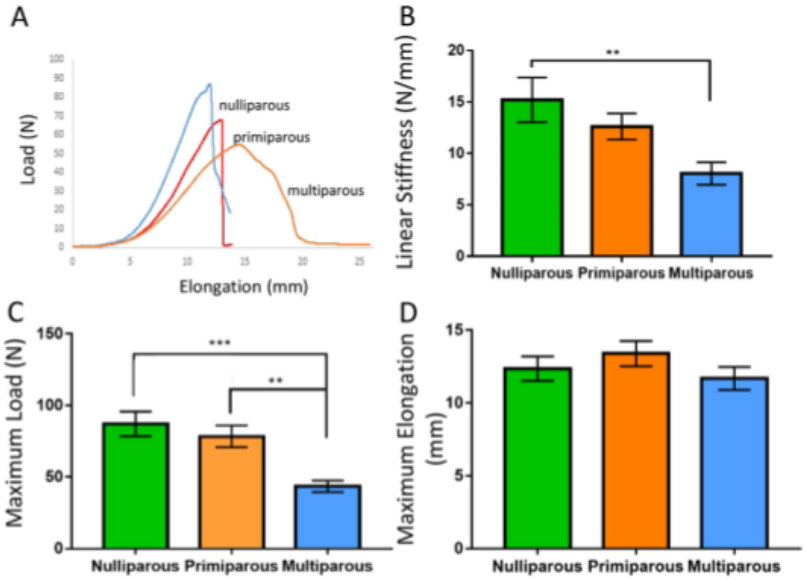

Figure 6. Biomechanical analysis of ovine vaginal tissue. Using biaxial tensile testing (**A**) representative load-elongation curves from nulliparous (blue), primiparous (red) and multiparous (orange) vaginal wall. (**B**) Linear stiffness, (**C**) Max Load and (**D**) Maximum Elongation. Data are mean +/− SEM from nulliparous n = 6, primiparous and multiparous n = 8 ewes/group. **p < 0.01, ***p < 0.001.

multiparous ewes suggest they may be a suitable model for assessing new treatments for POP, such as cell-based therapies[11,12].

Our data indicate the muscularis as a key structural determinant of biomechanical strength of the vaginal wall. However, a limitation of the biaxial tensiometry used in this study ("ballburst" test), is that a steel rod may not exert equivalent forces of a pelvic organ, with different shape and hardness. However, the vaginal wall is subject to high intra-abdominal pressures transmitted through pelvic organs pressing on the vaginal wall[39]. Vaginal tissue is anisotropic[19,40], thus biaxial testing is currently the most equivalent test available. It is superior to uniaxial biomechanical testing as this only measures properties in one direction, which does not represent the physiologic environment, in which strain is placed on the vaginal wall in all directions[18,26,41].

Limitations of our study include the lack of hormone measurement to determine oestrus cycle stage of the ewes, relatively small group size and lack of longitudinal measurements of POP-Q points or pressure sensor readings. Although the majority of our samples were from ewes in the follicular phase of the oestrus cycle, it is unknown whether the luteal stage would have affected our results. Given that the greatest damage to the vaginal wall occurs in women during their first vaginal birth and that the risk of POP rises incrementally with subsequent births[42–44] we expected to see greatest changes in these measurements between nulliparous and primiparous ewes compared to those between the primiparous and multiparous. While our small group sizes may have contributed to minimal changes observed in primiparous ewes at the POP-Q points Aa and Ba compared with nulliparous, we also showed trends toward greater changes for GH and PB than between primparous and multiparous and for Ap and Ba using the pressure sensor device. This suggests that the pressure sensor device may be more sensitive in detecting vaginal wall weakness than the relatively inexact POP-Q measurements and therefore may have value in assessing women with POP. Similarly, our small group size and lack of longitudinal data may have contributed to our observation of the greatest effect on muscularis and vaginal thickness in multiparous rather than primiparous ewes. Our data also suggests that the Ba measurement may not be as robust as other POP-Q points as significant correlations ($P < 0.0051$) were not observed at this point for muscularis thickness, elastic fibre content or maximum load. This may be due to the urethral opening positioned in the anterior vaginal wall, which is not the case in women and may explain why POP, while very common in the Ba position in women, is not in the ovine model[43]. Since vaginal surgical procedures in the ovine model are performed in the Ap region[45,46] rather than the anterior wall because of the urethra, we believe that the POP-Q and pressure sensor values at this point will provide a useful monitoring parameter.

In conclusion, we have observed vaginal muscularis thinning following multiple births in an ovine model which may significantly contribute to vaginal wall weakness and potential susceptibility to POP. In particular we identified that loss of smooth muscle in the vaginal muscularis is a key factor in vaginal muscularis thinning, and is associated with loss of strength and stiffness resulting in vaginal wall weakness in multiparous ewes. We

contend that it is the thinner muscularis of the multiparous vaginal wall that makes it vulnerable to rises in intra-abdominal pressure and allows the herniation of the pelvic organs, resulting in POP. Our data contributes to the understanding of the effect of parity on ovine vaginal tissue structure and mechanical properties, which will inform future studies that may use this large pre-clinical animal model for cell-based therapies for POP.

Methods

Ethics and Animals. Experimental procedures and animal husbandry were approved by the Monash Medical Centre Animal Ethics Committee A in accordance with the ethical guidelines of the National Health and Medical Research Council (NHMRC) of Australian Code for the Care and Use of Animals for Scientific Purposes 8th Edition. Border Leicester Merino (BLM) ewes were housed in the Monash Animal Service. Ewes were selected on their birth history; nulliparous (having never been pregnant, aged 2 years, n = 6), primiparous (having had one pregnancy, aged 3–4 years, n = 8) and multiparous (having more than one previous pregnancy, aged 4–5 years, n = 8) who had undergone zero, one and multiple lamb deliveries, respectively, with the last lamb delivered 12 months prior.

Modified Pelvic Organ Prolapse Quantification ("POP-Q") measurements. "POP-Q" measurements were undertaken by gynaecologists (NY, AR) in conscious ewes as previously described[18]. Briefly manual traction with forceps on the vaginal tissue in the Aa, Ba, Ap regions using the urethra as a reference point for Ba (proximal anterior) and mucocutaneous junction for Aa (distal anterior) and Ap (distal posterior), rather than the hymen as performed in women. The intraclass correlation coefficients for the POPQ measures Aa, Ap and Ba were 0.75, 0.83 and 0.64, respectively, and interclass correlation coeffeicents 0.73, 0.74 and 0.58 respectively. Vaginal length of each ewe was also recorded.

Vaginal pressure measurements. Immediately following "POP-Q" measurements, a modified speculum fitted with 8 fibre optic pressures sensors 10 mm apart on each parallel blade was inserted into the ovine vagina and pressure measurements recorded at 10 mm dilation following a maximal dilation of 20 mm. Mean pressures (mm Hg) at sensor 1–3, equivalent to Ba (anterior blade, lower proximal toward the cervix), and sensors 6–7 on each blade, equivalent to Aa (anterior blade, lower distal toward introitus) and Ap (upper posterior blade, distal toward introitus) were reported.

Tissues. Following euthanasia, the complete vaginal tract was removed, trimmed and incised in a longitudinal manner adjacent to the urethra (anterior wall) from the muco-cutaneous junction to the cervix (Supplemental Fig. 1) and dissected and frozen at −20 C for biomechanical analyses. Due to narrowing of the ewe vagina at the apical end, the 4 cm × 4 cm tissue required for biomechanical testing was taken from the mid-region of the posterior wall. Previous studies have demonstrated similarity in the biochemical and biomechanical properties of the lower-and-mid regions of the ovine vaginal wall[41]. To avoid the hymnal ring, tissue adjacent to the piece for biomechanical analysis was excised and fixed in 10% formalin, paraffin embedded and 5 μm sections were stained with Haemotoxylin and Eosin (H&E), Masson's Trichrome and Hart's elastic fibre stain in the Monash Histology Platform (MHP) facility. Additionally, ovaries were removed from each animal in order to determine the stage of oestrus cycle; 4/6 nulliparous, 7/8 primiparous and 8/8 multiparous ewes were in the follicular stage of the oestrus cycle.

Vaginal wall thickness. Massons Trichrome-stained sections were examined under an Olympus BX61 light microscope and three high resolution images per sample of the entire vaginal wall acquired using Olympus cellSense software. Both the lamina propria and muscularis were measured in microns (n = 3/region) and replicates averaged for calculating mean/ewe group. The total vaginal wall thickness was calculated by adding the length of the 2 regions and the relative percentage of each region to total vaginal wall thickness was calculated.

α-Smooth muscle actin immunohistochemistry and image analysis. Sections were dewaxed, rehydrated, then protein block (Dako Glostrup, Denmark) was applied for 30 min at RT. After three washes in PBS, sections were incubated with mouse anti-human α-smooth muscle actin (αSMA) antibody (Dako) for one hr at 37 °C at 1:50 dilution (71 μg/1 ml). Mouse IgG1 isotype control antibody (Dako) was used as the negative control at the same concentration. Sections were washed 3 times with PBS/2% BSA followed by anti-mouse secondary antibody (Dako) for 30 mins at RT, washed in PBS and chromogen added (3,3′-diaminobenzidine) (Sigma-Aldrich, St. Louis USA) for 3 min as previously published[18]. Slides were mounted in DPX (Sigma-Aldrich). Three images (10X magnification) were taken each of the lamina propria and muscularis regions using an Olympus BX61 light microscope and Olympus cellSens software and analysed using ImageJ software. Each image was color deconvoluted from haematoxylin and DAB staining, then converted into binary colour, with pixels above a threshold intensity of 20 considered as 1 (αSMA+) and everything else 0. The area of brown-stained smooth muscle in each region was then measured as a percentage of the area of interest, then averaged for the three replicates for each ovine sample and then averaged for each of the 3 groups.

Collagen analysis. Tissue sections were stained with Picro-Sirius Red using previously established protocols[47]. Briefly, slides were stained in Weigert's haematoxylin for 8 minutes, then washed in tap water for 10 minutes before staining in 0.1% Picro-Sirius red for one hour then washed in two changes of acidified water (0.5% glacial acetic acid, pH 3). Slides were allowed to air-dry, rinsed twice in Histoclear and mounted in DPX. Three images at 10X magnification were taken of the lamina propria and muscularis regions using an Olympus BX61 light microscope equipped with a polarising filter (Olympus T2 U-ANT and U-POT) using cellSens software and an Olympus DP80 camera to identify birefringent Sirius red-stained collagen fibres. Images were examined using

ImageJ software and separated into base colors red and green. An intensity threshold was set that converted any green or red pixel into a single colour with a count of 1, while a black pixel was considered 0. The red and green birefringent collagen fibres (Fig. 3A–C) were measured as percentage area of both the lamina propria and muscularis for three images/region. These replicates were averaged for each ovine sample and used to obtain means for each group.

Hydroxyproline Assay for Collagen. Supernatants from digested samples were immersed in 5 ml of 6 M HCl and 2 ml edible oil under nitrogen for 4 hours at 11.5 C, then transferred to a desiccator overnight. The solution beneath the oil was extracted and evaporated at 70 C. The precipitate was weighed in 4 ml of distilled water, then 0.5 ml of 0.05 M Chloramine T solution was added to each sample for 30 min at room temperature (RT). The reaction was continued by addition of 0.5 ml of 3.15 M Perchloric Acid Solution for 10 minutes at RT, followed by adding 0.5 ml 10% Paradimethylaminobenzaldehyde solution and incubated for 40 minutes at 60 C. Absorbance was read at A560 nm using distilled water as a blank. A standard curve using L-hydroxyproline (0–10 ug/ml (Sigma)) was used to ascertain the collagen content of each sample. Total collagen was calculated using hydroxyproline: collagen ratio of 0.143:1.

Elastic fibre analysis. Dewaxed and dehydrated paraffin sections were stained by Hart's method at the Monash Histology Platform. Briefly, sections were immersed in 0.25% potassium permanganate for 5 minutes, then rinsed in distilled water twice for 30 seconds each, and placed in 5% oxalic acid for 3 seconds before rinsing in tap water, then distilled water, twice for 30 seconds each followed by 10% Resorcin (w/v distilled water) Fuchsin (2% w/v distilled water) solution in acidified 70% ethanol overnight. Slides were again rinsed in tap then distilled water three times, each for 30 seconds and counterstained in 0.25% tartrazine in saturated picric acid for 3 minutes, dehydrated, cleared and mounted with DPX. Three images (10X magnification) were taken of the lamina propria and muscularis regions using an Olympus BX61 light microscope. Blood vessels in the images were outlined and removed electronically before a custom ImageJ macro was used to separate the image into black (elastic fibre) and yellow (background tissue) stained components, with a threshold of 20 considered as 1 (elastic fibre+) and everything else 0 and then generated the area percentage of elastic fibre and yellow-stained tissue in the area of interest (Fig. 5). The percentage area of elastic fibre was then divided by the area percentage of tissue to produce the percentage elastic fibre/region, then averaged for three replicates from each ovine sample and the average for each group then calculated.

Biomechanical analysis of ovine vaginal tissue. Frozen tissues were thawed overnight at 4 C and tested within 24 hr. Freeze-thawing vaginal tissue does not alter its mechanical properties and is more reliable as the same conditions are used for each specimen[48]. Samples ($\sim 30 \times 30$ mm) were excised from the explanted sample and kept moist using PBS until testing. The biaxial tensile properties of the tissue were measured using a ball burst test method using an Instron Tensile Tester (5557; Instron Corp, MA) with a load cell of 100N. Samples were secured between 2 embossed metal plates, both with an aperture of 15 mm (for penetration of the steel rod). Rubber sheeting was used to avoid sample slippage during testing. A rounded steel rod (10 mm diameter) was pushed through the tissue sample at a crosshead speed of 20 mm/min to break. Load-elongation curves were plotted from the generated data (Fig. 6A) and from these curves stiffness (N/mm) in the region of high stiffness (linear region), maximum load (N) and maximum elongation were calculated.

Statistical analysis. All data were assessed for normality using Shapiro-Wilk or Kolmogorov-Smirnov tests if the sample size was too small for Shapiro-Wilk test. Data were normally distributed. Differences in POP-Q scores, pressure sensor data, histological and biomechanical data by parity group (nulliparous, primiparous and parous) were assessed using a 1-Way ANOVA with Tukey's multiple comparison post hoc test. The correlation between the "POP-Q", biomechanical data and pressure sensor with histological parameters was assessed using the Pearson's correlations coefficient. Due to the multiple testing we performed a Benjamini-Hochberg false discovery rate calculation. All correlation p values < 0.0051 (2-tailed) were considered statistically significant. All analyses were undertaken using GraphPad Prism 6 for Windows 7, (GraphPad Software, La Jolla California USA) or the SPSS statistical package (SPSS 23, IBM Corp, Armonk, New York, USA).

References

1. DeLancey, J. O. The hidden epidemic of pelvic floor dysfunction: achievable goals for improved prevention and treatment. *American journal of obstetrics and gynecology* **192,** 1488–1495, doi: 10.1016/j.ajog.2005.02.028 (2005).
2. Deprest, J. *et al.* The biology behind fascial defects and the use of implants in pelvic organ prolapse repair. *Int Urogynecol J* **17** Suppl 1, S16–25, doi: 10.1007/s00192-006-0101-2 (2006).
3. Nygaard, I. *et al.* Prevalence of symptomatic pelvic floor disorders in US women. *Jama* **300,** 1311–1316, doi: 10.1001/jama.300.11.1311 (2008).
4. Barber, M. D. & Maher, C. Epidemiology and outcome assessment of pelvic organ prolapse. *Int Urogynecol J* **24,** 1783–1790, doi: 10.1007/s00192-013-2169-9 (2013).
5. Slieker-ten Hove, M. C. *et al.* The prevalence of pelvic organ prolapse symptoms and signs and their relation with bladder and bowel disorders in a general female population. *Int Urogynecol J* **20,** 1037–1045, doi: 10.1007/s00192-009-0902-1 (2009).
6. Diez-Itza, I., Aizpitarte, I. & Becerro, A. Risk factors for the recurrence of pelvic organ prolapse after vaginal surgery: a review at 5 years after surgery. *Int Urogynecol J* **18,** 1317–1324, doi: 10.1007/s00192-007-0321-0 (2007).
7. Vergeldt, T. F., Weemhoff, M., IntHout, J. & Kluivers, K. B. Risk factors for pelvic organ prolapse and its recurrence: a systematic review. *Int Urogynecol J* **26,** 1559–1573, doi: 10.1007/s00192-015-2695-8 (2015).
8. Drewes, P. G. *et al.* Pelvic organ prolapse in fibulin-5 knockout mice: pregnancy-induced changes in elastic fiber homeostasis in mouse vagina. *The American journal of pathology* **170,** 578–589, doi: 10.2353/ajpath.2007.060662 (2007).
9. Li, B. *et al.* [Expression and significance of elastin and fibulin-5 in anterior vaginal tissue of women with pelvic organ prolapse]. *Zhonghua fu chan ke za zhi* **44,** 514–517 (2009).

10. Zong, W. *et al.* Alteration of vaginal elastin metabolism in women with pelvic organ prolapse. *Obstetrics and gynecology* **115,** 953–961, doi: 10.1097/AOG.0b013e3181da7946 (2010).
11. Darzi, S., Werkmeister, J. A., Deane, J. A. & Gargett, C. E. Identification and Characterization of Human Endometrial Mesenchymal Stem/Stromal Cells and Their Potential for Cellular Therapy. *Stem cells translational medicine*, doi: 10.5966/sctm.2015-0190 (2016).
12. Emmerson, S. J. & Gargett, C. E. Endometrial mesenchymal stem cells as a cell based therapy for pelvic organ prolapse. *World journal of stem cells* **8,** 202–215, doi: 10.4252/wjsc.v8.i5.202 (2016).
13. Couri, B. M. *et al.* Animal models of female pelvic organ prolapse: lessons learned. *Expert review of obstetrics & gynecology* **7,** 249–260, doi: 10.1586/eog.12.24 (2012).
14. Zacharin, R. F. Genital prolapse in ruminants. *The Australian & New Zealand journal of obstetrics & gynaecology* **9,** 236–239 (1969).
15. Parkinson, L. A. *et al.* Real-time measurement of the vaginal pressure profile using an optical-fiber-based instrumented speculum. *Journal of biomedical optics* **21,** 127008, doi: 10.1117/1.jbo.21.12.127008 (2016).
16. Young, N. *et al.* Vaginal wall weakness in parous ewes: a potential preclinical model of pelvic organ prolapse. *Int Urogynecol J*, doi: 10.1007/s00192-016-3206-2 (2016).
17. Persu, C. *et al.* Pelvic Organ Prolapse Quantification System (POP-Q) - a new era in pelvic prolapse staging. *Journal of medicine and life* **4,** 75–81 (2011).
18. Ulrich, D. *et al.* Influence of reproductive status on tissue composition and biomechanical properties of ovine vagina. *PloS one* **9,** e93172, doi: 10.1371/journal.pone.0093172 (2014).
19. Feola, A. *et al.* Deterioration in biomechanical properties of the vagina following implantation of a high-stiffness prolapse mesh. *BJOG: an international journal of obstetrics and gynaecology* **120,** 224–232, doi: 10.1111/1471-0528.12077 (2013).
20. Alperin, M. & Moalli, P. A. Remodeling of vaginal connective tissue in patients with prolapse. *Current opinion in obstetrics & gynecology* **18,** 544–550, doi: 10.1097/01.gco.0000242958.25244.ff (2006).
21. Mosier, E., Lin, V. K. & Zimmern, P. Extracellular matrix expression of human prolapsed vaginal wall. *Neurourology and urodynamics* **29,** 582–586, doi: 10.1002/nau.20806 (2010).
22. Alarab, M. *et al.* Expression of extracellular matrix-remodeling proteins is altered in vaginal tissue of premenopausal women with severe pelvic organ prolapse. *Reproductive sciences (Thousand Oaks, Calif.)* **21,** 704–715, doi: 10.1177/1933719113512529 (2014).
23. Budatha, M. *et al.* Extracellular matrix proteases contribute to progression of pelvic organ prolapse in mice and humans. *The Journal of clinical investigation* **121,** 2048–2059, doi: 10.1172/jci45636 (2011).
24. Connell, K. A. *et al.* Diminished vaginal HOXA13 expression in women with pelvic organ prolapse. *Menopause (New York, N.Y.)* **16,** 529–533, doi: 10.1097/gme.0b013e31818fb0c2 (2009).
25. Ritz-Timme, S., Laumeier, I. & Collins, M. J. Aspartic acid racemization: evidence for marked longevity of elastin in human skin. *The British journal of dermatology* **149,** 951–959 (2003).
26. Rahn, D. D. *et al.* Biomechanical properties of the vaginal wall: effect of pregnancy, elastic fiber deficiency, and pelvic organ prolapse. *American Journal of Obstetrics and Gynecology* **198,** 590.e591–590.e596, doi: 10.1016/j.ajog.2008.02.022 (2008).
27. Gustilo-Ashby, A. M. *et al.* The impact of cesarean delivery on pelvic floor dysfunction in lysyl oxidase like-1 knockout mice. *Female pelvic medicine & reconstructive surgery* **16,** 21–30, doi: 10.1097/SPV.0b013e3181d00035 (2010).
28. Boreham, M. K. *et al.* Morphometric analysis of smooth muscle in the anterior vaginal wall of women with pelvic organ prolapse. *American journal of obstetrics and gynecology* **187,** 56–63 (2002).
29. Boreham, M. K. *et al.* Morphometric properties of the posterior vaginal wall in women with pelvic organ prolapse. *American journal of obstetrics and gynecology* **187,** 1501–1508, discussion 1508–1509 (2002).
30. Badlou, W. *et al.* Comparative histological analysis of anterior vaginal wall in women with pelvic organ prolapse or control subjects. A pilot study. *Int Urogynecol J* **19,** 723–729, doi: 10.1007/s00192-007-0516-4 (2008).
31. Takacs, P. *et al.* Vaginal smooth muscle cell apoptosis is increased in women with pelvic organ prolapse. *Int Urogynecol J* **19,** 1559–1564, doi: 10.1007/s00192-008-0690-z (2008).
32. Bump, R. C. *et al.* The standardization of terminology of female pelvic organ prolapse and pelvic floor dysfunction. *American journal of obstetrics and gynecology* **175,** 10–17 (1996).
33. Diez-Itza, I., Aizpitarte, I. & Becerro, A. Risk factors for the recurrence of pelvic organ prolapse after vaginal surgery: a review at 5 years after surgery. *International Urogynecology Journal Floor Dysfunction* **18,** 1317–1324, doi: 10.1007/s00192-007-0321-0 (2007).
34. Strohbehn, K., Jakary, J. A. & Delancey, J. O. Pelvic organ prolapse in young women. *Obstetrics and gynecology* **90,** 33–36, doi: 10.1016/s0029-7844(97)00218-4 (1997).
35. Tinelli, A. *et al.* Age-related pelvic floor modifications and prolapse risk factors in postmenopausal women. *Menopause (New York, N.Y.)* **17,** 204–212, doi: 10.1097/gme.0b013e3181b0c2ae (2010).
36. Gerten, K. A., Markland, A. D., Lloyd, L. K. & Richter, H. E. Prolapse and Incontinence Surgery in Older Women. *The Journal of Urology* **179,** 2111–2118, doi: 10.1016/j.juro.2008.01.089 (2008).
37. Feola, A. *et al.* Parity negatively impacts vaginal mechanical properties and collagen structure in rhesus macaques. *American journal of obstetrics and gynecology* **203,** 595.e591-598, doi: 10.1016/j.ajog.2010.06.035 (2010).
38. Knight, K. M. *et al.* Impact of parity on ewe vaginal mechanical properties relative to the nonhuman primate and rodent. *Int Urogynecol J* **27,** 1255–1263, doi: 10.1007/s00192-016-2963-2 (2016).
39. Spahlinger, D. M. *et al.* Relationship between intra-abdominal pressure and vaginal wall movements during Valsalva in women with and without pelvic organ prolapse: technique development and early observations. *Int Urogynecol J* **25,** 873–881, doi: 10.1007/s00192-013-2298-1 (2014).
40. Martins, P. *et al.* Biomechanical properties of vaginal tissue in women with pelvic organ prolapse. *Gynecologic and obstetric investigation* **75,** 85–92, doi: 10.1159/000343230 (2013).
41. Ulrich, D. *et al.* Regional variation in tissue composition and biomechanical properties of postmenopausal ovine and human vagina. *PloS one* **9,** e104972, doi: 10.1371/journal.pone.0104972 (2014).
42. Gyhagen, M., Bullarbo, M., Nielsen, T. F. & Milsom, I. Prevalence and risk factors for pelvic organ prolapse 20 years after childbirth: a national cohort study in singleton primiparae after vaginal or caesarean delivery. *BJOG: an international journal of obstetrics and gynaecology* **120,** 152–160, doi: 10.1111/1471-0528.12020 (2013).
43. Olsen, A. L. *et al.* Epidemiology of surgically managed pelvic organ prolapse and urinary incontinence. *Obstetrics and gynecology* **89,** 501–506, doi: 10.1016/s0029-7844(97)00058-6 (1997).
44. Tegerstedt, G., Maehle-Schmidt, M., Nyren, O. & Hammarstrom, M. Prevalence of symptomatic pelvic organ prolapse in a Swedish population. *International urogynecology journal and pelvic floor dysfunction* **16,** 497–503, doi: 10.1007/s00192-005-1326-1 (2005).
45. Darzi, S. *et al.* Tissue response to collagen containing polypropylene meshes in an ovine vaginal repair model. *Acta biomaterialia* **39,** 114–123, doi: 10.1016/j.actbio.2016.05.010 (2016).
46. de Tayrac, R., Alves, A. & Therin, M. Collagen-coated vs noncoated low-weight polypropylene meshes in a sheep model for vaginal surgery. A pilot study. *International urogynecology journal and pelvic floor dysfunction* **18,** 513–520, doi: 10.1007/s00192-006-0176-9 (2007).
47. Ulrich, D. *et al.* A Preclinical Evaluation of Alternative Synthetic Biomaterials for Fascial Defect Repair Using a Rat Abdominal Hernia Model. *(Alternative Biomaterials for Fascial Defect Repair).* **7,** e50044, doi: 10.1371/journal.pone.0050044 (2012).
48. Ulrich, D. *et al.* Changes in pelvic organ prolapse mesh mechanical properties following implantation in rats. *American journal of obstetrics and gynecology* **214,** 260.e261-268, doi: 10.1016/j.ajog.2015.08.071 (2016).

Acknowledgements

This work was supported by the National Health and Medical Research Council (NHMRC) of Australia Project grant #1081944 (CEG, JAW, JA, AR), a NHMRC Senior Research Fellowship #1042298 (CEG), and the Victorian Government's Operational Infrastructure Support Program. JA is funded by a South Australian Premier's Professorial Fellowship.

Author Contributions

S.E. performed the experiments, collected and assembled the data, analysed the data, and wrote manuscript. N.Y., A.R., L.P., S.L.E., A.V., J.W. performed the experiments, collected and assembled the data. M.D., K.E., C.L. analysed the data. C.E.G., J.A.W., A.R., and J.A. conceived and designed the experiments, provided the financial support, helped with data analysis and interpretation, editing and final approval of manuscript.

Additional Information

Supplementary information accompanies this paper at http://www.nature.com/srep

Competing Interests: The authors declare no competing financial interests.

How to cite this article: Emmerson, S. *et al.* Ovine multiparity is associated with diminished vaginal muscularis, increased elastic fibres and vaginal wall weakness: implication for pelvic organ prolapse. *Sci. Rep.* **7**, 45709; doi: 10.1038/srep45709 (2017).

Publisher's note: Springer Nature remains neutral with regard to jurisdictional claims in published maps and institutional affiliations.

This work is licensed under a Creative Commons Attribution 4.0 International License. The images or other third party material in this article are included in the article's Creative Commons license, unless indicated otherwise in the credit line; if the material is not included under the Creative Commons license, users will need to obtain permission from the license holder to reproduce the material. To view a copy of this license, visit http://creativecommons.org/licenses/by/4.0/

© The Author(s) 2017

Chapter 3

Optimisation of an ovine surgery model in preclinical trials of endometrial mesenchymal stem cell-seeded polyamide/gelatin tissue engineering constructs for treatment of pelvic organ prolapse.

Declaration

Monash University

Declaration for Thesis Chapter 3

In the case of Chapter 3, my contribution to the work involved the following:

Name	Nature of Contribution	Extent of contribution (%) for student co-authors only.
Stuart Emmerson	All experimental work. Manuscript Writing.	80%
Caroline Gargett	Scientific input	N
Jerome Werkmeister	Scientific input	N
Joan Melendez	Performed ovine surgeries	N
Sharon Edwards	PA+G mesh fabrication.	N
Anne Gibbon	Sheep anaesthesia & monitoring.	N
Ker Sin Tan	Technical assistance.	N
James Deane	Fluorescent Microscopy assistance.	N
Kirstin Elgass	ImageJ macros and image analysis	N
Shayanti Mukherjee	Ovine post-mortems	N

Student signature: **Date:** 10/06/2019

Introductory Statement

The ultimate fate of eMSC implanted *in vivo* as part of TE constructs, remains unknown. Our group has previously demonstrated that human eMSC do not persist beyond 14 days after being implanted in an immunocompromised rat model, suggesting their elimination by the host innate immune system. Autologous eMSC could be used to prevent host immune rejection, while labelling them with easy and quick non-biological labelling methods will answer many questions about their ultimate fate following implantation. However, this would require animal models that share close equivalence to women. To this end, ovine animal models are very promising due to their similar pelvic anatomy to women and ability to also undergo spontaneous POP. Additionally, with newly developed POP-Q methods for ewes, multiparous ewes with weakened vaginal walls can be specifically selected for participation in TE preclinical trials. This gives the investigation of stem cell-seeded TE constructs an animal model that are as close as possible to equivalence with POP-vulnerable women.

In this chapter, I first optimised the labelling of eMSC using superparamagnetic iron oxide nanoparticles (SPIONS), or IODEX and determined potential toxicity to eMSC. I then seeded IODEX+eMSC onto polyamide/gelatin (PA/G) scaffolds to create eMSC/PA/G constructs that were planted into the vaginal walls of multiparous ewes that were selected for vaginal wall weakness. I determined that IODEX is a useful eMSC labelling tool due to the ease and speed of labelling and its non-toxicity and vivid cellular labelling. I also observed that PA/G constructs integrated poorly into the vaginal walls, with high rates of exposure that masked any potential benefit the implanted eMSC might have had over the host immune system. Finally, I confirmed the persistence of IODEX+eMSC at 7 days in vaginal tissue and assessed the clonogenicity of eMSC samples before implantation.

I want to thank Ker Sin Tan for her invaluable help with laboratory experimental work and teaching me the necessary protocols. I also want to thank Dr Anne Gibbon and Dr Joan Melendez for their assistance with sheep gynaecological surgery, animal monitoring and post-mortems. I also want to thank Dr Sharon Edwards and Aditya Vashi of CSIRO for their assistance with the PA/G mesh preparation that I used throughout my study, and Dr Shayanti Mukherjee for her assistance during sheep post-mortems. Finally, I wish to thank Dr Kirstin Elgass for her help in image analysis and Dr James Deane for his help with the fluorescent microscopy.

3.1. Abstract

Tissue Engineering (TE) constructs that utilise biocompatible scaffolds with stem cells are a promising treatment for some clinical challenges faced by conventional medicine. However, little is known about the ultimate fate of implanted stem cells. Current efforts to track stem cell fate and migration are limited by various labelling methods and this study seeks to optimise a relatively new technique for labelling cells with iron oxide (IODEX) nanoparticles for tracking autologous endometrial mesenchymal stem cells (eMSC) during *in vivo* implantation. Here, IODEX labelling dosage was optimised to 10µg/100,000 cells. This labelled over 90% of cells and was not toxic. IODEX was retained within the cytoplasm following a week of cellular proliferation *in vitro*. Ovine $CD271^{+}/CD49f^{-}$ eMSC purity correlated with clonogenicity yet also varied considerably between ovine samples within the same passage numbers. The final IODEX-labelled eMSC were generally from passage 3 cells where the $CD271^{+}/CD49f^{-}$ purity varied from 23% to 64%. Adjusted equal concentrations of purified and labelled eMSCs were seeded onto polyamide/gelatin mesh (PA/G) and implanted into the vaginal walls of multiparous ewes that had been specifically selected for vaginal wall weakness as a large animal model of POP. Autologous eMSC were detectable after 7 days. However, PA/G implants were characterised by poor tissue integration, extensive folding and high rates of mesh exposure. This study shows the promising use of Pelvic Organ Prolapse-Quantification (POP-Q) selected ewes for use in future preclinical trials that feature nanoparticle-labelled eMSC for modulating wound sites in MSC-based TE in treating POP.

3.2. Introduction

Tissue engineering (TE) is a method of combining cells with scaffold materials to create a composite that can provide regeneration of damaged or lost tissue, such as muscle tissue and organs. The synthetic material used within TE typically provides a scaffold into which cells are incorporated to either re-grow tissues or organs or to accelerate healing by paracrine mechanisms when implanted into recipient host wound sites [209, 210]. TE approaches that utilise stem cells are common and the most promising, due to their ability to self-renew and differentiate into desired cell types. Such constructs have been used in developing new blood vessels [211], replaced damage cartilage[212] and making progress towards growing an entire bladder [213]. Advancement in this promising field requires the refinement of suitable scaffolding and ideal stem cell types.

There most commonly used transvaginal mesh is composed of polypropylene (PP) due to its strength, chemically inert nature and ease of production. However, the rates of adverse effects associated with PP mesh, such as exposure, fibrosis and chronic inflammatory responses, is cause for concern, and our previous research compared PP mesh with new meshes knitted from polyamide (PA) and polyamide with a gelatin coat (PA/G). When comparing PP, PA and PA/G mesh in rat and mice models, we observed the PA and PA/G mesh evoked a greatly reduced immune response compared to PP, while simultaneously improving collagen organisation and exhibiting biomechanical properties closer to that of human vaginal tissue [33, 34]. These advantages make the PA/G very attractive for advancement into preclinical trials for combining stem cells with mesh scaffolding for POP treatment.

The ideal cell type for TE use needs to be easily obtainable, accepted by the recipient immune system and effective in their purpose. Induced pluripotent stem cells (iPSC) have shown promise in this direction for an autologous source, but generating these cells is an expensive, time consuming and demanding process that makes them ill-suited for rapid, personalised medicine [214, 215]. Human embryonic stem cells (hESC) have also seen utilisation in tissue engineering, but the employment of these cells has ethical concerns and controversy [216]. In recent years, Mesenchymal Stem Cells (MSC), which are adult stem cells that can be isolated from most tissues, have emerged as a promising alternative [217, 218]**.** Among these, endometrial mesenchymal stem cells (eMSC) are an ideal choice as they can be acquired by a simple office-based procedure, are highly clonogenic, self-renew, can differentiate into various mesodermal lineages and have reported immune-modulating properties [34, 96]. These cells

have been proposed as a potential treatment for pelvic organ prolapse (POP). The ease of eMSC acquisition has seen their increasing use for pre-clinical *in vivo* research in animal models such as rats and mice using human eMSC [32, 34]. Our prior characterisation of ovine eMSC has marked them for investigation as a source of autologous cells for MSC-based therapy for POP, particularly after characterising the effect of parity on the ovine vaginal wall [219]. However, the persistence of eMSC following implantation remains an issue as few grafted stem cells remain detectable beyond 14 days [34]. Whether these cells are diminishing due to the host immune response or undergoing cell death is unclear. Tracking implanted eMSC will help determine their fate and role during implantation.

Fluorescent labelling and microscopy have been the methods of choice for detecting labelled cells from *in vitro* cultures and explanted *in vivo* tissues due to their ability to distinguish between target cells and surrounding tissues. There are several different ways of fluorescently labelling cells with different methods being suitable for different needs. Cellular dyes that stain the membrane of cells can be suitable for short-term tracking but are not persistent to permit long-term tracking of cells *in vivo* due to the eventual diminishment of the dye. Genetic labelling involves the use of lentiviral vectors that insert fluorescent protein genes into the host cell genome, permitting targeted and specific long-term tracking of implanted cells *in vivo* and has been demonstrated to persist for at least six months [220-223]. However, the process of genetically labelling cellular chromatin to express such marker proteins is costly, lengthy and, if such cells are to be implanted into farm animal models, may encounter formidable regulatory hurdles from government agencies such as in Australia. An additional risk with genetic labelling is the chance, however unlikely, of unwittingly creating point-mutations via insertion of vectors into the cellular genome [224]. A third option is cytoplasmic labelling with inorganic particles, such as dextran-coated Iron-Oxide ("IODEX"). IODEX are superparamagnetic iron oxide nanoparticles (SPIONs) conjugated with fluorescein isothiocyanate (FITC) that enter the cytoplasm of target cells via the tat protein, and which can be detected using fluorescent microscopy [225]. Their versatility is evidenced by their use to track cells implanted into ovine spinal columns for up to eight weeks [226]. The magnetic properties of the particles themselves has allowed their detection using magnetic resonance imaging (MRI) [227]. The lack of reported toxicity and the speed and ease with which they can be used to label target cells makes IODEX nanoparticles an attractive alternate to dyes or genetic labelling. However, as of writing this, no publication has investigated either potential toxicity of IODEX within eMSC cells or their retention within the cytoplasm following proliferation.

This was a pilot study to first optimise the concentration of IODEX nanoparticles for labelling ovine eMSC. We then implanted IODEX+eMSC seeded PA/G constructs into the vaginal walls of Pelvic Organ Prolapse-Quantification (POP-Q) matched multiparous ewes in the establishment of a new animal model for future preclinical trials of TE constructs in POP. We wished to also investigate any potential toxicity targeted cells and the retention of IODEX nanoparticles during eMSC proliferation was investigated in addition to the clonogenicity of eMSC or latter-passage eMSC populations.

3.3. Methods

3.3.1. Ethics and animals

Experimental procedures and animal husbandry were approved by the Monash Medical Centre Animal Ethics Committee A in accordance with the ethical guidelines of the National Health and Medical Research Council (NHMRC) of Australian Code for the Care and Use of Animals for Scientific Purposes 8th Edition. Border Leicester Merino (BLM) ewes were housed in the Monash Animal Research Platform in an enclosed barn or outdoor enclosures. Multiparous ewes aged 5-6 years (n = 19) who had undergone multiple lamb deliveries and delivered their last lambs at least 9 months prior were selected if they showed evidence of weakened vaginal tissue with POP-Q values lower than 0 at point Ap and at point Aa.

3.3.2. Ovine hysterectomy for collection of endometrial tissue

Subtotal hysterectomy was performed via ventral midline laparotomy on 7 ewes to collect endometrial tissue. Anaesthesia was induced by intravenous Medetomidine premedication (0.1-0.2 mg/kg), followed by intravenous Thiopentone (10mg/kg), and then maintained with Isoflurane (1-3% in 100% O_2). A short acting broad-spectrum antibiotic, Cefazolin (7.5mg/kg), was given intravenously prior to surgery, and a long-acting antibiotic, Duplocilin (5.75mg/kg), to continue coverage for 48 hours post-surgery. Suspensory ligaments of the ovary and feeding vessels to the uterus were ligated and transected before performing a supracervical amputation of the uterine body conserving the ovaries. Laparotomy was closed using absorbable sutures. Postoperative analgesia was with bupivacaine (5µg/ml) injection at the abdominal incision site. Pain relief was provided as Fentanyl (75µg/hr) transdermal patch applied before start of surgery and maintained for 3 days for postoperative pain relief, Carprofen (2mg/kg) given subcutaneously at start of surgery and Bupivicaine (6-10mL) given subcutaneously under the

incision line at end of surgery. The ewes recovered for up to four weeks from the abdominal surgery before they underwent vaginal surgery. They were housed at the Monash Medical Centre Animal Facilities/Monash Animal Research Platform (MMCAF/MARP) animal facility on Clayton campus in individual mobile cages/individual pens in sight of other ewes and moved into small holding pens as they recovered. The excised uterus was placed in ice-cold transport medium (HEPES-buffered DMEM/F-12 medium (Invitrogen) supplemented with 1% antibiotic Anti-Anti (100X, Life Technologies) (Bench Media), stored at 4°C and processed within 18 hours, as previously described.

3.3.3. Isolation of Ovine eMSC by Flow Cytometry Sorting Using CD271

Ovine eMSC were isolated from hysterectomy tissue as previously described [129]. Isolated cells (up to 1 x 10^7 cells/100µl) were incubated with phycoerythrin (PE)-conjugated anti-human CD271 (1:10, mouse IgG1; Miltenyi Biotec) and allophycocyanin (APC)-conjugated anti-human CD49f (1:10, clone GoH3, rat IgG2a; Miltenyi Biotec) in 2% fetal bovine serum/PBS (FBS/PBS) for 30 min on ice in the dark. Cells were then washed and resuspended in 1 µM Sytox Blue (Life Technologies) to distinguish live and dead cells. CD271+/CD49f-eMSC were isolated using fluorescence activated cell sorting (FACS) using a MoFlow flow cytometer (Beckman Coulter) or an Influx flow cytometer (Becton Dickinson Biosciences) using Monash University Flow Core services.

3.3.4. Cell Culture

Freshly sorted $CD271^+/CD49f^-$ cells were cultured in stromal medium containing DMEM/F-12 (Life Technologies), 10% fetal bovine serum (Life Technologies), 2 mM glutamine (Life Technologies), 0.5 mg/ml primocin antibiotic and incubated at 37°C in 5% CO_2. Medium was changed every 2–3 days and cells were passaged at 80% confluence.

3.3.5. IODEX Labelling for Optimisation and Implantation

Four batches of $1x10^5$ CD271+/CD49f-eMSC (Passage 3) were seeded separately in 6-well plates (BD Biosciences) and immediately incubated with four different concentrations of IODEX: 0.0µg (negative control), 1µg, 5µg and 10µg/100,000 cells. Cells were trypsinised after 6 hours using TrypLE™ (Life technologies, #12604-021) and processed for Flow Cytometry analysis as previously described [129]. For implantation, P2-4 cells were labelled with FITC-labelled IODEX paramagnetic particles at 10µg/100,000 cells concentration for 24

hours in 37°C incubator. Cells collected after trypsinisation were washed and resuspended in 100,000 cells/100 µl Bench Media.

3.3.6. Detection of IODEX+ eMSC in Cadaver Tissue - Proof of Concept

Four batches of $1x10^5$ CD271+/CD49f-eMSC (Passage 3) were incubated with 5ug/100,000 (n=2) and 10ug/100,000 (n=2) IODEX. After 6 hours, cells were collected and subcutaneously injected into the flanks of fresh C57BL/6 mouse cadavers, kept on warm surgical mats. After 30 minutes, the flanks were removed and fixed with 4% paraformaldehyde (PFA) overnight, before placing into 30% sucrose for 24 hours and then finally frozen in OCT. OCT blocks were cut into 8µm sections for immunofluorescent imaging at Monash Histology Platform (MHP).

3.3.7. Fluorescence Microscopy

Paraformaldehyde fixed frozen sections were stained with Hoechst 33258 (Molecular Probes) for 5 minutes to mark the cell nuclei. Slides were then mounted with fluorescent mounting medium (Dako). Confocal Microscopy was performed using MHTP Olympus FV1200 Confocal using Olympus CellSens software to detect FITC.

3.3.8. Toxicity and Retention

Six batches of $1x10^5$ CD271+/CD49f-eMSC (Passage 3) were seeded separately in 6-well plates (BD Biosciences) with 10ug/100,000 cells IODEX for 6 (n=2), 12 (n=2) and 24 (n=2) hour incubation. Media was then aspirated and replaced with fresh stromal medium, and cultures incubated for 6 days with fresh media changes every 2 days. Cells were then trypsinised, collected and prepared for flow cytometry analysis (see above).

3.3.9. Clonogenicity of IODEX-labelled eMSC

For colony forming assays, cells were seeded at very low seeding densities of 6-32 cells/cm^2 onto fibronectin-coated (10ug/ml, BD Biosciences) 10cm dishes (BD Biosciences) and cultured in stromal medium [129]. Colonies were monitored to ensure they were derived from single cells. Clonal cultures were fixed in 4% PFA at day 12 and stained with haematoxylin. Cloning efficiency was determined on plates yielding non-overlapping clones with >50 clones to ensure sufficient clones/plate for statistical purposes.

3.3.10. Fabrication of PA/G Meshes

PA meshes were fabricated from 80µm monofilament warp knitted into a pattern with large pore area of 0.99 +/- 0.10 mm, small pore area of 0.04 +/- 0.02 $mm^2$and weight of 42 g/m^2, similar to, but not identical to previously described heavier meshes using 100 µm monofilament [31, 33]. For PA/G constructs, PA mesh was dip-coated in 12% porcine gelatin (Type A, 300 bloom; Sigma; USA) in water. Once fully wet, the meshes were placed on ice-cold 0.5% glutaraldehyde (Sigma) for 8 minutes on each side to cross-link the gelatin, followed by 2% w/v glycine (Merck; Australia) in water for 15 minutes at RT, then 2% v/v H_2O_2 (Merck) in water for 15 minutes at RT, and 4% w/v glycerol (Merck) in water for 15 minutes at RT with washing steps in water in between. Mesh was air-dried and sterilised by gamma irradiation at 25 kGy prior to implantation [33].

3.3.11. Preparation of Autologous Ovine eMSC-seeded Mesh Constructs

Prior to seeding, PA/G 30 x 20 mm mesh pieces were soaked in 1:50 Anti-Anti (100X) antibiotic for 1 hour at 37°C, then transferred to 20µg/ml fibronectin (Sigma-Aldrich, Saint Louis) overnight at 37°C. PA/G meshes were manually seeded on the stabilized gelatin using a pipette at a seeding density of 100,000 cells/cm^2 in 100 ul medium/mesh (600,000 cells/mesh) and cultured for 24h and checked for cell adherence, and transported in bench medium on ice for surgical implantation. These constructs were termed eMSC/PA/G. Control meshes without cells underwent the same procedure but without cells and termed PA/G.

3.3.12. Transvaginal Surgery - Implantation of PA/G with and without eMSCs

BLM ewes were anaesthetised using the same protocol as for hysterectomy. Antibiotic prophylaxis was given. Ewes were placed into lithotomy position and POP-Q measurements were taken. Hydro dissection of the vaginal tissue layers was achieved with 20ml of lidocaine with 1ml of adrenaline (Aspen Pharmacare Australia, 1mg/ml). For 13 sheep having mesh implantation, a 40 mm, full-thickness midline vertical incision was made through the mucosa on the posterior vaginal wall and blunt dissection was used to open the rectovaginal space. eMSC/PA/G (n=7, using autologous cells) and PA/G (n=6) were surgically implanted by gynaecologist J Melendez. All inserted meshes were fixed with absorbable sutures into the rectovaginal space, and the vaginal mucosa closed using absorbable sutures. Ewes receiving cells were implanted with a tissue engineering construct delivering their own eMSC. For incisional controls (n=6), the vaginal incision was performed without placement of mesh and closed using absorbable sutures. Pain relief was with subcutaneous Carprofen (2mg/kg) given

at start of surgery and bupivicaine (6-10mL) given subcutaneously at the incision site at end of surgery.

3.3.13. Post Mortem and Harvest of ovine Vaginal Mesh/tissue Complexes

Ewes were euthanised after 30 days using Lethabarb (110mg/kg, Virbac (Australia) Pty Limited,) and POP-Q measures were taken immediately. The entire vaginal tract was removed with adjacent tissues, trimmed and incised in a longitudinal manner adjacent to the urethra (anterior wall) from the muco-cutaneous junction to the cervix and dissected for analyses as shown in **Figure 1**. The distal mesh/tissue complex was dissected into further pieces for histology and qPCR (in RNAlater) analyses, and biomechanical analysis (Bm, not performed due to poor mesh/tissue integration). Tissues for histology were fixed in 10% formalin and then processed to paraffin or 4% paraformaldehyde overnight, then placed in 30% sucrose for 48 hours and frozen in OCT.

3.3.14. Histology

Formalin fixed paraffin embedded tissues were sectioned at 4μm and stained with Haemotoxylin and Eosin (H&E), Masson's Trichrome and Hart's elastic fibre stain in the Monash Histology Platform (MHP) facility using previously published methods [219]. OCT-embedded tissue was cryosectioned into 8μm sections for immunohistochemistry and immunofluorescence staining.

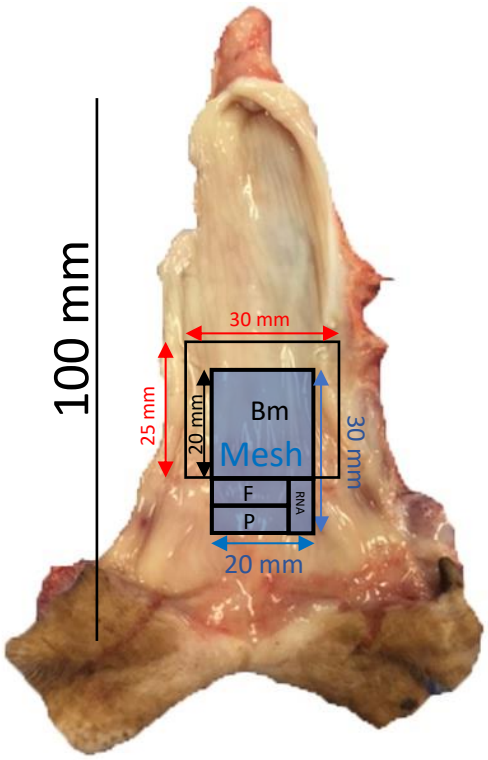

Figure 1: Dissection of ovine vaginal tissue at post-mortem. Blue region is mesh, black outlines sections of tissue retrieved for biomechanical (Bm), histological (F, frozen and P, paraffin) and qPCR (RNA) analysis.

3.3.15. Immunofluorescence and IODEX+eMSC *in vivo* Detection

Frozen sections were thawed and blocked with protein block (Dako) for 1 hour at RT, and immunostained with mouse anti αSMA to mark smooth muscle bundles or anti-CD45 antibodies to mark total leukocytes **(Table 1)** for 1 hour at RT. Isotype-matched antibodies (Dako Mouse IgG1) were used as negative controls and applied at the same concentrations. Anti-mouse Alexa-Fluor-568-conjugated secondary antibody (Thermo Fisher Scientific) was then incubated for 30 minutes at RT for both primary antibodies. The same procedure was followed for Ki-67 staining (rabbit anti Ki-67 antibody kindly donated by the Moss Laboratory, Hudson Institute of Medical Research), with donkey anti-rabbit-Alexa Fluor 568 f and Rabbit IgG1 isotype (Thermo Fisher Scientific) used for negative control. Nuclei were stained with Hoechst 33258 (Molecular Probes) for 5 minutes and the slides were mounted with fluorescent mounting medium (Dako). Direct fluorescent microscopy was also used to track the IODEX+eMSC *in vivo* on frozen sections following Hoechst 33258 nuclei staining. All fluorescent microscopy used an MHTP Olympus FV1200 Confocal Microscope and Olympus CellSens software was used for image acquisition.

3.3.16 Immunohistochemistry Image Analysis

Frozen sections were washed 3 times with PBS then protein block (Dako Glostrup, Denmark) was applied for 30min at RT. After three washes in PBS, sections were incubated with primary antibodies (CD45, CD86 and CD163, **Table 1**) for one hr at 37°C. Mouse IgG1 isotype control antibody (Dako) was used as the negative control at the same concentration. Sections were washed 3 times with PBS followed by anti-mouse secondary antibody HRP-labelled polymer (Dako) for 40mins at RT, washed in PBS and chromogen added (3,3′-diaminobenzidine) (Sigma-Aldrich, St. Louis USA) for 3 min as previously published [27]. Slides were mounted in DPX (Sigma-Aldrich). Images were taken at 10x magnification using an Olympus BX61 light microscope and Olympus cellSens software and analysed using ImageJ software. Using custom macros provided by Dr Kirstin Elgass, Monash University Micro Imaging, Monash Health Translational Precinct (MHTP), a region was drawn either around mesh filaments, or the edge of the implant tissue interface if no mesh filaments were present. Analyses were then conducted in a 50µm increment around either mesh filaments or adjacent tissue edge, using the same colour deconvolution method as previously reported [219]. Five to 10 images per sample of regions containing mesh filaments were taken

Table 1: Antibodies used for immunostaining.

Primary Antibodies	Final Concentration (µg/mL)	Isotype	Supplier
CD45	0.5	Mouse IgG1	BioRad
CD86	0.5	Mouse IgG1	BioRad
CD163	0.5	Mouse IgG1	BioRad
A-Smooth Muscle Actin (αSMA)	0.71	Mouse IgG2a	Dako
Ki-67	1.0	Rabbit IgG1	Thermo Fisher Scientific

3.3.17. Statistical Analysis

All data were analysed using GraphPad Prism 7.02 for Windows 10 64-bit, (GraphPad Software, La Jolla California USA) and initially assessed for normality using Shapiro-Wilk or Kolmogorov-Smirnov tests. Image analysis of histological data was assessed using a 1-Way ANOVA with Tukey's multiple comparison post hoc test. Kruskal-Wallis with Dunn's multiple comparisons test were used for non-parametric data. Regression analysis was performed using Microsoft Excel Version 1808 (Build 10730.20304).

3.4. Results

3.4.1. Optimal IODEX Concentration for Labelling Ovine eMSC

For an autologous cell-based therapy it is essential to label the transplanted cells to track their movements following implantation. Three groups of eMSC each received an increasing dose of IODEX nanoparticles while another was left blank to serve as a control. Labelling was assessed by flow cytometry after 6 hours **(Fig 2)**. FITC+eMSC (%) increased with concentration (µg/cells) until 5µg/100,000 at which point it plateaued where both 5µg **(Fig 2C)** and 10µg **(Fig 2D)** of IODEX per 100,000 cells labelled close to 100% of ovine eMSC within 6 hours. Both 5µg and 10µg concentrations were used for further IODEX-labelling optimisation.

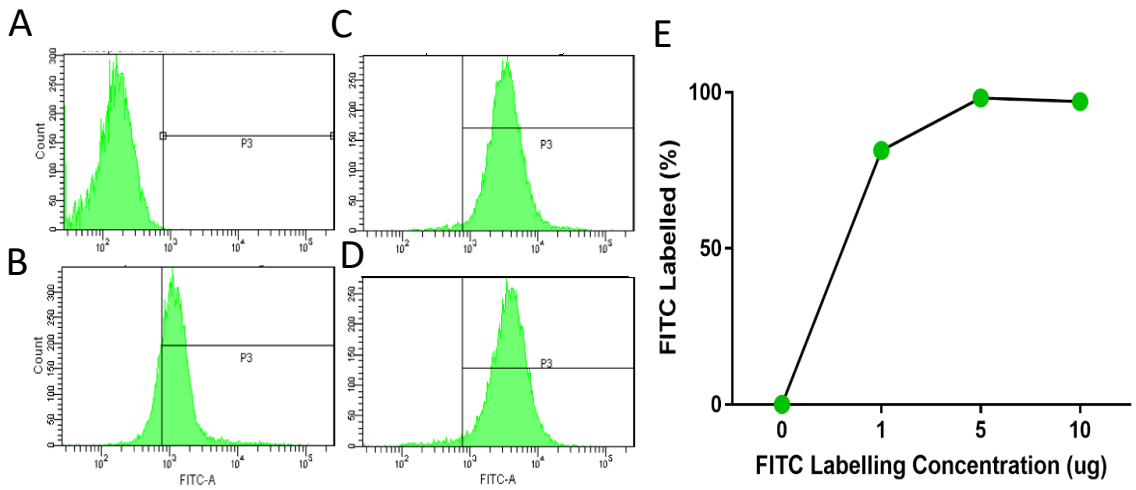

Figure 2: IODEX labelling optimisation for ovine eMSC: Flow Cytometry was used to determine the degree of IODEX-FITC labelling at different concentrations after 6 hours incubation at **A)** 0.0µg (control), **B)** 1µg, **C)** 5µg and **D)** 10µg of IODEX per 100,000 passage 2-3 cells. **E)** Graphical representation of flow data.

3.4.2. IODEX+eMSC are Detectable in Explanted Mouse Tissue

To measure and optimise our ability to image IODEX+eMSC in tissues following implantation, IODEX+eMSC were injected into the flanks of mouse cadavers. IODEX^{+}eMSC was injected immediately following animal culling, tissue was harvested after 30 minutes and subjected to fluorescent imaging. Several IODEX+eMSC clusters were observed, which were distinct from surrounding cells due to the IODEX-FITC conjugate **(Fig 3)**, at both 5µg/100,000 (**Fig 3A)** and 10µg/100,000 cells **(Fig 3B)**. However, 10µg/100,000 cells were much more vibrant and clearly visible due to greater IODEX saturation per cell **(Fig 3B)**.

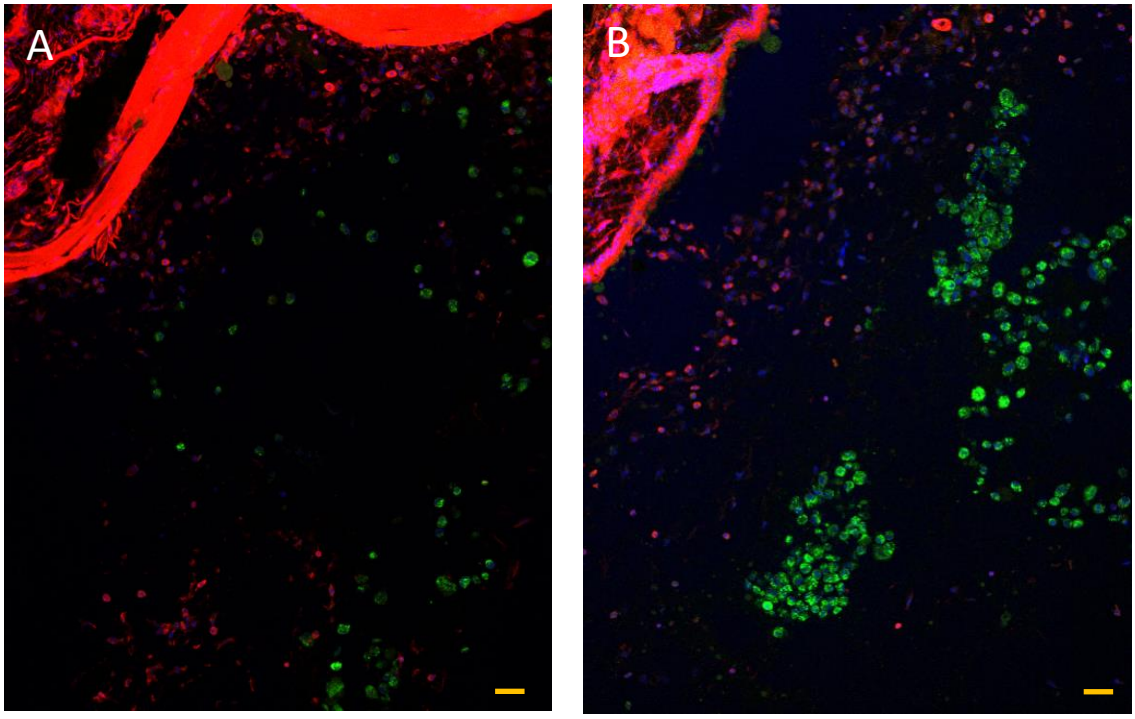

Figure 3: IODEX+eMSC detection *in vivo*: IODEX+eMSC were injected into the flanks of fresh C57BL/6 mouse cadavers at two concentrations: **A)** 5µg and **B)** 10µg per 100,000 cells. Scalebars – 100µm.

3.4.3. Lack of IODEX Toxicity on eMSC and Signal Dilution by Cellular Proliferation

To determine any potential IODEX cellular toxicity, 1x10^{5} ovine eMSC were labelled with 10µg IODEX/100,000 eMSC for 6, 12 and 24 hours (each n=2) and maintained in culture for 6 days post labelling. All incubation times revealed no loss of cells between experimental groups **(Fig 4A)**. After 6 days, all groups had increased cell numbers around 7-fold with just under 3 cell doublings over the 6 days. After 6 days of cell proliferation, cells were analysed by flow cytometry for (%) FITC^{+} IODEX retention and approximately 20% of IODEX was retained by the eMSC incubated with IODEX for 24 hours **(Fig 4B)** which was the highest retention of any incubation time. Though 6 hours was proven sufficient for IODEX labelling

of eMSC (as seen in 3.1), 24 hour incubation time permitted greater uptake of IODEX by eMSC, which is likely why more was retained after 6 days. This could be confirmed in future studies that use FACS to measure fluorescent intensity per cell.

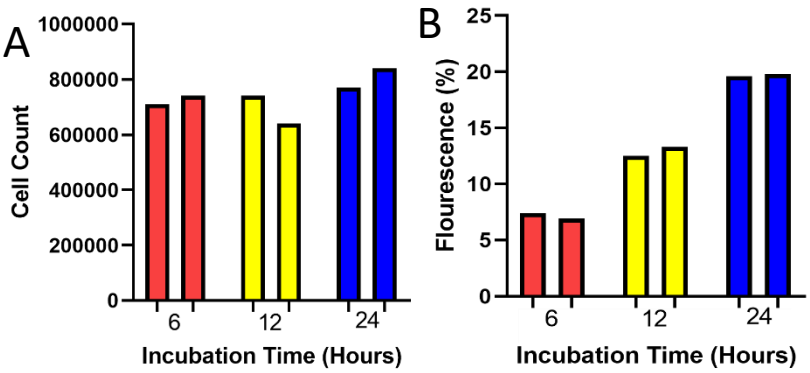

Figure 4: IODEX toxicity and retention during proliferation in vitro: eMSC ($1x10^5$ cells/well) were labelled with 10µg/100,000 FITC-IODEX for several different incubation times (X axis) and cultured for 6 days, then analysed for %+ FITC labelled cells by flow cytometry **A)** raw counts **B)** % FITC+. (each time-point n=2)

3.4.4. eMSC Purity Correlates with eMSC Clonogenicity

To determine if $CD271^+/CD49f^-$ (%) purity in ovine eMSC cultures reflected MSC purity, cloning efficiency was examined using replicate samples of eMSC intended for eMSC/PA/G implantation. Cloning efficiency correlated with the $CD271^+/CD49f^-$ (%) purity **(Fig 5)** with R^2 =0.46, though the y-intercept was not significant (p=0.3251). The cells used were Passage 2 (n=1), Passage 3 (n=4) and Passage 4 (n=1), and a drop in $\%CD271^+/CD49f^-$ occurred with increasing passages **(Table 2)**. There was also considerable variance for samples within the same-passage number, with a variance of 41% between the highest and lowest $CD271^+/CD49f^-$Passage 3 samples. This could be due to the length of time each sample spent in culture to generate sufficient numbers of cells. It is possible that significance can be gained by the use of more samples. Though not statistically significant, the trend does align with current literature which has observed a decline in the clonogenicity of stem cells in sequential passages [209], and eMSC are no exception. This result encouraged the use of eMSC at as low a passage as possible.

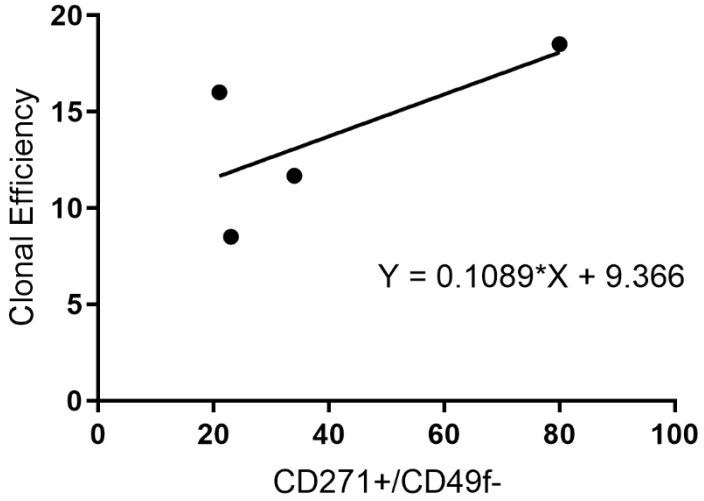

Figure 5: Correlation between % ovine eMSC and clonogenicity: Clonal assays were performed using eMSC before implantation. $R^2 = 0.46$, p=0.3251.

Table 2: Passage number and $CD271^+/CD49f^{neg}$ purity of implanted eMSC

Passage Number	CD271+/CD49f- (%)
2	80
3	64
3	55
3	30
3	23
4	21

3.4.5. Ovine Demographics

Given that some multiparous ewes have evidence of weakened vaginal walls [183, 204], multiparous ewes were selected on a common and comparable characteristic the POP-Q measurement at 2 points of the vaginal wall. The POP-Q system has been adapted for ewes [183] in which tissue distensibility is measured at three key points, Posterior Point A (Ap), Anterior Point A (Aa) and Anterior Point B (Ba) (See Section 1.6.8, Chapter 1). As Ap was the location receiving the implants and Aa was on the anterior less accessible location for surgical implants), ewes with an Ap and/or Aa value between -1 to 1 (-3 is normal) were selected as

having vaginal wall weakness and were distributed into three similar experimental groups (PA/G, eMSC/PA/G and Incision control) **(Table 3)** with matched Aa (p=0.8483) and Ap (p=0.7776) measurements.

Table 3: POP-Q Measurements for experimental group selection

	PA/G	eMSC/PA/G	Incision	p-value
Ap	0 (-1 - 0)	0 (-1 - 0)	0 (-1 - 1)	0.7776
Aa	0 (-1 - 1)	0 (-1 - 1)	0 (-1 - 1)	0.8483

Data are median (range) at POP-Q points Ap, Aa; PA/G; polyamide gelatin +/- eMSC.

3.4.6. PA/G Constructs Integrate Poorly into Ovine Vaginal Tissue

As this was our first experience in using transvaginal mesh surgery in the ovine model, a pilot study was conducted, and the ewes were assessed only 7 days following implantation of the constructs. H&E staining was used to determine the anatomical effect of PA/G construct implantation on the vaginal wall. A significant disruption to the muscularis and lamina propria of the vaginal wall was observed in both PA/G **(Fig 6A)** and eMSC/PA/G **(Fig 6B)** explants, with mesh folding a prominent characteristic of each explant. In our initial explants blood clotting around the implanted mesh **(Fig 6A)** was observed, so all subsequent procedures in ewes included adrenaline in the hydro dissection fluid to minimize bleeding. This resulted in no blood clots **(Fig 6B)**. One of the most common adverse effects of commercial transvaginal mesh is exposure through the vaginal wall. Exposure rates were between 17% (PA/G) and 33% (eMSC/PA/G) of implanted constructs **(Table 4)**.

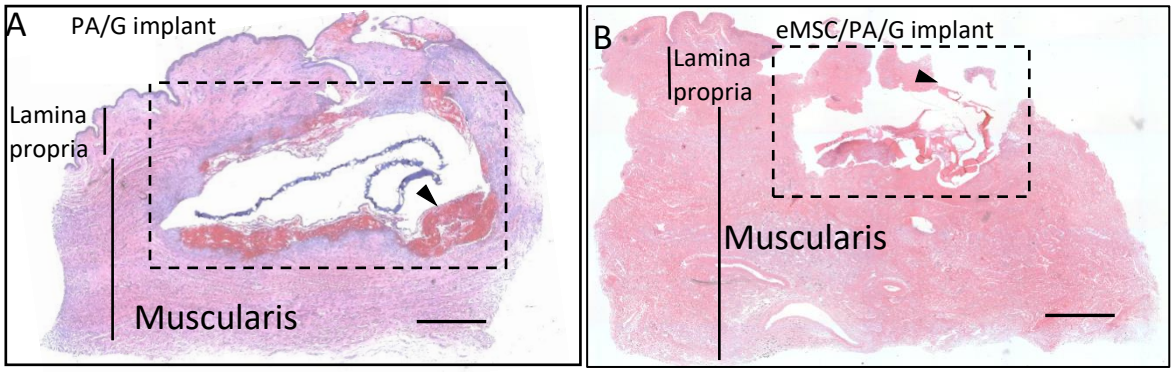

Figure 6: Poor Mesh/Tissue integration of eMSC/PA/G and PA/G constructs into the ovine vaginal wall of multiparous ewes: H&E stained vaginal wall sections showing, PA/G constructs **A)** without and **B)** with eMSC after 7 days. Note the blood clot (black arrow) in (A) and the exposure of eMSC/PA/G (black arrow) in (A). Scalebars – 2mm.

Table 4: Mesh exposure into the vaginal wall

	Exposure	No Exposure	p-value*
PA/G	1	5	0.505
eMSC/PA/G	2	4	

*Chi-square test

3.4.7. Implanted Autologous Ovine eMSC Persist for 7 Days

Fluorescent microscopy was used to first detect IODEX-labelled eMSC seeded on the PA/G constructs 1 day following labelling in culture **(Fig 7A).** As expected, the labelled cells were in close proximity to the TE construct, and the morphology of a blue nuclei surrounded by IODEX-FITC saturated cytoplasm is similar to my observation in the mouse cadaver proof-of-concept. Day 1 eMSC-IODEX cells are also vibrant in their cell labelling prior to implantation for 7 days. This contrasts with eMSC-IODEX cells in frozen sections of day 7 vaginal tissue explants in which the cytoplasm contains significant volumes of IODEX-FITC, but not enough to fully envelope the nuclei **(Fig 7B**, yellow arrows). The overall numbers of detected cells *in vivo* appear small relative to the numbers that were implanted; however this is a 4µm thick section of a $1cm^3$ block of tissue so the observed number of cells was expected. The detected eMSC were also all in close proximity to the gelatin upon which they had been seeded for implantation, suggesting that they had not migrated in the 7 days since their delivery into the wound site. Additionally, all of the IODEX particles were observed in the cytoplasm within the cytoplasm of the eMSC. No FITC fluorescence were recorded that would suggest eMSC were being taken up by macrophages. However, double staining with macrophage specific antibodies will confirm this.

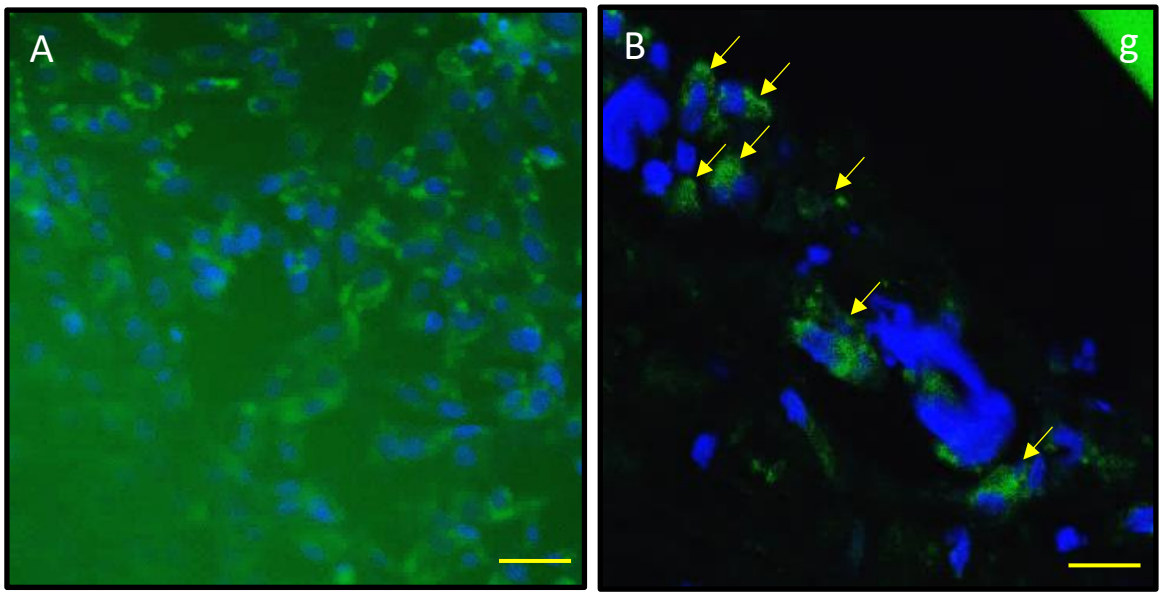

Figure 7: IODEX-FITC-labelled eMSC *in vitro* and *in vivo*: IODEX-labelled eMSC were cultured *in vitro* for **A)** 1 day and implanted into the ovine vaginal wall of the same ewe for 7 days. eMSC were observed with punctuate green nanoparticles in the cytoplasm (yellow arrows) in **B)** eMSC/PA/G explants close to the gelatin (g). Scalebars – 50µm.

3.4.8. Implanted eMSC do not Proliferate *in vivo* within 7 Days

To confirm if eMSC were proliferating *in vivo* following implantation, immunofluorescent staining was performed on frozen sections using Ki67 nuclear protein antibody, which can act as a marker of proliferation. Fig 8A shows positive Ki-67 staining in cells within positive control lamb neural tissue, with staining localised to the blue nuclei which produces a distinctive colour. This immunostaining was absent from all of the IODEX+eMSC sections that were analysed suggesting implanted eMSCs do not proliferate *in vivo* **(Fig 8B)**. There was very little Ki-67 staining in IODEX+eMSC frozen sections.

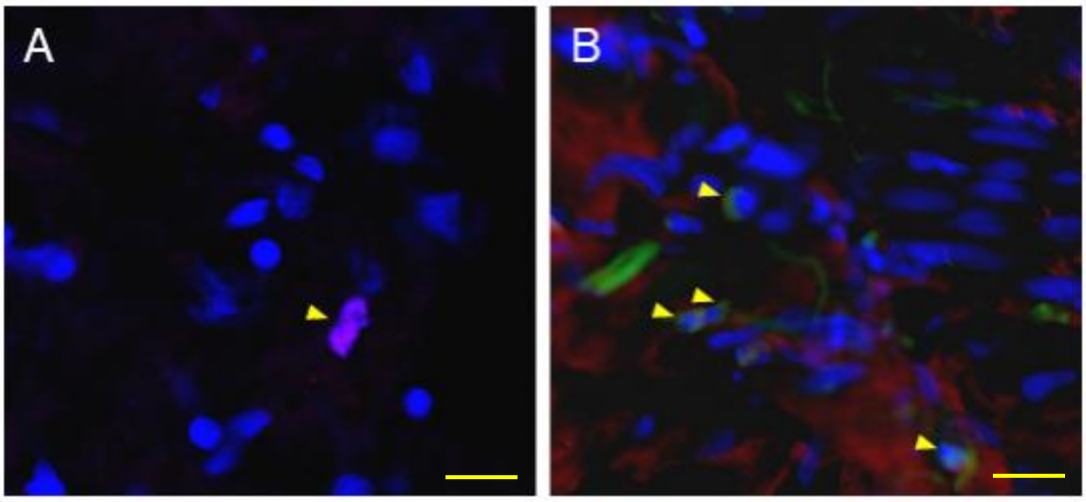

Figure 8: Ki-67 expression in proliferating cells *in vivo*: Frozen sections of **A)** positive lamb neural tissue where the proliferation-marker Ki-67 is localised to the nucleus of cells (yellow arrow). In explanted **B)** ovine eMSC/PA/G treated vaginal tissue, no IODEX+eMSC cells exhibited Ki-67 staining (yellow arrows). Scalebars – 50µm.

3.4.9. Implanted Autologous eMSC do not Alter Macrophage Phenotype by 7 Days

To assess the inflammatory response to implanted PA/G with and without eMSC, immunohistochemistry staining using the pan-leukocyte marker CD45 was undertaken on tissue explants **(Fig 9).** Fig 9A shows concentration of leukocytes at the tissue edge close to the implanted gelatin, similar to the gradient observed in prior experiments in rat models [210]. Similar levels of macrophages were revealed with PA/G and eMSC/PA/G meshes within a 0-50µm increment of the mesh tissue interface and, although appeared higher than the incision control, this was not significant. **(Fig 9D)**. To determine the specific macrophage populations surrounding the implant, sections were stained with CD86 antibody for M1 macrophages **(Fig 9B)** and CD163 antibody for M2 macrophages **(Fig 9C)**. The M1 and M2 response was similar for all groups **(Fig 9E-F).** The staining for M1 and M2 macrophages is noticeably less than that of the pan-leukocyte marker CD45+, which suggests an increased presence of non-macrophage white blood cells such as neutrophils and monocytes, both of which are present early within the wound healing process.

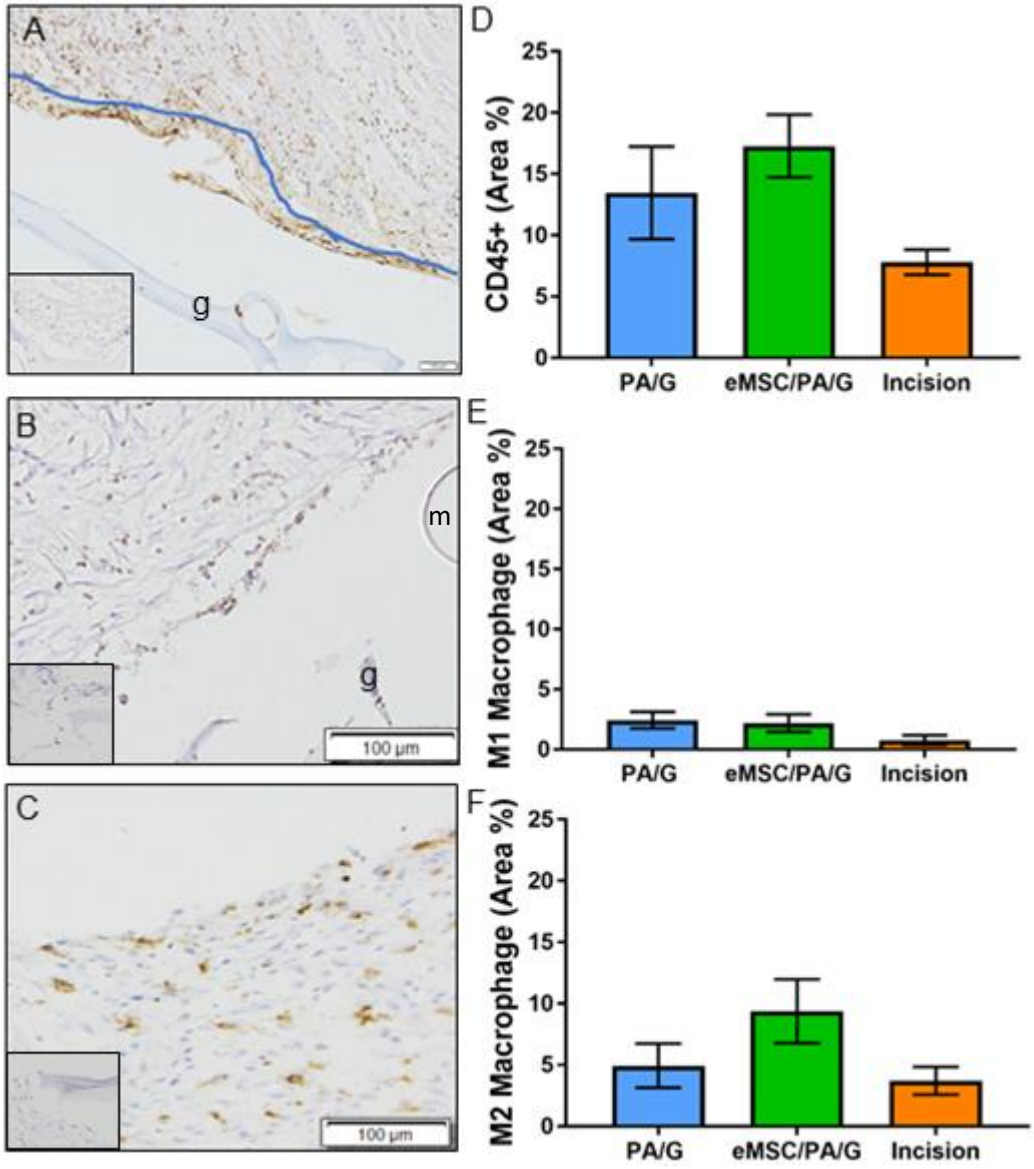

Figure 9: Immune response at the mesh-tissue interface of implanted PA/G constructs after 7 days: A) CD45+ leukocytes (brown), **B)** CD86+ M1 macrophages and **C)** CD163+ M2 macrophages in PA/G explants were analysed in the 0-50µm increment around the mesh implant (blueline). Graphs showing image analysis quantification of % positive stained area for **D)** CD45+ leukocytes, **E)** CD86+ M1 macrophages and **F)** CD163+ M2 macrophages. Insets are negative controls. g, gelatin, m, mesh filament. Scalebars – 100µm. Data are mean +/- SEM from n=6 animals/group, except eMSC/PA/G n=4

3.5. Discussion

The main findings of this pilot optimisation study were demonstrating the feasibility of using POP-Q selected ewes for TE construct implantation and tracking, the successful labelling and detection of IODEX^{+}eMSC *in vivo* and the lack of *in vivo* proliferation of implanted eMSC. Continued culture of CD271^{+}/CD49f^{-} showed loss of eMSC marker purity with corresponding lower clonal efficiency. Finally, PA/G and eMSC/PA/G TE constructs implanted into the weakened vaginal walls of selected multiparous ewes were characterised by poor integration at 7 days despite the presence of eMSC, which was observed in greater numbers of CD45+ leukocytes near implanted PA/G constructs.

The use of MSC in TE constructs holds considerable potential, but the ultimate fate, migratory patterns and mechanisms of action of the included cells within implanted tissue is still not fully understood [211, 212]. The use of cell labelling techniques has contributed significantly to uncovering the eventual fate of implanted cells, with dyes, genetic labelling and IODEX being used with varying results. Our previous use of human eMSC in TE implanted into immunocompromised rat models used cells labelled with Vybrant^{TM} DiO Cell-Labelling Solution dye and revealed that only very few cells were retained beyond 14 days [34]. This was likely due to the immune system eliminating the implanted human eMSC, particularly as we observed that the remaining few eMSC do not proliferate *in vivo* in the ovine model. However, Vybrant^{TM} DiO system labels the outer membrane of cells and has had diminished labelling saturation within the first seven days of labelling [228]. This encouraged us to seek longer-lasting labelling systems, such as lentiviral vectors or superparamagnetic iron oxide nanoparticles (SPIONs) such as IODEX. Lentiviral vectors were unavailable for this study due to the lengthy process involved in meeting governmental regulations and obtaining approval. IODEX, however, was plentiful in supply (thanks to the kind donation of the Prof. Kishore Bhakoo, Translational Molecular Imaging Group, Singapore) and posed no regulatory risk due to non-biological composition [229]. As the goal was to have strong labelling for prolonged visualisation *in vivo*, toxicity was an important parameter to be assessed. Though IODEX has not impaired the function of mesenchymal stromal cells [225], it is unknown if this was true with eMSC. It is clear from the images acquired that the IODEX particles were occupying considerable space within the cytoplasm of labelled eMSC, a space in which protein synthesis, transportation and intracellular homeostasis occurs. It is possible that this level of saturation affects the exosome secretory pathways, which could alter the paracrine effect of eMSCs. qPCR performed on *in vitro* eMSC with and without IODEX labelling could be used to

investigate this possibility. Additionally, ELISA's could be performed on collected supernatants to compare protein production between controls and IODEX-saturated eMSC. Nevertheless, it was quicker to label eMSC with IODEX nanoparticles than lentiviral vectors. IODEX only required an overnight incubation that lost no cells yet produced almost complete cellular labelling that was ready to be implanted the following day. In contrast, lentiviral labelling requires a lengthier process that involves further passaging, harsh transduction methods, FACS cell sorting and extended time in culture to proliferate and regain cell numbers. For extended cell tracking, the lentiviral vector is more favourable as it is unknown how long IODEX persists within the cytoplasm of eMSC. But for shorter term trials in which low cell passage number s is a key factor, IODEX does have its advantages.

The loss of MSC functional properties (eg clonogenicity), including eMSC, during expansion in culture is a well-known phenomenon that may influence their usefulness during MSC-based TE. Culturing and proliferation of bone marrow MSC has resulted in observed diminishment of the telomere lengths and loss of regenerative potential [97, 230, 231]. This is the conundrum of using mesenchymal stem cells for medicinal purposes: after acquisition they must be cultured to expand to sufficient numbers but this results in diminishing stemness and reduced efficacy when implanted [209]. In our research, Passage 2-4 cells were used for implantation, with a median Passage 3, because they were the earliest passages that yielded enough cells. Since we had previously shown loss of human eMSC stemness with culture [142], eMSC purity was measured as a percentage of $CD271^{+}/CD49f^{-}$ cells, as CD271 is the only MSC biomarker expressed by ovine eMSC and is used for cell isolation[129], and marks the clonogenic ovine eMSC. A moderate correlation was found between $CD271^{+/}CD49f^{-}$ (%) and clonal efficiency, though this was not significant. This raises several questions, such as whether Passage 3 and 4 ovine eMSC can influence wound healing as effectively as passage 2 cells. An issue with defining a set passage number is the variation of the number of functional eMSC in the one passage number. In our current study, the phenotypic disparity of passage 3 eMSC varied from 23% to 64% potency as assessed by clonogenicity. Overall, it should be considered how the stemness of each sample would affect their efficacy when implanted *in vivo*, as the clonal efficiency ranged from 20-80% across the six samples. Current research suggests decreased MSC clonogenicity are a consequence of increasing passage number, presumably associated with loss of stemness [232]. Though eMSC are particularly dynamic due to their origin from a cyclically rapidly regenerating tissue, there is evidence that human eMSC undergo similar loss

of potency when cultured for extended periods of time [140, 141]. At present CD271 is the only biomarker for ovine eMSC [27], but there may be other biomarkers more aligned with the stemness and potency of related cells in the ovine endometrium or bone marrow. However, it should be appreciated that this study was performed as a pilot initiative to optimise a variety of parameters for a larger study over longer incubation times, making it more difficult to draw complete conclusions.

The biocompatibility of TE constructs is central to their feasibility as an effective method of treatment for any tissue injury including POP. Thus, the relatively poor mesh/tissue integration of the day 7 PA/G explants, and the apparent ineffectiveness of eMSC in controlling this, was a major concern. This lack of integration in our current study contrasted with good integration in our previous studies that used rat hernia or skin wound repair models [27, 33, 34] indicates the importance of both the anatomical implantation site as well as the animal model. In other studies that used similar ovine animal models for PP mesh [184, 233], poor tissue integration coincided with high rates of mesh exposure [28, 29, 233], similar to our current study where exposure rates were high, 17% for PA/G explants and 33% for eMSC/PA/G explants using a PA/G mesh. This could also be due to the lack of biomechanical match-up between the PA/G constructs and the ovine vaginal tissue. Alternatively, a significant body foreign body response or the gelatin coating itself could be preventing integration; this study did not include a non-gelatin coated PA mesh to provide data on which to make that comparison. This is our first study featuring such an early time-point for PA/G mesh implants into ovine transvaginal animal models as our prior work with gelatin-coated polyamide mesh featured 60 and 90 day time points in rat and mice models, meaning there is little precedent on which to make predictions. Therefore, this degree of poor tissue integration at 7 days could be a normal part of the recovery process. Until later time-points are conducted the full significance of these data will remain unclear. However, it points out the importance of mimicking human anatomy as closely as possible, and we have demonstrated this is possible with POP-Q selected ovine model that presents with vaginal weakness similar to that of POP-vulnerable women. These will be crucial factors moving forward into preclinical trials.

The poor integration of the TE mesh into the host tissues made detection and confirmation of the IODEX-labelled eMSC particularly difficult. IODEX-labelled cells have been tracked for up to 8 weeks in sheep spinal columns using MRI[226]. However, as MRI was unavailable for this study, immunofluorescence confocal microscopy was used but was impaired by the

inadequately healed tissue. The IODEX-labelled eMSC resided close to the gelatin/mesh implant, making it difficult to locate them in poorly integrated tissue. This suggests that the eMSC do not migrate far from their site of implantation, which supports the current literature to date that has shown that eMSC operate in a paracrine manner rather than migrating to target areas and differentiating into required tissue cells [32]. This lack of eMSC mobility poses further questions, such as whether the implanted eMSC would eventually leave the implant region and incorporate into vaginal smooth muscle cells. The muscularis thins in the vaginal wall in response to damage incurred by vaginal delivery [213]. Thickening this layer by implanting eMSCs that eventually differentiate into smooth muscle cells, would be contribute significantly towards successful clinical treatment of POP and prevention of future herniations.

Modulating the host immune response to implanted TE constructs is a greatly desired outcome of TE. By using autologous eMSC to minimise the innate immune response that is activated and likely responsible for removing the implanted human eMSC trialled in our rat skin wound repair model within 14 days [34]. Broadly speaking, the two main populations of macrophages at a wound site are M1 "pro-inflammatory" macrophages and M2 "wound healing" macrophages. A property of eMSC is their ability to modulate the immune response by promoting the switching of M1 macrophages to M2 macrophages. Significant differences were not found between overall leukocyte infiltration between experimental groups, nor in M1 and M2 macrophage populations. However, the CD45 antibody is a pan-leuokocyte marker, and so it is likely that it also reacted with other white blood cells that were present this early in the wound healing process, such as M0 macrophages and neutrophils. Though it was not statistically significant, there was a trend of greater M2 polarisation in the eMSC/PA/G explants in percentage of CD163+ stained area. This suggests the possibility that the full, measurable response was masked by the poor mesh/tissue integration, mesh exposure and folding, which is a limitation of this study that should be considered. Later time points that allow the tissue to fully heal could provide clearer data.

3.6. Conclusion

This study demonstrated the potential use of sheep as large animal model for POP research to track *in vivo* behaviour of IODEX-labelled autologous ovine eMSC following implantation. IODEX labelling dosage was optimised to 10µg/100,000 cells which labelled over 90% of cells and produced vivid fluorescent imaging after 24 hr incubation, demonstrating no cellular toxicity and around 20% label retention within the cytoplasm following a week of cellular

proliferation associated with around 3 cell doublings. A moderate link between MSC passage number of a cell population and clonogenicity was found, that reflected cell potency and stemness. When seeded onto PA/G mesh and implanted into the vaginal walls of multiparous ewes with objective measurement of "POP", eMSC were detectable after 7 days but did not appear to have a significant influence over the host immune response. eMSC improve poor tissue integration of PA/G implants, which were characterised by heavy folding and high rates of mesh exposure. These factors need to be optimised and overcome in further preclinical studies.

Chapter 4

Composite mesh design for delivery of autologous mesenchymal stem cells influences mesh integration, exposure and biocompatibility in an ovine model of pelvic organ prolapse

Introductory Statement

In Chapter 3 we observed poor biocompatibility of PA/G constructs with and without autologous eMSC. This was a surprising outcome as prior research in mouse models had observed good mesh integration of PA/G constructs into surrounding tissues. It was hypothesised that the stiffer glutaraldehyde-crosslinked gelatin coat of the PA/G constructs was causing biomechanical mismatch between the construct and surrounding tissues, resulting in poor biocompatibility. In this chapter we compared the biocompatibility of two different mesh designs, both with and without autologous eMSC: PA mesh coated in glutaraldehyde-cross linked gelatin, and PA mesh first implanted into the vaginal wall and then receiving a mixture of eMSC and ruthenium-based gelatin that is then photoseal cross-linked *in situ*. I also used this chapter to assess the persistence of autologous eMSC 30 days after implantation and their effect on wound healing and modulating the host immune response. I performed all the experimental work except where noted in the following acknowledgements. First, I would like to thank Dr Paivi Karjalainen and Dr Joan Melendez for performing the gynaecological implantation surgery within our ovine animal models, and Dr Anne Gibbon for assisting them and monitoring the ewe's post-surgery. I would also like to thank Dr Shayanti Mukherjee for assisting with and Dr Ilias Nitsos for performing the ovine post-mortems. I also want to thank Dr Saeedeh Darzi for assisting with learning the protocols required to apply ruthenium-based gelatin, as well as Dr Kirsin Elgass and for their help with image analysis. Finally, I want to thank Dr Sharon Edwards for her expertise and efforts in mesh preparation and performing the biomechanical testing on vaginal tissue explants.

Manuscript submitted to Biomaterials

Composite mesh design for delivery of autologous mesenchymal stem cells influences mesh integration, exposure and biocompatibility in an ovine model of pelvic organ prolapse

Emmerson S[1,2], Mukherjee S[1], Melendez J[4], Cousins F[1], Edwards SL[3], Karjalainen P[4], Ng M[5], Tan, KS[1], Darzi S[1,2], Bhakoo K[5], Rosamilia A[4], Werkmeister JA[1,2], Gargett CE[1,2].

[1]Ritchie Centre, Hudson Institute of Medical Research, 27-31 Wright Street, Clayton, Melbourne, Australia.
[2]Department of Obstetrics and Gynaecology, Monash University, Wellington Road, Clayton, Melbourne, Australia.
[3]CSIRO Manufacturing, Research Way, Clayton, Melbourne, Australia.
[4]Monash Health, 126/128 Cleeland St, Dandenong, Melbourne, Australia.
[5]Singapore Bioimaging Consortium, 1 Agency for Science, Technology and Research (A*STAR), 1 Biopolis Way, Singapore.

Corresponding Author:

Professor Caroline Gargett,
The Ritchie Centre
Hudson Institute of Medical Research
Translation Research Facility Level 5
27-31 Wright Street
Clayton, Victoria, 3168, Australia
Ph: +61 3 8572 2795
Email: caroline.gargett@hudson.org.au

Keywords: Tissue engineering, Pelvic Organ Prolapse, endometrial MSC, MSC, polyamide, ovine, autologous, mesh exposure

4.1. Abstract

The widespread use of synthetic transvaginal polypropylene mesh for treating Pelvic Organ Prolapse (POP) has been curtailed due to serious adverse effects highlighted in 2008 and 2011 FDA warnings and subsequent legal action. We are developing new synthetic meshes to deliver endometrial mesenchymal stem cells (eMSC) to improve mesh biocompatibility and restore strength to prolapsed vaginal tissue. Here we evaluated mechanically matched knitted polyamide mesh in an ovine multiparous model using transvaginal implantation and matched for the degree of POP. Polyamide mesh dip-coated in gelatin and stabilised with 0.5% glutaraldehyde (PA/G) were used either alone or seeded with autologous ovine eMSC (eMSC/PA/G), which resulted in substantial mesh folding, poor tissue integration and 42% mesh exposure in the ovine model. In contrast, a two-step insertion protocol, whereby the uncoated PA mesh alone was inserted transvaginally followed by application of autologous eMSC in a gelatin hydrogel onto the mesh and crosslinked with blue light (PA+eMSC/G), integrated well with little folding and no mesh exposure. The autologous ovine eMSC survived 30 days *in vivo* but had no effect on mesh integration. The stiff PA/G constructs provoked greater myofibroblast and inflammatory responses in the vaginal wall, disrupted the muscularis layer and reduced elastin fibres compared to PA+eMSC/G constructs. This study identified the superiority of a two-step protocol for implanting synthetic mesh in cellular compatible composite constructs and simpler surgical application, providing additional translational value.

4.2. Introduction

Pelvic Organ Prolapse (POP) is the herniation of the pelvic organs into the vagina[234, 235]. POP is common, affecting approximately a quarter of all women, particularly post-menopausal women, causing bladder, bowel and sexual dysfunction, incontinence and, considerable distress [234, 235]. Although the underlying cause of POP is not yet fully understood, the main risk factors are vaginal birth, forceps delivery, older age at first child delivery, obesity and aging [2, 236, 237]. The genetic contribution to POP susceptibility indicates that alterations in the synthesis and regulation of fibulin, elastin and collagen could be contributing factors [201, 238, 239].

We are developing a tissue engineering approach using a new polyamide/gelatin composite mesh biomechanically matched to vaginal tissue as a scaffold for implanting autologous endometrial mesenchymal stem cells (eMSC) to treat POP. Perivascular eMSC were chosen due to their ease of acquisition from endometrial biopsy tissues without anaesthetic, and the ability to purify them using specific markers [96, 127]. Polyamide (PA) was initially selected from a range of custom knitted polymers following evaluation using *in vitro* biomechanical testing tools where PA mesh exhibited preferable biomechanical properties [31] and *in vivo* testing in a rat abdominal hernia model as it elicited a milder host immune response [31, 33]. eMSC/PA/G constructs were made by dip coating knitted PA meshes in gelatin, then seeding with human eMSC [34] and were assessed in a xenogeneic rat skin repair model [13,14]. In this model, eMSC seeded PA/G constructs promoted angiogenesis, reduced the chronic inflammatory response, promoted deposition of physiological crimped collagen and improved the biomechanical properties (reduced stiffness and increased mesh/tissue explant extensibility) [34]. However, PA/G constructs also exhibited greater rigidity than PA alone, and it is currently unknown how the presence of a glutaraldehyde-crosslinked gelatin-coating would influence the efficacy of mesh performance and impact effective delivery of autologous eMSC. To address these concerns, uncoated PA mesh alone was first implanted and eMSC were then delivered using a more elastic light crosslinked gelatin. Prior to clinical translation of these mesh types, mesh performance is being assessed in a preclinical ovine POP model with transvaginal insertion of autologous eMSC/PA/G constructs. Sheep are an attractive animal model due to their similar vaginal dimensions and anatomy to women, the spontaneous development of POP occurs in some older, multiparous animals, and their relative cost effectiveness [175, 176, 183, 185]. Indeed, ovine models have been proposed for training surgeons in vaginal surgery specifically for treating POP in women [186].

The use of ovine animal models has substantially increased our understanding of the effect of multiparity (i.e multiparity lamb deliveries) and implanting transvaginal mesh into the vaginal wall. The ovine model has shown that multiparity was associated with weakened vaginal walls as measured by the distensibility of vaginal tissue using a modified clinical score, Pelvic Organ Prolapse Quantification (POP-Q) [183], and a novel fibre optic pressure sensor device [204, 219]. Previous work has shown that multiparity is associated with a decrease in smooth muscle thickness and an increase in elastin fibre content in the ovine vaginal wall [219], resulting in reduced biomechanical strength. Parous sheep also exhibited greater POP-Q scores [219] as well as weakened regions in the anterior and posterior vaginal walls as measured by a pressure sensor device [204] compared with nulliparous sheep.

Disruption of the vaginal muscularis in macaques following commercial mesh implantation, albeit using sacrocolpopexy [240], compounds the damage incurred by herniation of the pelvic organs and alters the expressions of extracellular matrix proteins, such as elastin fibres [239]. This emphasises the importance of mesh design in promoting mesh integration for POP treatment. Coating mesh with various collagen matrices to minimize the host response to the mesh and its subsequent exposure has been tested in ovine models [27-29]. It was hypothesised that the collagen coating would improve mesh implant integration [27-29, 241]. However, the results have been inconsistent and stand as testimony to the challenge of developing an ideal biomaterial for treating POP.

Central to the biocompatibility of synthetic mesh-based treatments for POP is the host immune response. All implanted meshes elicit a chronic inflammatory response mediated by M1 pro-inflammatory macrophages which can limit or delay the M2 pro-wound healing macrophage response. Mesh design itself can also influence M1/M2 macrophage polarisation. For example, lightweight, Restorelle mesh implanted in the Rhesus vagina provoked a milder M1 pro-inflammatory macrophage response compared to heavier commercially available Gynemesh [242], while PA and gelatin-coated PA (PA/G) mesh evoked a milder host inflammatory response compared to polypropylene (PP) mesh in rat models [33].

The aim of this study was to compare two methods for transvaginal delivery of autologous eMSC on polyamide synthetic mesh using an ovine model of vaginal wall weakness (POP). The second aim was to determine the retention of implanted autologous eMSC and to assess

their effect on the extracellular matrix and inflammatory response to the implanted gelatin-coated and non-coated PA mesh. In order to track the eMSC post implantation, they were labelled with dextran coated iron oxide nanoparticles (IODEX) conjugate with TAT-FITC.

4.3. Methods

4.3.1. Ethics and Animals

Experimental procedures and animal husbandry were approved by the Monash Medical Centre Animal Ethics Committee A in accordance with the ethical guidelines of the National Health and Medical Research Council (NHMRC) of Australian Code for the Care and Use of Animals for Scientific Purposes 8th Edition. Border Leicester Merino (BLM) ewes were housed in the Monash Animal Research Platform in an enclosed barn or outdoor enclosures. Multiparous ewes, aged 5-6 years (n=30) who had undergone multiple lamb deliveries (n≥3) and delivered their last lamb(s) at least 9 months prior, were selected if they showed evidence of weakened vaginal tissue with POP-Q values higher than -3 (medians were -1 at point Ap and 0 at point Aa **(Table 1)**).

4.3.2. Pelvic Organ Quantification "POP-Q" Measurements

Quantification of POP was done using a modified POP-Q (Pelvic Organ Prolapse Quantification) system as previously described [183]. Pre-surgery measurements were undertaken by a gynaecologist (JM) in conscious ewes. Briefly, manual traction with forceps was applied to the vaginal tissue at the Aa, Ba and Ap points using the urethra as a reference point for Ba (proximal anterior) and mucocutaneous junction for Aa (distal anterior) and Ap (distal posterior). Ewes were divided into four experimental groups (n=6/group) and one incisional control group (n=6) ensuring POP-Q scores were matched between the groups (Table 1). Postmortem POP-Q measurements were acquired immediately following euthanasia (SE).

4.3.3. Ovine hysterectomy for Collection of Endometrial Tissue

Subtotal hysterectomy was performed via ventral midline laparotomy on 12 ewes to collect uterine tissue. Anaesthesia was induced by intravenous Medetomidine premedication (0.1-0.2 mg/kg), followed by intravenous Thiopentone (10mg/kg), and then maintained with Isoflurane (1-3% in 100% O_2). Pain relief was provided before start of surgery as Fentanyl (75µg/hr) transdermal patch and Carprofen (2mg/kg) given subcutaneously. A short acting broad-spectrum antibiotic, Cefazolin (7.5mg/kg), was given intravenously prior to surgery, and a long-acting antibiotic, Duplocilin (5.75mg/kg), to continue coverage for 48 hours post-surgery.

Suspensory ligaments of the ovary and feeding vessels to the uterus were ligated and transected before performing a supracervical amputation of the uterine body conserving the ovaries. Laparotomy was closed using absorbable sutures. Postoperative pain relief was with Bupivicaine (5µg/ml) given by subcutaneous injection under the incision site at end of surgery and the fentanyl patch (75µg/hr) was maintained for 3 days. The ewes recovered for four weeks from the abdominal surgery before they underwent vaginal surgery. They were cared for at animal facility at Monash University Animal Research Platform in individual pens in sight of other ewes and moved into small holding pens as they recovered. The excised uterus was placed in ice-cold transport medium (HEPES-buffered DMEM/F-12 medium (Invitrogen) supplemented with 1% antibiotic Anti-Anti (100X, Life Technologies) (Bench Medium), stored at 4°C and processed within 18 hours, as previously described [129].

4.3.4. Isolation of Ovine eMSC by Flow Cytometry Sorting sing CD271

Ovine eMSC were isolated from hysterectomy tissue as previously described [129]. Isolated cells (up to 1 x 10^7 cells/100µl) were incubated with phycoerythrin (PE)-conjugated anti-human CD271 (1:10, mouse IgG1; Miltenyi Biotec) and allophycocyanin (APC)-conjugated anti-human CD49f (1:10, clone GoH3, rat IgG2a; Miltenyi Biotec) in 2% fetal bovine serum/PBS (FBS/PBS) for 30 min on ice in the dark using our established protocols [129]. Cells were then washed and resuspended in 1µM Sytox Blue (Life Technologies) in fetal bovine serum (FBS)/PBS to exclude dead cells. $CD271^+CD49f^-$ eMSC were isolated using fluorescence activated cell sorting (FACS) with a MoFlow flow cytometer (Beckman Coulter) or an Influx flow cytometer (Becton Dickinson Biosciences) using Monash University Flow Core services.

4.3.5. Cell Culture

Freshly sorted cells were cultured in stromal medium containing DMEM/F-12 (Life Technologies), 10% fetal bovine serum (Life Technologies), 2mM glutamine (Life Technologies), 0.5 mg/ml primocin antibiotic and incubated at 37°C in 5% CO_2. Medium was changed every 2–3 days and cells were passaged at 80% confluence.

4.3.6. eMSC Labelling

Before implantation, passage (P) 3-4 cells were labelled with FITC-TAT IODEX paramagnetic nanoparticles at a concentration used previously [226]. Cells were incubated with 10µg of IODEX per 100,000 cells for 24 hours at 37°C. Cells collected after trypsinisation with 1X

TrypLE^{TM} (Life Technologies, #12604-021)), washed and resuspended at 100,000 cells/100µl Bench Medium.

4.3.7. Fabrication of PA and PA/G Meshes

PA meshes were fabricated from 80µm monofilament warp knitted into an open pore pattern with large pore area of 0.99 +/- 0.10 mm^2, small pore area of 0.04 +/- 0.02 mm^2 and mass per unit area 42 g/m^2, similar to, but not identical to previously described heavier meshes using 100 µm monofilaments [31, 33]. For PA/G constructs, PA mesh was dip-coated in 12% porcine gelatin, cross linked on ice-cold 0.5% (v/v) glutaraldehyde (Sigma) for 8 minutes/side followed by 2% w/v glycine (Merck; Australia) in water for 15 minutes, then 2% v/v H_2O_2 (Merck) in water for 15 minutes, and 4% w/v glycerol (Merck) in water for 15 minutes, all at RT with washing steps in water in between. Mesh was air-dried and sterilised by gamma irradiation at 25 kGy prior to implantation [33]. PA mesh was used in both the PA and PA/G constructs. (see below).

4.3.8. Preparation of Autologous Ovine eMSC-seeded Mesh Constructs

Prior to seeding, PA/G 30 x 20 mm mesh pieces were soaked in 1:50 Anti-Anti (100X) antibiotic for 1 hour at 37°C, then transferred to 20ug/ml fibronectin (Sigma-Aldrich, Saint Louis) overnight at 37°C. Coated stabilised PA/G meshes were manually seeded with labelled sorted eMSC at a seeding density of 100,000 cells/cm^2 in 100 ul medium/mesh (600,000 cells/mesh) and cultured for 24h, checked for cell adherence, and transported in bench medium on ice for surgical implantation. These constructs were termed eMSC/PA/G. PA/G without cells underwent the same procedure but without cells. A second set of meshes were implanted in a two-step procedure, with PA meshes first implanted into the vaginal wall and then 600,000 eMSC suspended in 0.5ml 12% porcine gelatin, 2mM ruthenium metal complex (Ru) (2,2′-bipyridyl) dichloro ruthenium (II) hexahydrate [Ru II(bpy)3]$^{2+}$ (Sigma-Aldrich) and 10mM sodium persulfate (SPS) (Sigma-Aldrich). Half the cell/gelatin mixture was applied to the surface of the PA mesh *in situ*, and the gelatin cross-linked using a LED dental lamp (460nm, 1200cm mW/cm^3, 3M Epilar Free Light 2) for 20 seconds before the other half was applied and cross-linked, as described previously [32, 36]. These constructs were termed PA+eMSC/G. Control PA meshes without cells were incubated in bench medium only and implanted without gelatin. Each ewe received autologous eMSC previously acquired from her endometrium (see above).

4.3.9. Transvaginal Surgery - Implantation of PA/G, PA+G Mesh with and without eMSC

BLM ewes were anaesthetised using the same protocol as for hysterectomy. Antibiotic prophylaxis was given. Ewes were placed into lithotomy position and POP-Q measurements were taken. Hydrodissection of the vaginal tissue layers was achieved with 20ml of bupivacaine (5mg/ml) with 1ml of adrenaline (Aspen Pharmacare Australia, 1mg/ml). For 24 sheep having mesh implantation, a 40 mm, full-thickness midline incision was made on the posterior vaginal wall and the rectovaginal space was dissected. eMSC/PA/G (n=6), PA/G (n=6), PA (n=12) were surgically implanted. Autologous ovine eMSC/G were then applied to the 6 PA meshes (PA+eMSC/G) and the gelatin crosslinked (see above). All inserted meshes were fixed with absorbable sutures into the rectovaginal space, and the vaginal epithelium closed using absorbable sutures. Ewes receiving cells were implanted with a tissue engineering construct delivering autologous eMSC. For incisional controls (n=6), the vaginal incision was performed without placement of mesh and closed using absorbable sutures. Pain relief was with subcutaneous Carprofen (2mg/kg) given at start of surgery and bupivicaine (5mg/ml) given subcutaneously at the incision site at end of surgery.

4.3.10. Post Mortem and Harvest of Ovine Vaginal Mesh/Tissue Explants

Ewes were euthanised after 30 days using Lethabarb (110mg/kg, Virbac (Australia) Pty Limited,) and POP-Q measures were taken immediately. The entire vaginal tract was removed with adjacent tissues, trimmed and incised in a longitudinal manner adjacent to the urethra (anterior wall) from the muco-cutaneous junction to the cervix and dissected for analyses as shown in **Supplemental Figure 1**. For biomechanical analyses, a 25 mm x 30 mm piece was taken from the proximal mesh/tissue explant and frozen at -20^{o}C. The remaining distal mesh/tissue explants were further dissected for qPCR (in RNAlater) analysis and histology (fixed in 10% formalin and processed to paraffin (FFPE), or 4% paraformaldehyde overnight, then placed in 30% sucrose for 48 hours and frozen in OCT).

4.3.11. Histology

FFPE tissues were sectioned at 4μm and stained with H&E, Masson's Trichrome and Hart's elastin fibre stain in the Monash Histology Platform (MHP) facility using previously published methods. Three images of the muscularis region at and away from the surgical site were captured for each tissue explant and measured for elastin fibre content for comparison. OCT-

embedded tissue was cryosectioned into 8μm sections for immunohistochemistry and immunofluorescence staining.

4.3.12. Collagen Analysis using Sirius Red Birefringence

FFPE tissue sections were stained with 0.1% picro-sirius red [219]. Images were captured on an Olympus BX61 light microscope equipped with a polarising filter (Olympus T2 U-ANT and U-POT). cellSens software and an Olympus DP80 camera was to identify birefringent sirius red-stained collagen fibres; images underwent image analysis (below) and birefringence was separated into red (mature collagen) and green (immature collagen) with pixel intensity thresholds defined and counted as 1 for each as described previously [21].

4.3.13. Image Analysis

Images were taken at 10x magnification using an Olympus BX61 light microscope and Olympus cellSens software and analysed using ImageJ software. Using custom macros provided by Dr Kirstin Elgass, Monash University Micro Imaging, Monash Health Translational Precinct (MHTP), a region was drawn either around mesh filaments, or the edge of the implant disruption if no mesh filaments were present. Analyses were then conducted in a 250μm increment around the region of interest for collagen and αSMA analysis, 50μm for elastin fibres and immunohistochemistry, using colour deconvolution as previously reported [219]. All the visible mesh filament regions were imaged, ranging between 5-10 replicates per sample.

4.3.14. Immunofluorescence

Frozen sections were thawed and blocked with protein block (Dako, Glostrup, Denmark) for 1 hour at RT, and immunostained with mouse anti αSMA antibody to mark smooth muscle bundles or CD45 to mark total leukocytes **(Supplemental Table 1)** for 1 hour at RT. Isotype-matched antibodies (Dako Mouse IgG1 for CD45, IgG2A for αSMA) were used as negative controls and applied at the same concentrations, as previously reported [219]. Anti-mouse Alexa-Fluor-568-conjugated secondary antibody (Thermo Fisher Scientific) was then incubated for 30 minutes at RT for both primary antibodies. Nuclei were stained with Hoechst 33258 (Molecular Probes) for 5 minutes and the slides were mounted with fluorescent mounting medium (Dako). FITC-IODEX-labelled eMSC were detected using Olympus FV1200 Confocal Microscope and Olympus CellSens software and their persistence (%) was determined by first calculating the number of average labelled cells around visible mesh

filaments in 6-9 images/sheep, then dividing this number by the number of labelled cells that were injected and multiplying by 100 for % cell persistence.

4.3.15. Immunohistochemistry

FFPE 8μm sections were dehydrated and antigen retrieval performed using 0.1M citrate buffer and endogenous peroxidase was blocked with 3% hydrogen peroxide. Sections were then incubated with protein block (Dako) for 30 min at RT, followed by primary antibody (CD45 or αSMA, **Supplemental Table 1**) in 2% BSA/PBS for one hour at RT. Mouse IgG1 (Dako) was used as the negative isotype control at the same concentration. HRP-labelled polymer (Dako) conjugated anti-mouse secondary antibody was applied for 40 mins at RT, DAB chromogen (Sigma-Aldrich) diluted 1:2 for αSMA and 1:10 for CD45 in substrate peroxidase buffer (Pierce, Thermo Fisher Scientific, Waltham USA) for 5 min, counterstained with hematoxylin as previously published [219]. Frozen 4μm sections were used for immunostaining with antibodies to CD86 (M1 macrophage marker) and CD163 (M2 macrophage marker **(Supplemental Table 1)** using the same procedure, but without antigen retrieval. In addition to analysis around mesh filaments (see image analysis above), 4 measurements were taken of the lamina propria, muscularis and implant/disruption region of each tissue explant and averaged to calculate the percentage of vaginal wall disrupted by implantation of mesh constructs.

4.3.16. Quantitative qPCR

RNA was isolated using PureLink® RNA mini Kit (Life technologies, #12183018A) and treated with DNase (PureLinkTM DNase, Invitrogen) to obtain DNA-free total RNA. First-strand cDNA was synthesized using SuperScript III first-strand synthesis system (Invitrogen). 100ng of cDNA was amplified and detected using Green Super Mix and primers for *COL1A1*, *COL3A1*, *FBN5*, *ELN* (**Supplemental Table 2,** Bioneer Corporation). The PCR conditions were initial denaturation at 95°C for 10 minutes, followed by 40 cycles of denaturation at 95 °C for 15 seconds and annealing/polymerisation at 60°C for 60 seconds. 18S was used as an endogenous control to normalise the target gene expression and fold change was calculated using the $2^{-\Delta\Delta CT}$ method.

4.3.17. Biomechanical Analysis of the Ovine Vaginal Mesh/Tissue Explants

Frozen mesh/tissue explants were thawed overnight at 4° C, and tensile testing was performed within 24 hr using the ball burst method in an Instron Tensile Tester (5557; Instron Corp, MA) with a 100N load cell. Samples were secured between 2 embossed metal plates, both with an aperture of 15 mm. Rubber sheeting was used to avoid sample slippage between the plates during testing. The force required to rupture the explant using a rounded steel rod (10 mm diam) was recorded at a crosshead speed of 20 mm/min as previously described [219]. Load (N)/elongation (mm) curves were plotted from the generated data and stiffness (N/mm) was defined as the gradient of the load/elongation curve in the linear region of the curve.

4.3.18. Statistical Analysis

All data were analysed using GraphPad Prism 7.02 for Windows 10 64-bit, (GraphPad Software, La Jolla California USA) and initially assessed for normality using Shapiro-Wilk or Kolmogorov-Smirnov tests. Image analysis of immunohistochemistry, vaginal disruption and qPCR data were assessed using a One-way ANOVA with Tukey's multiple comparison post hoc test. αSMA and elastin were assessed using unpaired t-tests as the data were parametric and collagen was assessed by Mann-Whitney U test for nonparametric data. Differences in POP-Q Aa and Ap measurements used for selection of ewes with vaginal weakness were analysed using Kruskal-Wallis One-way ANOVA. Differences in pre- and post- surgery POP-Q measurements were analysed in each experimental group using Wilcoxon signed rank test for paired nonparametric data. Differences in mesh exposure were measured using a Chi-square test.

4.4. Results

4.4.1. Ovine Demographics

To identify multiparous ewes with vaginal wall weakness (i.e "POP") for use in this study, we undertook a modified human POP-Q we previously developed [183]. Ewes with Aa and/or Ap values between -2 to 0 (-3 is normal) were selected as having vaginal wall weakness and were then distributed into the five experimental groups (PA/G, PA, eMSC/PA/G, PA+eMSC/G, and incision control) to ensure matching between groups **(Table 1)**. The Aa and Ap measurement of each group were similar (p=0.2289 and p=0.3275 respectively). Ap is the most significant POP-Q point as PA/G and PA constructs were implanted into the posterior wall of the ovine vagina at the Ap location. POP-Q measurements taken at the time of construct explantation (**Fig 1**) showed no significant change after one month of mesh implantation for PA/G (**Fig 1A,**

C) or PA groups **(Fig 1B, D)** both with or without eMSC. There was neither improvement or worsening of vaginal wall weakness. The results were similar for the incision control.

4.4.2. Mesh Exposure into the Vaginal Wall

One of the major adverse events associated with transvaginal polypropylene mesh was vaginal exposure. Almost half (42%) of the 12 PA/G implants showed vaginal exposure by 30 days with 4 exposures in PA/G explants and 1 in eMSC/PA/G explants **(Table 2)**. In contrast no mesh exposures were observed in any of the 12 PA construct explants, significantly different to PA/G meshes **(**p=0.012, **Table 2)**.

4.4.3. Integration and Location of PA/G and PA Mesh Implants in the Ovine Vaginal Wall

H&E stained mesh/tissue explants showed similar distribution of the implanted PA/G and PA constructs in the ovine vagina; 2 PA/G constructs were implanted into the lamina propria, 6 in the muscularis and 4 into both the lamina propria and muscularis, whereas 2 PA constructs were implanted into the lamina propria, 9 in the muscularis and 1 both in the lamina propria and muscularis. PA/G constructs were characterised by poor mesh integration and substantial folding **(Fig 2A)**, while PA constructs exhibited superior mesh integration (**Fig 2B)**.

4.4.4. Mesh Constructs Disrupt Smooth Muscle Architecture and Content of the Ovine Vaginal Wall

Our observations of mesh placement in H&E sections suggested that the muscularis layer was disrupted (**Fig 2A**) as previously reported for polypropylene mesh implanted in the macaque vagina [240]. Low magnification panorama images of αSMA immunostained mesh/tissue explants **(Fig 2C)** clearly delineated the smooth muscle layers and enabled measurement of lamina propria, muscularis and implant region thickness to determine the extent of vaginal wall disruption by the implanted mesh constructs. The disrupted region was significantly increased for implanted PA/G constructs without cells **(Fig 2D,** $p<0.05$**)** but not the PA constructs compared to incisional controls. The disrupted area appeared reduced in both mesh constructs with eMSC, **(Fig 2E)** however they were not significantly different from the corresponding mesh constructs without cells.

4.4.5. αSMA+ Cell Types are Differentially Altered in eMSC/PA/G Compared To PA+eMSC/G Constructs

αSMA immunostaining detected a differential myofibroblast response **(Fig 3A-E)** around the filaments of the two different mesh constructs in the presence of eMSC. There was no significant difference between PA/G and PA αSMA^+ myofibroblast area, with the αSMA^+ staining of PA explants demonstrating more vasculature and few myofibroblasts **(Fig 3A, C)** but no difference in aSMA staining (**Fig 3F)**. The percentage area of myofibroblasts was significantly greater at the mesh/tissue interface of eMSC/PA/G explants compared to PA+eMSC/G **(Fig 3G,** $p<0.01$**)** and similarly most αSMA^+ cells were marking the vasculature in the latter (**Fig 3D vs 3B**)**.**

4.4.6. Collagen Organisation of the Ovine Vagina was not Affected by Construct Implantation

Although large bands of collagen-like material were observed around the implanted mesh in the disrupted zone **(Fig 4A)**, sirius red birefringence analysis of collagen organisation within a 250 μm radius around individual mesh filaments **(Fig 4B, E)** showed a similar percentage of mature **(**red birefringence, **Fig 4C, D**) and immature **(**green birefringence **Fig 4F, G**) collagen after 30 days for each of the two constructs (ie PA/G and PA), irrespective of the presence of eMSC.

4.4.7. PA/G Constructs Diminish Elastin Fibre Content of the Ovine Vagina

It was previously shown that multiparous ewes with "POP" had higher elastin fibre levels in the vaginal wall than nulliparous ewes [219]. We therefore assessed elastin fibre densities by Hart's stain within a 0-50 μm increment around mesh filaments in PA/G (**Fig 5A, D)** and PA explant groups **(Fig 5B, E)**. Elastin fibre content was retained in PA explants compared to PA/G **(Fig 5C**, $p<0.001$), which showed a significant reduction whether or not eMSC were present (eMSC/PA/G) (**Fig 5F,** $p<0.01$). Elastin fibre densities were also examined in the distant muscularis away from the implant site in PA/G **(Fig 5G, J)** and PA explant groups **(Fig 5H, K)**. Similarly, the elastin fibre content was retained in the distant muscularis of PA and PA+eMSC/G explant tissue **(Fig 5I, L** respectively, $p<0.05$ for both**)** when compared with PA/G explants. However, there was no difference in % elastin area **(Fig 5O)** at the point of incision **(Fig 5M)** and the distant muscularis **(Fig 5N)** in the incisional controls.

4.4.8. Implanted Autologous eMSC Persist in the Vagina for 30 Days

Allogeneic and xenogeneic implantation of MSC do not survive long when implanted *in vivo* [32, 34, 243]. Since we hypothesised that autologous cells would survive longer *in vivo* following transplantation, we sought to assess retention of autologous ovine eMSC labelled with FITC-conjugated IODEX paramagnetic nanoparticles. By confocal microscopy, IODEX-FITC-labelled eMSC were observed *in vitro* on PA/G scaffolds 1 day following labelling **(Fig 6A.i)** and *in vivo* in frozen sections of the vaginal tissue implanted with eMSC/PA/G **(Fig 6A.ii)** and PA+eMSC/G **(Fig 6A.iii)** at 30 days. To determine if IODEX-FITC-labelled eMSC incorporated into vaginal smooth muscle, dual colour immunofluorescence was performed. FITC-labelled eMSC (green) did not co-localise with A568-α-SMA^{+} smooth muscle fibres (red) **(Fig 6B)**, nor were any found within resident A568-CD45^{+} leukocytes **(Fig 6C)**. The mean percentage of persisting IODEX-labelled eMSC was calculated to be 5.7 ± 2.3 % (mean ± SEM) of implanted cells at day 30 for the 12 samples implanted with eMSC (PA/G and P + G).

4.4.9. eMSC Alter Extracellular Matrix Gene Expression

To further investigate the effects of the PA/G and PA eMSC constructs on extracellular matrix (ECM) metabolism, qPCR was used to analyse expression of ECM-associated genes *COL1A1*, *COL3A1*, *FBN5 and ELN* after 30 days implantation. eMSC/PA/G explants exhibited upregulated expression of *COL1A1* (**Fig 7A,** $p<0.01$), *COL3A1* (**Fig 7C**, $p<0.01$), *FBN5* (**Fig 7E,** $p<0.05$) and *ELN* **(Fig 7G**, $p<0.01$) compared to controls. In contrast, PA explants without eMSC exhibited decreased expression of *COL1A1* (**Fig 7B,** $p<0.05$p) and *COL3A1* (**Fig 7D,** $p<0.05$p) compared to controls. PA explants showed similar *ELN* and *FBN5* gene expression levels to incisional controls **(Fig 7F and H)**, although the fold changes were markedly lower than for the PA/G and eMSC/PA/G meshes **(Fig 7E and G)**.

4.4.10. Leukocyte Response to Implanted PA/G and PA Constructs

The foreign body response to implanted mesh is a major determinant of mesh biocompatibility and is mediated by leukocytes. Immunohistochemistry for the pan-leukocyte marker, CD45 and image analysis was used to quantify the immune response in the first 50μm increment around individual mesh filaments to implanted PA/G and PA constructs. As shown previously in rodent models [32, 34], CD45^{+} cells were concentrated at the mesh tissue interface of individual mesh filaments **(Fig 8A)**. The CD45 positive area (%) was significantly greater in PA/G explants without cells compared to PA alone **(Fig 8D**, $p<0.01$).

To determine which leukocyte subsets were surrounding mesh filaments, immunostaining for M1 macrophages using a sheep cross-reactive mouse anti-bovine CD86 antibody was undertaken **(Fig 8B)**. Significant differences between the controls and PA/G constructs within the 0-50 μm increment at the mesh-tissue interface was noted, irrespective of the presence of eMSC **(Fig 8E**, $p<0.01$ for both**)**. PA/G explants exhibited greater M1 area staining than PA explants ($p<0.01$), and similarly for eMSC/PA/G versus PA+eMSC/G ($p<0.001$). These results show that the PA/G constructs provoked a greater pro-inflammatory M1 macrophage response than PA constructs, irrespective of the seeding of autologous eMSC.

CD163 was used to measure the M2 macrophage response at the filament tissue interface within a 0-50 μm radius **(Fig 8C)**. PA explants alone or with cells exhibited a stronger M2 response compared with controls ($p<0.001$ and $p<0.01$, respectively, **Fig 8F**)**.**

4.4.11. Biomechanical Properties of Vaginal Tissue Implanted with PA/G and PA Mesh Constructs

Biomechanical properties of mesh tissue explants explanted from the ovine vagina were assessed using the ball burst method. Average load/elongation curves found explanted PA and PA/G meshes were not different in stiffness following 30 days implantation **(Supp. Fig 2A)** and were less than normal vaginal tissue [20]. Both meshes with eMSC had higher average stiffness, at higher compressive extensions, with higher breaking load for the PA+eMSC/G meshes **(Supp. Fig 2B)**. The PA+eMSC/G mesh exceeded the incision control in stiffness that is closer to normal vaginal tissue stiffness (**Supp. Fig 2C**).

4.5. Discussion

The main finding of our study was that mesh design was critical to mesh performance in an ovine model of objectively measured vaginal wall weakness. PA constructs with and without eMSC were characterised by a lack of mesh exposure, one of the most important adverse events associated with the clinical use of PP meshes. Several factors contributed to this lack of exposure. PA meshes without cells had high drape and were easily inserted into the vagina. For PA+eMSC/G constructs, the blue light crosslinking of gelatin tyrosine residues resulted in a highly elastic hydrogel[36] containing eMSCs. In contrast, PA/G mesh comprising a more densely glutaraldehyde crosslinked gelatin showed exposures irrespective of the presence of eMSCs. The stiffness of these latter constructs may not be the only factor in the poorer biocompatibility observed between PA/G with or without eMSC and PA or PA+eMSC/G. While pre-seeding eMSCs onto the PA/G may have provided an advantage as eMSCs attached to the gelatin surface and connected with each other *in vitro* before implantation, this did not prevent exposures. In contrast, eMSC/G applied to the implanted PA would have only attached to gelatin motifs *in vivo*, however, this disadvantage did not appear to affect the good integration observed with this construct design, suggesting that construct stiffness may be the main contributing factor in the exposure of the PA/G meshes that was minimally influenced by the eMSCs. An extra control group comprising PA+G would have further clarified this mechanism. The excellent integration of PA with or without eMSC constructs into host tissues was further demonstrated by lesser tissue disruption to the vaginal muscularis and a reduced myofibroblast response compared to PA/G constructs. Additional evidence of PA biocompatibility was shown by maintenance or increased elastin fibre content at the mesh tissue interface and in the distant muscularis, compared to the diminished elastin fibres observed in PA/G explants. The two-step PA *in situ* hydrogel delivery protocol also proved more surgeon-friendly and easier to handle during surgical implantation. When implanted, autologous FITC-IODEX-labelled eMSC persisted for at least 30 days in the ovine vagina. These eMSC upregulated collagen gene expression in the poorly integrated eMSC/PA/G explants and maintained collagen synthesis genes in PA+eMSC/G explants. PA explants exhibited a greater M2 response at the mesh-tissue interface than incisional controls. PA/G constructs with and without cells, by contrast, provoked a greater pro-inflammatory M1 macrophage response. We have also demonstrated, for the first time, the potential of using POP-Q selected ewes with vaginal wall weakness as an animal model for POP research, particularly as recipients of autologous cell-based therapies and tissue engineered constructs. While ovine transvaginal surgery models have been previously reported [183, 185, 186], this

study is the first where mesh performance has been examined in a sub-group of multiparous ewes that had been selected and matched for defined POP.

The integrity of the muscularis is vital to the strength of vaginal tissue and potentially its capacity to resist POP [219], and this integrity may be severely disrupted by the implantation of synthetic mesh [240]. Our study clearly shows that naked PA meshes integrate well into the tissue with minimal disruption, suggesting that the PA constructs with or without eMSC would be the preferred surgical synthetic mesh for future applications. Histologically, we observed significant disruption to the vaginal muscularis but only in PA/G explants, with less disruption when eMSC were incorporated into these implants, suggesting a role for eMSC in either replenishing smooth muscle cells or retaining them following injury. In either case, neither the post-surgery POP-Q measurements nor the biomechanical distensibility and strength of the vaginal wall was altered following mesh implantation. This was as expected due to the short 30 day time point. Our previous studies reported a correlation between reduced thickness of the muscularis layer and abnormal POP-Q Ap and Aa measurements and decreased maximum tensile load [219]. There was also a positive correlation between elastic fibre content and Aa and Ap POP-Q values in the muscularis (and lamina propria), indicating greater elastic fibre content in the weakened ovine vagina. In murine vagina smooth muscle this has been shown to contribute to the biomechanical strength of the tissue [244]. These data suggest that the smooth muscle of the vagina plays an important role in providing biomechanical strength and that preservation of vaginal smooth muscle is an important goal for POP treatment. We hypothesise that autologous eMSC implanted in vaginal tissue may assist in replenishing vaginal smooth muscle, as we have previously shown that eMSC differentiate into mature smooth muscle cells on PA/G scaffolds *in vitro* [245].

The biocompatibility of synthetic transvaginal mesh is of central importance in its clinical application for treating POP. The impetus for using warp knitted mesh was mesh flexibility and an open pore structure, both of which are favourable to tissue conformation and integration *in vivo*. This knitted PA mesh also exhibited excellent biocompatibility in rodent models [33]. Ovine models are an established animal model for mesh evaluation, particularly for assessing the value of different collagen coatings on the performance of PP mesh [28, 241, 246]. However, the surprising difference between the poor integration of the PA/G constructs in the ovine vaginal wall compared with good integration in our previous studies using rat hernia and subcutaneous wound repair models [33, 34] indicates the importance of anatomical equivalence

in pre-clinical trials. We were concerned by the poor integration of PA/G explants and the high number of exposures following implantation, especially as we implanted them as deep as possible to minimise this possibility. PA constructs were less stiff compared to PA/G, where the glutaraldehyde cross-linked gelatin increased the stiffness and bending rigidity of the mesh [31]. The glutaraldehyde cross-links between the abundant amine groups in gelatin, appeared too stiff in the ovine preclinical vaginal surgery model, despite titrating it to a minimal concentration for coating the mesh. In contrast, the photochemical crosslinking of less common tyrosine residues in the gelatin, originally used as a highly elastic surgical sealant [36], provided a more elastic and flexible material for delivering eMSC to the vaginal wall. This made surgical implantation easier and was likely responsible for the lack of mesh exposure as the mesh may have moved with the tissue rather than through the planes of the tissue [247]. Both PA/G and PA construct groups were implanted as deep as possible. However, the ovine vaginal wall is thin, including the rectovaginal septum, so care was taken not to perforate the rectum during initial dissection. Histological examination showed that the majority of implanted meshes were located in the adventitia and muscularis layers of the vagina for both construct groups. Additionally, the PA constructs were easier to prepare and simpler to handle during the surgery and implantation, considerations that would not have emerged with smaller animal models. As these two construct types are being investigated for clinical purposes with eMSC, the case of surgical ease and superior integration singles out using the 2-step insertion procedure with the uncoated PA mesh.

Coating PP and PA meshes have been evaluated before in both small and large animal models, particularly ewes [27-29, 241]. The initial purpose in coating monofilament PP was an attempt to avoid adverse reactions and gradually integrate the implant into host tissues by modulating the immune response. These studies also showed that while the anatomical implantation site is critical for mesh evaluation, the choice of animal model is also crucial as there are currently no recorded instances of mesh exposure in smaller animal models such as mice or rats which limits model equivalency to the human condition. In smaller animal models, mesh is implanted into alternative sites, due to the size of the vagina, which can affect results due to lack of human equivalency. Earlier studies in a rabbit vaginal model showed no exposures of collagen-coated and uncoated PP meshes [246], while in sheep vaginal models, overall exposure rates were around 22-25% in all PP meshes with or without collagen coatings [28, 29, 241]. Mesh exposure was a recurring problem in these studies with occurrences as high as 50% in uncoated PP meshes with reduced exposures varying from 8% to 25% depending on the type of collagen

coatings [28, 29]. These studies are in contrast to our current findings where no exposures were found with our new PA meshes and cross-linked gelation coatings were detrimental to mesh performance. Gelatin was considered for coating due to its cost effectiveness, biocompatibility, and afforded an excellent scaffold for eMSC delivery in a rodent model [34]. In contrast, our PA+eMSC/G constructs used a highly flexible, elastic gelatin tissue sealant based on a rapid *in situ* photopolymerised gelatin ("photoseal gelatin") to separately deliver eMSC after surgical implantation of the PA mesh [32]. This approach has previously been shown to evoke no inflammatory response *in vivo* [36]. Employing this system as a two-part protocol for delivering autologous eMSC resulted in a greatly reduced immune response and excellent tissue integration, possibly due to greater elasticity of the photoseal coating, that combined with its adhesive properties created an *in vivo* construct that moved with the intra-vaginal forces of a larger animal model.

This study showed that different synthetic mesh designs impacted the ECM of the ovine vaginal wall. Elastin fibres were disrupted following 30 days of implantation with PA/G, with local depletion at the PA/G mesh/tissue interface and the distant muscularis. In contrast, elastin fibres were maintained or even increased in PA meshes. eMSC did not influence the loss or retention of elastin fibers, already detrimentally affected in prolapsed tissue [239]. In our study, expression of the fibulin-5 elastin precursor was increased in the eMSC/PA/G samples, possibly in response to the loss of elastin protein. eMSC influence ECM remodelling, most likely by modulating M2 macrophage polarisation as shown in our previous studies [34, 170], and aligns with other findings demonstrating a link between macrophage activation, polarisation and tissue remodelling [248, 249]. Furthermore, eMSC upregulated collagen gene expression in eMSC/PA/G explants and was possibly mediated by increased M2 macrophages or eMSC themselves [250].

Fibrosis was an intended consequence of implanted mesh in order to thicken or strengthen the vaginal wall to protect it against further herniation. However, chronic fibrosis and wound contraction is a common adverse effect [251], both of which are associated with myofibroblasts [252]. PA/G implants provoked a significantly detrimental myofibroblast response at the mesh/tissue interface compared with the PA meshes where the predominant αSMA staining was reduced and appeared to be mainly neovasculature rather than myofibroblasts. eMSC that retain their stemness properties *in vitro* downregulate myofibroblast and ECM genes [250],

which could explain why the lowest myofibroblast area was observed around filaments in PA+eMSC/G explants. Additionally, the superior design of the PA meshes and better integration could also have contributed to the lower myofibroblast response. Conversely, the greater disruption of the smooth muscle layer caused by PA/G implants could have provoked the greater myofibroblast response, rather than the material itself. Longer time-points will help answer this question. Regardless, due to their antifibrotic effects, the use of this mesh in POP treatment could minimise common adverse effects.

MSC have low immunogenicity and are often used in allogeneic applications without immunosuppression. However, recent studies show that subsequent doses of allogeneic MSC are cleared more rapidly from the body [253]. One advantage of autologous MSC is their inherent compatibility with host tissues, allowing the administration of repeated doses. In the present study, to the best of our knowledge, we have demonstrated the longest persistence of autologous eMSC, showing approximately 6% survived 30 days *in vivo*. The longer MSC persist in the body, the greater their effect is likely to be, particularly in repairing damaged tissues or modulating the foreign body response to foreign grafts or mesh [106]. Human eMSC only survived up to 14 days in immunocompromised rats, despite having positive wound healing effects on the local tissues [34]. We showed that resident CD45+ leukocytes had not phagocytosed the implanted autologous eMSC. The exact fate of the eMSC over the time period remains unknown, but Ki-67 staining (see Chapter 3, Section 3.4.8) showed that implanted eMSC were not proliferating *in vivo* at day 30. The precise life span of MSC in general is also not yet known [254]. It is expected that senescence and cell death may be responsible for lack of transplanted MSC persistence in tissues. Arrest of this process or transplanting undifferentiated cultured MSC is expected to extend persistence when deployed during stem cell-based therapy [142]. Culture methods are now available that prevent apoptosis, senescence and spontaneous differentiation of human eMSC into fibroblasts [142, 250]. We did not observe spontaneous differentiation of IODEX-labelled eMSC to αSMA+ cells *in vivo*, and neither did we see a toxic effect on eMSC viability or proliferative capacity *in vitro*, as has been shown in prior research using the same concentration [226]. The gradual expulsion of IODEX nanoparticles from the eMSC cytoplasm from cellular processes is another possibility, however the retention of IODEX nanoparticles has been observed in MSC for up to eight weeks in ovine spinal columns, and therefore seems unlikely [227]. However, a lentiviral labelling vector incorporating a fluorescent dye gene that integrates into the host

DNA could be used [32] to avoid any risk of IODEX dilution from cell division, which cannot be ruled out as only one time point (30 days) was examined.

The immune system plays a central role in the biocompatibility of mesh implants, and a significant factor is the macrophage. Broadly speaking, there are two main populations of macrophages at a wound site, classically activated "pro-inflammatory" M1 macrophages and "pro-wound healing" M2 macrophages [255]. We observed a different histological immune response to eMSC/PA/G and eMSC+PA/G implants, with a greater M1 macrophage and reduced M2 response to implanted PA/G constructs compared with PA. There was reduced overall leukocyte infiltration in PA+eMSC/G explants, yet greater M1 and M2 positive staining area. Our results confirm that of our prior study using an immunocompromised rat model and observed particular macrophage activity immediately following surgery (favouring M1 macrophages) and later days (favouring M2 macrophages), but not significant activity at 30 days [34]. It is possible that 30 days is not the ideal time point to investigate the effect of implanted eMSC on the host immune system, and a more definitive result may be possible at earlier (7 days) or later (90 days) time points. In either case, our studies demonstrate the ability of eMSC to modulate the immune system to facilitate wound healing and mesh biocompatibility in rat, mouse [32, 34, 170] and for the first time in an ovine model.

There are some limitations to our study. Firstly, there was not a PA+G control group to determine whether the lightly photo-crosslinked gelatin had any effect on the tissue response. However, our data shows that the eMSC on PA+eMSC/G constructs had negligible effect compared to PA alone, indicating that if the photo-crosslinked gelatin was having an independent effect, we would have observed this. Our most significant findings, such as the lack of expsoure of photo-crosslinked PA gelatin coating compared to stiffer PA/G meshes stabilised with glutaraldehyde, persistence of autologous eMSC for at least 30 days in the ovine vagina and optimisation of the ovine animal model for transvaginal mesh surgery by selecting multiparous ewes on the basis of abnormal POP-Q values were not impacted by the lack of this control group. Our single 30 day time point also limits our ability to fully observe mesh exposure rates in the longer term (eg. 90 days). Secondly, our method of analysing M1/M2 populations at the tissue-mesh interface, though innovative in its objectivity, was performed using a single section for each sample. It is possible that analysis of multiple sections per sample could yield more accurate results. Thirdly, while we attempted to surgically implant

the PA/G and PA constructs between the muscularis and adventitia of the vagina, the ovine vaginal tissue is thin and the mesh location varied between these layers. We used urogynaecology training fellows (JM, PK) to surgically insert the mesh to ensure accurate positioning. It is unknown to what extend this has impacted the results, but future studies will make every effort to standardise the position of the implant.

5. Conclusion

This study demonstrated that the composition and design of tissue engineering constructs for delivering a cell-based therapy is important for transvaginal repair surgery in a novel multiparous ovine model of POP. Unlike previous studies using multiparous ewes, we pre-selected sheep and experimental groups were matched on their POP-Q results. In a 2-step surgeon friendly procedure, PA mesh with excellent drapeability, implanted first with eMSC delivered subsequently in situ, shows better integration than a composite mesh of PA/G. However, we were unable to fully distinguish the impact of the gelatin cross-linking method (glutaraldeyde vs blue light) through lack of a PA+no cells/G control. Implanted autologous eMSC persisted for 30 days in the vagina near mesh filaments, influencing both the host immune response, ECM remodelling and fibrotic response, demonstrating the value of an autologous approach. This study provides new materials for POP research and an improved animal model of POP, but it also demonstrates the complexity of the problem. In a time when commercial mesh has been withdrawn from several major markets, new bioengineering approaches tested in an authentic preclinical POP model offers potential therapies for women with POP who currently have few effective treatment options. Such an approach has potential to advance towards clinical studies.

4.7. Acknowledgements

This work was supported by the National Health and Medical Research Council (NHMRC) of Australia Project grant #1081944 (CEG, JAW, AR), a NHMRC Senior Research Fellowship #1042298 (CEG), and the Victoria Government's Operational Infrastructure Support Program.

4.8. Tables

Table 1: POP-Q measurements for experimental group selection.

	PA/G	PA	eMSC/PA/G	PA+eMSC/G	Incision	p-value*
Ap	-1 (-2 – 0)	-1 (-1 – 0)	-1 (-2 – 0)	-1 (-1 – 0)	-2 (-2 – 0)	0.3275
Aa	0 (-2 – 0)	-1 (-1 – 0)	0 (0 – 1)	0 (-1 – 0)	0 (-2 – 1)	0.2289

Data are median (range) at POP-Q points Ap and Aa; PA/G; polyamide dip-coated in gelatin +/- eMSC; PA+eMSC/G, polyamide with eMSC in gelatin added following implantation and blue light crosslinked. (Kruskal-Wallis)

Table 2: Mesh exposure into the vaginal wall.

	Exposure	No Exposure	p-value*
PA/G	5	7	0.012
PA	0	12	

*Chi-square test

Supplemental Table 1: Antibodies used for immunostaining.

Primary Antibodies	Concentration	Isotype	Supplier
CD45	(0.5µg/mL) 1/200	Mouse IgG1	BioRad
CD86	(0.5µg/mL) 1/1000	Mouse IgG1	BioRad
CD163	(0.5µg/mL) 1/200	Mouse IgG1	BioRad
alpha-Smooth Muscle Actin (αSMA)	(0.71µg/mL) 1/500	Mouse IgG2a	Dako

Supplemental Table 2: Primers used for qPCR.

GENE	PRIMER SEQUENCE
COL1A1	F: ATGACCGAGACGTGTGGAAA
	R: GACTTTGGCGTTAGGACAGT
COL3A1	F: AAGGGTGAAGATGGCAAAGA
	R: TTTCTCCTGGAAGGCCATTT
FBN5	F: GCGAATGTTCCCGGATCTTA
	R: CAGGTTTGTACACAGGGATT
ELN	F: CATCGCTGTTCCCCATGTCT
	R: AAACCGGACAAGGATGGAC

4.9. Figures

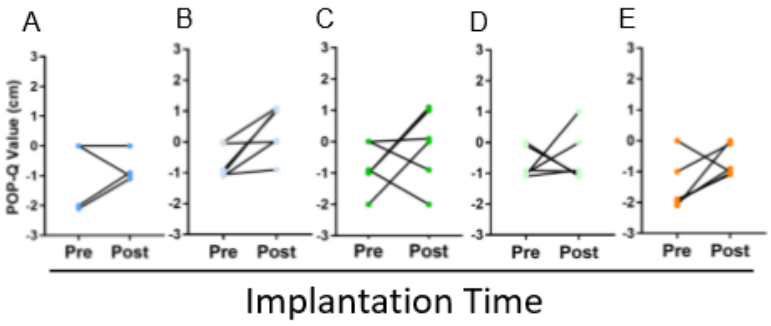

Figure 1: Change in POP-Q Ap measurements before and after 30 days after construct implantation: in **A)** PA/G, **B)** PA, **C)** eMSC/PA/G, **D)** PA + eMSC/G and **E)** incision control. Data are from n=6 animals/group. (Wilcoxon signed rank test)

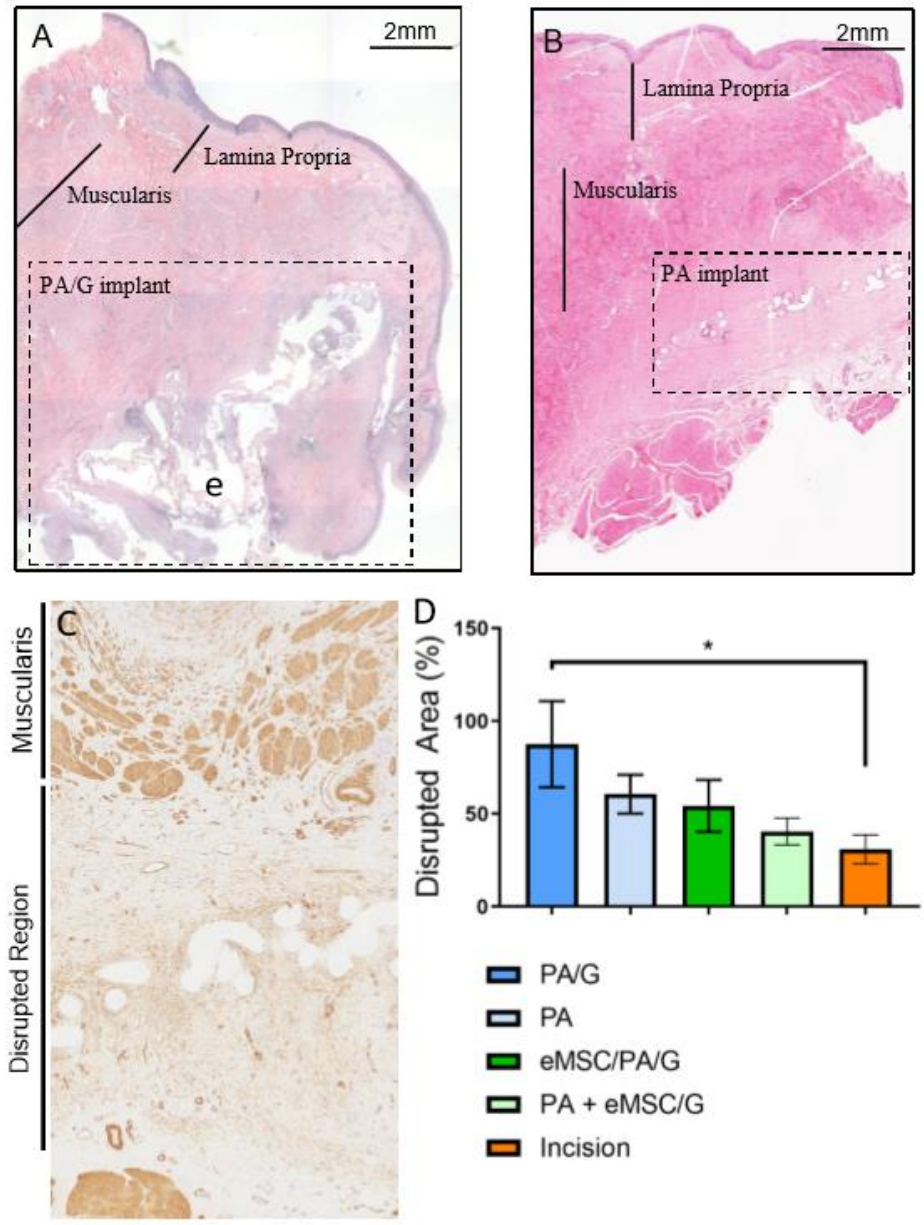

Figure 2: Mesh integration and vaginal muscularis disruption 30 days after PA/G and PA construct implantation: H&E stained vaginal wall sections showing, **A)** PA/G explant characterised by poor mesh integration, folding and exposure (e), **B)** PA explant characterised by superior mesh integration and no exposure. **C)** Representative image showing smooth muscle disruption after construct implantation into the vaginal wall. Measured disruption of total vaginal wall after implantation of **D-E)** mesh alone and with **E)** mesh with eMSC Data are mean +/- SEM of n=6 animals/group, except PA+eMSC/G & PA/G n=5. * $p<0.05$. (One-way ANOVA)

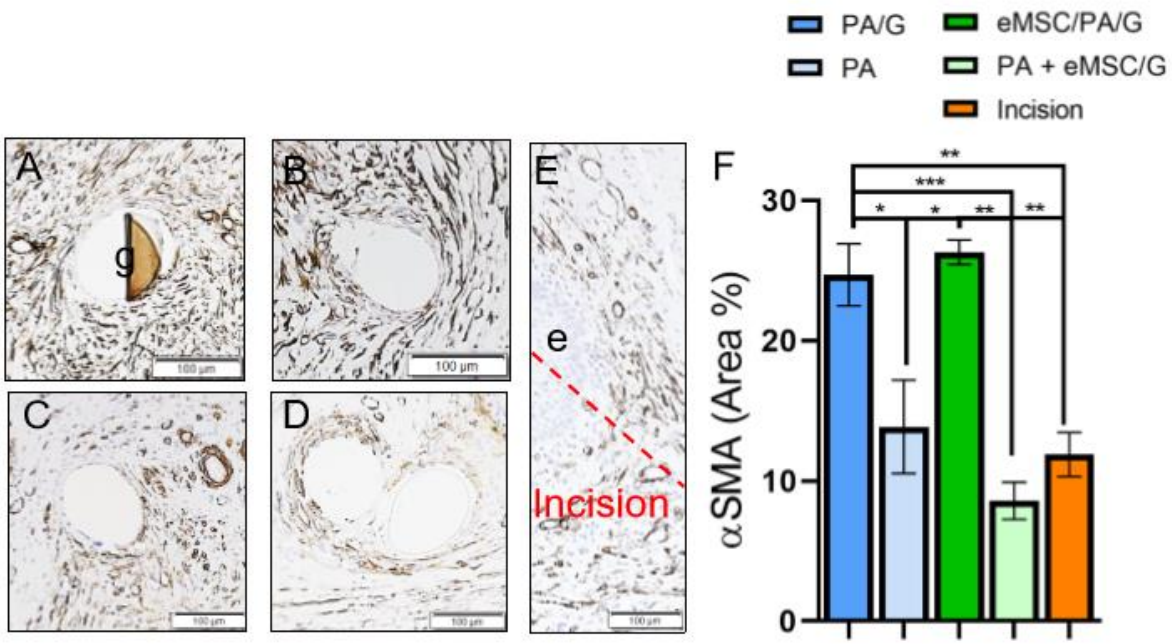

Figure 3: αSMA immunostaining of myofibroblasts and vasculature in the ovine vaginal wall of **A)** PA/G, **B)** eMSC/PA/G, **C)** PA, **D)** PA + eMSC/G explants and **E)** incision control (dotted line indicates line of incision, (e) epithelium). Image analysis of % aSMA area (myofibroblasts, (A, B) and vasculature (C, D)) are shown in **F)** in a 0-250 µm increment around mesh filaments. g, gelatin, Data are mean +/- SEM from n=6 animals/group, except eMSC/PA/G n=3 and PA+eMSC/G n=5, * $p<0.05$, ** $p<0.01$, *** $p<0.001$. (One-way ANOVA)

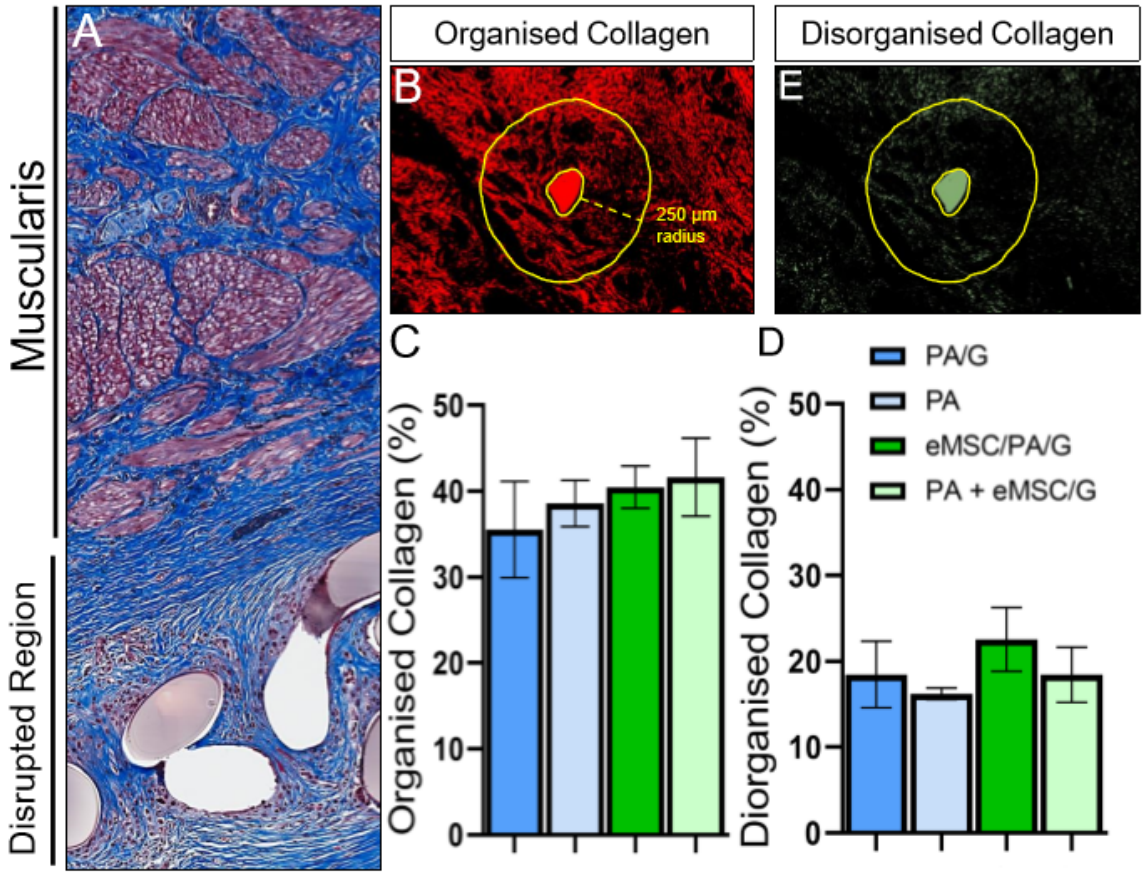

Figure 4: Organised and disorganised collagen content of ovine vaginal wall 30 days following implantation of PA/G and PA constructs: A) Mason Trichrome staining of PA explant show collagen deposition around the mesh/tissue interface. Birefringence images of Sirius Red stained tissues showing **B)** large, organised red and **E)** thinner disorganised collagen fibrils. Yellow lines show the 0-250µm increment around the mesh filaments used for quantification by image analysis of % area organised collagen in PA/G and PA explants **C)** without and with eMSC, and disorganised collagen **D)** without and with eMSC. Data are mean +/- SEM from n=6 animals/groups, except eMSC/PA/G n=4, PA+eMSC/G n=5. (One-way ANOVA)

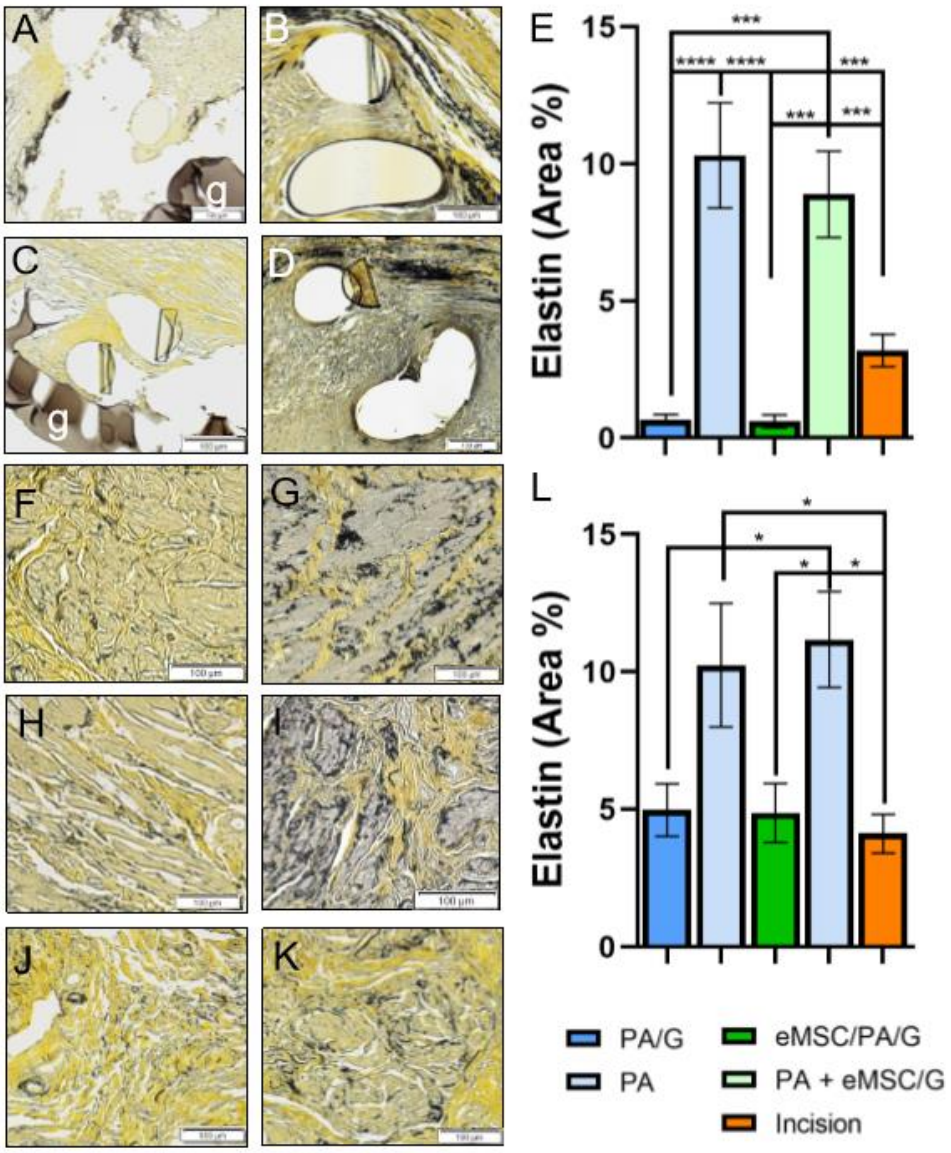

Figure 5: Elastin fibre retention around mesh filaments and in distant vaginal muscularis following implantation of PA/G and PA constructs, shown as black fibres in Hart's-stained tissue in representative images of the mesh/tissue interface following implantation of **A)** PA/G, **B)** PA, **C)** eMSC/PA/G and **D)** PA+eMSC/G constructs. **(C)** Black elastin fibres were quantified in a 0-50 µm increment around mesh filaments. Elastin fibres in muscularis distant from point of implantation in **F)** PA/G and **G)** PA, **H)** eMSC/PA/G and **I)** PA+eMSC/G constructs, **J)** point of incision and **K)** distant muscularis was measured as **L)** % area elastin.. g,gelatin. Data are mean +/- SEM from PA/G and PA n=6, eMSC/PA/G and PA + eMSC/PA/G n=5 animals/group, * $p<0.05$, ** $p<0.01$, *** $p<0.001$. (One-way ANOVA)

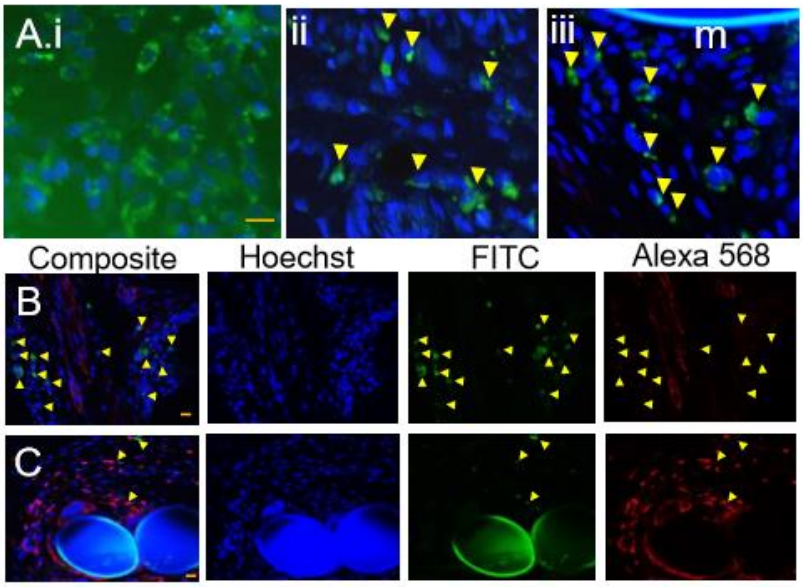

Figure 6: Iodex-FITC-labelled eMSC *in vitro* and *in vivo*. Iodex-FITC-labelled eMSC **A.i)** cultured *in vitro* for 1 day, **A.ii)** implanted *in vivo* for 30 days in eMSC/PA/G mesh appearing as punctate green particles in the cytoplasm of eMSC (yellow arrows, nuclei blue) or as **A.iii)** PA+eMSC/G explants in close proximity to mesh (m). eMSC (yellow arrowheads) did not **B)** co-localise with αSMA+ smooth muscle cells (red), nor were **C)** taken up by CD45+ resident macrophages (red). Yellow scalebars - 50μm.

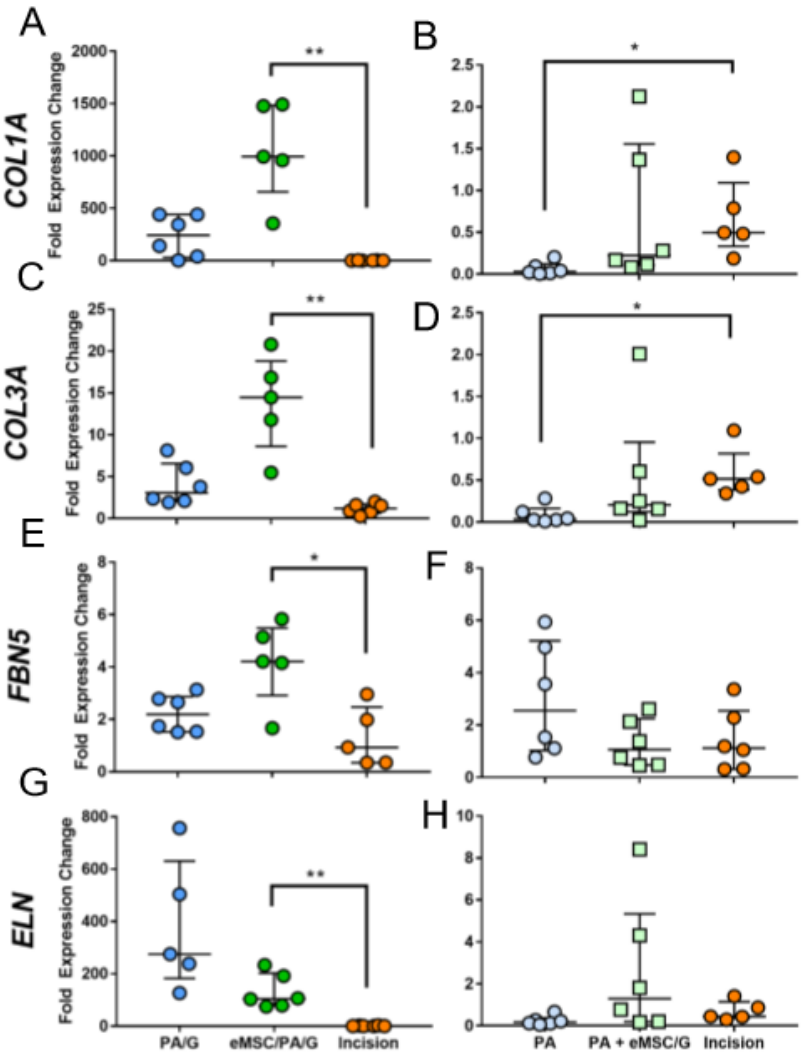

Figure 7: qPCR analysis of ECM gene expression within ovine vaginal wall 30 days after implantation of PA/G and PA constructs. **A, C, E** and **G** are PA/G explants and **B, D, F** and **H** are PA explants. Data are mean +/- SEM from n=6 animals/group, *p<0.05, **p<0.01. (One-way ANOVA)

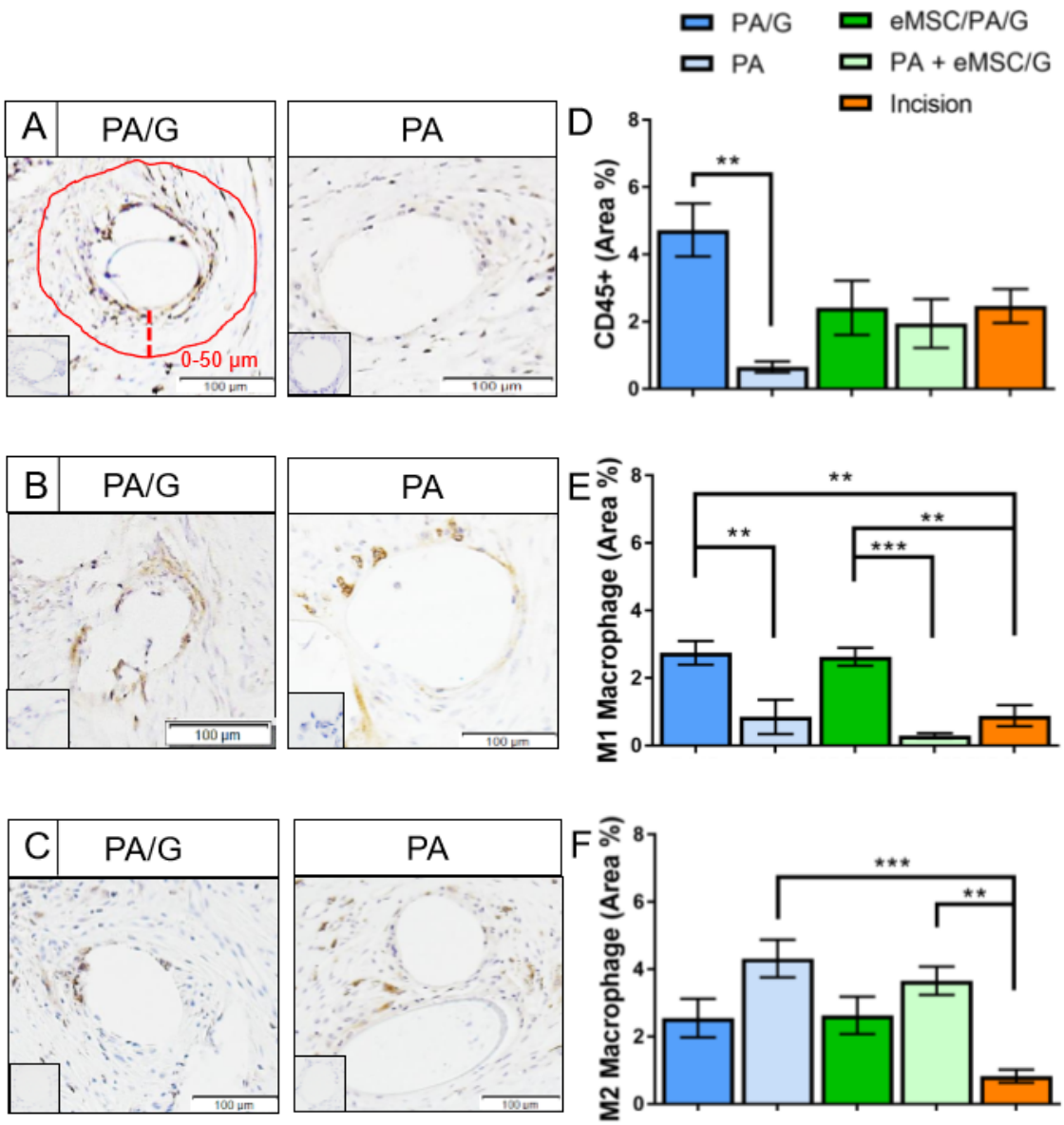

Figure 8: Immune response around mesh filaments in PA/G and PA constructs after 30 days: A) CD45+ leukocytes, **B)** CD86+ M1 macrophages and **C)** CD163+ M2 macrophages in PA/G and PA explants was measured within a 0-50 µm increment of mesh filaments (outlined in red). Quantification of % positive area staining for **D)** CD45+ leukocyte, **E)** CD86+ M1 macrophages and **F)** CD163+ M2 macrophages. Inserts are negative controls. Data are mean +/- SEM from n=6 animals/group except PA/G n=5, ** p<0.01, ***p<0.001. (One-way ANOVA)

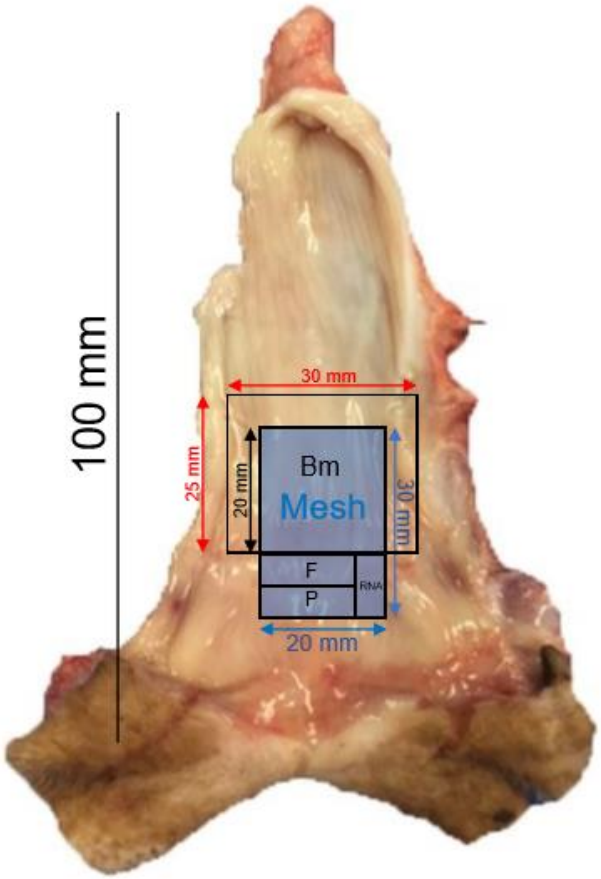

Supplemental Figure 1: Diagram of post-mortem tissue harvest of ovine vaginal tissue. Blue region is mesh, black outlines sections of tissue retrieved for biomechanical (Bm), histological (f, frozen and p, paraffin) and qPCR (RNA) analysis.

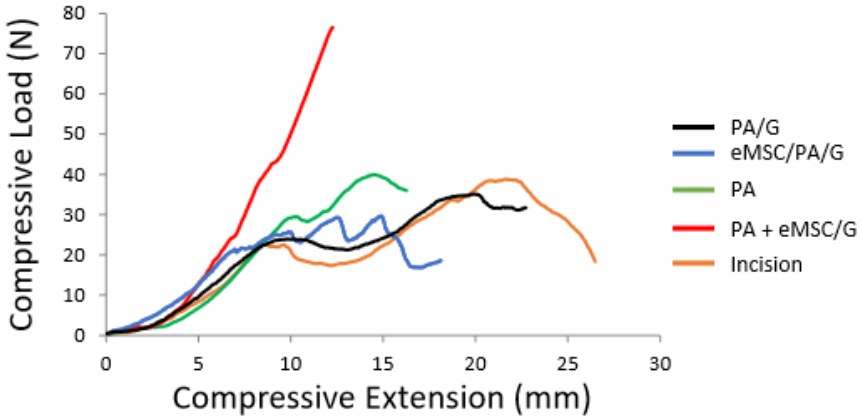

Supplemental Figure 2: Biomechanical stiffness of ovine vaginal tissue 30 days following implantation of PA/G and PA constructs: PA/G and eMSC/PA/G, PA, PA+eMSC/G and incisional control. (Plots are means, n=6 animals/group)

Chapter 5

General Discussion

The main goal of this thesis was to optimise a functional large animal model of POP as a test system for evaluating new scaffolds intended for the delivery of eMSC to support and repair weakened vaginal walls. For my thesis I focused on refining the ovine animal model and demonstrated the importance of mesh design for treating POP. I first characterised the vaginal tissue in the ovine animal model using clinical, physical, histological, biochemical and biomechanical approaches. I observed that increasing parity thinned the muscularis of the vaginal wall and increased the elastic fibre content, which correlated with a weakened and more flexible vagina in multiparous ewes. I utilised a modified clinical POP-Q evaluation system that measures vaginal tissue distensibility [183]. This allowed the specific selection of ewes with vaginal wall weakness and the matching of animals between experimental groups. I observed the importance of mesh design and biomechanical compliance, as the stiffer glutaraldehyde stabilised gelatin-coated polyamide mesh (PA/G) integrated poorly and had high rates of exposure during both the pilot study and 30 day trial. In comparison, a two-step protocol in which the same PA mesh without gelatin was implanted followed by a cell/gelatin mixture applied and photocross-linked *in situ* (creating a very elastic/flexible gelatin scaffold), proved the superior mesh scaffold system for delivery of eMSC into the vaginal wall. Using this animal model allowed us to demonstrate autologous IODEX-labelled eMSC persisted until 30 days after implantation.

The ovine animal model is emerging as one of the most human-equivalent models available for studying the pathology and treatment of POP. Not only do ewes develop POP spontaneously at relatively high rates, around 15%, but the most typically affected ewes are older and multiparous, similar to onset in women [227, 251, 256]. Similar to women, ewes have a comparable vaginal length and diameter, a pelvic anatomy with a tri-level support system, and a large head-to-pelvis ratio that impacts vaginally-delivered young [179, 257]. These properties have seen the use of ovine models expand rapidly over the past decade, with efforts to map the biomechanical and anatomical composition of their vaginal tissue leading to a wealth of information for their use as models in the development of POP treatment [175, 258-260]. We have further refined the ovine animal model by using the modified POP-Q to select ewes for our experimental groups by selecting ewes with abnormal POP-Q measurements at points Aa and Ap for use in our TE 7 day implantation pilot and 30 day trial. I identified adverse outcomes that did not occur in smaller animal models, such as lack of biocompatibility of PA/G composite constructs exemplified by mesh exposure that would have undoubtedly arisen in any preclinical trial with women. The optimisation and use of the ovine model has provided insight

into the practicality of the surgical procedure itself, particularly the implantation of the TE construct. The PA/G constructs were difficult in both handling and implanting, with surgeons often commenting on the stiffness of the gelatin-coated mesh and the challenge they posed to implant into the vaginal wall. In contrast, non-coated PA mesh was easy to handle and draped over the tissue without difficulty. Minimalizing difficulties associated with cell-seeded TE constructs through the use of a simpler 2 step insertion procedure will minimize the learning curve required for urogynaecologists to apply this new approach and would contribute to the success of future TE-based POP treatment.

In the first aim of my thesis I assessed the effect of parity on the ovine vaginal wall by correlating histological, biochemical and biomechanical results with POP-Q and pressure sensor measurements in nulliparous, primiparous and multiparous ewes. The two most significant alterations to the multiparous vaginal wall was the reduction of the total smooth muscle area (muscularis) and the increased elastic fibre content of the lamina propria. These two main findings were associated with a mechanically weaker and more flexible vaginal tissue, which is similar to what we observed during our previous analysis of ovine vaginal tissue from the same region [180]. It is interesting to consider that the original aim of synthetic mesh implantation was to instigate a fibrotic response that would thicken the vaginal wall with mostly collagenous scar-tissue. However, our data (from both Aims 1 and 3) suggests that the vaginal tissue contains sufficient collagen, meaning that the majority of herniation resistance is provided by a thinned layer of smooth muscle. Histological examination of prolapsed vaginal tissue from parous women exhibited disorganised smooth muscle cells that had been displaced by increased collagen III deposition [45]. This was similar to our findings in our ovine model with a reduced smooth muscle area and increased lamina propria (composed mostly of collagen) portion of the vaginal wall, which supports our suggestion that the integrity of the muscularis is important for resisting POP. Other research investigating the effect of parity on the structure of the pelvic floor muscles showed increased fibre length and decreased muscle tensile strength in older women, likely contributing to POP vulnerability [261]. The preservation of the muscularis layer should be a prime consideration for any future mesh research, either through surgical avoidance of damaging muscularis integrity or possibly through treatment targeting smooth muscle cell replenishment. Though neither of these were within the scope of my research project, it would be interesting to investigate the potential for targeted smooth muscle restoration within the muscularis, or to prevent its loss, as an alternative means of treatment for POP. eMSC are capable of differentiating into smooth

muscle cells *in vitro*, though no evidence was observed for this having occurred *in vivo* at 30 days in my study [262]. Our laboratory is currently investigating POP-prevention by assessing the effect of autologous ovine eMSC injected into balloon-injured vaginal walls of nulliparous ewes as a model of first birth injury, as the most damage occurs during first vaginal delivery in women [47]. Promoting the healing of the muscularis layer damaged by vaginal birth could prevent the need for future POP treatment altogether and would be a preferable alternative to surgically implanted synthetic materials [166, 263].

Ovine animal models are growing in popularity, but the selection of ewes on the basis of POP-Q measurements has not previously been undertaken. Our innovation in using an ovine model with POP-Q confirmed-vaginal weakness is, we believe, the closest model of recapitulating women with POP. The importance of this progress is supported by findings from my first aim, where we showed that multiparous vaginal tissue was considerably weaker with reduced stiffness than either nulliparous and primiparous ewes. The difference between multiparous and primiparous ewes was only the delivery of a single lamb, reinforcing the importance of vaginal trauma during first vaginal delivery [47]. Our study was innovative by also correlating histological findings with both POP-Q and pressure sensor measurements. Using this method, we were able to observe the anatomical effect of parity and statistically link those effects with POP-Q measurements of tissue distensibility.

In the second aim of my thesis, I optimised both the IODEX labelling of eMSC and the ovine animal model we would use for future preclinical trials of TE constructs to track eMSC fate. The fate of IODEX-labelled eMSC implanted in ovine vagina on a TE construct is currently unknown. The use of IODEX nanoparticles (a type of superparamagnetic iron oxide nanoparticle, or SPION) are well documented for labelling other cell types [225, 226], and similar to previous studies using IODEX nanoparticles to label many other cell types, my optimisation studies for labelling eMSC showed similar concentrations (10ug/100,000 cells)were optimal. Even after 6 days culture, IODEX-labelled eMSC still retained 20% of the initial IODEX label. Despite poor PA/G mesh integration into ovine vaginal tissue, considerable retention of IODEX within the cytoplasm was detected *in vivo* suggesting proliferation of the labelled eMSC. However, no Ki-67^{+} eMSC were detected, suggesting the eMSC were not proliferating *in vivo* and neither were they cleared by macrophages *in vivo*. At 30 days the implanted IODEX-labelled eMSC remain near the implantation site, most likely secreting pro-wound healing cytokines until either being taken up by resident macrophages or

remaining in the surrounding tissues. This supports the current evidence in rats that eMSCs exert a paracrine mechanism of action in improving PA/G mesh integration rather than incorporating into surrounding tissues. [34]. The ease and speed of IODEX labelling and their nontoxicity to eMSC, makes FITC-IODEX nanoparticles an attractive method of cell tracking for short-term time-points of TE construct implantation.

One concern was the variation in the purity of $CD271^{+}/CD49f^{-}$ eMSC in the samples used for implantation, even though they were cultured for similar passages. Our measure of ovine eMSC "stemness" was using the percentage of $CD271^{+}/CD49f^{-}$ cells, the same markers used to isolate eMSC from ovine endometrium [129]. This variability could be due to biological variation between individual ewes or perhaps that the ovine eMSC spontaneously differentiated into fibroblasts during culture expansion as shown for human eMSC [141, 142]. MSC populations losing stemness with is supported by the established literature [142, 232]. Arresting this loss in passaged eMSC has been achieved by culturing in a serum-free medium containing the transforming growth factor beta (TGFβ) receptor inhibitor, A83-01. A83-01 prevents SMAD2/3 phosphorylation [142]. Its inclusion in cultures of late-passage eMSC maintained clonogenicity and differentiation potential while blocking senescence and apoptosis. As a small molecule inhibitor, A8301 is potentially a useful alternative to current methods of culturing eMSC for POP treatment and should be used in future TE preclinical research involving eMSC.

I demonstrated for the first time that autologous eMSC persist for up to 30 days following implantation into host recipient vaginal tissue. Our previous research, using human eMSC on PA/G meshes implanted into an immunocompromised rat model, showed limited eMSC retention. By 14 days most DIO-labelled human eMSC were no longer detectable in rat models and it was hypothesised that host macrophages phagocytosed implanted human eMSC. The results generated in my third aim supports this hypothesis, due to the persistence of IODEX-labelled autologous ovine eMSC in sheep for up to 30 days. The lack of phagocytosed IODEX nanoparticles observed in immunostained CD45+ leukocytes in vaginal tissues implanted with autologous eMSC suggests they avoid host immune rejection and therefore persist for the long-term. Xenogenic human eMSC were taken up by the macrophages of the immunocompromised rat model after 14 days, yet their influence persisted 30 and 90 days after implantation, likely due to the initial secretion of exosomes and cytokines [250]. If xenogeneic eMSC have this far-reaching influence weeks after their removal, the potential of autologous eMSC for influencing

long-term wound healing is an exciting prospect worthy of exploration in longer term (90 days) in the ovine vaginal surgery model.

In Aim 3 my comparison between PA/G and PA constructs with incisional controls showed that the PA/G constructs were poorly integrated and highly folded, with high rates of exposure. This also could have masked detectable changes in the distribution of CD86+ M1 inflammatory macrophages and CD163+ M2 macrophages at the filament/tissue interface, hindering interpretation on the effect of autologous eMSC on the innate immune system. This is in contrast to the well-integrated PA constructs, which exhibited an increase in the M2 population compared to incisional controls. The lack of significant difference in macrophage response between the 2 mesh designs (PA vs PA/G construct groups) by the presence of autologous eMSC was unexpected, given our prior research observing the immune-modulatory properties of eMSC by 30 days [34]. In contrast, the PA constructs integrated well regardless of the presence of eMSC, with only slight differences in the immune response between PA constructs with and without eMSC. Though these data might suggest that the presence of eMSC is not necessary and that mesh design takes precedence, our time point was too early to witness any potential long-term benefits of eMSC. Longer time points could further explore the long-term effects (ie 90 days) of the implanted eMSC.

My third aim also demonstrated the suitability of our improved ovine model of POP and the importance of mesh material design on tissue integration and adverse events associated with transvaginal implantation of mesh. We used PA mesh which was synthesised by monofilament warp knitted to have both large (0.99 +/- 0.10 mm2) and small (0.04 +/- 0.02 mm2) pore areas. Established literature on mesh material demonstrated that porosity is of particular importance to the biocompatibility and integration of mesh implants [10, 264]. This suggests part of the failure of our monofilament PA/G constructs to integrate into the vagina of a large animal model was due to the pores of the PA mesh being completely filled with gelatin, which resulted in a stiffer, less drapeable mesh [31]. The purpose of the gelatin-coating was to provide a biocompatible scaffold to deliver high numbers of eMSC for implantation. However, the porcine gelatin we used is aqueous at body temperature. Cross-linking the gelatin with glutaraldehyde stabilised the gelatin as a high-density gelatin-coat which provided an adequate PA/G scaffold in our smaller animal models [34, 170]. This coat also increased the stiffness of the resulting construct compared to PA mesh on its own, which was not apparent in smaller animal models but which became evident in our ovine animal model through high rates of

exposure. This is likely due to biomechanical mismatching between the PA/G constructs and surrounding tissues. The exposure we observed is similar to other studies that also used coated-mesh implanted into ovine animal models and experienced high rates of exposure [28, 29]. The alternative elastic-based gelatin containing eMSC which was cross-linked in a two-step protocol that involved a ruthenium-based photo-crosslinking agent produced a less dense and more flexible gelatin that biomechanically matched the surrounding tissue [36]. The lack of coating is also the likely reason the PA mesh on its own was more drapeable. In addition to the increased drapability of PA mesh, the two-step procedure for implanting mesh and cells is significantly easier for the surgeons to use. This is an important consideration for clinical translation of MSC-based TE treatment for POP, as surgical implantation is a critical step which already varies with the skill of individual surgeons.

The implantation process of a TE construct was traumatic to the vaginal tissue, particularly the recipients of PA/G constructs with disruption of the muscularis layer and diminishment of elastic fibre content compared to controls. Both TE constructs were traumatic, but the PA construct was more compliant with the natural tissue, easier to handle and retained ECM and smooth muscle content that could be conducive to successful long-term recovery. Furthermore, the target for this proposed treatment would be women who already have POP and require TE construct insertion to repair the herniation and restore damaged tissue. According to my first aim, this muscle layer will have thinned in multiparous, older women who experience POP. This should serve to guide future mesh development to not only support the herniated tissue, but also regeneration of the thinned vaginal muscularis. Preserving the elastic fibre content and assuaging the myofibroblast response in weakened vaginal tissue has promise to improve surgical POP repair operations. Our unique multiparous ovine transvaginal surgery model using ewes with weakened vaginal tissue and the two-step PA and eMSC implantation protocol demonstrated not only a superior method of cell delivery, but also of tissue preservation. It is likely such an approach would doubtless improve the regenerative potential of implanted autologous MSC. To this end, nanofiber constructs are being investigated for their potential to treat POP with an electrospun nanofiber mat that is both extremely light and flexible, [265] and are showing potential as a scaffold for the delivery of cells [149, 166, 266-268] where gelatin polymer blends are showing excellent biocompatibility. I have performed an innovative refinement of the ovine animal model of POP, which could provide these new mesh types with a human equivalent model needed to further investigate their potential for clinical translation.

References

1. Burrows, L.J., L.A. Meyn, M.D. Walters and A.M. Weber, *Pelvic symptoms in women with pelvic organ prolapse.* Obstet Gynecol, 2004. **104**(5 Pt 1): p. 982-8.
2. Lee, U.J., M.H. Kerkhof, S.A. van Leijsen and J.P. Heesakkers, *Obesity and pelvic organ prolapse.* Curr Opin Urol, 2017. **27**(5): p. 428-434.
3. Ward, R.M., D.R. Velez Edwards, T. Edwards, A. Giri, R.N. Jerome and J.M. Wu, *Genetic epidemiology of pelvic organ prolapse: a systematic review.* American journal of obstetrics and gynecology, 2014. **211**(4): p. 326-335.
4. Subak, L.L., L.E. Waetjen, S. van den Eeden, D.H. Thom, E. Vittinghoff and J.S. Brown, *Cost of pelvic organ prolapse surgery in the United States.* Obstet Gynecol, 2001. **98**(4): p. 646-51.
5. Australian Commission on Safety and Quality in Health Care, *Treatment Options for Pelvic Organ Prolapse.* 2018.
6. Stanford, E.J., A. Cassidenti and M.D. Moen, *Traditional native tissue versus mesh-augmented pelvic organ prolapse repairs: providing an accurate interpretation of current literature.* Int Urogynecol J, 2012. **23**(1): p. 19-28.
7. Gerten, K.A., A.D. Markland, L.K. Lloyd and H.E. Richter, *Prolapse and incontinence surgery in older women.* J Urol, 2008. **179**(6): p. 2111-8.
8. Sung, V.W., S. Weitzen, E.R. Sokol, C.R. Rardin and D.L. Myers, *Effect of patient age on increasing morbidity and mortality following urogynecologic surgery.* Am J Obstet Gynecol, 2006. **194**(5): p. 1411-7.
9. Iyer, S. and S.M. Botros, *Transvaginal mesh: a historical review and update of the current state of affairs in the United States.* Int Urogynecol J, 2017. **28**(4): p. 527-535.
10. Liang, R., K. Knight, S. Abramowitch and P.A. Moalli, *Exploring the basic science of prolapse meshes.* Current opinion in obstetrics & gynecology, 2016. **28**(5): p. 413-419.
11. Feola, A., S. Abramowitch, Z. Jallah, S. Stein, W. Barone, S. Palcsey and P. Moalli, *Deterioration in biomechanical properties of the vagina following implantation of a high-stiffness prolapse mesh.* Bjog, 2013. **120**(2): p. 224-232.
12. Wein, A.J., *Re: Implications of the FDA statement on transvaginal placement of mesh: the aftermath.* J Urol, 2015. **193**(2): p. 606-7.
13. Pott, P.P., M.L.R. Schwarz, R. Gundling, K. Nowak, P. Hohenberger and E.D. Roessner, *Mechanical properties of mesh materials used for hernia repair and soft tissue augmentation.* PloS one, 2012. **7**(10): p. e46978-e46978.
14. Baylón, K., P. Rodríguez-Camarillo, A. Elías-Zúñiga, J.A. Díaz-Elizondo, R. Gilkerson and K. Lozano, *Past, Present and Future of Surgical Meshes: A Review.* Membranes, 2017. **7**(3): p. 47.
15. Amid, P.K., *Classification of biomaterials and their related complications in abdominal wall hernia surgery.* Hernia, 1997. **1**(2): p. 70-70.
16. Todros, S., P.G. Pavan and A.N. Natali, *Synthetic surgical meshes used in abdominal wall surgery: Part I-materials and structural conformation.* J Biomed Mater Res B Appl Biomater, 2017. **105**(3): p. 689-699.
17. Klinge, U., B. Klosterhalfen, V. Birkenhauer, K. Junge, J. Conze and V. Schumpelick, *Impact of polymer pore size on the interface scar formation in a rat model.* J Surg Res, 2002. **103**(2): p. 208-14.
18. Orenstein, S.B., E.R. Saberski, D.L. Kreutzer and Y.W. Novitsky, *Comparative analysis of histopathologic effects of synthetic meshes based on material, weight, and pore size in mice.* J Surg Res, 2012. **176**(2): p. 423-9.
19. Weyhe, D., W. Cobb, J. Lecuivre, A. Alves, S. Ladet, D. Lomanto and Y. Bayon, *Large pore size and controlled mesh elongation are relevant predictors for mesh integration quality and low*

shrinkage--Systematic analysis of key parameters of meshes in a novel minipig hernia model. Int J Surg, 2015. **22**: p. 46-53.
20. Cobb, W.S., K.W. Kercher and B.T. Heniford, *The argument for lightweight polypropylene mesh in hernia repair.* Surg Innov, 2005. **12**(1): p. 63-9.
21. Winters, J.C., M.P. Fitzgerald and M.D. Barber, *The use of synthetic mesh in female pelvic reconstructive surgery.* BJU Int, 2006. **98 Suppl 1**: p. 70-6; discussion 77.
22. Brown, C.N. and J.G. Finch, *Which mesh for hernia repair?* Annals of the Royal College of Surgeons of England, 2010. **92**(4): p. 272-278.
23. Klinge, U., J. Otto and T. Mühl, *High structural stability of textile implants prevents pore collapse and preserves effective porosity at strain.* BioMed research international, 2015. **2015**: p. 953209-953209.
24. Klinge, U., J.K. Park and B. Klosterhalfen, *'The ideal mesh?'.* Pathobiology, 2013. **80**(4): p. 169-75.
25. Zhu, L.M., P. Schuster and U. Klinge, *Mesh implants: An overview of crucial mesh parameters.* World J Gastrointest Surg, 2015. **7**(10): p. 226-36.
26. Cervigni, M., F. Natale, C. La Penna, M. Saltari, A. Padoa and M. Agostini, *Collagen-coated polypropylene mesh in vaginal prolapse surgery: an observational study.* Eur J Obstet Gynecol Reprod Biol, 2011. **156**(2): p. 223-7.
27. Darzi, S., I. Urbankova, K. Su, J. White, C. Lo, D. Alexander, J.A. Werkmeister, C.E. Gargett and J. Deprest, *Tissue response to collagen containing polypropylene meshes in an ovine vaginal repair model.* Acta Biomater, 2016. **39**: p. 114-123.
28. Endo, M., I. Urbankova, J. Vlacil, S. Sengupta, T. Deprest, B. Klosterhalfen, A. Feola and J. Deprest, *Cross-linked xenogenic collagen implantation in the sheep model for vaginal surgery.* Gynecol Surg, 2015. **12**(2): p. 113-122.
29. Feola, A., M. Endo, I. Urbankova, J. Vlacil, T. Deprest, S. Bettin, B. Klosterhalfen and J. Deprest, *Host reaction to vaginally inserted collagen containing polypropylene implants in sheep.* Am J Obstet Gynecol, 2015. **212**(4): p. 474.e1-8.
30. Blazquez, R., F.M. Sanchez-Margallo, V. Alvarez, A. Uson, F. Marinaro and J.G. Casado, *Fibrin glue mesh fixation combined with mesenchymal stem cells or exosomes modulates the inflammatory reaction in a murine model of incisional hernia.* Acta Biomater, 2018. **71**: p. 318-329.
31. Edwards, S.L., J.A. Werkmeister, A. Rosamilia, J.A. Ramshaw, J.F. White and C.E. Gargett, *Characterisation of clinical and newly fabricated meshes for pelvic organ prolapse repair.* J Mech Behav Biomed Mater, 2013. **23**: p. 53-61.
32. Darzi, S., J.A. Deane, C.A. Nold, S.E. Edwards, D.J. Gough, S. Mukherjee, S. Gurung, K.S. Tan, A.V. Vashi, J.A. Werkmeister and C.E. Gargett, *Endometrial Mesenchymal Stem/Stromal Cells Modulate the Macrophage Response to Implanted Polyamide/Gelatin Composite Mesh in Immunocompromised and Immunocompetent Mice.* Scientific Reports, 2018. **8**(1): p. 6554.
33. Ulrich, D., S.L. Edwards, J.F. White, T. Supit, J.A. Ramshaw, C. Lo, A. Rosamilia, J.A. Werkmeister and C.E. Gargett, *A preclinical evaluation of alternative synthetic biomaterials for fascial defect repair using a rat abdominal hernia model.* PLoS One, 2012. **7**(11): p. e50044.
34. Ulrich, D., S.L. Edwards, K. Su, K.S. Tan, J.F. White, J.A.M. Ramshaw, C. Lo, A. Rosamilia, J.A. Werkmeister and C.E. Gargett, *Human Endometrial Mesenchymal Stem Cells Modulate the Tissue Response and Mechanical Behavior of Polyamide Mesh Implants for Pelvic Organ Prolapse Repair.* Tissue Engineering. Part A, 2014. **20**(3-4): p. 785-798.
35. Rosen, M.J., *Polyester-based mesh for ventral hernia repair: is it safe?* Am J Surg, 2009. **197**(3): p. 353-9.
36. Elvin, C.M., T. Vuocolo, A.G. Brownlee, L. Sando, M.G. Huson, N.E. Liyou, P.R. Stockwell, R.E. Lyons, M. Kim, G.A. Edwards, G. Johnson, G.A. McFarland, J.A. Ramshaw and J.A.

Werkmeister, *A highly elastic tissue sealant based on photopolymerised gelatin.* Biomaterials, 2010. **31**(32): p. 8323-31.
37. Badylak, S.F., *Decellularized allogeneic and xenogeneic tissue as a bioscaffold for regenerative medicine: factors that influence the host response.* Ann Biomed Eng, 2014. **42**(7): p. 1517-27.
38. Porzionato, A., E. Stocco, S. Barbon, F. Grandi, V. Macchi and R. De Caro, *Tissue-Engineered Grafts from Human Decellularized Extracellular Matrices: A Systematic Review and Future Perspectives.* International journal of molecular sciences, 2018. **19**(12): p. 4117.
39. Lupinacci, R.M., A.S. Gizard, E. Rivkine, C. Debove, F. Menegaux, C. Barrat, P. Wind and C. Tresallet, *Use of a bioprosthetic mesh in complex hernia repair: early results from a French multicenter pilot study.* Surg Innov, 2014. **21**(6): p. 600-4.
40. Adelman, D.M. and K.G. Cornwell, *Bioprosthetic Versus Synthetic Mesh: Analysis of Tissue Adherence and Revascularization in an Experimental Animal Model.* Plastic and reconstructive surgery. Global open, 2018. **6**(5): p. e1713-e1713.
41. FitzGerald, J.F. and A.S. Kumar, *Biologic versus Synthetic Mesh Reinforcement: What are the Pros and Cons?* Clinics in colon and rectal surgery, 2014. **27**(4): p. 140-148.
42. Liang, R., K. Knight, D. Easley, S. Palcsey, S. Abramowitch and P.A. Moalli, *Towards rebuilding vaginal support utilizing an extracellular matrix bioscaffold.* Acta Biomater, 2017. **57**: p. 324-333.
43. East, B., M. Plencner, M. Kralovic, M. Rampichova, V. Sovkova, K. Vocetkova, M. Otahal, Z. Tonar, Y. Kolinko, E. Amler and J. Hoch, *A polypropylene mesh modified with poly-epsilon-caprolactone nanofibers in hernia repair: large animal experiment.* Int J Nanomedicine, 2018. **13**: p. 3129-3143.
44. Vashaghian, M., C.M. Diedrich, B. Zandieh-Doulabi, A. Werner, T.H. Smit and J.P. Roovers, *Gentle cyclic straining of human fibroblasts on electrospun scaffolds enhances their regenerative potential.* Acta Biomater, 2019. **84**: p. 159-168.
45. Vetuschi, A., A. D'Alfonso, R. Sferra, D. Zanelli, S. Pompili, F. Patacchiola, E. Gaudio and G. Carta, *Changes in muscularis propria of anterior vaginal wall in women with pelvic organ prolapse.* European journal of histochemistry : EJH, 2016. **60**(1): p. 2604-2604.
46. Meijerink, A.M., R.H. van Rijssel and P.J. van der Linden, *Tissue composition of the vaginal wall in women with pelvic organ prolapse.* Gynecol Obstet Invest, 2013. **75**(1): p. 21-7.
47. Kamisan Atan, I., S. Lin, H.P. Dietz, P. Herbison and P.D. Wilson, *It is the first birth that does the damage: a cross-sectional study 20 years after delivery.* Int Urogynecol J, 2018. **29**(11): p. 1637-1643.
48. Memon, H.U. and V.L. Handa, *Vaginal childbirth and pelvic floor disorders.* Womens Health (Lond), 2013. **9**(3): p. 265-77; quiz 276-7.
49. Rahn, D.D., J.F. Acevedo and R.A. Word, *Effect of vaginal distention on elastic fiber synthesis and matrix degradation in the vaginal wall: potential role in the pathogenesis of pelvic organ prolapse.* American journal of physiology. Regulatory, integrative and comparative physiology, 2008. **295**(4): p. R1351-R1358.
50. Feola, A., S. Abramowitch, K. Jones, S. Stein and P. Moalli, *Parity negatively impacts vaginal mechanical properties and collagen structure in rhesus macaques.* Am J Obstet Gynecol, 2010. **203**(6): p. 595.e1-8.
51. Xelhuantzi, N., J. Rodríguez-Antolín, L. Nicolás, F. Castelán, E. Cuevas and M. Martínez-Gómez, *Tissue alterations in urethral and vaginal walls related to multiparity in rabbits.* The Anatomical Record, 2014. **297**(10): p. 1963-1970.
52. Larsson, C., K. Kallen and E. Andolf, *Cesarean section and risk of pelvic organ prolapse: a nested case-control study.* Am J Obstet Gynecol, 2009. **200**(3): p. 243.e1-4.
53. Richardson, A.C., J.B. Lyon and N.L. Williams, *A new look at pelvic relaxation.* Am J Obstet Gynecol, 1976. **126**(5): p. 568-73.

54. Rahn, D.D., M.D. Ruff, S.A. Brown, H.F. Tibbals and R.A. Word, *Biomechanical properties of the vaginal wall: effect of pregnancy, elastic fiber deficiency, and pelvic organ prolapse.* Am J Obstet Gynecol, 2008. **198**(5): p. 590.e1-6.
55. Vazin, T. and W.J. Freed, *Human embryonic stem cells: derivation, culture, and differentiation: a review.* Restorative neurology and neuroscience, 2010. **28**(4): p. 589-603.
56. Vats, A., N.S. Tolley, A.E. Bishop and J.M. Polak, *Embryonic stem cells and tissue engineering: delivering stem cells to the clinic.* Journal of the Royal Society of Medicine, 2005. **98**(8): p. 346-350.
57. Telpalo-Carpio, S., J. Aguilar-Yañez, M. Gonzalez-Garza, D.E. Cruz-Vega and J. Moreno-Cuevas, *iPS cells generation: an overview of techniques and methods.* Journal of stem cells & regenerative medicine, 2013. **9**(1): p. 2-8.
58. Singh, V.K., M. Kalsan, N. Kumar, A. Saini and R. Chandra, *Induced pluripotent stem cells: applications in regenerative medicine, disease modeling, and drug discovery.* Frontiers in cell and developmental biology, 2015. **3**: p. 2-2.
59. Takahashi, K. and S. Yamanaka, *Induced pluripotent stem cells in medicine and biology.* Development, 2013. **140**(12): p. 2457-61.
60. Zhao, T., Z.N. Zhang, Z. Rong and Y. Xu, *Immunogenicity of induced pluripotent stem cells.* Nature, 2011. **474**(7350): p. 212-5.
61. Garreta, E., S. Sanchez, J. Lajara, N. Montserrat and J.C.I. Belmonte, *Roadblocks in the Path of iPSC to the Clinic.* Current transplantation reports, 2018. **5**(1): p. 14-18.
62. Montagnani, S., M.A. Rueger, T. Hosoda and D. Nurzynska, *Adult Stem Cells in Tissue Maintenance and Regeneration.* Stem cells international, 2016. **2016**: p. 7362879-7362879.
63. Gonzalez, M.A. and A. Bernad, *Characteristics of adult stem cells.* Adv Exp Med Biol, 2012. **741**: p. 103-20.
64. Clevers, H. and F.M. Watt, *Defining Adult Stem Cells by Function, not by Phenotype.* Annu Rev Biochem, 2018. **87**: p. 1015-1027.
65. Blau, H.M., B.D. Cosgrove and A.T. Ho, *The central role of muscle stem cells in regenerative failure with aging.* Nat Med, 2015. **21**(8): p. 854-62.
66. Carr, L.K., M. Robert, P.L. Kultgen, S. Herschorn, C. Birch, M. Murphy and M.B. Chancellor, *Autologous muscle derived cell therapy for stress urinary incontinence: a prospective, dose ranging study.* J Urol, 2013. **189**(2): p. 595-601.
67. Jankowski, R.J., B.M. Deasy and J. Huard, *Muscle-derived stem cells.* Gene Ther, 2002. **9**(10): p. 642-7.
68. Tare, R.S., J. Kanczler, A. Aarvold, A.M. Jones, D.G. Dunlop and R.O. Oreffo, *Skeletal stem cells and bone regeneration: translational strategies from bench to clinic.* Proc Inst Mech Eng H, 2010. **224**(12): p. 1455-70.
69. Xu, X., K.J. Wilschut, G. Kouklis, H. Tian, R. Hesse, C. Garland, H. Sbitany, S. Hansen, R. Seth, P.D. Knott, W.Y. Hoffman and J.H. Pomerantz, *Human Satellite Cell Transplantation and Regeneration from Diverse Skeletal Muscles.* Stem Cell Reports, 2015. **5**(3): p. 419-34.
70. Ho, M.H., S. Heydarkhan, D. Vernet, I. Kovanecz, M.G. Ferrini, N.N. Bhatia and N.F. Gonzalez-Cadavid, *Stimulating vaginal repair in rats through skeletal muscle-derived stem cells seeded on small intestinal submucosal scaffolds.* Obstet Gynecol, 2009. **114**(2 Pt 1): p. 300-9.
71. Chapple, C., N. Osman and S. MacNeil, *Developing tissue-engineered solutions for the treatment of extensive urethral strictures.* Eur Urol, 2013. **63**(3): p. 539-41.
72. Meyer, S., C. Achtari, P. Hohlfeld and L. Juillerat-Jeanneret, *The contractile properties of vaginal myofibroblasts: is the myofibroblasts contraction force test a valuable indication of future prolapse development?* Int Urogynecol J Pelvic Floor Dysfunct, 2008. **19**(10): p. 1399-403.
73. Ruiz-Zapata, A.M., M.H. Kerkhof, B. Zandieh-Doulabi, H.A. Brolmann, T.H. Smit and M.N. Helder, *Functional characteristics of vaginal fibroblastic cells from premenopausal women with pelvic organ prolapse.* Mol Hum Reprod, 2014. **20**(11): p. 1135-43.

74. Sieira Gil, R., C.M. Pages, E.G. Diez, S. Llames, A.F. Fuertes and J.L. Vilagran, *Tissue-engineered oral mucosa grafts for intraoral lining reconstruction of the maxilla and mandible with a fibula flap.* J Oral Maxillofac Surg, 2015. **73**(1): p. 195.e1-16.
75. Roman, S., A. Mangera, N.I. Osman, A.J. Bullock, C.R. Chapple and S. MacNeil, *Developing a tissue engineered repair material for treatment of stress urinary incontinence and pelvic organ prolapse-which cell source?* Neurourol Urodyn, 2014. **33**(5): p. 531-7.
76. Mangera, A., A.J. Bullock, S. Roman, C.R. Chapple and S. MacNeil, *Comparison of candidate scaffolds for tissue engineering for stress urinary incontinence and pelvic organ prolapse repair.* BJU Int, 2013. **112**(5): p. 674-85.
77. Le Blanc, K. and D. Mougiakakos, *Multipotent mesenchymal stromal cells and the innate immune system.* Nat Rev Immunol, 2012. **12**(5): p. 383-96.
78. Bianco, P., X. Cao, P.S. Frenette, J.J. Mao, P.G. Robey, P.J. Simmons and C.Y. Wang, *The meaning, the sense and the significance: translating the science of mesenchymal stem cells into medicine.* Nat Med, 2013. **19**(1): p. 35-42.
79. James, A.W., J.N. Zara, M. Corselli, A. Askarinam, A.M. Zhou, A. Hourfar, A. Nguyen, S. Megerdichian, G. Asatrian, S. Pang, D. Stoker, X. Zhang, B. Wu, K. Ting, B. Peault and C. Soo, *An abundant perivascular source of stem cells for bone tissue engineering.* Stem Cells Transl Med, 2012. **1**(9): p. 673-84.
80. Parekkadan, B. and J.M. Milwid, *Mesenchymal stem cells as therapeutics.* Annu Rev Biomed Eng, 2010. **12**: p. 87-117.
81. Caplan, A.I., *Adult mesenchymal stem cells for tissue engineering versus regenerative medicine.* J Cell Physiol, 2007. **213**(2): p. 341-7.
82. Caplan, A.I., *Why are MSCs therapeutic? New data: new insight.* J Pathol, 2009. **217**(2): p. 318-24.
83. Chan, R.W., K.E. Schwab and C.E. Gargett, *Clonogenicity of human endometrial epithelial and stromal cells.* Biol Reprod, 2004. **70**(6): p. 1738-50.
84. Gargett, C.E., K.E. Schwab, R.M. Zillwood, H.P. Nguyen and D. Wu, *Isolation and culture of epithelial progenitors and mesenchymal stem cells from human endometrium.* Biol Reprod, 2009. **80**(6): p. 1136-45.
85. Kadekar, D., V. Kale and L. Limaye, *Differential ability of MSCs isolated from placenta and cord as feeders for supporting ex vivo expansion of umbilical cord blood derived CD34(+) cells.* Stem Cell Research & Therapy, 2015. **6**: p. 201.
86. Zuk, P.A., M. Zhu, P. Ashjian, D.A. De Ugarte, J.I. Huang, H. Mizuno, Z.C. Alfonso, J.K. Fraser, P. Benhaim and M.H. Hedrick, *Human adipose tissue is a source of multipotent stem cells.* Mol Biol Cell, 2002. **13**(12): p. 4279-95.
87. Rustad, K.C. and G.C. Gurtner, *Mesenchymal Stem Cells Home to Sites of Injury and Inflammation.* Adv Wound Care (New Rochelle), 2012. **1**(4): p. 147-152.
88. Estrela, C., A.H. Alencar, G.T. Kitten, E.F. Vencio and E. Gava, *Mesenchymal stem cells in the dental tissues: perspectives for tissue regeneration.* Braz Dent J, 2011. **22**(2): p. 91-8.
89. Le Blanc, K., *Mesenchymal stromal cells: Tissue repair and immune modulation.* Cytotherapy, 2006. **8**(6): p. 559-61.
90. Wong, S.P., J.E. Rowley, A.N. Redpath, J.D. Tilman, T.G. Fellous and J.R. Johnson, *Pericytes, mesenchymal stem cells and their contributions to tissue repair.* Pharmacol Ther, 2015. **151**: p. 107-20.
91. Li, M. and S. Ikehara, *Bone-marrow-derived mesenchymal stem cells for organ repair.* Stem Cells Int, 2013. **2013**: p. 132642.
92. Gronthos, S., M. Mankani, J. Brahim, P.G. Robey and S. Shi, *Postnatal human dental pulp stem cells (DPSCs) in vitro and in vivo.* Proc Natl Acad Sci U S A, 2000. **97**(25): p. 13625-30.
93. Tran, C. and M.S. Damaser, *The potential role of stem cells in the treatment of urinary incontinence.* Therapeutic advances in urology, 2015. **7**(1): p. 22-40.

94. Estes, B.T., B.O. Diekman, J.M. Gimble and F. Guilak, *Isolation of adipose-derived stem cells and their induction to a chondrogenic phenotype.* Nat Protoc, 2010. **5**(7): p. 1294-311.
95. Murphy, M.B., K. Moncivais and A.I. Caplan, *Mesenchymal stem cells: environmentally responsive therapeutics for regenerative medicine.* Experimental & Molecular Medicine, 2013. **45**(11): p. e54.
96. Ulrich, D., R. Muralitharan and C.E. Gargett, *Toward the use of endometrial and menstrual blood mesenchymal stem cells for cell-based therapies.* Expert Opin Biol Ther, 2013. **13**(10): p. 1387-400.
97. Baxter, M.A., R.F. Wynn, S.N. Jowitt, J.E. Wraith, L.J. Fairbairn and I. Bellantuono, *Study of telomere length reveals rapid aging of human marrow stromal cells following in vitro expansion.* Stem Cells, 2004. **22**(5): p. 675-82.
98. Gargett, C.E. and H. Masuda, *Adult stem cells in the endometrium.* Mol Hum Reprod, 2010. **16**(11): p. 818-34.
99. Katare, R., F. Riu, J. Rowlinson, A. Lewis, R. Holden, M. Meloni, C. Reni, C. Wallrapp, C. Emanueli and P. Madeddu, *Perivascular delivery of encapsulated mesenchymal stem cells improves postischemic angiogenesis via paracrine activation of VEGF-A.* Arterioscler Thromb Vasc Biol, 2013. **33**(8): p. 1872-80.
100. Melief, S.M., S.B. Geutskens, W.E. Fibbe and H. Roelofs, *Multipotent stromal cells skew monocytes towards an anti-inflammatory interleukin-10-producing phenotype by production of interleukin-6.* Haematologica, 2013. **98**(6): p. 888-95.
101. Bourin, P., B.A. Bunnell, L. Casteilla, M. Dominici, A.J. Katz, K.L. March, H. Redl, J.P. Rubin, K. Yoshimura and J.M. Gimble, *Stromal cells from the adipose tissue-derived stromal vascular fraction and culture expanded adipose tissue-derived stromal/stem cells: a joint statement of the International Federation for Adipose Therapeutics and Science (IFATS) and the International Society for Cellular Therapy (ISCT).* Cytotherapy, 2013. **15**(6): p. 641-8.
102. Varma, M.J., R.G. Breuls, T.E. Schouten, W.J. Jurgens, H.J. Bontkes, G.J. Schuurhuis, S.M. van Ham and F.J. van Milligen, *Phenotypical and functional characterization of freshly isolated adipose tissue-derived stem cells.* Stem Cells Dev, 2007. **16**(1): p. 91-104.
103. Kim, J.H., S.C. Choi, C.Y. Park, J.H. Park, J.H. Choi, H.J. Joo, S.J. Hong and D.S. Lim, *Transplantation of Immortalized CD34+ and CD34- Adipose-Derived Stem Cells Improve Cardiac Function and Mitigate Systemic Pro-Inflammatory Responses.* PLoS One, 2016. **11**(2): p. e0147853.
104. Sidney, L.E., M.J. Branch, S.E. Dunphy, H.S. Dua and A. Hopkinson, *Concise review: evidence for CD34 as a common marker for diverse progenitors.* Stem Cells, 2014. **32**(6): p. 1380-9.
105. Nielsen, J.S. and K.M. McNagny, *Novel functions of the CD34 family.* J Cell Sci, 2008. **121**(Pt 22): p. 3683-92.
106. Darzi, S., J.A. Werkmeister, J.A. Deane and C.E. Gargett, *Identification and Characterization of Human Endometrial Mesenchymal Stem/Stromal Cells and Their Potential for Cellular Therapy.* Stem cells translational medicine, 2016. **5**(9): p. 1127-1132.
107. Bressan, E., D. Botticelli, S. Sivolella, F. Bengazi, R. Guazzo, L. Sbricoli, S. Ricci, L. Ferroni, C. Gardin, J.U. Velez and B. Zavan, *Adipose-Derived Stem Cells as a Tool for Dental Implant Osseointegration: an Experimental Study in the Dog.* Int J Mol Cell Med, 2015. **4**(4): p. 197-208.
108. Wang, L., J. Deng, W. Tian, B. Xiang, T. Yang, G. Li, J. Wang, M. Gruwel, T. Kashour, J. Rendell, M. Glogowski, B. Tomanek, D. Freed, R. Deslauriers, R.C. Arora and G. Tian, *Adipose-derived stem cells are an effective cell candidate for treatment of heart failure: an MR imaging study of rat hearts.* Am J Physiol Heart Circ Physiol, 2009. **297**(3): p. H1020-31.
109. Manavella, D.D., L. Cacciottola, C.M. Desmet, B.F. Jordan, J. Donnez, C.A. Amorim and M.M. Dolmans, *Adipose tissue-derived stem cells in a fibrin implant enhance neovascularization in a peritoneal grafting site: a potential way to improve ovarian tissue transplantation.* Hum Reprod, 2018. **33**(2): p. 270-279.

110. Zhu, Y., Y. Yang, Y. Zhang, G. Hao, T. Liu, L. Wang, T. Yang, Q. Wang, G. Zhang, J. Wei and Y. Li, *Placental mesenchymal stem cells of fetal and maternal origins demonstrate different therapeutic potentials.* Stem Cell Research & Therapy, 2014. **5**(2): p. 48-48.
111. Mathews, S., K. Lakshmi Rao, K. Suma Prasad, M.K. Kanakavalli, A. Govardhana Reddy, T. Avinash Raj, K. Thangaraj and G. Pande, *Propagation of pure fetal and maternal mesenchymal stromal cells from terminal chorionic villi of human term placenta.* Scientific reports, 2015. **5**: p. 10054-10054.
112. Gonzalez, P.L., C. Carvajal, J. Cuenca, F. Alcayaga-Miranda, F.E. Figueroa, J. Bartolucci, L. Salazar-Aravena and M. Khoury, *Chorion Mesenchymal Stem Cells Show Superior Differentiation, Immunosuppressive, and Angiogenic Potentials in Comparison With Haploidentical Maternal Placental Cells.* Stem Cells Transl Med, 2015. **4**(10): p. 1109-21.
113. Portmann-Lanz, C.B., A. Schoeberlein, A. Huber, R. Sager, A. Malek, W. Holzgreve and D.V. Surbek, *Placental mesenchymal stem cells as potential autologous graft for pre- and perinatal neuroregeneration.* Am J Obstet Gynecol, 2006. **194**(3): p. 664-73.
114. In 't Anker, P.S., S.A. Scherjon, C. Kleijburg-van der Keur, G.M. de Groot-Swings, F.H. Claas, W.E. Fibbe and H.H. Kanhai, *Isolation of mesenchymal stem cells of fetal or maternal origin from human placenta.* Stem Cells, 2004. **22**(7): p. 1338-45.
115. Barlow, S., G. Brooke, K. Chatterjee, G. Price, R. Pelekanos, T. Rossetti, M. Doody, D. Venter, S. Pain, K. Gilshenan and K. Atkinson, *Comparison of human placenta- and bone marrow-derived multipotent mesenchymal stem cells.* Stem Cells Dev, 2008. **17**(6): p. 1095-107.
116. Komaki, M., Y. Numata, C. Morioka, I. Honda, M. Tooi, N. Yokoyama, H. Ayame, K. Iwasaki, A. Taki, N. Oshima and I. Morita, *Exosomes of human placenta-derived mesenchymal stem cells stimulate angiogenesis.* Stem Cell Res Ther, 2017. **8**(1): p. 219.
117. Liang, L., Z. Li, T. Ma, Z. Han, W. Du, J. Geng, H. Jia, M. Zhao, J. Wang, B. Zhang, J. Feng, L. Zhao, A. Rupin, Y. Wang and Z.C. Han, *Transplantation of Human Placenta-Derived Mesenchymal Stem Cells Alleviates Critical Limb Ischemia in Diabetic Nude Rats.* Cell Transplant, 2017. **26**(1): p. 45-61.
118. Jabbour, H.N., R.W. Kelly, H.M. Fraser and H.O. Critchley, *Endocrine regulation of menstruation.* Endocr Rev, 2006. **27**(1): p. 17-46.
119. Gargett, C.E., R.W. Chan and K.E. Schwab, *Hormone and growth factor signaling in endometrial renewal: role of stem/progenitor cells.* Mol Cell Endocrinol, 2008. **288**(1-2): p. 22-9.
120. Gargett, C.E., *Uterine stem cells: what is the evidence?* Hum Reprod Update, 2007. **13**(1): p. 87-101.
121. Dominici, M., K. Le Blanc, I. Mueller, I. Slaper-Cortenbach, F. Marini, D. Krause, R. Deans, A. Keating, D. Prockop and E. Horwitz, *Minimal criteria for defining multipotent mesenchymal stromal cells. The International Society for Cellular Therapy position statement.* Cytotherapy, 2006. **8**(4): p. 315-7.
122. Dimitrov, R., T. Timeva, D. Kyurkchiev, M. Stamenova, A. Shterev, P. Kostova, V. Zlatkov, I. Kehayov and S. Kyurkchiev, *Characterization of clonogenic stromal cells isolated from human endometrium.* Reproduction, 2008. **135**(4): p. 551-8.
123. Masuda, H., Y. Matsuzaki, E. Hiratsu, M. Ono, T. Nagashima, T. Kajitani, T. Arase, H. Oda, H. Uchida, H. Asada, M. Ito, Y. Yoshimura, T. Maruyama and H. Okano, *Stem cell-like properties of the endometrial side population: implication in endometrial regeneration.* PLoS One, 2010. **5**(4): p. e10387.
124. Cervello, I., A. Mas, C. Gil-Sanchis, L. Peris, A. Faus, P.T. Saunders, H.O. Critchley and C. Simon, *Reconstruction of endometrium from human endometrial side population cell lines.* PLoS One, 2011. **6**(6): p. e21221.
125. Schwab, K.E. and C.E. Gargett, *Co-expression of two perivascular cell markers isolates mesenchymal stem-like cells from human endometrium.* Hum Reprod, 2007. **22**(11): p. 2903-11.

126. Schwab, K.E., P. Hutchinson and C.E. Gargett, *Identification of surface markers for prospective isolation of human endometrial stromal colony-forming cells.* Hum Reprod, 2008. **23**(4): p. 934-43.
127. Masuda, H., S.S. Anwar, H.J. Buhring, J.R. Rao and C.E. Gargett, *A novel marker of human endometrial mesenchymal stem-like cells.* Cell Transplant, 2012. **21**(10): p. 2201-14.
128. Ulrich, D., K.S. Tan, J. Deane, K. Schwab, A. Cheong, A. Rosamilia and C.E. Gargett, *Mesenchymal stem/stromal cells in post-menopausal endometrium.* Hum Reprod, 2014. **29**(9): p. 1895-905.
129. Letouzey, V., K.S. Tan, J.A. Deane, D. Ulrich, S. Gurung, Y.R. Ong and C.E. Gargett, *Isolation and characterisation of mesenchymal stem/stromal cells in the ovine endometrium.* PLoS One, 2015. **10**(5): p. e0127531.
130. Spitzer, T.L., A. Rojas, Z. Zelenko, L. Aghajanova, D.W. Erikson, F. Barragan, M. Meyer, J.S. Tamaresis, A.E. Hamilton, J.C. Irwin and L.C. Giudice, *Perivascular human endometrial mesenchymal stem cells express pathways relevant to self-renewal, lineage specification, and functional phenotype.* Biol Reprod, 2012. **86**(2): p. 58.
131. Sivasubramaniyan, K., A. Harichandan, S. Schumann, M. Sobiesiak, C. Lengerke, A. Maurer, H. Kalbacher and H.J. Buhring, *Prospective isolation of mesenchymal stem cells from human bone marrow using novel antibodies directed against Sushi domain containing 2.* Stem Cells Dev, 2013. **22**(13): p. 1944-54.
132. Sobiesiak, M., K. Sivasubramaniyan, C. Hermann, C. Tan, M. Orgel, S. Treml, F. Cerabona, P. de Zwart, U. Ochs, C.A. Muller, C.E. Gargett, H. Kalbacher and H.J. Buhring, *The mesenchymal stem cell antigen MSCA-1 is identical to tissue non-specific alkaline phosphatase.* Stem Cells Dev, 2010. **19**(5): p. 669-77.
133. Murakami, K., Y.H. Lee, E.S. Lucas, Y.W. Chan, R.P. Durairaj, S. Takeda, J.D. Moore, B.K. Tan, S. Quenby, J.K. Chan, C.E. Gargett and J.J. Brosens, *Decidualization induces a secretome switch in perivascular niche cells of the human endometrium.* Endocrinology, 2014. **155**(11): p. 4542-53.
134. Schuring, A.N., N. Schulte, R. Kelsch, A. Ropke, L. Kiesel and M. Gotte, *Characterization of endometrial mesenchymal stem-like cells obtained by endometrial biopsy during routine diagnostics.* Fertil Steril, 2011. **95**(1): p. 423-6.
135. Fafián-Labora, J.A., M. Morente-López and M.C. Arufe, *Effect of aging on behaviour of mesenchymal stem cells.* World journal of stem cells, 2019. **11**(6): p. 337-346.
136. Rozemuller, H., H.J. Prins, B. Naaijkens, J. Staal, H.J. Buhring and A.C. Martens, *Prospective isolation of mesenchymal stem cells from multiple mammalian species using cross-reacting anti-human monoclonal antibodies.* Stem Cells Dev, 2010. **19**(12): p. 1911-21.
137. Buhring, H.J., S. Treml, F. Cerabona, P. de Zwart, L. Kanz and M. Sobiesiak, *Phenotypic characterization of distinct human bone marrow-derived MSC subsets.* Ann N Y Acad Sci, 2009. **1176**: p. 124-34.
138. Crisan, M., M. Corselli, W.C. Chen and B. Peault, *Perivascular cells for regenerative medicine.* J Cell Mol Med, 2012. **16**(12): p. 2851-60.
139. Li, L. and T. Xie, *Stem cell niche: structure and function.* Annu Rev Cell Dev Biol, 2005. **21**: p. 605-31.
140. Barragan, F., J.C. Irwin, S. Balayan, D.W. Erikson, J.C. Chen, S. Houshdaran, T.T. Piltonen, T.L. Spitzer, A. George, J.T. Rabban, C. Nezhat and L.C. Giudice, *Human Endometrial Fibroblasts Derived from Mesenchymal Progenitors Inherit Progesterone Resistance and Acquire an Inflammatory Phenotype in the Endometrial Niche in Endometriosis.* Biol Reprod, 2016. **94**(5): p. 118.
141. Gargett, C.E. and S. Gurung, *Endometrial Mesenchymal Stem/Stromal Cells, Their Fibroblast Progeny in Endometriosis, and More.* Biol Reprod, 2016. **94**(6): p. 129.

142. Gurung, S., J.A. Werkmeister and C.E. Gargett, *Inhibition of Transforming Growth Factor-beta Receptor signaling promotes culture expansion of undifferentiated human Endometrial Mesenchymal Stem/stromal Cells.* Sci Rep, 2015. **5**: p. 15042.
143. Alcayaga-Miranda, F., J. Cuenca, P. Luz-Crawford, C. Aguila-Diaz, A. Fernandez, F.E. Figueroa and M. Khoury, *Characterization of menstrual stem cells: angiogenic effect, migration and hematopoietic stem cell support in comparison with bone marrow mesenchymal stem cells.* Stem Cell Res Ther, 2015. **6**: p. 32.
144. Mukherjee, S., S. Darzi, K. Paul, J. Werkmeister and C. Gargett, *Mesenchymal Stem Cell based Bioengineered Constructs: Foreign Body Response, Cross-talk with Macrophages and Impact of Biomaterial Design Strategies for Pelvic Floor Disorders* Interface Focus, 2019.
145. Kim, M.H., W. Liu, D.L. Borjesson, F.R. Curry, L.S. Miller, A.L. Cheung, F.T. Liu, R.R. Isseroff and S.I. Simon, *Dynamics of neutrophil infiltration during cutaneous wound healing and infection using fluorescence imaging.* J Invest Dermatol, 2008. **128**(7): p. 1812-20.
146. Rodero, M.P. and K. Khosrotehrani, *Skin wound healing modulation by macrophages.* International journal of clinical and experimental pathology, 2010. **3**(7): p. 643-653.
147. Brancato, S.K. and J.E. Albina, *Wound macrophages as key regulators of repair: origin, phenotype, and function.* The American journal of pathology, 2011. **178**(1): p. 19-25.
148. Martinez, F.O. and S. Gordon, *The M1 and M2 paradigm of macrophage activation: time for reassessment.* F1000Prime Rep, 2014. **6**: p. 13.
149. Mukherjee, S., S. Darzi, A. Rosamilia, V. Kadam, Y. Truong, J.A. Werkmeister and C.E. Gargett, *Blended Nanostructured Degradable Mesh with Endometrial Mesenchymal Stem Cells Promotes Tissue Integration and Anti-Inflammatory Response in Vivo for Pelvic Floor Application.* Biomacromolecules, 2019. **20**(1): p. 454-468.
150. Gordon, S. and L. Martinez-Pomares, *Physiological roles of macrophages.* Pflugers Archiv : European journal of physiology, 2017. **469**(3-4): p. 365-374.
151. Ferrante, C.J. and S.J. Leibovich, *Regulation of Macrophage Polarization and Wound Healing.* Advances in wound care, 2012. **1**(1): p. 10-16.
152. Ju, C. and P. Mandrekar, *Macrophages and Alcohol-Related Liver Inflammation.* Alcohol research : current reviews, 2015. **37**(2): p. 251-262.
153. Italiani, P. and D. Boraschi, *From Monocytes to M1/M2 Macrophages: Phenotypical vs. Functional Differentiation.* Frontiers in immunology, 2014. **5**: p. 514-514.
154. Bertani, F.R., P. Mozetic, M. Fioramonti, M. Iuliani, G. Ribelli, F. Pantano, D. Santini, G. Tonini, M. Trombetta, L. Businaro, S. Selci and A. Rainer, *Classification of M1/M2-polarized human macrophages by label-free hyperspectral reflectance confocal microscopy and multivariate analysis.* Scientific reports, 2017. **7**(1): p. 8965-8965.
155. Shechter, R., A. London, C. Varol, C. Raposo, M. Cusimano, G. Yovel, A. Rolls, M. Mack, S. Pluchino, G. Martino, S. Jung and M. Schwartz, *Infiltrating blood-derived macrophages are vital cells playing an anti-inflammatory role in recovery from spinal cord injury in mice.* PLoS Med, 2009. **6**(7): p. e1000113.
156. Wheeler, K.C., M.K. Jena, B.S. Pradhan, N. Nayak, S. Das, C.D. Hsu, D.S. Wheeler, K. Chen and N.R. Nayak, *VEGF may contribute to macrophage recruitment and M2 polarization in the decidua.* PLoS One, 2018. **13**(1): p. e0191040.
157. Shechter, R., O. Miller, G. Yovel, N. Rosenzweig, A. London, J. Ruckh, K.W. Kim, E. Klein, V. Kalchenko, P. Bendel, S.A. Lira, S. Jung and M. Schwartz, *Recruitment of beneficial M2 macrophages to injured spinal cord is orchestrated by remote brain choroid plexus.* Immunity, 2013. **38**(3): p. 555-69.
158. Martinez, F.O., L. Helming, R. Milde, A. Varin, B.N. Melgert, C. Draijer, B. Thomas, M. Fabbri, A. Crawshaw, L.P. Ho, N.H. Ten Hacken, V. Cobos Jimenez, N.A. Kootstra, J. Hamann, D.R. Greaves, M. Locati, A. Mantovani and S. Gordon, *Genetic programs expressed in resting and IL-4 alternatively activated mouse and human macrophages: similarities and differences.* Blood, 2013. **121**(9): p. e57-69.

159. Roszer, T., *Understanding the Mysterious M2 Macrophage through Activation Markers and Effector Mechanisms.* Mediators Inflamm, 2015. **2015**: p. 816460.
160. Deryugina, E.I. and J.P. Quigley, *Tumor angiogenesis: MMP-mediated induction of intravasation- and metastasis-sustaining neovasculature.* Matrix Biol, 2015. **44-46**: p. 94-112.
161. Vinnakota, K., Y. Zhang, B.C. Selvanesan, G. Topi, T. Salim, J. Sand-Dejmek, G. Jonsson and A. Sjolander, *M2-like macrophages induce colon cancer cell invasion via matrix metalloproteinases.* J Cell Physiol, 2017. **232**(12): p. 3468-3480.
162. Nakagomi, D., K. Suzuki, K. Meguro, J. Hosokawa, T. Tamachi, H. Takatori, A. Suto, H. Matsue, O. Ohara, T. Nakayama, S. Shimada and H. Nakajima, *Matrix metalloproteinase 12 is produced by M2 macrophages and plays important roles in the development of contact hypersensitivity.* J Allergy Clin Immunol, 2015. **135**(5): p. 1397-400.
163. Barbay, V., M. Houssari, M. Mekki, S. Banquet, F. Edwards-Levy, J.P. Henry, A. Dumesnil, S. Adriouch, C. Thuillez, V. Richard and E. Brakenhielm, *Role of M2-like macrophage recruitment during angiogenic growth factor therapy.* Angiogenesis, 2015. **18**(2): p. 191-200.
164. Contreras, R.A., F.E. Figueroa, F. Djouad and P. Luz-Crawford, *Mesenchymal Stem Cells Regulate the Innate and Adaptive Immune Responses Dampening Arthritis Progression.* Stem cells international, 2016. **2016**: p. 3162743-3162743.
165. Darzi, S., J.A. Deane, C.A. Nold, S.E. Edwards, D.J. Gough, S. Mukherjee, S. Gurung, K.S. Tan, A.V. Vashi, J.A. Werkmeister and C.E. Gargett, *Endometrial Mesenchymal Stem/Stromal Cells Modulate the Macrophage Response to Implanted Polyamide/Gelatin Composite Mesh in Immunocompromised and Immunocompetent Mice.* Sci Rep, 2018. **8**(1): p. 6554.
166. Gargett, C.E., S. Gurung, S. Darzi, J.A. Werkmeister and S. Mukherjee, *Tissue engineering approaches for treating pelvic organ prolapse using a novel source of stem/stromal cells and new materials.* Curr Opin Urol, 2019.
167. Deprest, J., F. Zheng, M. Konstantinovic, F. Spelzini, F. Claerhout, A. Steensma, Y. Ozog and D. De Ridder, *The biology behind fascial defects and the use of implants in pelvic organ prolapse repair.* Int Urogynecol J Pelvic Floor Dysfunct, 2006. **17 Suppl 1**: p. S16-25.
168. Emmerson, S.J. and C.E. Gargett, *Endometrial mesenchymal stem cells as a cell based therapy for pelvic organ prolapse.* World journal of stem cells, 2016. **8**(5): p. 202-215.
169. Darzi, S., J.A. Werkmeister, J.A. Deane and C.E. Gargett, *Identification and Characterization of Human Endometrial Mesenchymal Stem/Stromal Cells and Their Potential for Cellular Therapy.* Stem Cells Transl Med, 2016. **5**(9): p. 1127-32.
170. Edwards, S.L., D. Ulrich, J.F. White, K. Su, A. Rosamilia, J.A. Ramshaw, C.E. Gargett and J.A. Werkmeister, *Temporal changes in the biomechanical properties of endometrial mesenchymal stem cell seeded scaffolds in a rat model.* Acta Biomater, 2015. **13**: p. 286-94.
171. Takacs, P., M. Nassiri, A. Viciana, K. Candiotti, A. Fornoni and C.A. Medina, *Fibulin-5 expression is decreased in women with anterior vaginal wall prolapse.* Int Urogynecol J Pelvic Floor Dysfunct, 2009. **20**(2): p. 207-11.
172. Chin, K., C. Wieslander, H. Shi, S. Balgobin, T.I. Montoya, H. Yanagisawa and R.A. Word, *Pelvic Organ Support in Animals with Partial Loss of Fibulin-5 in the Vaginal Wall.* PLoS One, 2016. **11**(4): p. e0152793.
173. Rahn, D.D., J.F. Acevedo, S. Roshanravan, P.W. Keller, E.C. Davis, L.Y. Marmorstein and R.A. Word, *Failure of pelvic organ support in mice deficient in fibulin-3.* Am J Pathol, 2009. **174**(1): p. 206-15.
174. Rahn, D.D., M.D. Ruff, S.A. Brown, H.F. Tibbals and R.A. Word, *Biomechanical Properties of The Vaginal Wall: Effect of Pregnancy, Elastic Fiber Deficiency, and Pelvic Organ Prolapse.* American journal of obstetrics and gynecology, 2008. **198**(5): p. 590.e1-590.e6.
175. Abramowitch, S.D., A. Feola, Z. Jallah and P.A. Moalli, *Tissue mechanics, animal models, and pelvic organ prolapse: a review.* Eur J Obstet Gynecol Reprod Biol, 2009. **144 Suppl 1**: p. S146-58.

176. Couri, B.M., A.T. Lenis, A. Borazjani, M.F. Paraiso and M.S. Damaser, *Animal models of female pelvic organ prolapse: lessons learned.* Expert Rev Obstet Gynecol, 2012. **7**(3): p. 249-260.
177. Tardif, S.D., K. Coleman, T.R. Hobbs and C. Lutz, *IACUC review of nonhuman primate research.* Ilar j, 2013. **54**(2): p. 234-45.
178. Bristol, F.M. and S. Djurickovic, *Hyperestrogenism in female swine as the result of feeding mouldy corn.* Can Vet J, 1971. **12**(6): p. 132-5.
179. Krause, H. and J. Goh, *Sheep and rabbit genital tracts and abdominal wall as an implantation model for the study of surgical mesh.* J Obstet Gynaecol Res, 2009. **35**(2): p. 219-24.
180. Ulrich, D., S.L. Edwards, V. Letouzey, K. Su, J.F. White, A. Rosamilia, C.E. Gargett and J.A. Werkmeister, *Regional variation in tissue composition and biomechanical properties of postmenopausal ovine and human vagina.* PLoS One, 2014. **9**(8): p. e104972.
181. Scott, P.R. and M.E. Gessert, *Ultrasonographic examination of 12 ovine vaginal prolapses.* Vet J, 1998. **155**(3): p. 323-4.
182. Parkinson, L.A., C.E. Gargett, N. Young, A. Rosamilia, A.V. Vashi, J.A. Werkmeister, A.W. Papageorgiou and J.W. Arkwright, *Real-time measurement of the vaginal pressure profile using an optical-fiber-based instrumented speculum.* J Biomed Opt, 2016. **21**(12): p. 127008.
183. Young, N., A. Rosamilia, J. Arkwright, J. Lee, M. Davies-Tuck, J. Melendez, J. Werkmeister and C.E. Gargett, *Vaginal wall weakness in parous ewes: a potential preclinical model of pelvic organ prolapse.* Int Urogynecol J, 2017. **28**(7): p. 999-1004.
184. Manodoro, S., M. Endo, P. Uvin, M. Albersen, J. Vlacil, A. Engels, B. Schmidt, D. De Ridder, A. Feola and J. Deprest, *Graft-related complications and biaxial tensiometry following experimental vaginal implantation of flat mesh of variable dimensions.* Bjog, 2013. **120**(2): p. 244-250.
185. Urbankova, I., K. Vdoviakova, R. Rynkevic, N. Sindhwani, D. Deprest, A. Feola, P. Herijgers, L. Krofta and J. Deprest, *Comparative Anatomy of the Ovine and Female Pelvis.* Gynecol Obstet Invest, 2017. **82**(6): p. 582-591.
186. Mansoor, A., S. Curinier, S. Campagne-Loiseau, L. Platteeuw, B. Jacquetin and B. Rabischong, *Development of an ovine model for training in vaginal surgery for pelvic organ prolapse.* Int Urogynecol J, 2017. **28**(10): p. 1595-1597.
187. Ulrich, D., S.L. Edwards, D.L. Alexander, A. Rosamilia, J.A. Werkmeister, C.E. Gargett and V. Letouzey, *Changes in pelvic organ prolapse mesh mechanical properties following implantation in rats.* Am J Obstet Gynecol, 2016. **214**(2): p. 260.e1-8.
188. Alperin, M. and P.A. Moalli, *Remodeling of vaginal connective tissue in patients with prolapse.* Curr Opin Obstet Gynecol, 2006. **18**(5): p. 544-50.
189. Mosier, E., V.K. Lin and P. Zimmern, *Extracellular matrix expression of human prolapsed vaginal wall.* Neurourol Urodyn, 2010. **29**(4): p. 582-6.
190. Alarab, M., H. Kufaishi, S. Lye, H. Drutz and O. Shynlova, *Expression of Extracellular Matrix-Remodeling Proteins Is Altered in Vaginal Tissue of Premenopausal Women With Severe Pelvic Organ Prolapse.* Reproductive Sciences, 2014. **21**(6): p. 704-715.
191. Budatha, M., S. Roshanravan, Q. Zheng, C. Weislander, S.L. Chapman, E.C. Davis, B. Starcher, R.A. Word and H. Yanagisawa, *Extracellular matrix proteases contribute to progression of pelvic organ prolapse in mice and humans.* J Clin Invest, 2011. **121**(5): p. 2048-59.
192. Connell, K.A., M.K. Guess, A. Tate, V. Andikyan, R. Bercik and H.S. Taylor, *Diminished vaginal HOXA13 expression in women with pelvic organ prolapse.* Menopause, 2009. **16**(3): p. 529-33.
193. Ritz-Timme, S., I. Laumeier and M.J. Collins, *Aspartic acid racemization: evidence for marked longevity of elastin in human skin.* Br J Dermatol, 2003. **149**(5): p. 951-9.
194. Liu, X., Y. Zhao, B. Pawlyk, M. Damaser and T. Li, *Failure of elastic fiber homeostasis leads to pelvic floor disorders.* Am J Pathol, 2006. **168**(2): p. 519-28.

195. Rahn, D.D., J.F. Acevedo and R.A. Word, *Effect of vaginal distention on elastic fiber synthesis and matrix degradation in the vaginal wall: potential role in the pathogenesis of pelvic organ prolapse.* Am J Physiol Regul Integr Comp Physiol, 2008. **295**(4): p. R1351-8.
196. Drewes, P.G., H. Yanagisawa, B. Starcher, I. Hornstra, K. Csiszar, S.I. Marinis, P. Keller and R.A. Word, *Pelvic organ prolapse in fibulin-5 knockout mice: pregnancy-induced changes in elastic fiber homeostasis in mouse vagina.* Am J Pathol, 2007. **170**(2): p. 578-89.
197. Boreham, M.K., C.Y. Wai, R.T. Miller, J.I. Schaffer and R.A. Word, *Morphometric analysis of smooth muscle in the anterior vaginal wall of women with pelvic organ prolapse.* Am J Obstet Gynecol, 2002. **187**(1): p. 56-63.
198. Takacs, P., M. Gualtieri, M. Nassiri, K. Candiotti and C.A. Medina, *Vaginal smooth muscle cell apoptosis is increased in women with pelvic organ prolapse.* Int Urogynecol J Pelvic Floor Dysfunct, 2008. **19**(11): p. 1559-64.
199. Vitale, S.G., V.L. La Rosa, A.M.C. Rapisarda and A.S. Laganà, *The Importance of a Multidisciplinary Approach or Women with Pelvic Organ Prolapse and Cystocele.* Oman medical journal, 2017. **32**(3): p. 263-264.
200. Persu, C., C.R. Chapple, V. Cauni, S. Gutue and P. Geavlete, *Pelvic Organ Prolapse Quantification System (POP-Q) - a new era in pelvic prolapse staging.* Journal of medicine and life, 2011. **4**(1): p. 75-81.
201. Khadzhieva, M.B., S.V. Kamoeva, A.G. Chumachenko, A.V. Ivanova, I.V. Volodin, I.S. Vladimirov, S.K. Abilev and L.E. Salnikova, *Fibulin-5 (FBLN5) gene polymorphism is associated with pelvic organ prolapse.* Maturitas, 2014. **78**(4): p. 287-92.
202. Martins, P., A. Lopes Silva-Filho, A.M. Rodrigues Maciel da Fonseca, A. Santos, L. Santos, T. Mascarenhas, R.M. Natal Jorge and A.J. Ferreira, *Biomechanical properties of vaginal tissue in women with pelvic organ prolapse.* Gynecol Obstet Invest, 2013. **75**(2): p. 85-92.
203. Lei, L., Y. Song and R. Chen, *Biomechanical properties of prolapsed vaginal tissue in pre- and postmenopausal women.* Int Urogynecol J Pelvic Floor Dysfunct, 2007. **18**(6): p. 603-7.
204. Parkinson, L., C. Gargett, N. Young, A. Rosamilia, A. Vashi, J. Werkmeister, A. W Papageorgiou and J. Arkwright, *Real-time measurement of the vaginal pressure profile using an optical-fiber- based instrumented speculum Real-time measurement of the vaginal pressure profile using an optical-fiber-based instrumented speculum*. Vol. 21. 2016.
205. Ulrich, D., S.L. Edwards, K. Su, J.F. White, J.A. Ramshaw, G. Jenkin, J. Deprest, A. Rosamilia, J.A. Werkmeister and C.E. Gargett, *Influence of reproductive status on tissue composition and biomechanical properties of ovine vagina.* PLoS One, 2014. **9**(4): p. e93172.
206. Zacharin, R.F., *Genital prolapse in ruminants.* Aust N Z J Obstet Gynaecol, 1969. **9**(4): p. 236-9.
207. Barber, M.D. and C. Maher, *Epidemiology and outcome assessment of pelvic organ prolapse.* Int Urogynecol J, 2013. **24**(11): p. 1783-90.
208. Slieker-ten Hove, M.C., A.L. Pool-Goudzwaard, M.J. Eijkemans, R.P. Steegers-Theunissen, C.W. Burger and M.E. Vierhout, *The prevalence of pelvic organ prolapse symptoms and signs and their relation with bladder and bowel disorders in a general female population.* Int Urogynecol J Pelvic Floor Dysfunct, 2009. **20**(9): p. 1037-45.
209. Baraniak, P.R. and T.C. McDevitt, *Stem cell paracrine actions and tissue regeneration.* Regenerative medicine, 2010. **5**(1): p. 121-143.
210. Wang, Y., P. Yin, G.-L. Bian, H.-Y. Huang, H. Shen, J.-J. Yang, Z.-Y. Yang and Z.-Y. Shen, *The combination of stem cells and tissue engineering: an advanced strategy for blood vessels regeneration and vascular disease treatment.* Stem cell research & therapy, 2017. **8**(1): p. 194-194.
211. Zhao, J., L. Liu, J. Wei, D. Ma, W. Geng, X. Yan, J. Zhu, H. Du, Y. Liu, L. Li and F. Chen, *A novel strategy to engineer small-diameter vascular grafts from marrow-derived mesenchymal stem cells.* Artif Organs, 2012. **36**(1): p. 93-101.

212. Kalamegam, G., A. Memic, E. Budd, M. Abbas and A. Mobasheri, *A Comprehensive Review of Stem Cells for Cartilage Regeneration in Osteoarthritis.* Adv Exp Med Biol, 2018. **1089**: p. 23-36.
213. Serrano-Aroca, Á., C.D. Vera-Donoso and V. Moreno-Manzano, *Bioengineering Approaches for Bladder Regeneration.* International journal of molecular sciences, 2018. **19**(6): p. 1796.
214. Medvedev, S.P., A.I. Shevchenko and S.M. Zakian, *Induced Pluripotent Stem Cells: Problems and Advantages when Applying them in Regenerative Medicine.* Acta naturae, 2010. **2**(2): p. 18-28.
215. Ohnuki, M. and K. Takahashi, *Present and future challenges of induced pluripotent stem cells.* Philosophical transactions of the Royal Society of London. Series B, Biological sciences, 2015. **370**(1680): p. 20140367-20140367.
216. Sun, Q., Z. Zhang and Z. Sun, *The potential and challenges of using stem cells for cardiovascular repair and regeneration.* Genes & diseases, 2014. **1**(1): p. 113-119.
217. Kim, H.J. and J.-S. Park, *Usage of Human Mesenchymal Stem Cells in Cell-based Therapy: Advantages and Disadvantages.* Development & reproduction, 2017. **21**(1): p. 1-10.
218. Robey, P., *"Mesenchymal stem cells": fact or fiction, and implications in their therapeutic use.* F1000Research, 2017. **6**: p. F1000 Faculty Rev-524.
219. Emmerson, S., N. Young, A. Rosamilia, L. Parkinson, S.L. Edwards, A.V. Vashi, M. Davies-Tuck, J. White, K. Elgass, C. Lo, J. Arkwright, J.A. Werkmeister and C.E. Gargett, *Ovine multiparity is associated with diminished vaginal muscularis, increased elastic fibres and vaginal wall weakness: implication for pelvic organ prolapse.* Sci Rep, 2017. **7**: p. 45709.
220. Cousin, C., M. Oberkampf, T. Felix, P. Rosenbaum, R. Weil, S. Fabrega, V. Morante, D. Negri, A. Cara, G. Dadaglio and C. Leclerc, *Persistence of Integrase-Deficient Lentiviral Vectors Correlates with the Induction of STING-Independent CD8(+) T Cell Responses.* Cell Rep, 2019. **26**(5): p. 1242-1257.e7.
221. Escors, D. and K. Breckpot, *Lentiviral vectors in gene therapy: their current status and future potential.* Archivum immunologiae et therapiae experimentalis, 2010. **58**(2): p. 107-119.
222. Kita-Matsuo, H., M. Barcova, N. Prigozhina, N. Salomonis, K. Wei, J.G. Jacot, B. Nelson, S. Spiering, R. Haverslag, C. Kim, M. Talantova, R. Bajpai, D. Calzolari, A. Terskikh, A.D. McCulloch, J.H. Price, B.R. Conklin, H.S. Chen and M. Mercola, *Lentiviral vectors and protocols for creation of stable hESC lines for fluorescent tracking and drug resistance selection of cardiomyocytes.* PLoS One, 2009. **4**(4): p. e5046.
223. Merten, O.-W., M. Hebben and C. Bovolenta, *Production of lentiviral vectors.* Molecular therapy. Methods & clinical development, 2016. **3**: p. 16017-16017.
224. Modlich, U., S. Navarro, D. Zychlinski, T. Maetzig, S. Knoess, M.H. Brugman, A. Schambach, S. Charrier, A. Galy, A.J. Thrasher, J. Bueren and C. Baum, *Insertional transformation of hematopoietic cells by self-inactivating lentiviral and gammaretroviral vectors.* Mol Ther, 2009. **17**(11): p. 1919-28.
225. Hansen, L., A.B. Hansen, A.B. Mathiasen, M. Ng, K. Bhakoo, A. Ekblond, J. Kastrup and T. Friis, *Ultrastructural characterization of mesenchymal stromal cells labeled with ultrasmall superparamagnetic iron-oxide nanoparticles for clinical tracking studies.* Scand J Clin Lab Invest, 2014. **74**(5): p. 437-46.
226. Summers, J., D. Oehme, C. Handley, J. Troupis, J. Finnie, J. Manavis, C. McDonald, A. Gibbon, K. Bhakoo, G. Egan, M. Eager, R. Vreys, A. Ng, P. Ghosh, T. Goldschlager and G. Jenkin, *In vivo MRI tracking of mesenchymal precursor cells labelled with iron oxide fluorescent nanoparticles (IODEX) in an ovine model of disc degeneration.* The Spine Journal, 2015. **15**(3): p. S69.
227. Mathiasen, A.B., L. Hansen, T. Friis, C. Thomsen, K. Bhakoo and J. Kastrup, *Optimal labeling dose, labeling time, and magnetic resonance imaging detection limits of ultrasmall superparamagnetic iron-oxide nanoparticle labeled mesenchymal stromal cells.* Stem cells international, 2013. **2013**: p. 353105-353105.

228. Lehmann, T.P., W. Juzwa, K. Filipiak, P. Sujka-Kordowska, M. Zabel, J. Głowacki, M. Głowacki and P.P. Jagodziński, *Quantification of the asymmetric migration of the lipophilic dyes, DiO and DiD, in homotypic co-cultures of chondrosarcoma SW-1353 cells.* Molecular medicine reports, 2016. **14**(5): p. 4529-4536.
229. Feng, J., H. Liu, L. Zhang, K. Bhakoo and L. Lu, *An insight into the metabolic responses of ultra-small superparamagnetic particles of iron oxide using metabonomic analysis of biofluids.* Nanotechnology, 2010. **21**(39): p. 395101.
230. Banfi, A., G. Bianchi, R. Notaro, L. Luzzatto, R. Cancedda and R. Quarto, *Replicative aging and gene expression in long-term cultures of human bone marrow stromal cells.* Tissue Eng, 2002. **8**(6): p. 901-10.
231. Stolzing, A., E. Jones, D. McGonagle and A. Scutt, *Age-related changes in human bone marrow-derived mesenchymal stem cells: consequences for cell therapies.* Mech Ageing Dev, 2008. **129**(3): p. 163-73.
232. Kretlow, J.D., Y.Q. Jin, W. Liu, W.J. Zhang, T.H. Hong, G. Zhou, L.S. Baggett, A.G. Mikos and Y. Cao, *Donor age and cell passage affects differentiation potential of murine bone marrow-derived stem cells.* BMC Cell Biol, 2008. **9**: p. 60.
233. de Tayrac, R., A. Alves and M. Therin, *Collagen-coated vs noncoated low-weight polypropylene meshes in a sheep model for vaginal surgery. A pilot study.* Int Urogynecol J Pelvic Floor Dysfunct, 2007. **18**(5): p. 513-20.
234. Weber, A.M. and H.E. Richter, *Pelvic organ prolapse.* Obstet Gynecol, 2005. **106**(3): p. 615-34.
235. Elneil, S., *Complex pelvic floor failure and associated problems.* Best Pract Res Clin Gastroenterol, 2009. **23**(4): p. 555-73.
236. Tinelli, A., A. Malvasi, S. Rahimi, R. Negro, D. Vergara, R. Martignago, M. Pellegrino and C. Cavallotti, *Age-related pelvic floor modifications and prolapse risk factors in postmenopausal women.* Menopause, 2010. **17**(1): p. 204-12.
237. Vergeldt, T.F.M., M. Weemhoff, J. IntHout and K.B. Kluivers, *Risk factors for pelvic organ prolapse and its recurrence: a systematic review.* International Urogynecology Journal, 2015. **26**(11): p. 1559-1573.
238. Lim, V.F., J.K. Khoo, V. Wong and K.H. Moore, *Recent studies of genetic dysfunction in pelvic organ prolapse: the role of collagen defects.* Aust N Z J Obstet Gynaecol, 2014. **54**(3): p. 198-205.
239. Zong, W., S.E. Stein, B. Starcher, L.A. Meyn and P.A. Moalli, *Alteration of vaginal elastin metabolism in women with pelvic organ prolapse.* Obstetrics and gynecology, 2010. **115**(5): p. 953-961.
240. Jallah, Z., R. Liang, A. Feola, W. Barone, S. Palcsey, S.D. Abramowitch, N. Yoshimura and P. Moalli, *The impact of prolapse mesh on vaginal smooth muscle structure and function.* BJOG : an international journal of obstetrics and gynaecology, 2016. **123**(7): p. 1076-1085.
241. de Tayrac, R., A. Alves and M. Thérin, *Collagen-coated vs noncoated low-weight polypropylene meshes in a sheep model for vaginal surgery. A pilot study*. Vol. 18. 2007. 513-20.
242. Brown, B.N., D. Mani, A.L. Nolfi, R. Liang, S.D. Abramowitch and P.A. Moalli, *Characterization of the host inflammatory response following implantation of prolapse mesh in rhesus macaque.* Am J Obstet Gynecol, 2015. **213**(5): p. 668.e1-10.
243. Wang, J., A. Najjar, S. Zhang, B. Rabinovich, J.T. Willerson, J.G. Gelovani and E.T. Yeh, *Molecular imaging of mesenchymal stem cell: mechanistic insight into cardiac repair after experimental myocardial infarction.* Circ Cardiovasc Imaging, 2012. **5**(1): p. 94-101.
244. Clark Gabrielle, L., P. Pokutta-Paskaleva Anastassia, J. Lawrence Dylan, H. Lindsey Sarah, L. Desrosiers, R. Knoepp Leise, L. Bayer Carolyn, L. Gleason Rudolph and S. Miller Kristin, *Smooth muscle regional contribution to vaginal wall function.* Interface Focus, 2019. **9**(4): p. 20190025.

245. Su, C., S.L. Edwards, K.S. Tan, J.F. White, S. Kandel, J.A.M. Ramshaw, C.E. Gargett and J.A. Werkmeister, *Induction of endometrial mesenchymal stem cells into tissue-forming cells suitable for fascial repair.* Acta Biomater, 2014. **10**(12): p. 5012-5020.
246. Huffaker, R.K., T.W. Muir, A. Rao, S.S. Baumann, T.J. Kuehl and L.M. Pierce, *Histologic response of porcine collagen-coated and uncoated polypropylene grafts in a rabbit vagina model.* Am J Obstet Gynecol, 2008. **198**(5): p. 582.e1-7.
247. Jambusaria, L.H., M. Murphy and V.R. Lucente, *One-year functional and anatomic outcomes of robotic sacrocolpopexy versus vaginal extraperitoneal colpopexy with mesh.* Female Pelvic Med Reconstr Surg, 2015. **21**(2): p. 87-92.
248. Valentin, J.E., A.M. Stewart-Akers, T.W. Gilbert and S.F. Badylak, *Macrophage participation in the degradation and remodeling of extracellular matrix scaffolds.* Tissue Eng Part A, 2009. **15**(7): p. 1687-94.
249. Yates, C.C., M. Rodrigues, A. Nuschke, Z.I. Johnson, D. Whaley, D. Stolz, J. Newsome and A. Wells, *Multipotent stromal cells/mesenchymal stem cells and fibroblasts combine to minimize skin hypertrophic scarring.* Stem Cell Res Ther, 2017. **8**(1): p. 193.
250. Gurung, S., S. Williams, J.A. Deane, J.A. Werkmeister and C.E. Gargett, *The Transcriptome of Human Endometrial Mesenchymal Stem Cells Under TGFβR Inhibition Reveals Improved Potential for Cell-Based Therapies.* Frontiers in cell and developmental biology, 2018. **6**: p. 164-164.
251. Heneghan, C.J., B. Goldacre, I. Onakpoya, J.K. Aronson, T. Jefferson, A. Pluddemann and K.R. Mahtani, *Trials of transvaginal mesh devices for pelvic organ prolapse: a systematic database review of the US FDA approval process.* BMJ open, 2017. **7**(12): p. e017125-e017125.
252. Bochaton-Piallat, M.-L., G. Gabbiani and B. Hinz, *The myofibroblast in wound healing and fibrosis: answered and unanswered questions.* F1000Research, 2016. **5**: p. F1000 Faculty Rev-752.
253. Isakova, I.A., C. Lanclos, J. Bruhn, M.J. Kuroda, K.C. Baker, V. Krishnappa and D.G. Phinney, *Allo-reactivity of mesenchymal stem cells in rhesus macaques is dose and haplotype dependent and limits durable cell engraftment in vivo.* PLoS One, 2014. **9**(1): p. e87238.
254. Eggenhofer, E., F. Luk, M.H. Dahlke and M.J. Hoogduijn, *The life and fate of mesenchymal stem cells.* Frontiers in immunology, 2014. **5**: p. 148-148.
255. Morrison, T.J., M.V. Jackson, E.K. Cunningham, A. Kissenpfennig, D.F. McAuley, C.M. O'Kane and A.D. Krasnodembskaya, *Mesenchymal Stromal Cells Modulate Macrophages in Clinically Relevant Lung Injury Models by Extracellular Vesicle Mitochondrial Transfer.* American journal of respiratory and critical care medicine, 2017. **196**(10): p. 1275-1286.
256. Rink, B.E., T. Beyer, H.M. French, E. Watson, C. Aurich and F.X. Donadeu, *The Fate of Autologous Endometrial Mesenchymal Stromal Cells After Application in the Healthy Equine Uterus.* Stem Cells Dev, 2018. **27**(15): p. 1046-1052.
257. Barnhart, K.T., A. Izquierdo, E.S. Pretorius, D.M. Shera, M. Shabbout and A. Shaunik, *Baseline dimensions of the human vagina.* Hum Reprod, 2006. **21**(6): p. 1618-22.
258. Ueberrueck, T., J. Tautenhahn, L. Meyer, O. Kaufmann, H. Lippert, I. Gastinger and T. Wahlers, *Comparison of the ovine and porcine animal models for biocompatibility testing of vascular prostheses.* J Surg Res, 2005. **124**(2): p. 305-11.
259. Urbankova, I., G. Callewaert, N. Sindhwani, A. Turri, L. Hympanova, A. Feola and J. Deprest, *Transvaginal Mesh Insertion in the Ovine Model.* J Vis Exp, 2017(125).
260. Vogels, R.R.M., R. Kaufmann, L.C.L. van den Hil, S. van Steensel, M.H.F. Schreinemacher, J.F. Lange and N.D. Bouvy, *Critical overview of all available animal models for abdominal wall hernia research.* Hernia : the journal of hernias and abdominal wall surgery, 2017. **21**(5): p. 667-675.

261. Alperin, M., M. Cook, L.J. Tuttle, M.C. Esparza and R.L. Lieber, *Impact of vaginal parity and aging on the architectural design of pelvic floor muscles.* American journal of obstetrics and gynecology, 2016. **215**(3): p. 312.e1-312.e3129.
262. Werkmeister, J.A., S. Edwards, C. Su, S. Gurung, A. Vashi, J. White, D. Ulrich, A. Rosamilia and C.E. Gargett, *A holistic tissue engineering approach from laboratory to small and large animal models for treatment of pelvic organ dysfunction.* Frontiers in Bioengineering and Biotechnology.
263. Callewaert, G., M. Da Cunha, N. Sindhwani, M. Sampaolesi, M. Albersen and J. Deprest, *Cell-based secondary prevention of childbirth-induced pelvic floor trauma.* Nat Rev Urol, 2017. **14**(6): p. 373-385.
264. Bilsel, Y. and I. Abci, *The search for ideal hernia repair; mesh materials and types.* Int J Surg, 2012. **10**(6): p. 317-21.
265. Hansen, S.G., M.B. Taskin, M. Chen, L. Wogensen, J. Vinge Nygaard and S.M. Axelsen, *Electrospun nanofiber mesh with fibroblast growth factor and stem cells for pelvic floor repair.* J Biomed Mater Res B Appl Biomater, 2019.
266. Hympanova, L., R. Rynkevic, S. Roman, M. Mori da Cunha, E. Mazza, M. Zundel, I. Urbankova, M.R. Gallego, J. Vange, G. Callewaert, C. Chapple, S. MacNeil and J. Deprest, *Assessment of Electrospun and Ultra-lightweight Polypropylene Meshes in the Sheep Model for Vaginal Surgery.* Eur Urol Focus, 2018.
267. Gigliobianco, G., C.K. Chong and S. MacNeil, *Simple surface coating of electrospun poly-L-lactic acid scaffolds to induce angiogenesis.* J Biomater Appl, 2015. **30**(1): p. 50-60.
268. Vashaghian, M., A.M. Ruiz-Zapata, M.H. Kerkhof, B. Zandieh-Doulabi, A. Werner, J.P. Roovers and T.H. Smit, *Toward a new generation of pelvic floor implants with electrospun nanofibrous matrices: A feasibility study.* Neurourol Urodyn, 2017. **36**(3): p. 565-573.

Appendices

Chapter 4 Appendices Images

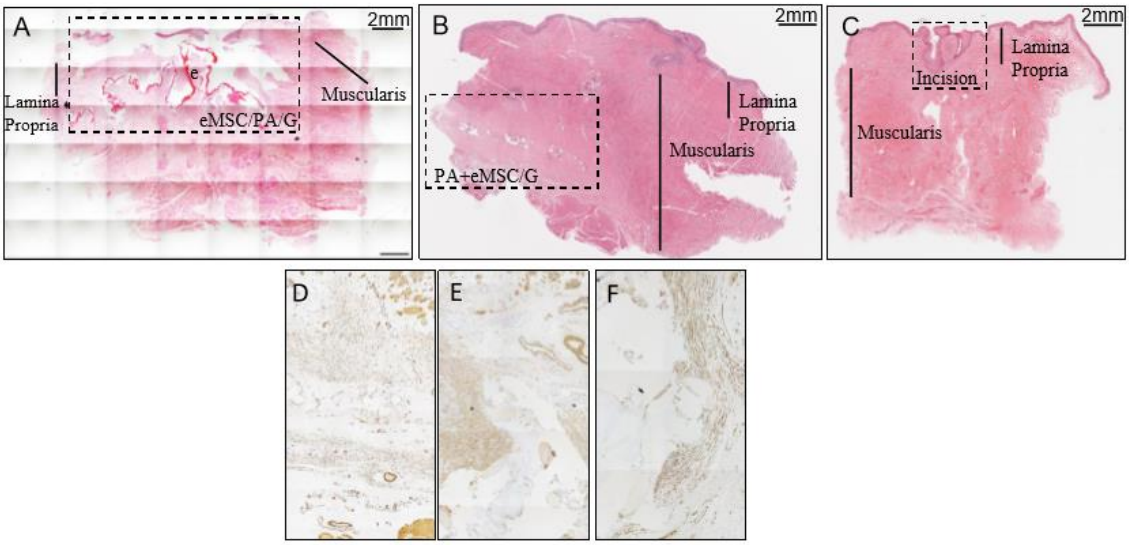

Appendix Figure 2: Mesh integration and vaginal muscularis disruption 30 days after PA/G and PA construct implantation: H&E stained vaginal wall sections showing, **A)** eMSC/PA/G explant characterised by poor mesh integration, folding and exposure (e), **B)** PA+eMSC/G explant characterised by superior mesh integration and no exposure and **C)** incisional control. Representative image showing smooth muscle disruption after **D)** PA, **E)** PA/G and **F)** eMSC/PA/G construct implantation into the vaginal wall.

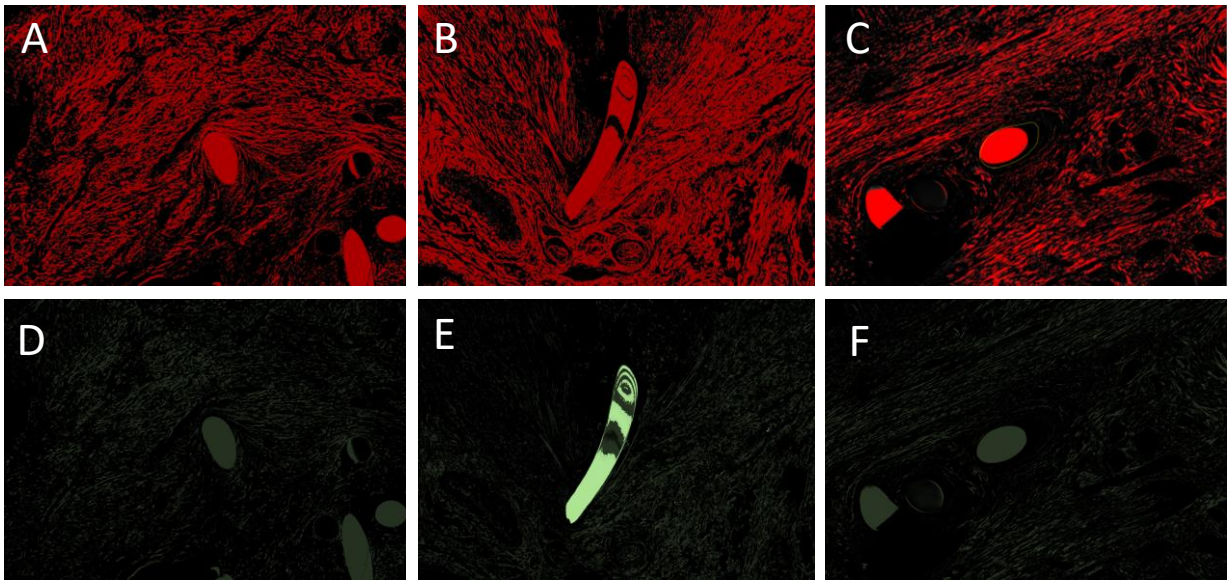

Appendix Figure 4: Organised and disorganised collagen content of ovine vaginal wall 30 days following implantation of PA/G and PA constructs: Birefringence images of Sirius Red stained tissues showing large, organised red fibrils in **A)** PA/G, **B)** eMSC/PA/G and **C)** PA+eMSC/G explants. Thinner, disorganised, green collagen fibrils were observed in **D)** PA/G, **E)** eMSC/PA/G**, F)** PA+eMSC/G explants.

Published Review – World Journal of Stem Cells

World Journal of Stem Cells

Submit a Manuscript: http://www.wjgnet.com/esps/
Help Desk: http://www.wjgnet.com/esps/helpdesk.aspx
DOI: 10.4252/wjsc.v8.i5.202

World J Stem Cells 2016 May 26; 8(5): 202-215
ISSN 1948-0210 (online)
© 2016 Baishideng Publishing Group Inc. All rights reserved.

REVIEW

Endometrial mesenchymal stem cells as a cell based therapy for pelvic organ prolapse

Stuart J Emmerson, Caroline E Gargett

Stuart J Emmerson, Caroline E Gargett, the Ritchie Centre, Hudson Institute of Medical Research, Melbourne, Victoria 3168, Australia

Stuart J Emmerson, Caroline E Gargett, Department of Obstetrics and Gynaecology, Monash University, Melbourne, Victoria 3168, Australia

Author contributions: Emmerson SJ contributed to the acquisition of data, analysis and interpretation of data, drafting, writing the article and approved the final version; Gargett CE contributed to the conception and design of the study, critical revision related to the important intellectual content, editing and approval of the final version.

Conflict-of-interest statement: The authors have no conflicts of interest.

Open-Access: This article is an open-access article which was selected by an in-house editor and fully peer-reviewed by external reviewers. It is distributed in accordance with the Creative Commons Attribution Non Commercial (CC BY-NC 4.0) license, which permits others to distribute, remix, adapt, build upon this work non-commercially, and license their derivative works on different terms, provided the original work is properly cited and the use is non-commercial. See: http://creativecommons.org/licenses/by-nc/4.0/

Correspondence to: Caroline E Gargett, PhD, Associate Professor, the Ritchie Centre, Hudson Institute of Medical Research, 27-31 Wright Street, Melbourne, Victoria 3168, Australia. caroline.gargett@hudson.org.au
Telephone: +61-3-85722795
Fax: +61-3-95947439

Received: October 30, 2015
Peer-review started: November 4, 2015
First decision: November 30, 2015
Revised: December 23, 2015
Accepted: February 14, 2016
Article in press: February 16, 2016
Published online: May 26, 2016

Abstract

Pelvic organ prolapse (POP) occurs when the pelvic organs (bladder, bowel or uterus) herniate into the vagina, causing incontinence, voiding, bowel and sexual dysfunction, negatively impacting upon a woman's quality of life. POP affects 25% of all women and results from childbirth injury. For 19% of all women, surgical reconstructive surgery is required for treatment, often augmented with surgical mesh. The surgical treatment fails in up to 30% of cases or results in adverse effects, such as pain and mesh erosion into the bladder, bowel or vagina. Due to these complications the Food and Drug Administration cautioned against the use of vaginal mesh and several major brands have been recently been withdrawn from market. In this review we will discuss new cell-based approaches being developed for the treatment of POP. Several cell types have been investigated in animal models, including a new source of mesenchymal stem/stromal cells (MSC) derived from human endometrium. The unique characteristics of endometrial MSC, methods for their isolation and purification and steps towards their development for good manufacturing practice production will be described. Animal models that could be used to examine the potential for this approach will also be discussed as will a rodent model showing promise in developing an endometrial MSC-based therapy for POP. The development of a preclinical large animal model for assessing tissue engineering constructs for treating POP will also be mentioned.

Key words: Endometrium; Mesenchymal stem cells; Endometrial mesenchymal stem cells; Pelvic organ prolapse; Mesh; Tissue engineering; Regenerative medicine

© **The Author(s) 2016.** Published by Baishideng Publishing Group Inc. All rights reserved.

Core tip: Pelvic organ prolapse is the herniation of pelvic organs into the vaginal cavity and affects approximately 25% of all women. Traditional mesh-augmented surgical treatments cause complications such as pain and mesh erosion. A tissue engineering approach using endometrial mesenchymal stem cells seeded on new composite mesh show promise in animal models through their modulation of the chronic inflammatory response and promotion of physiological and biomechanically compliant neotissue.

Emmerson SJ, Gargett CE. Endometrial mesenchymal stem cells as a cell based therapy for pelvic organ prolapse. *World J Stem Cells* 2016; 8(5): 202-215 Available from: URL: http://www.wjgnet.com/1948-0210/full/v8/i5/202.htm DOI: http://dx.doi.org/10.4252/wjsc.v8.i5.202

INTRODUCTION

The repair of damage to tissues and organs constitutes almost half of all medical expenses[1]. In the early 1990s in the United States alone, $400 billion was spent per annum treating conditions linked with tissue and organ failure[1]. Despite both this enormous cost and high demand for tissue and organ repair, therapies currently available are unable to fully restore tissues and organs. With an ageing population and increasing demand for organ and tissue replacement the emerging field of tissue engineering and regenerative medicine offers hope for a possible solution for many intractable clinical problems[2].

TISSUE ENGINEERING

Tissue engineering combines both biological sciences and engineering to develop treatments that restore, maintain or improve tissue function[1,3,4]. Though similar to regenerative medicine, an important distinction resides in the potential use of synthetic and semisynthetic materials in tissue engineering[4-6]. This separation can be better understood by considering the three major components of tissue engineering: Metabolically active cells[7], polymeric micro-carriers or scaffolds[8] and bioreactors to produce the tissue engineered construct for implantation[9].

The application of stem cells to tissue engineering applications has been a major recent advance in the field. Although a variety of stem cell types exist, including human embryonic cells and induced pluripotent stem cells, this review will focus on mesenchymal stem/stromal cells (MSCs). The potential for using MSCs for clinical purposes is an expanding area, for both their relative ease of acquisition and their versatility although many utilize their immunomodulatory and anti-inflammatory properties rather than generating new tissue[10-12]. Polymeric micro-carriers, hydrogels and scaffolds are essential components for supporting the reconstitution of damaged tissue. Seeding a scaffold with viable adult stem cells enables their differentiation into the cells desired when implanted into the body[13]. One key question in the tissue engineering field is the choice of polymer, particularly whether to use synthetic or biodegradable polymers. Bioreactors are generally defined as devices in which biological and/or biochemical processes for generating the tissue engineering construct are developed under closely monitored and tightly controlled environmental and operating conditions, *i.e.,* Good Manufacturing Practice[14]. In modern tissue engineering, bioreactors are powerful tools to support and direct *in vitro* development of stem cell populations into functional tissues by simulating an appropriate biological, physical and mechanical environment. In essence, bioreactors are the means by which the desired tissue is generated *in vitro* and directed in its development for transplanting into the patient.

PELVIC ORGAN PROLAPSE

Pelvic organ prolapse (POP) is the herniation of pelvic organs into the vagina (Figure 1)[15,16]. Symptoms of POP include bowel and urinary incontinence, pain, voiding, bowel and sexual dysfunction, severely affecting the quality of life of affected women[17]. POP is a common condition, affecting approximately 25% of all women in the United States and Western countries, and is particularly prevalent in post-menopausal women. The main risk factor is vaginal birth and age. However, obesity is also a contributing factor, particularly in regard to POP recurrence[18]. Though not as well understood, a genetic predisposition to POP is a factor in some cases, particularly in genes regulating collagen and elastin synthesis in the pelvic floor and vaginal walls[19-21]. Given that the United States, Europe and Australia face increasing obesity rates and an aging population, the prevalence and severity of POP will only increase over the coming years. The economic and healthcare costs are considerable, approximating US$1 billion each year[22].

Surgical reconstruction for treatment of POP

Currently the standard treatment for POP is native tissue repair conducted transvaginally (colporrhaphy) or abdominally (sacral colpopexy). This surgical treatment has a high failure rate with 30% of patients requiring one or more further surgeries due to recurrence of POP[23]. Additionally, reconstructive procedures in older women have complication rates from 15.5% to 33%, with the majority related to urinary tract infections, febrile morbidity and blood loss requiring transfusion[24]. Indeed, the mortality from urogynecological surgery increases with each decade of life, with the most common complications occurring in women 80 years or older[25].

The first generation of augmented treatments for POP involved the implantation of polypropylene mesh into the vaginal walls to alleviate the herniation

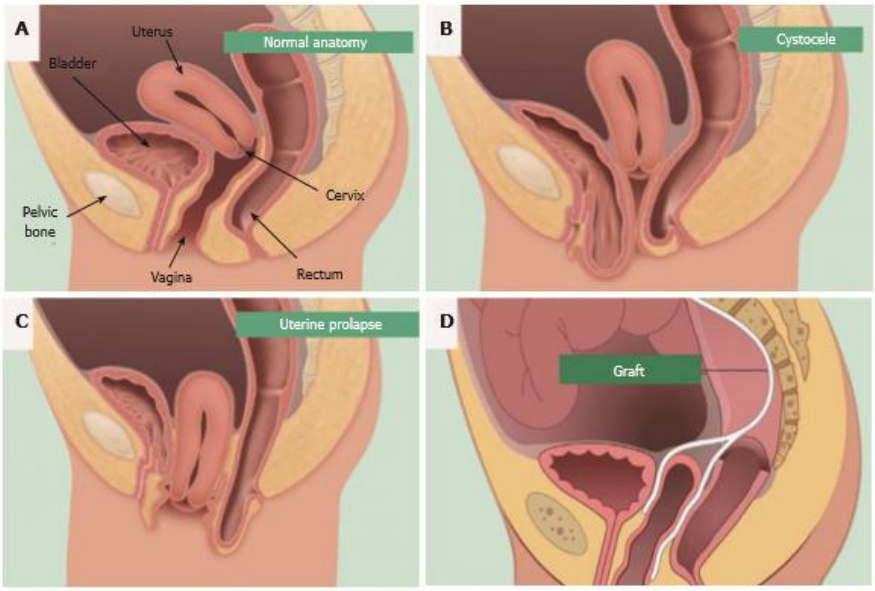

Figure 1 Pelvic organ prolapse mesh treatment. Normal pelvic anatomy (A) and herniation of the bladder (B) and uterus into the vagina (C). Synthetic mesh augmentation of vaginal walls as a colporrhaphy treatment for pelvic organ prolapse (D). Hysterectomies are also used to treat uterine prolapse (reproduced with permission from BARD medical).

and support the pelvic organs (Figure 1D)[26]. Mesh has been available since the 1950s for the repair of abdominal hernias[26]. Though successful for many women, up to 30% will require subsequent surgery while also enduring other complications such as fibrosis, mesh erosion into the vagina, bladder or bowel, chronic inflammation and mesh shrinkage[24,26,27]. This resulted in worldwide recalls of many of the leading brands of meshes for vaginal surgery, leaving women with fewer options for treatment once again.

CANDIDATE CELLS FOR TISSUE ENGINEERING APPLICATIONS FOR POP

Skeletal muscle derived stem cells

Skeletal muscle has been identified previously as a potential source of progenitor stem cells capable of differentiating into myogenic and osteogenic cell lineages in rat models[28-33]. The use of skeletal muscle stem cells to deliver gene therapy is being explored for treating muscular dystrophy and stress urinary incontinence, another pelvic floor disorder involving the urethra[28]. In addition, they are being used to regenerate both skeletal and cardiac muscle, bone and cartilage. As a potential source of cells for treating POP, muscle-derived stem cells (MDSC) are particularly attractive as they can now be isolated from human skeletal muscles and differentiated into skeletal myotubes, *in vitro* and *in vivo*[33]. In rat models MDSC have been used to treat fibrosis. The ability of MDSC to promote vaginal epithelial regeneration and vaginal wall repair in a rat model makes them candidates for treating POP[34]. However to avoid the risk of immune rejection from allogeneic sources, MDSC are better derived from the patient's own muscle tissue. Such an autologous procedure is expensive and invasive, causing significant pain and morbidity for the patient. An alternative source of cells for POP treatment could prove more beneficial and practical for the patient.

Fibroblasts and myofibroblasts

As major producers of collagen and an essential cell for the formation of connective tissue, fibroblasts have also been suggested as an alternative cell source for POP treatment[35]. Vaginal myofibroblasts from nulliparous women have higher contractile strength compared to those from parous women, suggesting that vaginal delivery and overstretching of the vaginal wall affects myofibroblast function[36]. However, the use of autologous vaginal fibroblasts from patients for treating their pelvic floor disorders raises concerns about the quality of cells utilised. Other studies have observed that vaginal fibroblasts derived from prolapsed tissues have impaired function, such as delayed fibroblast-mediated collagen contraction and lower production of collagen synthesising enzymes[21]. This could be avoided if women have a vaginal biopsy to collect and cryopreserve fibroblasts before childbirth in order to

obtain better quality cells, however long-term planning and storage facilities are not available to most women. The invasive method of acquiring human vaginal fibroblasts and subsequent morbidity is unfortunately an obstacle in their use as the main source of cells for a tissue engineering-based approach to treating POP.

Buccal mucosal fibroblasts (BMF), however offer a readily available and plentiful source of cells and could prove an alternative to human vaginal fibroblasts. BMF are harvested from the inside of the cheek lining and express the typical MSC/fibroblast surface markers but do not function as MSC[37]. They produce important components of the extracellular matrix, collagen I and elastin, both of which are required for strengthening the vaginal walls to alleviate and prevent herniation[35,38]. The interaction of BMF with various biodegradable scaffolds has been examined *in vitro* for potential treatment of PFDs including POP[38]. Although BMF offer a potential candidate for the treatment of POP, they currently remain untested for this purpose in animal models and their ultimate suitability remains unknown.

MSCs

MSC have been extensively used as cell-based therapies predominantly for their anti-inflammatory and immunomodulatory non-stem cell properties[39,40]. However they also have potential for tissue engineering purposes for regenerating new tissues or promoting the activity of endogenous stem cells[10,13,41]. MSC populations have the capacity for self-renewal, high proliferative potential and differentiate into a variety of mesodermal and other lineages[42]. Recent advances in cellular identification using more specific markers has shown that MSC can be extracted from most tissues including bone marrow, umbilical cord, placenta, adipose tissue and endometrium, although not all of these sources have demonstrated clonogenicity for their MSC populations[43-47]. Typically, MSC actively respond to stress or injury in a similar manner to the way cells of the innate immune system respond to pathogen exposure. When supplied systemically, exogenous MSCs home to sites of injury in response to inflammation[48]. Here MSCs operate in a paracrine manner secreting large amounts of diverse proteins, growth factors, cytokines and chemokines that promote a variety of effects including neo-angiogenesis, tissue regeneration and remodelling, immune cell activation, suppression of inflammation and cellular recruitment[13,41,49-51].

The potential of MSC as a cell-based therapy has recently been explored in numerous clinical applications. The ability to direct bone marrow MSC differentiation into other cell types and lineages has shown that these cells maintain a phenotype lacking tissue-specific characteristics until exposed to signals in damaged tissues[52]. MSC obtained from dental pulp have been used to repair related tissues such as periodontal ligament, dental papilla and dental follicle[53]. The ability of adipose tissue and bone marrow MSC to act as precursor cells has also been exploited by directing their differentiation toward the chondrogenic lineage in order to produce cartilage-synthesising chondrocytes[54]. Although MSC show promise as cell-based therapies, more understanding of their mechanism of action and utilising their potential is needed. Early use of MSC has not always met expectations, often producing inconsistent results[55]. This may be due to lesser refined methods of isolating and cultivating MSC resulting in the administration of fibroblasts and myofibroblasts rather than undifferentiated MSC[56]. Until recently, production of significant numbers of MSCs posed a challenge, as the regenerative potential of MSC declined during culture expansion[57,58], which is required due to the small numbers of perivascular MSC present within tissues[59]. For tissue engineering applications and tissue repair following ischaemia (*e.g.,* cardiac muscle), local rather than systemic delivery is desirable and will likely result in greater local concentration of MSC at the desired tissue site, even when the mechanism of action is paracrine[60]. A further consideration is allogeneic *vs* autologous. Seeding MSC onto scaffolds, such as polyamide/gelatin (PA + G) for POP or poly-lactic-co-glycolic acid nano-fibers appears to produce better outcomes in preclinical studies[57,61]. MSCs are a versatile and promising stem/stromal cell which can be used for a variety of regenerative medicine applications. Additionally, MSC have greater capacity to regenerate tissues from which they are derived[39]. With this in mind, MSC obtained from the lining of the uterus could be useful in the development of treatments for other regions of the female reproductive tract, *e.g.,* vaginal wall tissue in cases of POP.

ENDOMETRIUM AS A NOVEL SOURCE OF MSC

Regenerative potential of endometrium

The endometrial lining of the uterus serves as the site of embryo implantation, placentation and the development of the embryo and foetus during pregnancy[62]. The upper functional layer of the human endometrium undergoes extensive growth, differentiation and shedding each menstrual cycle under the influence of sex steroid hormone fluctuations[63]. Following menstruation, the remaining basal layer regenerates the new functional layer, which undergoes rapid cellular proliferation followed by differentiation (Figure 2). If an embryo does not implant, the terminally differentiated epithelium and stroma is shed during menstruation[64]. Much like the continuously renewing small intestinal mucosa, the endometrial mucosa undergoes many cycles of regeneration during a woman's lifetime, indicative of its highly dynamic and regenerative capacity.

Endometrial MSC

The existence of stem/progenitor cells within the endometrium and their role as progenitor cells for regenerating endometrial tissue has only recently been

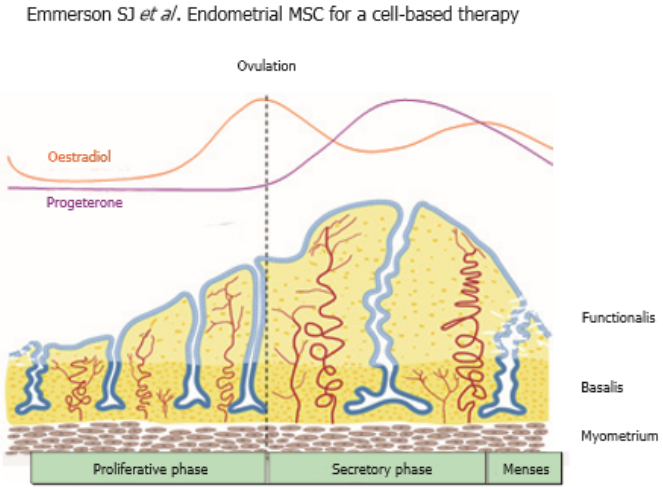

Figure 2 Schematic of changes in the human endometrium during the menstrual cycle, illustrating the growth, differentiation and shedding of the functionalis layer. The functionalis layer regenerates 4-10 mm during the proliferative phase (10 d) as cells proliferate in response to rising circulating estrogen levels. During the secretory phase, progesterone induces differentiation of the epithelium and stroma to generate an endometrium receptive to implantation of an embryo. This entire process occurs over 400 times during a woman's reproductive life indicating the regenerative potential of human endometrium (reproduced from ref.[63] with permission).

reported. Endometrial MSC (eMSC) are clonogenic, multipotent, differentiating into four mesodermal lineages: Osteoblasts, chondrocytes, smooth muscle cells and adipocytes *in vitro* (Figure 3) and expressing the typical pattern of MSC surface markers[44,65,66]. Endometrial side population (SP cells) also demonstrate MSC properties[67,68]. Serial clonal culture shows that clonogenic eMSC undergo self-renewal *in vitro* and have high proliferative potential[44]. The population of clonogenic eMSC within human endometrium is small approximating 1.3%, necessitating the identification of specific surface markers to allow their prospective isolation and enrichment from endometrial biopsies[69,70].

Prospective isolation of eMSC

In order to exploit the regenerative ability of eMSC, they must first be isolated from the heterogeneous population of cells obtained from dissociated endometrial tissue. Ideally this requires the identification of unique surface markers on eMSC that will identify their *in vivo* niche and separate them from undesired stromal fibroblasts and other cells. Indeed several sets of specific surface markers have been identified on eMSC[70-73]. Almost all clonogenic human endometrial stromal cells with MSC properties are found in the $CD140b^{+}CD146^{+}$ population, comprising 1.5% of the stromal fraction[70]. These markers revealed a perivascular niche for eMSC adjacent to endothelial cells suggesting they are pericytes (Figure 4). The transcriptome of the co-expressing $CD140b^{+}CD146^{+}$ cells indicates they are distinct from $CD140b^{-}CD146^{+}$ endothelial cells, but more similar to endometrial $CD140b^{+}CD146^{-}$ stromal fibroblasts[73]. To obtain these co-expressing cells, a flow cytometry sorter must be used, which limits the utility of this marker set, given the damaging effects of automated cell sorting on cell viability[70]. To overcome this problem a single perivascular marker was sought for isolating eMSC. The W5C5 antibody identified a population of perivascular endometrial stromal cells with typical MSC properties that also reconstituted stromal tissue *in vivo* when transplanted beneath the kidney capsule[72]. The $W5C5^{+}$ cells comprised 4.4% of endometrial stromal cells. The epitope recognised by the W5C5 antibody is the Sushi Domain-containing 2 (SUSD2) adhesion molecule[74]. A single marker enables magnetic bead sorting, a gentler protocol than using a cell sorter as evidenced by increased clonogencity of $SUSD2^{+}$ cells compared to $CD140b^{+}CD146^{+}$ cells[72]. TNAP (tissue non-specific alkaline phosphatase) is another single marker that identifies eMSC, but has less utility as the epitope is also expressed by endometrial epithelial cells[75]. Another perivascular marker (AOC3) identified by RNA sequencing $SUSD2^{+}$ and $SUSD2^{-}$ cells may have utility for isolating eMSC[76], but the common bone marrow MSC marker Stro-1 does not enrich for endometrial stromal cells with MSC properties[69]. All these markers revealed that the perivascular eMSC were found in both the functionalis and basalis layers of human endometrium, indicating that eMSC will be found in menstrual blood and can be isolated from biopsies and curettage as well as hysterectomies[56,77].

EMSC can also be obtained from post-menopausal women following short term (8 wk) estrogen replacement which regenerates their atrophic endometrial tissue[78]. Collection of menstrual blood or an endometrial biopsy are convenient sources not requiring anaesthesia, with the latter available as a simple office based procedure. Such tissue sources are ideal for cell-based therapies (Figure 5). Despite their great promise, eMSC and menstrual blood MSC have yet to

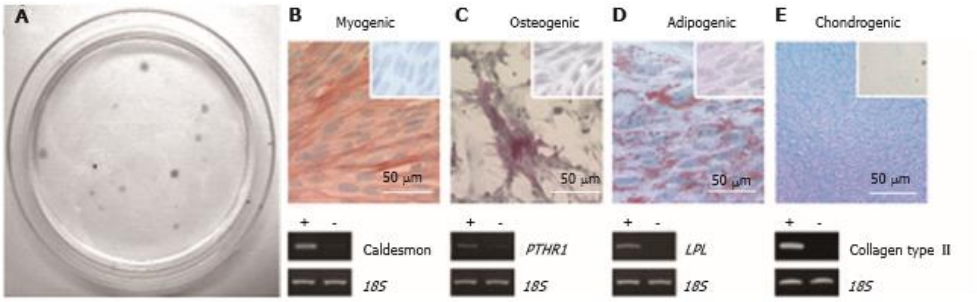

Figure 3 Endometrial mesenchymal stem cells. Clonogenic (A); and differentiate into 4 mesodermal lineages from a single clonogenic cell (B-E); myocytes (B); osteocytes (C); adipocytes (D); chondrocytes (reproduced from ref. [44] with permission) (E). PTHR1: Parathyroid hormone 1 receptor; LPL: Lipoprotein lipase.

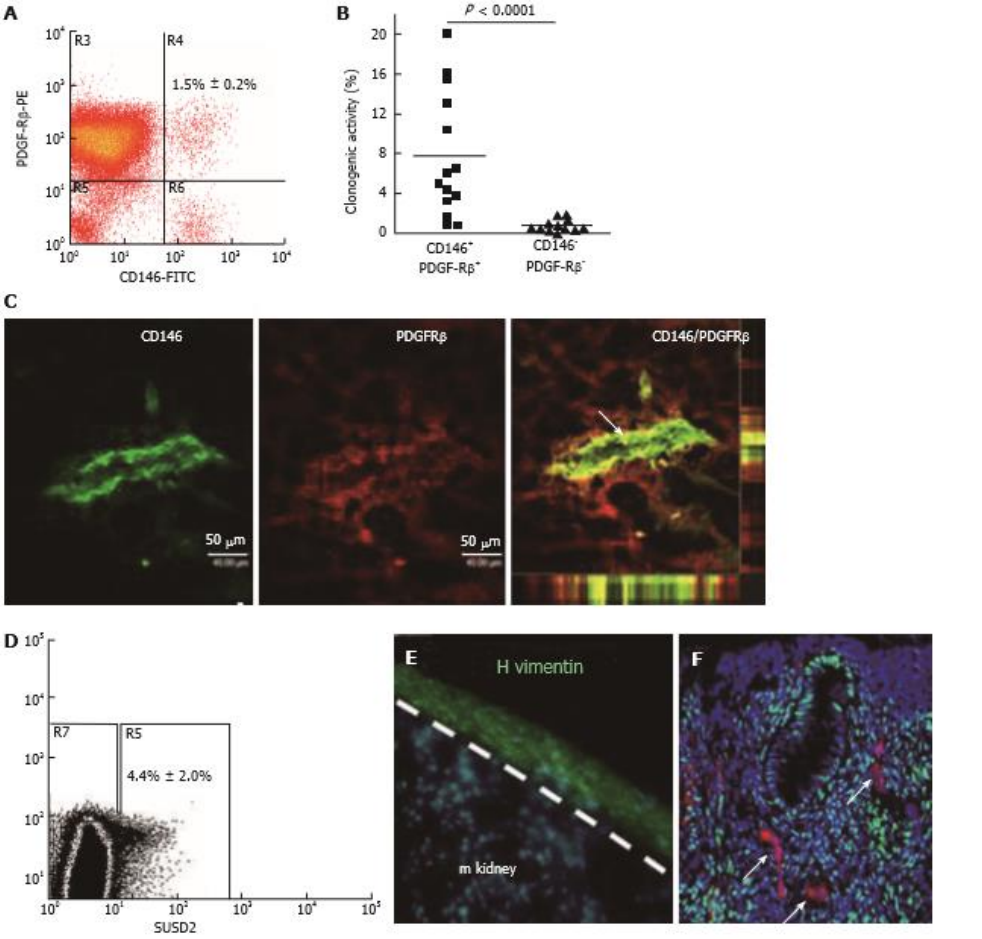

Figure 4 Specific enriching for endometrial mesenchymal stem cells. Flow cytometry plot of CD146$^+$PDGFRB$^+$ fraction (A) which contains most of the clonogenic stromal cells (B) and reveals their pericyte identity *in vivo* (C); SUSD2$^+$ cells in endometrial cell suspensions (D) which E reconstitute human vimentin+ stromal tissue when transplanted under the kidney capsule of NSG mice, and F have a perivascular location in human endometrium. SUSD2$^+$ cells (red) do not express estrogen receptor-α (green), but endometrial stromal cells do (DNA blue). The white arrow indicates perivascular SUSD2$^+$ cells (reproduced ref. [70,72,78] with permission).

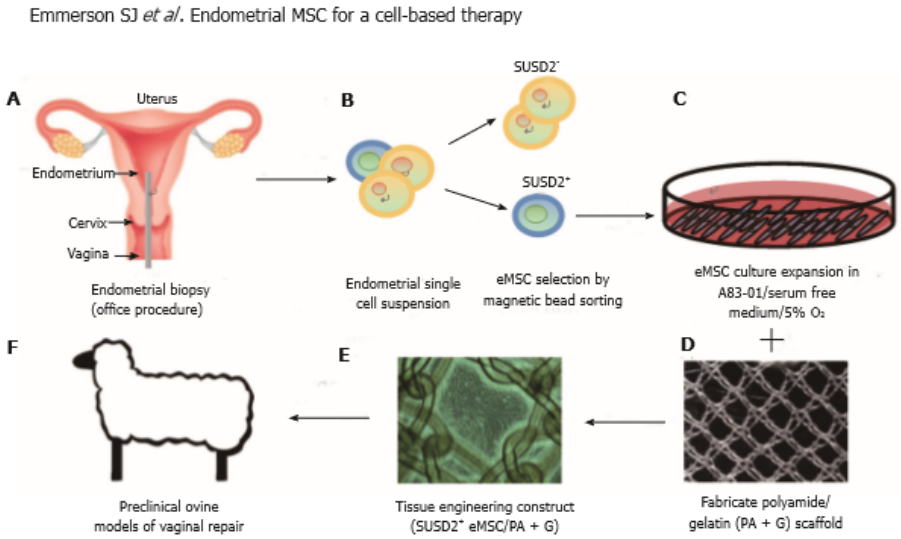

Figure 5 Isolation and application of e-mesenchymal stem cells in pelvic organ prolapse vaginal repair. (A) simple office based endometrial biopsies can be used to obtain patients' tissues, which are dissociated, then (B) eMSC selected using SUSD2 magnetic bead sorting, followed by (C) culture expansion in A83-01/serum free medium in 5% O_2 to generate large numbers of undifferentiated SUSD2$^+$ eMSC (90%-95%) for (D) seeding onto fabricated scaffolds which will create an (E) eMSC/PA-G tissue engineering construct for implantation into (F) a large animal preclinical model to assess their efficacy in vaginal repair of parous ewes with evidence of POP (reproduced with permission from ref.[57,103] with permission). POP: Pelvic organ prolapse; MSC: Mesenchymal stem cells.

be significantly explored as therapeutic agents for stem cells therapies. There are certain endometrial disorders where caution maybe required eg endometriosis. However this disorder affects young infertile women who will not have the opportunity to develop POP. Indeed, it will be important to ensure no underlying uterine or other pathology (*e.g.,* malignant tumour) in identifying suitable patients for cell harvesting to treat their POP. For example, should a woman have uterine cancer, it would not be possible to use her eMSC for cell-based therapies. Similarly, it would also be contraindicated to use another source of autologous MSC in case tumour cells have spread to organs such as bone. These important issues should be considered in developing the potential of eMSC as cell-based therapies.

Large animal models are usually required to provide data for regulatory bodies prior to translating potential cell-based therapies into the clinic. If autologous applications are being evaluated, it becomes necessary to derive MSC from species such as ovine, porcine, canine, equine and non-human primates[79,80]. Often antibodies used as biomarkers to derive MSC from human or mouse do not cross react with these species. For example, neither CD140b, CD146 nor SUSD2 cross react with ovine endometrial tissue[81]. However, the bone marrow MSC surface marker CD271[82] cross reacts with ovine endometrial stromal cells enriching for eMSC demonstrating clonogenicity, *in vitro* self-renewal and the ability to differentiate into adipogenic, myogenic, osteogenic and chondrogenic lineages[81]. The CD271$^+$ ovine eMSC were identified in a perivascular niche around arterioles and venules *in vivo*, but unlike human eMSC which have a pericyte location, ovine CD271$^+$ stromal cells occupied the adventitia in the periphery of these vessels (Figure 6). In human bone marrow and adipose tissue, vascular adventitial cells show similar MSC properties as those located in the pericyte position[83].

eMSC phenotype and gene profile

Cell fate decisions made by somatic stem cells to self-renew or undergo differentiation depends upon the cellular microenvironment or niche from signals emanating from cells and extracellular matrix that comprise this niche[84]. In this context, understanding both the extrinsic and intrinsic gene regulation pathways operating in undifferentiated eMSC and their more differentiated progeny could shed light on their function in endometrial regeneration. Gene expression profiling comparing purified endometrial cell populations of CD140b$^+$CD146$^+$ eMSC, CD140b$^+$CD146$^-$ stromal fibroblasts and CD140b$^-$CD146$^+$ endothelial cells showed that eMSC differentially expressed 762 and 1518 genes, respectively[73]. The eMSC gene expression profile was typical of stem cells, showing upregulation of self-renewal genes of the *TGFβ*, *FGF2*, *WNT*, *IGF* and Hedgehog signalling pathways in comparison with the endometrial stromal fibroblasts and endothelial cells. The expression of SUSD2 was also elevated in the double positive eMSC population. G-protein coupled receptor- and cAMP-mediated signalling were also upregulated in the CD140b$^+$CD146$^+$ population, similar to genes involved in maintaining the undifferentiated state of

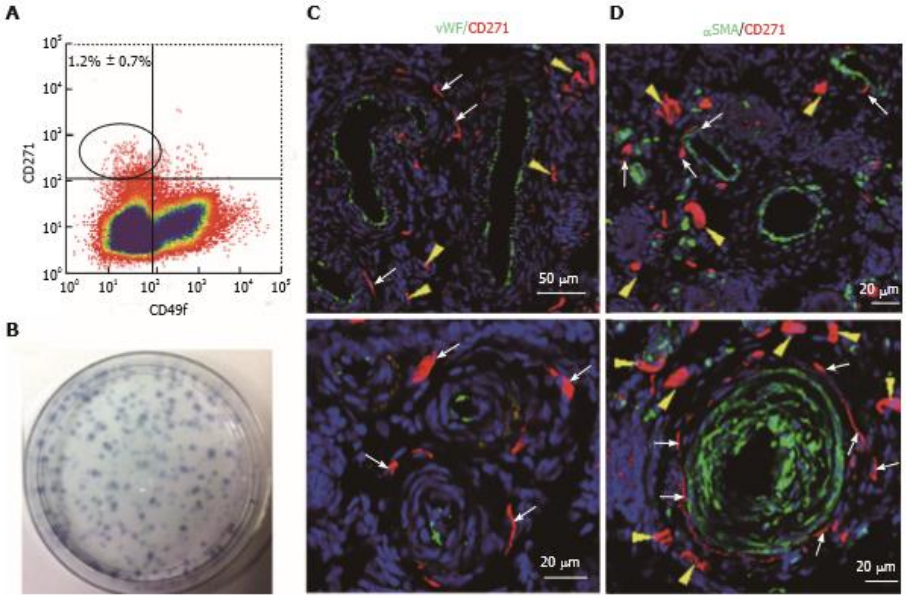

Figure 6 Specific markers for ovine e-mesenchymal stem cells. Flow cytometry plot of ovine endometrial cells immunolabelled with CD271 and CD49f antibodies (A). The CD271$^+$CD49f$^-$ population enriches; Clonogenic stromal cells (B); Immunofluorescence images of ovine endometrium stained with CD271 (red) and vascular markers reveals their *in vivo* perivascular location in the adventitia of veins and arteries (C, D); vWF an endothelial marker (green), showing CD271$^+$ cells are perivascular but not pericytes (C); αSMA, a perivascular marker (green) showing CD271$^+$ cells located adjacent to αSMA$^+$ cells in the adventitia of vessels rather than expressing αSMA themselves (D). White arrows: perivascular CD271$^+$ cells; yellow arrows: CD271$^+$ cells not associated with vessels (reproduced from ref.[81] with permission). vWF: Von Willebrand factor; αSMA: Alpha smooth muscle actin.

bone marrow MSC. The CD140b$^+$CD146$^+$ population also showed upregulation of immunomodulatory and immunosuppressive genes[73]. eMSC displayed increased expression of Cyclin D1 (CCND1) which ensures their progression through the G1 phase of the cell cycle[73]. Gene profiling has confirmed human eMSC as pericytes, while RNA sequencing of cultured endometrial SUSD2$^+$ and SUSD2$^-$ cells revealed 134 differentially expressed genes, with many of those in the SUSD2$^+$ population characteristic of perivascular cells[76]. The *in vivo* differentiation pathway for eMSC is to decidualised perivascular cells and decidual cells of the endometrial stroma, a process mediated by the post-ovulation sex steroid hormone, progesterone, *via* production of cAMP. The perivascular location of eMSC in the spiral arterioles renders them well situated to participate in the regeneration of the uterine lining and formation of the placenta during embryo implantation and subsequent pregnancy[76].

Tissue engineering for POP repair

Given the problem associated with mesh implantation for POP repair, and the need for physical support, a tissue engineering approach may provide a more durable treatment. The ideal treatment for POP would be an implantable autograft that alleviated herniation and regenerated the damaged tissue within the vaginal wall.

In vitro studies

For a cell based treatment to be practical, methods for procuring and expanding the necessary cells need to be developed. Culturing and expanding eMSC *in vitro* has been optimised in serum-free conditions, showing that fibronectin is the optimal substrate for attachment[85]. Additionally, hypoxic conditions of 5% O_2 increased the proliferation rate and yield of eMSC, whilst maintaining multipotency and their expression of CD140b, CD146 and SUSD2. Culturing eMSC on a polyamide/gelatin composite scaffold with exogenous TGFβ1 and PDGF-BB induced their differentiation into smooth muscle cells expressing SM22α and SM-myosin heavy chain[86]. Incubation with connective tissue growth factor induced the eMSC to differentiate into collagen-producing fibroblasts. The differentiated smooth muscle cells and fibroblasts no longer expressed the eMSC marker SUSD2, confirming their differentiation into these desired cell types for POP repair[86]. Although these *in vitro* studies show promise, it is also essential to confirm smooth muscle and fibroblast differentiation *in vivo* to gain mechanistic understanding prior to transferring this technology into clinical applications.

Methodology has now been developed for culture expansion of eMSC in serum free medium containing A83-01, a TGFβ1 receptor inhibitor, that maintains eMSC stemness and SUSD2 phenotype[87]. TGFβ1-mediated apoptosis and senescence is prevented and proliferation promoted in A83-01-treated eMSC cultures maintaining the percentage of SUSD2$^+$ cells to more than 90% for all samples. This effect of A83-01 is mediated *via* Smad2/3 phosphorylation. A83-01 treated eMSC are more clonogenic than untreated control cells and retain their MSC properties[87]. A major advantage of this culture method is that a reproducible percentage of SUSD2$^+$ eMSC is achievable for all patient samples, an important consideration for scale out culture expansion of autologous cells.

In vivo studies

As outlined earlier there are substantial problems with current mesh augmentation of POP surgery. The use of autografts increases morbidity at the donor tissue site, biological materials often fail due to their rapid and unpredictable degradation[16], and the synthetic PP mesh currently used is biomechanically too stiff and often erodes into adjacent organs[56]. A better solution may be to combine the advantages of both the synthetic and biological approaches. This could utilise a synthetic mesh as a scaffold to not only support the prolapsed tissue but also provide a vehicle upon which to seed eMSC for delivery to sites of vaginal damage[26,88]. The eMSC could serve by modulating the inflammatory and immune responses and perhaps more importantly incorporating into the vaginal wall to regenerate the lost or damaged tissue or promoting endogenous stem cell populations to initiate repair which mesh alone cannot do.

Small animal rodent models

Recent efforts to test this possibility show potential utility. A non-degradable, polyamide (PA) mesh with biomechanical properties more closely matching vaginal tissue was coated with gelatin[88] to provide a substrate for seeding with SUSD2$^+$ eMSC. This tissue engineering construct was then implanted into a fascial defect on the dorsum of immunocompromised rats and assessed following necropsy at several time points over 90 d[57]. In the explanted eMSC/PA + G tissue complexes, greater neovascularisation was observed early on at 7 d compared with PA + G controls. Initially there was a greater influx of M1 inflammatory macrophages around the eMSC-seeded mesh. At 60 d these macrophages had changed to a M2 wound healing phenotype and by 90 d there were fewer CD68$^+$ macrophages around the cell-seeded PA + G filaments in comparison to PA + G alone, indicating a milder chronic inflammatory response in the long term. Importantly in these studies the cellular response at the mesh interface was assessed quantitatively in 50 μm increments around individual filaments using image analysis rather than subjective scoring[57,88]. Similar quantities of new collagen were generated around the PA + G mesh filaments, irrespective of the inclusion of eMSC, which was derived from rat fibroblasts rather than derivatives of the implanted human eMSC. However, this new collagen around the eMSC/PA + G mesh filaments showed physiological crimping by scanning electron microscopy, while more scar-like collagen was deposited around the PA + G mesh without eMSC[89]. This deposition of physiological collagen likely contributed to the improved biomechanical properties of the mesh/tissue complexes harvested at 90 d, where a longer toe region and lower stiffness was observed in the stress strain curves of the cell-seeded PA + G mesh compared with PA + G alone (Figure 7)[57]. The improved tissue organisation around the mesh filaments shown by histological staining suggests that eMSC promoted tissue regeneration and improved the biocompatibility of the synthetic PA + G mesh[57,89]. In this xenogeneic model, the eMSC survived a maximum of 14 d indicating that they exerted a paracrine effect in promoting vascularisation and reducing fibrosis similar to MSC effects on many other tissues[13]. However the percentage of SUSD2$^+$ cells in the single sample of passage 6 cells used for the entire study was only 10%. It will be of interest to determine whether more than a paracrine effect will be observed if > 90% of the cells are SUSD2$^+$, now a possibility by culturing them in A83-01-containing medium[87].

Despite the significant biological differences between human females and rodents, mouse models have proven invaluable for the investigation of the underlying biochemical mechanisms involved in the development of POP. The use of genetically modified mice has allowed exploration of the genetic underpinnings of POP, such as lysyl oxidase like-1 (LOXL1), an enzyme involved in elastin biosynthesis within vaginal tissue walls, and fibulin 5 (FBLN5) which regulates expression of collagen and elastin. Depletion of either LOXL1 or FBLN5 has been associated with POP[20,90]. The LOXL1 deficient mouse creates a POP-like condition where the mice develop an obvious bulge in the perineal region. It would be of interest to determine if an injectable MSC-based cell therapy alleviates the prolapse symptoms of LOXL-1 deficient mice. While extremely useful for investigating genetic contribution, transgenic mice are limited in their utility as models for exploring tissue engineering based treatments for POP due to the small size of their vagina.

Large animal preclinical models

Of the large animal models available for assessing cell-based therapies for POP, the domestic sheep is the most promising candidate due to their ready availability and physiological similarity to the human female pelvis in size and structure. Ewes also have a similar oestrus cycle of 17 d, a long labour and deliver a foetus with a large head to body ratio that is closer to humans than rodents[91,92]. Like humans, ewes undergo spontaneous POP with similar frequency and predisposing factors, such as parity, age and breeds with a large rump[91,93].

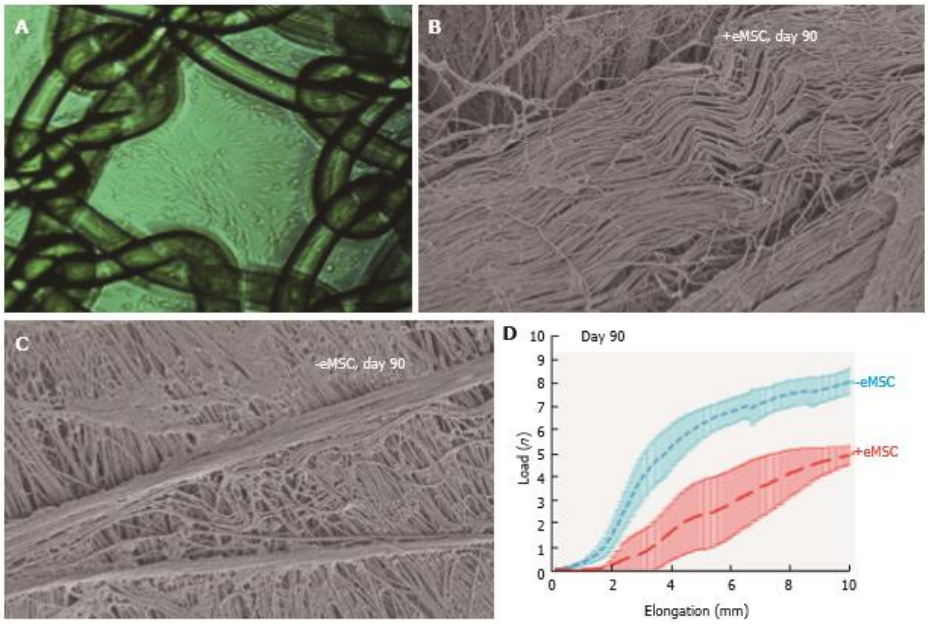

Figure 7 Human e-mesenchymal stem cells improves the biocompatibility of polyamide/gelatin (PA + G) mesh in a fascial wound defect in nude rats. PA + G mesh seeded with 100000 eMSC/cm^2 and cultured for 48 h, prior to implantation (A); Physiological crimped collagen deposited around eMSC$^+$/PA + G mesh (B); Scar-like collagen in PA + G mesh alone as observed by SEM (C); Load-elongation curves of explanted meshes with (red) and without (blue) eMSC showing less stiffness (slope) and longer toe region for mesh seeded with eMSC, indicating improved biomechanical properties (reproduced from ref.[57,86,89] with permission) (D). MSC: Mesenchymal stem cells; PA : Polyamide; G: Gelatin.

Although the ovine species are quadrupeds with a horizontal rather than vertical pelvic floor subject to differing forces, the overall arrangement of the pelvic organs and the similar vaginal dimensions to women make them a useful model for assessing new mesh and tissue engineering constructs[56]. Additionally, the ovine vagina has a similar histological structure, biochemical and biomechanical properties to that of women. Finally, the most common form of prolapse in sheep involves the bladder (cystocele) as it is for women Sheep have already been vaginally implanted with various POP mesh materials for evaluation of their efficacy and adverse effects in female pelvic reconstructive surgery[16,92,94,95]. The biochemical and biomechanical properties of ovine vaginal tissue has already been examined by quantitative histological imaging, biochemical collagen/GAG/elastin assays and biomechanical analyses, providing a platform for the evaluation of next generation eMSC-seeded mesh in the ovine vaginal repair model[96,97]. It is now possible to evaluate autologous eMSC since methods have been developed for obtaining MSC from the ovine bone marrow[79] and endometrium (Figure 5)[81].

Additional large animal models for assessing cell-based therapies for POP surgery include cows, pigs and non-human primates. Cows develop prolapse with similar predisposition and frequency to humans and sheep[98], however their purchase, handling and agistment costs make them a less practical model. Pigs are a common preclinical model for various clinical conditions but their foetuses do not have the large head-to body-ratio responsible for inducing spontaneous POP in the ovine model, reducing their utility[99]. Non-human primates such as Rhesus macaques and squirrel monkeys offer useful animal models due to a similar pelvic anatomy to humans and their more upright posture[100,101]. Furthermore, the Rhesus species develop spontaneous POP. Non-human primates have been used for assessing new POP meshes and for investigating the mechanism of action of their deleterious effects[27,102]. However ethical limitations, prohibitive cost of handling and necessary specialist expertise limit their availability for many investigators. Despite these limitations, assessment of tissue engineering constructs in the macaque model, particularly in retired breeders with evidence of POP, might provide the ultimate model of postmenopausal women with POP in which to assess a cell-based therapy. However it would be necessary to develop methods for obtaining MSC populations from the macaque species, for both autologous and allogeneic use.

CONCLUSION

POP is a common hidden disease burden for large numbers of women. Compounding this burden is the

inadequacies of current surgical treatments with or without mesh. To overcome this clinical challenge, recent advances in cellular phenotyping and gene profiling suggest endometrial MSC as a possible compliment to mesh-based POP treatment. The eMSC capacity for regenerating tissue is exemplified during a woman's reproductive life, where they regenerate at least one centimetre of endometrial lining each menstrual cycle for over 400 menstrual cycles. By seeding eMSC onto polyamide/gelatin composite mesh and implanting into vaginal walls, it may be possible to favourably modulate the innate immune response and accelerate organised tissue rehabilitation. That the first attempt at combining eMSC and mesh to treat a fascial defect has been successful using rodent models is encouraging, suggesting that further development of this approach using the ovine model is warranted.

REFERENCES

1 **Langer R**, Vacanti JP. Tissue engineering. *Science* 1993; **260**: 920-926 [PMID: 8493529]
2 **Berthiaume F**, Maguire TJ, Yarmush ML. Tissue engineering and regenerative medicine: history, progress, and challenges. *Annu Rev Chem Biomol Eng* 2011; **2**: 403-430 [PMID: 22432625 DOI: 10.1146/annurev-chembioeng-061010-114257]
3 **Freed LE**, Langer R, Martin I, Pellis NR, Vunjak-Novakovic G. Tissue engineering of cartilage in space. *Proc Natl Acad Sci USA* 1997; **94**: 13885-13890 [PMID: 9391122]
4 **Vogel G**. Tissue engineering. Mending the youngest hearts. *Science* 2011; **333**: 1088-1089 [PMID: 21868648 DOI: 10.1126/science.333.6046.1088]
5 **Marx V**. Tissue engineering: Organs from the lab. *Nature* 2015; **522**: 373-377 [PMID: 26085275 DOI: 10.1038/522373a]
6 **Vacanti JP**, Langer R. Tissue engineering: the design and fabrication of living replacement devices for surgical reconstruction and transplantation. *Lancet* 1999; **354** Suppl 1: SI32-SI34 [PMID: 10437854]
7 **Buehrer BM**, Cheatham B. Isolation and characterization of human adipose-derived stem cells for use in tissue engineering. *Methods Mol Biol* 2013; **1001**: 1-11 [PMID: 23494415 DOI: 10.1007/978-1-62703-363-3_1]
8 **Park JH**, Pérez RA, Jin GZ, Choi SJ, Kim HW, Wall IB. Microcarriers designed for cell culture and tissue engineering of bone. *Tissue Eng Part B Rev* 2013; **19**: 172-190 [PMID: 23126371 DOI: 10.1089/ten.TEB.2012.0432]
9 **Yeatts AB**, Geibel EM, Fears FF, Fisher JP. Human mesenchymal stem cell position within scaffolds influences cell fate during dynamic culture. *Biotechnol Bioeng* 2012; **109**: 2381-2391 [PMID: 22422570 DOI: 10.1002/bit.24497]
10 **Caplan AI**. Adult mesenchymal stem cells for tissue engineering versus regenerative medicine. *J Cell Physiol* 2007; **213**: 341-347 [PMID: 17620285 DOI: 10.1002/jcp.21200]
11 **Dimarino AM**, Caplan AI, Bonfield TL. Mesenchymal stem cells in tissue repair. *Front Immunol* 2013; **4**: 201 [PMID: 24027567 DOI: 10.3389/fimmu.2013.00201]
12 **Lindroos B**, Suuronen R, Miettinen S. The potential of adipose stem cells in regenerative medicine. *Stem Cell Rev* 2011; **7**: 269-291 [PMID: 20853072 DOI: 10.1007/s12015-010-9193-7]
13 **Parekkadan B**, Milwid JM. Mesenchymal stem cells as therapeutics. *Annu Rev Biomed Eng* 2010; **12**: 87-117 [PMID: 20415588 DOI: 10.1146/annurev-bioeng-070909-105309]
14 **Sensebé L**, Gadelorge M, Fleury-Cappellesso S. Production of mesenchymal stromal/stem cells according to good manufacturing practices: a review. *Stem Cell Res Ther* 2013; **4**: 66 [PMID: 23751270 DOI: 10.1186/scrt217]
15 **DeLancey JO**. The hidden epidemic of pelvic floor dysfunction: achievable goals for improved prevention and treatment. *Am J Obstet Gynecol* 2005; **192**: 1488-1495 [PMID: 15902147 DOI: 10.1016/j.ajog.2005.02.028]
16 **Deprest J**, Zheng F, Konstantinovic M, Spelzini F, Claerhout F, Steensma A, Ozog Y, De Ridder D. The biology behind fascial defects and the use of implants in pelvic organ prolapse repair. *Int Urogynecol J Pelvic Floor Dysfunct* 2006; **17** Suppl 1: S16-S25 [PMID: 16738743 DOI: 10.1007/s00192-006-0101-2]
17 **Claes L**. The mechanical and morphological properties of bone beneath internal fixation plates of differing rigidity. *J Orthop Res* 1989; **7**: 170-177 [PMID: 2918416]
18 **Diez-Itza I**, Aizpitarte I, Becerro A. Risk factors for the recurrence of pelvic organ prolapse after vaginal surgery: a review at 5 years after surgery. *Int Urogynecol J Pelvic Floor Dysfunct* 2007; **18**: 1317-1324 [PMID: 17333439 DOI: 10.1007/s00192-007-0321-0]
19 **Aboushwareb T**, McKenzie P, Wezel F, Southgate J, Badlani G. Is tissue engineering and biomaterials the future for lower urinary tract dysfunction (LUTD)/pelvic organ prolapse (POP)? *Neurourol Urodyn* 2011; **30**: 775-782 [PMID: 21661029 DOI: 10.1002/nau.21101]
20 **Rahn DD**, Ruff MD, Brown SA, Tibbals HF, Word RA. Biomechanical properties of the vaginal wall: effect of pregnancy, elastic fiber deficiency, and pelvic organ prolapse. *Am J Obstet Gynecol* 2008; **198**: 590.e1-590.e6 [PMID: 18455541 DOI: 10.1016/j.ajog.2008.02.022]
21 **Ruiz-Zapata AM**, Kerkhof MH, Zandieh-Doulabi B, Brölmann HA, Smit TH, Helder MN. Functional characteristics of vaginal fibroblastic cells from premenopausal women with pelvic organ prolapse. *Mol Hum Reprod* 2014; **20**: 1135-1143 [PMID: 25189765 DOI: 10.1093/molehr/gau078]
22 **Subak LL**, Waetjen LE, van den Eeden S, Thom DH, Vittinghoff E, Brown JS. Cost of pelvic organ prolapse surgery in the United States. *Obstet Gynecol* 2001; **98**: 646-651 [PMID: 11576582]
23 **Stanford EJ**, Cassidenti A, Moen MD. Traditional native tissue versus mesh-augmented pelvic organ prolapse repairs: providing an accurate interpretation of current literature. *Int Urogynecol J* 2012; **23**: 19-28 [PMID: 22068321 DOI: 10.1007/s00192-011-1584-z]
24 **Gerten KA**, Markland AD, Lloyd LK, Richter HE. Prolapse and incontinence surgery in older women. *J Urol* 2008; **179**: 2111-2118 [PMID: 18423726 DOI: 10.1016/j.juro.2008.01.089]
25 **Sung VW**, Weitzen S, Sokol ER, Rardin CR, Myers DL. Effect of patient age on increasing morbidity and mortality following urogynecologic surgery. *Am J Obstet Gynecol* 2006; **194**: 1411-1417 [PMID: 16647926 DOI: 10.1016/j.ajog.2006.01.050]
26 **Wein AJ**. Re: Implications of the FDA statement on transvaginal placement of mesh: the aftermath. *J Urol* 2015; **193**: 606-607 [PMID: 25617282 DOI: 10.1016/j.juro.2014.11.070]
27 **Feola A**, Abramowitch S, Jallah Z, Stein S, Barone W, Palcsey S, Moalli P. Deterioration in biomechanical properties of the vagina following implantation of a high-stiffness prolapse mesh. *BJOG* 2013; **120**: 224-232 [PMID: 23240801 DOI: 10.1111/1471-0528.12077]
28 **Carr LK**, Robert M, Kultgen PL, Herschorn S, Birch C, Murphy M, Chancellor MB. Autologous muscle derived cell therapy for stress urinary incontinence: a prospective, dose ranging study. *J Urol* 2013; **189**: 595-601 [PMID: 23260547 DOI: 10.1016/j.juro.2012.09.028]
29 **Blau HM**, Cosgrove BD, Ho AT. The central role of muscle stem cells in regenerative failure with aging. *Nat Med* 2015; **21**: 854-862 [PMID: 26248268 DOI: 10.1038/nm.3918]
30 **Jankowski RJ**, Deasy BM, Huard J. Muscle-derived stem cells. *Gene Ther* 2002; **9**: 642-647 [PMID: 12032710 DOI: 10.1038/sj.gt.3301719]
31 **van der Schaft DW**, van Spreeuwel AC, Boonen KJ, Langelaan ML, Bouten CV, Baaijens FP. Engineering skeletal muscle tissues from murine myoblast progenitor cells and application of electrical stimulation. *J Vis Exp* 2013; **(73)**: e4267 [PMID: 23542531 DOI: 10.3791/4267]
32 **Tare RS**, Kanczler J, Aarvold A, Jones AM, Dunlop DG, Oreffo RO. Skeletal stem cells and bone regeneration: translational

strategies from bench to clinic. *Proc Inst Mech Eng H* 2010; **224**: 1455-1470 [PMID: 21287831]
33 **Xu X**, Wilschut KJ, Kouklis G, Tian H, Hesse R, Garland C, Sbitany H, Hansen S, Seth R, Knott PD, Hoffman WY, Pomerantz JH. Human Satellite Cell Transplantation and Regeneration from Diverse Skeletal Muscles. *Stem Cell Reports* 2015; **5**: 419-434 [PMID: 26352798 DOI: 10.1016/j.stemcr.2015.07.016]
34 **Ho MH**, Heydarkhan S, Vernet D, Kovanecz I, Ferrini MG, Bhatia NN, Gonzalez-Cadavid NF. Stimulating vaginal repair in rats through skeletal muscle-derived stem cells seeded on small intestinal submucosal scaffolds. *Obstet Gynecol* 2009; **114**: 300-309 [PMID: 19622991]
35 **Chapple C**, Osman N, MacNeil S. Developing tissue-engineered solutions for the treatment of extensive urethral strictures. *Eur Urol* 2013; **63**: 539-541 [PMID: 23031675 DOI: 10.1016/j.eururo.2012.09.046]
36 **Meyer S**, Achtari C, Hohlfeld P, Juillerat-Jeanneret L. The contractile properties of vaginal myofibroblasts: is the myofibroblasts contraction force test a valuable indication of future prolapse development? *Int Urogynecol J Pelvic Floor Dysfunct* 2008; **19**: 1399-1403 [PMID: 18511996 DOI: 10.1007/s00192-008-0643-6]
37 **Roman S**, Mangera A, Osman NI, Bullock AJ, Chapple CR, MacNeil S. Developing a tissue engineered repair material for treatment of stress urinary incontinence and pelvic organ prolapse-which cell source? *Neurourol Urodyn* 2014; **33**: 531-537 [PMID: 23868812 DOI: 10.1002/nau.22443]
38 **Mangera A**, Bullock AJ, Roman S, Chapple CR, MacNeil S. Comparison of candidate scaffolds for tissue engineering for stress urinary incontinence and pelvic organ prolapse repair. *BJU Int* 2013; **112**: 674-685 [PMID: 23773418 DOI: 10.1111/bju.12186]
39 **Bianco P**, Cao X, Frenette PS, Mao JJ, Robey PG, Simmons PJ, Wang CY. The meaning, the sense and the significance: translating the science of mesenchymal stem cells into medicine. *Nat Med* 2013; **19**: 35-42 [PMID: 23296015 DOI: 10.1038/nm.3028]
40 **Le Blanc K**, Mougiakakos D. Multipotent mesenchymal stromal cells and the innate immune system. *Nat Rev Immunol* 2012; **12**: 383-396 [PMID: 22531326 DOI: 10.1038/nri3209]
41 **James AW**, Zara JN, Corselli M, Askarinam A, Zhou AM, Hourfar A, Nguyen A, Megerdichian S, Asatrian G, Pang S, Stoker D, Zhang X, Wu B, Ting K, Péault B, Soo C. An abundant perivascular source of stem cells for bone tissue engineering. *Stem Cells Transl Med* 2012; **1**: 673-684 [PMID: 23197874 DOI: 10.5966/sctm.2012-0053]
42 **Caplan AI**. Why are MSCs therapeutic? New data: new insight. *J Pathol* 2009; **217**: 318-324 [PMID: 19023885 DOI: 10.1002/path.2469]
43 **Chan RW**, Schwab KE, Gargett CE. Clonogenicity of human endometrial epithelial and stromal cells. *Biol Reprod* 2004; **70**: 1738-1750 [PMID: 14766732 DOI: 10.1095/biolreprod.103.024109]
44 **Gargett CE**, Schwab KE, Zillwood RM, Nguyen HP, Wu D. Isolation and culture of epithelial progenitors and mesenchymal stem cells from human endometrium. *Biol Reprod* 2009; **80**: 1136-1145 [PMID: 19228591 DOI: 10.1095/biolreprod.108.075226]
45 **Kadekar D**, Kale V, Limaye L. Differential ability of MSCs isolated from placenta and cord as feeders for supporting ex vivo expansion of umbilical cord blood derived CD34(+) cells. *Stem Cell Res Ther* 2015; **6**: 201 [PMID: 26481144 DOI: 10.1186/s13287-015-0194-y]
46 **Zuk PA**, Zhu M, Ashjian P, De Ugarte DA, Huang JI, Mizuno H, Alfonso ZC, Fraser JK, Benhaim P, Hedrick MH. Human adipose tissue is a source of multipotent stem cells. *Mol Biol Cell* 2002; **13**: 4279-4295 [PMID: 12475952 DOI: 10.1091/mbc.E02-02-0105]
47 **Crisan M**, Yap S, Casteilla L, Chen CW, Corselli M, Park TS, Andriolo G, Sun B, Zheng B, Zhang L, Norotte C, Teng PN, Traas J, Schugar R, Deasy BM, Badylak S, Buhring HJ, Giacobino JP, Lazzari L, Huard J, Péault B. A perivascular origin for mesenchymal stem cells in multiple human organs. *Cell Stem Cell* 2008; **3**: 301-313 [PMID: 18786417 DOI: 10.1016/j.stem.2008.07.003]
48 **Rustad KC**, Gurtner GC. Mesenchymal Stem Cells Home to Sites of Injury and Inflammation. *Adv Wound Care* (New Rochelle) 2012; **1**: 147-152 [PMID: 24527296 DOI: 10.1089/wound.2011.0314]
49 **Estrela C**, Alencar AH, Kitten GT, Vencio EF, Gava E. Mesenchymal stem cells in the dental tissues: perspectives for tissue regeneration. *Braz Dent J* 2011; **22**: 91-98 [PMID: 21537580]
50 **Le Blanc K**. Mesenchymal stromal cells: Tissue repair and immune modulation. *Cytotherapy* 2006; **8**: 559-561 [PMID: 17148032 DOI: 10.1080/14653240601045399]
51 **Wong SP**, Rowley JE, Redpath AN, Tilman JD, Fellous TG, Johnson JR. Pericytes, mesenchymal stem cells and their contributions to tissue repair. *Pharmacol Ther* 2015; **151**: 107-120 [PMID: 25827580 DOI: 10.1016/j.pharmthera.2015.03.006]
52 **Li M**, Ikehara S. Bone-marrow-derived mesenchymal stem cells for organ repair. *Stem Cells Int* 2013; **2013**: 132642 [PMID: 23554816 DOI: 10.1155/2013/132642]
53 **Gronthos S**, Mankani M, Brahim J, Robey PG, Shi S. Postnatal human dental pulp stem cells (DPSCs) in vitro and in vivo. *Proc Natl Acad Sci USA* 2000; **97**: 13625-13630 [PMID: 11087820 DOI: 10.1073/pnas.240309797]
54 **Estes BT**, Diekman BO, Gimble JM, Guilak F. Isolation of adipose-derived stem cells and their induction to a chondrogenic phenotype. *Nat Protoc* 2010; **5**: 1294-1311 [PMID: 20595958 DOI: 10.1038/nprot.2010.81]
55 **Murphy MB**, Moncivais K, Caplan AI. Mesenchymal stem cells: environmentally responsive therapeutics for regenerative medicine. *Exp Mol Med* 2013; **45**: e54 [PMID: 24232253 DOI: 10.1038/emm.2013.94]
56 **Ulrich D**, Muralitharan R, Gargett CE. Toward the use of endometrial and menstrual blood mesenchymal stem cells for cell-based therapies. *Expert Opin Biol Ther* 2013; **13**: 1387-1400 [PMID: 23930703 DOI: 10.1517/14712598.2013.826187]
57 **Ulrich D**, Edwards SL, Su K, Tan KS, White JF, Ramshaw JA, Lo C, Rosamilia A, Werkmeister JA, Gargett CE. Human endometrial mesenchymal stem cells modulate the tissue response and mechanical behavior of polyamide mesh implants for pelvic organ prolapse repair. *Tissue Eng Part A* 2014; **20**: 785-798 [PMID: 24083684]
58 **Baxter MA**, Wynn RF, Jowitt SN, Wraith JE, Fairbairn LJ, Bellantuono I. Study of telomere length reveals rapid aging of human marrow stromal cells following in vitro expansion. *Stem Cells* 2004; **22**: 675-682 [PMID: 15342932 DOI: 10.1634/stemcells.22-5-675]
59 **Gargett CE**, Masuda H. Adult stem cells in the endometrium. *Mol Hum Reprod* 2010; **16**: 818-834 [PMID: 20627991 DOI: 10.1093/molehr/gaq061]
60 **Katare R**, Riu F, Rowlinson J, Lewis A, Holden R, Meloni M, Reni C, Wallrapp C, Emanueli C, Madeddu P. Perivascular delivery of encapsulated mesenchymal stem cells improves postischemic angiogenesis via paracrine activation of VEGF-A. *Arterioscler Thromb Vasc Biol* 2013; **33**: 1872-1880 [PMID: 23766261 DOI: 10.1161/atvbaha.113.301217]
61 **Isakova IA**, Lanclos C, Bruhn J, Kuroda MJ, Baker KC, Krishnappa V, Phinney DG. Allo-reactivity of mesenchymal stem cells in rhesus macaques is dose and haplotype dependent and limits durable cell engraftment in vivo. *PLoS One* 2014; **9**: e87238 [PMID: 24489878 DOI: 10.1371/journal.pone.0087238]
62 **Jabbour HN**, Kelly RW, Fraser HM, Critchley HO. Endocrine regulation of menstruation. *Endocr Rev* 2006; **27**: 17-46 [PMID: 16160098 DOI: 10.1210/er.2004-0021]
63 **Gargett CE**, Chan RW, Schwab KE. Hormone and growth factor signaling in endometrial renewal: role of stem/progenitor cells. *Mol Cell Endocrinol* 2008; **288**: 22-29 [PMID: 18403104 DOI: 10.1016/j.mce.2008.02.026]
64 **Gargett CE**. Uterine stem cells: what is the evidence? *Hum Reprod Update* 2007; **13**: 87-101 [PMID: 16960017 DOI: 10.1093/humupd/dml045]
65 **Dimitrov R**, Timeva T, Kyurkchiev D, Stamenova M, Shterev A, Kostova P, Zlatkov V, Kehayov I, Kyurkchiev S. Characterization of clonogenic stromal cells isolated from human endometrium. *Reproduction* 2008; **135**: 551-558 [PMID: 18367513 DOI: 10.1530/REP-07-0428]
66 **Dominici M**, Le Blanc K, Mueller I, Slaper-Cortenbach I, Marini F, Krause D, Deans R, Keating A, Prockop Dj, Horwitz E. Minimal

criteria for defining multipotent mesenchymal stromal cells. The International Society for Cellular Therapy position statement. *Cytotherapy* 2006; **8**: 315-317 [PMID: 16923606 DOI: 10.1080/14653240600855905]

67 **Cervelló I**, Mas A, Gil-Sanchis C, Peris L, Faus A, Saunders PT, Critchley HO, Simón C. Reconstruction of endometrium from human endometrial side population cell lines. *PLoS One* 2011; **6**: e21221 [PMID: 21712999 DOI: 10.1371/journal.pone.0021221]

68 **Masuda H**, Matsuzaki Y, Hiratsu E, Ono M, Nagashima T, Kajitani T, Arase T, Oda H, Uchida H, Asada H, Ito M, Yoshimura Y, Maruyama T, Okano H. Stem cell-like properties of the endometrial side population: implication in endometrial regeneration. *PLoS One* 2010; **5**: e10387 [PMID: 20442847 DOI: 10.1371/journal.pone.0010387]

69 **Schwab KE**, Hutchinson P, Gargett CE. Identification of surface markers for prospective isolation of human endometrial stromal colony-forming cells. *Hum Reprod* 2008; **23**: 934-943 [PMID: 18305000 DOI: 10.1093/humrep/den051]

70 **Schwab KE**, Gargett CE. Co-expression of two perivascular cell markers isolates mesenchymal stem-like cells from human endometrium. *Hum Reprod* 2007; **22**: 2903-2911 [PMID: 17872908 DOI: 10.1093/humrep/dem265]

71 **Lv FJ**, Tuan RS, Cheung KM, Leung VY. Concise review: the surface markers and identity of human mesenchymal stem cells. *Stem Cells* 2014; **32**: 1408-1419 [PMID: 24578244 DOI: 10.1002/stem.1681]

72 **Masuda H**, Anwar SS, Bühring HJ, Rao JR, Gargett CE. A novel marker of human endometrial mesenchymal stem-like cells. *Cell Transplant* 2012; **21**: 2201-2214 [PMID: 22469435 DOI: 10.3727/096368911x637362]

73 **Spitzer TL**, Rojas A, Zelenko Z, Aghajanova L, Erikson DW, Barragan F, Meyer M, Tamaresis JS, Hamilton AE, Irwin JC, Giudice LC. Perivascular human endometrial mesenchymal stem cells express pathways relevant to self-renewal, lineage specification, and functional phenotype. *Biol Reprod* 2012; **86**: 58 [PMID: 22075475 DOI: 10.1095/biolreprod.111.095885]

74 **Sivasubramaniyan K**, Harichandan A, Schumann S, Sobiesiak M, Lengerke C, Maurer A, Kalbacher H, Bühring HJ. Prospective isolation of mesenchymal stem cells from human bone marrow using novel antibodies directed against Sushi domain containing 2. *Stem Cells Dev* 2013; **22**: 1944-1954 [PMID: 23406305 DOI: 10.1089/scd.2012.0584]

75 **Sobiesiak M**, Sivasubramaniyan K, Hermann C, Tan C, Orgel M, Treml S, Cerabona F, de Zwart P, Ochs U, Müller CA, Gargett CE, Kalbacher H, Bühring HJ. The mesenchymal stem cell antigen MSCA-1 is identical to tissue non-specific alkaline phosphatase. *Stem Cells Dev* 2010; **19**: 669-677 [PMID: 19860546 DOI: 10.1089/scd.2009.0290]

76 **Murakami K**, Lee YH, Lucas ES, Chan YW, Durairaj RP, Takeda S, Moore JD, Tan BK, Quenby S, Chan JK, Gargett CE, Brosens JJ. Decidualization induces a secretome switch in perivascular niche cells of the human endometrium. *Endocrinology* 2014; **155**: 4542-4553 [PMID: 25116707]

77 **Schüring AN**, Schulte N, Kelsch R, Röpke A, Kiesel L, Götte M. Characterization of endometrial mesenchymal stem-like cells obtained by endometrial biopsy during routine diagnostics. *Fertil Steril* 2011; **95**: 423-426 [PMID: 20864098 DOI: 10.1016/j.fertnstert.2010.08.035]

78 **Ulrich D**, Tan KS, Deane J, Schwab K, Cheong A, Rosamilia A, Gargett CE. Mesenchymal stem/stromal cells in post-menopausal endometrium. *Hum Reprod* 2014; **29**: 1895-1905 [PMID: 24964924 DOI: 10.1093/humrep/deu159]

79 **Gronthos S**, McCarty R, Mrozik K, Fitter S, Paton S, Menicanin D, Itescu S, Bartold PM, Xian C, Zannettino AC. Heat shock protein-90 beta is expressed at the surface of multipotential mesenchymal precursor cells: generation of a novel monoclonal antibody, STRO-4, with specificity for mesenchymal precursor cells from human and ovine tissues. *Stem Cells Dev* 2009; **18**: 1253-1262 [PMID: 19327008 DOI: 10.1089/scd.2008.0400]

80 **Rozemuller H**, Prins HJ, Naaijkens B, Staal J, Bühring HJ, Martens AC. Prospective isolation of mesenchymal stem cells from multiple mammalian species using cross-reacting anti-human monoclonal antibodies. *Stem Cells Dev* 2010; **19**: 1911-1921 [PMID: 20367498 DOI: 10.1089/scd.2009.0510]

81 **Letouzey V**, Tan KS, Deane JA, Ulrich D, Gurung S, Ong YR, Gargett CE. Isolation and characterisation of mesenchymal stem/stromal cells in the ovine endometrium. *PLoS One* 2015; **10**: e0127531 [PMID: 25992577 DOI: 10.1371/journal.pone.0127531]

82 **Bühring HJ**, Treml S, Cerabona F, de Zwart P, Kanz L, Sobiesiak M. Phenotypic characterization of distinct human bone marrow-derived MSC subsets. *Ann N Y Acad Sci* 2009; **1176**: 124-134 [PMID: 19796240 DOI: 10.1111/j.1749-6632.2009.04564.x]

83 **Crisan M**, Corselli M, Chen WC, Péault B. Perivascular cells for regenerative medicine. *J Cell Mol Med* 2012; **16**: 2851-2860 [PMID: 22882758 DOI: 10.1111/j.1582-4934.2012.01617.x]

84 **Li L**, Xie T. Stem cell niche: structure and function. *Annu Rev Cell Dev Biol* 2005; **21**: 605-631 [PMID: 16212509 DOI: 10.1146/annurev.cellbio.21.012704.131525]

85 **Rajaraman G**, White J, Tan KS, Ulrich D, Rosamilia A, Werkmeister J, Gargett CE. Optimization and scale-up culture of human endometrial multipotent mesenchymal stromal cells: potential for clinical application. *Tissue Eng Part C Methods* 2013; **19**: 80-92 [PMID: 22738377 DOI: 10.1089/ten.TEC.2011.0718]

86 **Su K**, Edwards SL, Tan KS, White JF, Kandel S, Ramshaw JA, Gargett CE, Werkmeister JA. Induction of endometrial mesenchymal stem cells into tissue-forming cells suitable for fascial repair. *Acta Biomater* 2014; **10**: 5012-5020 [PMID: 25194931 DOI: 10.1016/j.actbio.2014.08.031]

87 **Gurung S**, Werkmeister JA, Gargett CE. Inhibition of Transforming Growth Factor-β Receptor signaling promotes culture expansion of undifferentiated human Endometrial Mesenchymal Stem/stromal Cells. *Sci Rep* 2015; **5**: 15042 [PMID: 26461813 DOI: 10.1038/srep15042]

88 **Ulrich D**, Edwards SL, White JF, Supit T, Ramshaw JA, Lo C, Rosamilia A, Werkmeister JA, Gargett CE. A preclinical evaluation of alternative synthetic biomaterials for fascial defect repair using a rat abdominal hernia model. *PLoS One* 2012; **7**: e50044 [PMID: 23185528 DOI: 10.1371/journal.pone.0050044]

89 **Edwards SL**, Ulrich D, White JF, Su K, Rosamilia A, Ramshaw JA, Gargett CE, Werkmeister JA. Temporal changes in the biomechanical properties of endometrial mesenchymal stem cell seeded scaffolds in a rat model. *Acta Biomater* 2015; **13**: 286-294 [PMID: 25462845 DOI: 10.1016/j.actbio.2014.10.043]

90 **Takacs P**, Nassiri M, Viciana A, Candiotti K, Fornoni A, Medina CA. Fibulin-5 expression is decreased in women with anterior vaginal wall prolapse. *Int Urogynecol J Pelvic Floor Dysfunct* 2009; **20**: 207-211 [PMID: 18989607 DOI: 10.1007/s00192-008-0757-x]

91 **Couri BM**, Lenis AT, Borazjani A, Paraiso MF, Damaser MS. Animal models of female pelvic organ prolapse: lessons learned. *Expert Rev Obstet Gynecol* 2012; **7**: 249-260 [PMID: 22707980 DOI: 10.1586/eog.12.24]

92 **Krause H**, Goh J. Sheep and rabbit genital tracts and abdominal wall as an implantation model for the study of surgical mesh. *J Obstet Gynaecol Res* 2009; **35**: 219-224 [PMID: 19708169 DOI: 10.1111/j.1447-0756.2008.00930.x]

93 **Nakamura A**, Osonoi T, Terauchi Y. Relationship between urinary sodium excretion and pioglitazone-induced edema. *J Diabetes Investig* 2010; **1**: 208-211 [PMID: 24843434 DOI: 10.1111/j.2044-3870.2010.tb00263.x]

94 **Feola A**, Endo M, Urbankova I, Vlacil J, Deprest T, Bettin S, Klosterhalfen B, Deprest J. Host reaction to vaginally inserted collagen containing polypropylene implants in sheep. *Am J Obstet Gynecol* 2015; **212**: 474.e1-474.e8 [PMID: 25446700 DOI: 10.1016/j.ajog.2014.11.008]

95 **de Tayrac R**, Alves A, Thérin M. Collagen-coated vs noncoated low-weight polypropylene meshes in a sheep model for vaginal surgery. A pilot study. *Int Urogynecol J Pelvic Floor Dysfunct* 2007; **18**: 513-520 [PMID: 16941070 DOI: 10.1007/s00192-006-0176-9]

96 **Ulrich D**, Edwards SL, Letouzey V, Su K, White JF, Rosamilia A, Gargett CE, Werkmeister JA. Regional variation in tissue composition and biomechanical properties of postmenopausal ovine and human vagina. *PLoS One* 2014; **9**: e104972 [PMID: 25148261

DOI: 10.1371/journal.pone.0104972]
97 **Ulrich D**, Edwards SL, Alexander DLJ, Rosamilia A, Werkmeister JA, Gargett CE, Letouzey V. Changes in pelvic organ prolapse mesh mechanical properties following implantation in rats. *Am J Obstet Gynecol* 2016; **214**: 260.e1-e8 [PMID: 26348376 DOI: 10.1016/j.ajog.2015.08.071]
98 **Gardner IA**, Reynolds JP, Risco CA, Hird DW. Patterns of uterine prolapse in dairy cows and prognosis after treatment. *J Am Vet Med Assoc* 1990; **197**: 1021-1024 [PMID: 2243033]
99 **Finegold AA**, Schafer WR, Rine J, Whiteway M, Tamanoi F. Common modifications of trimeric G proteins and ras protein: involvement of polyisoprenylation. *Science* 1990; **249**: 165-169 [PMID: 1695391]
100 **Abramowitch SD**, Feola A, Jallah Z, Moalli PA. Tissue mechanics, animal models, and pelvic organ prolapse: a review. *Eur J Obstet Gynecol Reprod Biol* 2009; **144** Suppl 1: S146-S158 [PMID: 19285776 DOI: 10.1016/j.ejogrb.2009.02.022]
101 **Otto LN**, Slayden OD, Clark AL, Brenner RM. The rhesus macaque as an animal model for pelvic organ prolapse. *Am J Obstet Gynecol* 2002; **186**: 416-421 [PMID: 11904600 DOI: 10.1067/mob.2002.121723]
102 **Liang R**, Abramowitch S, Knight K, Palcsey S, Nolfi A, Feola A, Stein S, Moalli PA. Vaginal degeneration following implantation of synthetic mesh with increased stiffness. *BJOG* 2013; **120**: 233-243 [PMID: 23240802 DOI: 10.1111/1471-0528.12085]
103 **Edwards SL**, Werkmeister JA, Rosamilia A, Ramshaw JA, White JF, Gargett CE. Characterisation of clinical and newly fabricated meshes for pelvic organ prolapse repair. *J Mech Behav Biomed Mater* 2013; **23**: 53-61 [PMID: 23651550 DOI: 10.1016/j.jmbbm.2013.04.002]

P- Reviewer: Bussolati B, Sacco E, Tsai EM, Tan BK
S- Editor: Qiu S **L- Editor**: A **E- Editor**: Wu HL